4 Polyethylene Terephthalate-Based Blends: Thermoplastic and Thermoset

Rabindra Kumar Padhan[1,2] and Anurag A. Gupta[1]

[1]Bitumen Department, Executive Director, Indian Oil R&D Centre, Faridabad, Haryana, India

[2]Chemical Engineering Department, University of Petroleum and Energy Studies, Dehradun, Uttarakhand, India

OUTLINE

4.1 Introduction

Design of new polymers with special properties by chemical synthesis is always more expensive than the costs of the constituent existing polymers and the blending operation. A proper selection and combination of polymeric components in a certain ratio might result in a blend material with optimal properties for a specific application. The resulting blend will be more successful; more of the desired properties of the components are expressed in its property profile. A remarkably broad spectrum of properties can often be achieved by blending polymer blend. The blending technology began in the plastics industry over five decades ago. These properties include mostly mechanical strength and stiffness, toughness, processability, heat distortion temperature, flame retardancy, thermal and dimensional stability, aging resistance, permeability, elongation, transparency, and gloss. The most common polymer blending is found with polyethylene terephthalate (PET).

Poly(Ethylene Terephthalate) Based Blends, Composites and Nanocomposites. http://dx.doi.org/10.1016/B978-0-323-31306-3.00004-X

The key reason for blending of PET with other thermoplastic polymer(s) or with other thermosets is to "tailor" new materials with improved performance, with beneficial cost profiles to meet actual application needs. This tailoring approach, which also opens up new markets and application potentials for the already versatile thermoplastic polyesters, does not need the heavy capital investment and long development times usually associated with development and manufacture. The key polymers that are blended with PET to develop high-performance polymer blends include thermoplastics such as polyethylene (PE), polypropylenes (PP), polycarbonates (PCs), polystyrene, ethylene vinyl acetate, acrylonitrile–butadiene–styrene copolymer, polyarylate, and thermosets of polymers such as epoxies, polyester resin, phenolic resin, and various elastomers such as ethylene propylene rubber, ethylene propylene diene monomer rubber, nitrile butadiene rubber, and styrene-butadiene rubber [1]. PET blends can be typically prepared by five techniques: graft copolymerization, melt solution, latex blending, partial block, and synthesis of interpenetrating networks. Melt blending is a simple mechanical process of creating a homogeneous mixture of two or more polymers. The major advantage of melt blending is the absence of any solvents that might be required in other methods of polymer blending.

A number of miscible polymer blends are only completely miscible and form one-phase systems over a limited concentration, temperature, and pressure range. Under certain conditions of temperature, pressure, and composition, miscible binary blends may phase separate into two liquid phases with different compositions. Important characteristics of this type of blend are the overall blend composition, the morphology, and the composition of the different phases. The development of new multiphase blend materials is dependent primarily on controlling interfacial chemistry and microstructures. There are several material parameters that could influence morphology: viscosity ratio, composition, elasticity, shear stress, and interfacial modification. The morphology can be improved by controlling these parameters to obtain an increase in the mechanical properties. Immiscible polymer blends have large interfacial tension, poor interfacial adhesion, and poor mechanical properties. To enhance these properties, it is necessary to improve adhesion between two phases in the blend [2]. But the major disadvantages are that mixing may be incomplete due to the kinetics involved in mixing large polymer molecules and the chemical nature of the polymer.

However, the compatibility of these heterogeneous blends can be improved by the addition of compatibilizers [3,4]. The two methods finding practical application are (1) incorporation of a separate chemical compatibilizer into an immiscible polymer blend during melt compounding and (2) "reactive" compounding to form an *in situ* compatibilizer. Thus, there are two blend types depending on the method of compatibilization: physically or nonreactively compatibilized and *in situ* or reactively compatibilized. In either type, the control of compatibility at the interface between the constituent polymer phases is the key to optimization of the desired property profile and to stability of the blend morphology. Since PET possesses hydroxyl and carboxyl functional groups at chain ends, *in situ* or reactive compatibilization is an effective approach for developing engineering thermoplastic blends from these materials. Sometimes, a reactive coupler, such as epoxide moiety, maleic anhydride, glycidyl methacrylate, etc., is used to compatibilize thermoplastic PET blends.

The most common industrial method of PET blend preparation involves melt blending in a mixer or a twin-screw extruder. However, the rheological properties of the blend components, the melt-blending conditions, and the method of morphology stabilization, for example, by controlled cooling, crystallization, chemical reaction, etc., are important for developing useful property profiles in the blends.

4.2 Polyethylene Terephthalate-Based Thermoplastic Blends

The thermoplastic polymers that blend with PET represent an important group of materials. The thermoplastic polymers used in such blends include PE, PP, PCs, liquid crystalline polymers, etc. for improving cost effectiveness or properties such as mechanical strength and stiffness, toughness, processability, heat distortion temperature, flame retardancy, thermal and dimensional stability, aging resistance, permeability, elongation, transparency, gloss, and chemical resistance. The main objective of the development of this group of blends is to partially exploit the higher-end property polymer, combined with cost effectiveness, with the use of less costly PET.

4.3 Preparation of Polyethylene Terephthalate-Based Thermoplastic Blends

The preparation of polymer blends of thermoplastic polymers such as PE, PP, PCs, polystyrene, ethylene vinyl acetate, acrylonitrile-butadiene-styrene

(co)polymer, poly(phenylene sulfide), etc. with PET are discussed.

4.3.1 Preparation of Polyethylene Terephthalate Blends with Polyolefins

The combination of PET with polyolefins represents yet another important group of PET blends. The use of recycled scrap from PET and polyolefins for ecological reasons, as the major portion of postconsumer waste especially packaging, beverage containers, soft drinks bottles, etc., is the main reason for developing blends of PET with polyolefins. The blending of high-density polyethylene (HDPE) scrap with PET bottle scrap from containers of carbonated beverages is a major commercial example. Another reason for the study of the blend of PET with polyolefins such as PP, HDPE, etc. could be to explore the possibility of developing new fiber- and filament-type materials for nonwoven applications.

PETs modified with polyolefins are often glass fiber reinforced and find applications in injection molded automotive and industrial components such as windshield wiper blade supports, industrial pump housings and impellers, gears, and bearings.

4.3.1.1 PET/HDPE Blends

HDPE and PET contain a major portion of postconsumer waste and are recycled to reduce waste, especially packaging. Blending of these polymers is an alternative method to reduce waste. However, HDPE and PET are immiscible [5]. Through a proper compatibilization strategy, the blends can combine the stiffness (dimensional stability) of PET with the good impact strength of HDPE. Also, an improvement in the solvent resistance of PET is achieved by virtue of the presence of HDPE in the blends. The impetus for the development of PET/HDPE blends comes mainly from waste utilization efforts.

Chareunkvun [6] prepared HDPE grafted with glycidyl methacrylate (HDPE-*g*-GMA) by using Hakke Rheomix 3000p equipped with 27 roller rotors. The composition of HDPE/DCP/GMA was 100/0.6/10 phr. All components were mixed collectively for 10 min at 180ºC with 60 rpm. Akkapeddi and Van Buskirk [7] studied the compatibilization of postconsumer PET/HDPE blends. The melt blends were prepared in a single-screw extruder and a corotating twin-screw extruder. Ethylene-glycidyl methacrylate (E-GMA) was used as a compatibilizing agent in PET/HDPE blends. Addition of 10% E-GMA in a PET/HDPE (1.8:1) blend significantly improved the heat resistance and toughness properties. Iniguez et al. [8] studied the morphological stability of postconsumer PET/HDPE blends at different compositions (10–90% by volume of PET in HDPE) with and without a compatibilizer. Kim et al. [9] studied the compatibilization of PET/HDPE blends. HDPE grafted with the blocked isocyanate group (HDPE-*g*-BHI) was used as a reactive compatibilizer for an immiscible PET/HDPE blend. The blend ratios of the PET/HDPE were 10/90, 30/70, 50/50, 70/30, and 90/10 by weight. During the melt blending in an internal mixer, a chemical reaction occurred between carboxyl and hydroxyl end groups of PET with the isocyanate group.

4.3.1.2 PET/PC Blends

Blends of PC with PET or polybutylene terephthalate constitute an important category of commercial blends. This section discusses the compositions based on combinations of PC with PET. Ignatov et al. [10] prepared a PET and PC mechanically dispersed polymer blend by one-step extrusion. Fast-reactive blending of 50/50 wt/wt ratio of PET/PC was taken in a pilot plant having a twin-screw corotating extruder “ICMA MC 33” (D = 30 ram; LID = 36; 4–7 kg/h; 100–150 rpm) at 270–280°C in the extruder’s head. The catalyst was dispersed on PET or PC pellets at a concentration of 0.015–0.09 wt% with respect to the final PET/PC blend. Duration of the extrusion under the above conditions was about 1 min. The extruded product was then cooled in water, pelletized, and dried in a vacuum oven for 12 h at 120°C and extruded with commercial stabilizers (Ultranox 626 and Irganox 1010t, 0.3 wt% of each of them with respect to the final product). Murff et al. [11] prepared a melt blend of PC and PET by continuous extrusion, injection molded into bars, and studied their thermal and mechanical behavior.

4.3.1.3 PET/LCP Blends

Blending of PET with 10–15 wt% of liquid crystalline polymers (LCPs) has the advantages of low cost and ease of processing PET coupled with superior mechanical, thermomechanical, and barrier properties of LCPs. The issues for exploiting all these advantages include optimization of the blend composition, compatibilization, and strict control of the morphology of LCP phases.

4.3.2 Properties of Polyethylene Terephthalate-Based Thermoplastic Blends

The polymers that are blended with PET to develop a high-performance polymer blend include PCs, polyolefins, and LCPs. A variety of polyester blends are already commercially available to provide competitive product advantages to the end users; the examples are PET/HDPE, PET/PC, PET/LCP, etc.

For uncompatibilized blends of 10, 20, and 30% by volume of PET, the modulus and tensile strength increased with PET concentration, while the elongation at break decreased. These tendencies coincided with the results obtained by Kim et al. [12].

Pawlak et al. [13] studied two blends of PET and HDPE in weight compositions of 75/25 and 25/75. Three compatibilizers such as E-GMA, SEBS-*g*-MA, and HDPE-*g*-MA with variable contents (2, 3, 4, 5, and 10 wt%) were used. The melt blends were prepared in a corotating twin-screw extruder. The uncompatibilized blends were brittle in tensile tests with very low elongation at break.

Adur and Bonis [14] published an interesting study on compatibilized blends of 90% PET with 10% LCP, exhibiting excellent properties (Table 4.1). In the compatibilized blends, the tensile strength of PET was increased by 2.5 times and the modulus by 5 times.

4.3.3 Application of Polyethylene Terephthalate Blends

PETs modified with polyolefins are often glass fiber-reinforced and find applications in injection-molded automotive and industrial components such as windshield wiper blade supports, industrial pump housings, and impellers, gears and bearings. For that reason the blending of PET with other polymers is a significant development on the part of resin suppliers, as well as processors and consumers. A variety of PET blends are already commercially available to provide competitive product advantages to the end users; examples are PET/HDPE, PET/PE, and PET/LLDP (low-density polyethylene). The issue of reuse and recycling will be another factor catalyzing the growth of blending. Through a detailed knowledge of end product performance requirements, it is possible to reuse the recycled PET blends in sequentially less-critical applications. Similarly, the targeted application areas for PET/LCP blends mainly include high-barrier films, packaging, and industrial fibers. In blends with LCPs, PET race well with the best barrier materials in packaging and with high modulus and low shrinkage fibers used in textiles industries.

Similarly typical applications of PET/PC include those requiring a combination of excellent toughness (often at low temperatures), chemical resistance, and heat resistance, such as:

1. Automotive – car bumpers, mirror housings and brackets, rear quarter panels
2. Telecommunications – radio housings, speaker grills, instrument housings
3. Outdoor power equipment – tractor shrouds and consoles, lawn mower decks
4. Sports goods – protective helmets, ski boots, and binding components.

Table 4.1 Properties of Films Made From Compatibilized and Uncompatibilized PET/LCP (90/10)

Film	Tensile Strength (MPa)	Tensile Modulus (MPa)	Break Elongation (%)	O_2 Barrier $\times 10^{13}$ $\left(\frac{cm^3\,cm}{cm^2\,s\,cm\,of\,Hg}\right)$	Moisture Permeability $\times 10^{13}$ $\left(\frac{cm^3\,cm}{cm^2\,s\,cm\,of\,Hg}\right)$
PET/LCP, compatibilized	102	9515	2.0	102	5.10
PET/LCP, uncompatibilized	41	2068	3.0	210–240	–
PET (Kodar A-150)	40	1379	25.0	240	10.79
LCP (Vectra A-950)	193	10,342	3.6	0.24	10.02

4.4 Polyethylene Terephthalate-Based Thermoset Blends

PET is used for many industrial products such as fibers, packaging, and beverage containers because of its good resistance to heat, resistance to chemicals, and mechanical and electrical properties. However, when it is used in the field of plastics to produce injection-molded products, many shortcomings are observed upon molding. Due to the high second-order transition temperature of PET, when it is molded especially at a low-mold temperature, at which it is usually molded by general molding machines for universally used thermoplastic resins, the shape stability of molded products is extremely poor. Furthermore, in addition to its taking a long residence time in molds and its showing poor mold releasability, it has a further disadvantage of generating potholes and scratch on the surface of the molded product obtained. To remedy such limitation, it is necessary to modify polymers or blend two or more polymers. Thermoplastic/thermoset miscible blends have been largely studied and reported over the year in the literature. Among the thermoplastic polymers PET is an important class of polymer and its global consumption is nearly 8%. Blends of PET with thermoset polymers represent a different group of materials. The thermoset polymers used in such blends include epoxy, polyester resins, polyurethanes, amide, urea, etc. for improving cost-effectiveness or properties such as mechanical strength and stiffness, toughness, processability, increased heat susceptible, heat distortion temperature, flame retardancy, thermal and dimensional stability, aging resistance, permeability, elongation, transparency, gloss, and chemical resistance. The main objective of the development and use of PET-based thermoset blends is to partially exploit the higher-end property polymer, combined with cost-effectiveness.

4.5 Preparation of Polyethylene Terephthalate-Based Thermoset Blends

This section of the chapter deals with preparation, properties, and application of PET-based thermoset blends. The preparation of polymer blends of thermoset polymers such as epoxy resin, polycarbodiimides, amides, etc. with PET is discussed.

4.5.1 Preparation of Polyethylene Terephthalate Blends with Epoxy Resin

PET is exceptionally resistant to many chemical attacks and has some outstanding mechanical properties. For these reasons, PET would normally be considered quite suitable for the production of injection-molded articles. However, in spite of its many encouraging properties, PET has not as yet been employed as a commercial injection-molding material and its market for this purpose is very limited. In particular, it has been confirmed that injection-molded articles consisting solely of PET are not dimensionally stable, especially at temperatures above the second-order transition point.

However, materials with epoxide functionality may react to form covalent bonds with both the hydroxyl and carboxylic acid end groups present in PET. The strong polarization of the hydroxyl group of carboxylic acids ensures speedy reaction between epoxy and carboxyl groups as shown in Figure 4.1

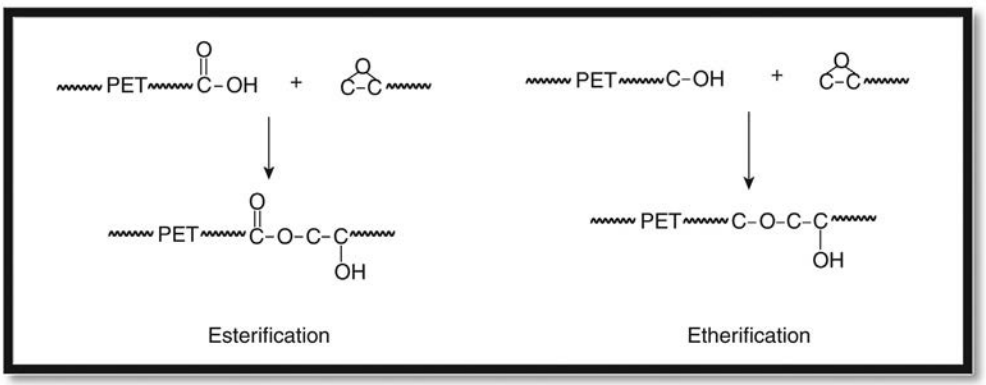

Figure 4.1 Schematic of PET, carboxylic, and alcohol group reactions with epoxides.

[15]. It has been suggested that injection-molded objects can be produced from PET by blending with epoxy compounds to improve the dimensional stability of injection-molded PET.

US Patent 3,560,605 [16] describes the modification of PET by diglycidyl ethers as obtained by the epoxidation of dihydric phenols to achieve highly improved injection-molding compositions and products. The procedures for preparing the PET/epoxy blends are given below.

Granulated PET and diglycidyl ether, commonly identified as epoxidized Bisphenol A, were intimately mixed with each other and then melt blended in a double-screw extruder for extrusion at 270–290°C into individual strands. The extruded strands were then cooled in water and cut into granules. By gentle heating at 130°C under a vacuum and an inert nitrogen atmosphere, the moisture content of the granulate was reduced to less than 0.01%. This granulate was further processed in a conventional injection-molding device to produce dimensionally stable and impact-resistant molded articles, e.g., cups, plates, bowls, combs, boxes, and the likes.

4.5.2 Preparation of Polyethylene Terephthalate Blends with Amide

Since PET and polyamides have reactive end groups, reactive compatibilization in an extruder is an integral part of PET/polyamide blend technology. Compatibilization is mainly achieved either through acid or phosphate-based catalyzed ester/amide interchange reaction or by reactive coupling reaction. Aharoni [17] used triphenyl phosphite as a catalyst to facilitate the interchange reaction between PET and PA6 (polyamide 6), resulting in the formation of block copolymers that compatibilized the blend components.

The PET/PA6 blend will be a promising blend if the rigidity of PET combines with the toughness of PA6. However, PET/PA6 blends without adding any compatibilizer have worse properties than those of virgin PET or PA6. Much research [3,4] has shown that the blending of PET and PA in the melt produces polyester–polyamide block copolymers, which could improve the compatibility of the blends.

Huang [18] studied and discussed the mechanism, morphology, and mechanical properties of PET/PA6 blends with low molecular weight Bisphenol-A epoxy resin/E44 as a reactive compatibilizer.

The preparations of the PET/PA6/E44 blends are as follows. Before compounding PET, PA6 and E44 were dried at 120, 80, and 120°C for 8, 12, and 5 h in a vacuum oven, respectively. All the melt compounding of the blends was carried out in a roller mixer of the Brabender Plasti-Corder Model XSS-300 with a temperature range of 295°C and roller speed of 32 rpm/5 min.

4.5.3 Preparation of Polyethylene Terephthalate Blends with Polycarbodiimides

Using polycarbodiimides as chain extenders for polyethylene terephthalate polymer is reported by Thomas (1978) [25]. The polycarbodiimides used were derived from oligomerization of toluene diisocyanate and were melt mixed with PET in a 28 mm W&P ZSK TSE at 254°C. The product was characterized by measuring impact strength, which showed an increase from 14.1 ft.-lb/in. to 19.8 ft.-lb/in. by using 1–2 phr polycarbodiimide. US patent 3,193,522 provided a process for stabilizing the polyester compounds against hydrolytic degradation by employing highly substituted polycarbodiimide additives having at least three carbodiimide groups in the molecules. US patents 3,193,523 and 3,193,524 disclose the use of monocarbodiimides to stabilize polyesters. Patent CA-1056985A1 attempts to stabilize polyesters by adding carbodiimide additives to polyesters having sufficient melt strength or die swell characteristics to improve extrusion applications.

4.5.4 Preparation of Polyethylene Terephthalate Blends with Polyurethane and Isocyanate

PET is a widely used thermoplastic polyester with a poor impact resistance when it is injection molded. The combination of PET with polyurethane (PU) is expected to raise its impact strength and increase compatibility when carbonyl groups of the polyester interact with the hydrogens of –NH groups of PU. Samios et al. [19] explained the preparation of PET/PU blends as follows.

PU was dried at 100°C for 24 h and PET at 150°C for 24 h *in vacuo*. Blends were prepared by melt mixing at ca. 260°C under a blanket of inert gas (argon) in a home-made stainless steel bob-and-cup type of mixer. The particular temperature was kept on the lower side by the T_m of PET and on the higher side by the onset of PU decomposition above 260°C. Films were prepared by compression molding between Teflon sheets backed by aluminum plates at 265°C and 5 MPa followed by quenching to 0°C.

US Patent 4,409,167 A describes the preparation of PET blended with an organic diisocyanate under conditions where carbon dioxide gas is vented smoothly, to achieve highly improved extruded articles. The procedures for preparing the PET/isocyanate blends are given below.

PET resin was granulated at dry ice temperature, then dried at 135°C. Methylene diphenyl diisocyanate was powdered and used 0.85% based on the weight of the PET resin was added under nitrogen. The cans were tumbled for 30 min. The blend was fed under a nitrogen blanket into a hopper by means of a twin-screw feeder made by K-Tron Corporation at a rate of 4.5 kg/h and was delivered by gravity from the hopper into a 28 mm Werner-Pfleiderer extruder. The melt pressure within the extruder was about 180–700 kPa and, at an average temperature of about 280–320°C, was maintained at a pressure of about 0.1–0.13 kPa. The screws were rotated at 40 rpm.

4.5.5 Properties of Polyethylene Terephthalate-Based Thermoset Blends

The behavior of blends depends upon the volume fractions of the phases, their shape, and on the nature of the constituents. PET-based thermoset blending is an economical way of diversifying and upgrading polymer properties. The blends of PET with thermoset polymers are used for improving the properties of mechanical strength and stiffness, toughness, processability, increased heat susceptible, heat distortion temperature, flame retardancy, thermal and dimensional stability, aging resistance, permeability, melt flow rate (MFR), elongation, transparency, gloss, and chemical resistance. Table 4.2 shows MFR and typical mechanical properties of the PET/PPE/epoxy/catalyst blends [20].

The MFR decreased with increasing polyphenylene-ether (PPE) concentration. However, epoxy concentration also plays a major role in the decrease of MFR. The tensile strength, tensile elongation, and flexural strength are higher for the blend having the composition of 70–90% of PET, 10–30% of PPE, and 0.3–0.5% of epoxy.

The mechanical properties of polymer blends are greatly influenced by their miscibility. Y. Huang and his coworker showed that [18] adding a small percentage of epoxy resin on the PET/PA6 blend, the mechanical properties of the blend increase. When the percentage of epoxy resin increases up to 5 wt%, the notched impact strength and flexural strength increase up to 500 and 400%, respectively [18].

Another important application of PET/polyamide blends mainly includes tough injection-molded automotive parts of hollow or solid configuration that would be exposed to severe conditions of corrosive

Table 4.2 Summarized Data on Melt Flow Rates (MFR) and Mechanical Properties

Composition	MFR (g/10 min)	Unnotch Impact (J/M)	Tensile Strength (MPa)	Tensile Elongation (%)	Flexural Strength (MPa)	Flexural Modulus (MPa)	G_c (J/m^2)
PET (IV – 1)/PPE/epoxy/cat.							
90/10	29.5	>900	53.2	424	87.3	2400	–
90/10/0.3	12.7	>900	57.3	541	93.3	2480	–
80/20	25.5	>900	54.6	44	90.6	2460	–
80/20/0.3	17.2	>900	58.7	84	94.4	2470	–
70/30	24.5	217	55.8	15	89.3	2410	4210
70/30/0.1	21.0	270	56.3	17	92.5	2480	5590
70/30/0.3	12.9	311	57.2	24	95.7	2520	6950
70/30/0.3/0.02	–	374	–	–	–	–	–
70/30/0.5	9.2	281	61.9	11	102.6	2600	9330
50/50	12.4	104	41.0	5.6	80.8	2520	–
50/50/0.3	5.0	195	48.0	6.8	83.4	2510	–
30/70	–	143	58.7	8.7	85.6	2330	–
30/70/0.3	–	244	59.6	8.7	88.9	2340	–

chemicals and high temperature during use. Automotive fuel intake manifolds and air suction and fume exhaust parts surrounding the engine are some of the classic examples of automotive parts where PET/polyamide blends are used, since the blends offer an excellent combination of mechanical, thermal, and chemical resistance.

In polycarbodiimide/PET blends, polycarbodiimides react with the terminal acid groups of PET and decrease the initial acid value of the polyester resin. Imashiro et al. [21] have described adding a carbodiimide compound to recycled PET such that the intrinsic viscosity and strength of the polyester resin during processing are retained.

4.5.6 Application of Polyethylene Terephthalate-Based Thermoset Blends

Blending of PET with thermoset polymers is a significant development on the part of resin suppliers, as well as processors, and, at times, consumers like automotive manufacturers. PET modified with epoxy resin has wide application in injection molding. The use of multifunctional epoxy-based modifiers to increase the melt strength of PET polymers has been investigated by Japon et al. [22,23] with the aim of producing PET foams by an extrusion process.

The chain extension of the PET approach is a simpler and cheaper technique for obtaining high molecular weight PET resins compared with the conventional solid postpolycondensation method. The chain extension of polyester in the melt using a high- reactivity diepoxy, diglycidyl tetrahydrophthalate has been extensively studied by Guo [24].

The diepoxide reacts with the hydroxyl and carboxyl end groups of PET at a relatively high temperature with very fast reaction rate. The melt flow index of the chain-extended PET decreased dramatically after addition of diepoxy compound. In addition, the notched Izod impact strength and elongation-at-break of the chain-extended PET was also found to increase. The chain-extended polyesters are also more stable thermally. Polycarbodiimide/PET blends are used as additives to provide long-term hydrolytic stability to PET components in service in moist and humid atmospheres. Again, PET/polyurethane blends are used as additives in packaging foam and to improve flame retardant qualities.

4.6 Conclusions

A remarkably broad spectrum of properties can often be achieved by blending two or more polymers. This chapter described the preparation, properties, and application of PET/thermoplastic and PET/thermoset polymer blends. The main objective of the development of this group of blends is to partially exploit the higher-end property polymer, combined with cost-effectiveness due to the use of less costly PET.

PETs modified with polyolefins are often glass fiber-reinforced and find applications in injection-molded automotive and industrial components. Similarly various applications of PET/PC include those requiring a combination of excellent toughness (often at low temperatures), chemical resistance, and heat resistance. However, compatibilizers play a major role to improve the mechanical, rheological, thermal, and morphological properties and density of the blends. The tensile, flexural, compressive, and impact strength and tensile strain at break improved in all compatible blends whereas tensile, flexural, and compressive modulus insignificantly changed for PET/polyolefin blends.

PET/thermoset-based blend materials are mainly used for the production of automotive, aeronautic, and electronic components. The major PET/thermoset blends are PET/epoxy resin, PET/polyamides, PET/polyurethane, and PET/polycarbodiimides. The thermal, mechanical, impact resistance, and flame retardant properties of PET substantially improve by adding thermoset polymers. These polymer blends have a wide spectrum of applications from domestic to industrial levels. Increasing use of PET-based blends increases the need to enhance the recycling option.

Acknowledgments

The author has not prepared any blends of PET with any other thermoplastic or thermoset polymer. However, the author extensively investigated the use of terephthalamide based on recycled PET plastic waste for the production of high-performance pavement material for the road construction industry. Terephthalamide from recycled PET offered a lower cost of materials for forming good quality pavement material.

References

[1] Y. Srithep, A. Javadi, S. Pilla, L.-S. Turng, S. Gong, C. Clemons, J. Peng, Processing and characterization of recycled poly(ethylene terephthalate) blends with chain extenders, thermoplastic elastomer, and/or poly(butylene adipate-*co*-terephthalate), Polym. Eng. Sci. 51 (2011) 1023–1032.

[2] A.F. Avila, M.V. Duarte, A mechanical analysis on recycled PET/HDPE composites, Polym. Degrad. Stab. 80 (2003) 373–382.

[3] T.L. Dimitrova, F.P. La Mantia, F. Pilati, M. Toselli, A. Valenza, A. Visco, On the compatibilization of PET/HDPE blends through a new class of copolyester, Polymer 41 (2000) 4817–4824.

[4] S.S. Dagli, K.M. Kamder, Effects of component addition protocol on the reactive compatibilization of HDPE/PET blends, Polym. Eng. Sci. 34 (23) (1994) 1709–1719.

[5] N. Torres, J.J. Robin, B. Boutevin, Study of compatibilization of HDPE-PET blends by adding grafted or statistical copolymers, J. Appl. Polym. Sci. 81 (2001) 2377–2386.

[6] S. Chareunkvun, A study of compatibilization and properties of recycled high density polyethylene (HDPE)/polyethylene terephthalate (PET) blends, Thesis, Suranaree University of Technology, 2007.

[7] M.K. Akkapeddi, B. Van Buskirk, On the compatibilization of PET-polyolefin blends, Polym. Mater. Sci. Eng. 67 (1992) 317–318.

[8] C.G. Iniguez, E. Michel, V.M. Gonzalez-Romero, R. Gonzalez-Nunez, Morphological stability of postconsumer PET/HDPE blends, Polym. Bull. 45 (2000) 295–302.

[9] D.H. Kim, K.Y. Park, J.Y. Kim, K.D. Suh, Improved compatibility of high-density polyethylene/poly(ethylene terephthalate) blend by the use of blocked isocyanate group, J. Appl. Polym. Sci. 78 (2000) 1017–1024.

[10] V.N. Ignatov, C. Carraro, V. Tartari, et al. PET/PC blends and copolymers by one-step extrusion: 1. Chemical structure and physical properties of 50/50 blends, Polymer 38 (1) (1997) 195–200.

[11] S.R. Murff, J.W. Barlow, D.R. Paul, Thermal and mechanical behavior of polycarbonate-poly(ethy1ene terephthalate) blends, J. Appl. Polym. Sci. 29 (1984) 3231–3240.

[12] D.H. Kim, K.Y. Park, J.Y. Kim, K.D. Suh, Improved compatibility of high-density polyethylene/poly(ethylene terephthalate) blend by the use of blocked isocyanate group, J. Appl. Polym. Sci. 78 (2000) 1017–1024.

[13] A. Pawlak, J. Morawiec, F. Pazzagli, M. Pracella, A. Galeski, Recycling of postconsumer poly(ethylene terephthalate) and high-density polyethylene by compatibilized blending, J. Appl. Polym. Sci. 86 (2002) 1473–1485.

[14] A.M Adur, L.J. Bonis, PET-LCP compatibilized alloys: a new unique developments, Proceedings of the FUTURE-PAK'94, Chicago, IL (1994) 2.48–2.58.

[15] M. Xanthos, U. Yilmazer, S.K. Dey, J. Quintans, Melt viscoelasticity of polyethylene terephthalate resins for low density extrusion foaming, Polym. Eng. Sci. 40 (3) (2000) 554–566.

[16] E.S. Siggel, W.O. Rein, H.-M. Koepp, Polyethylene terephthalate injection molding compositions containing a polyepoxide, US Patent 3,560,605.

[17] S.M. Aharoni, Microfibrillar-reinforced nylon-6/PET fibers with interfacial bonding, Int. J. Polym. Mater. Polym. Biomater. 38 (3–4) (1997) 173–203.

[18] Y. Huang, Y. Liu, C. Zhao, Morphology and properties of PET/PA-6/E-44 blends, J. Appl. Polym. Sci. 69 (8) (1998) 1505–1515.

[19] C.K. Samios, K.G. Gravalos, N.K. Kalfoglou, *In situ* compatibilization of polyurethane with poly(ethylene terephthalate), Eur. Polym. J. 36 (2000) 937–947.

[20] D.-W. Lo, C.-R. Chiang, F.-C. Chang, Reactive compatibilization of PET and PPE blends by epoxy couplers, J. Appl. Polym. Sci. 65 (4) (1997) 739–753.

[21] Y. Imashiro, I. Takahashi, N. Horie, S. Suzuki, Method for obtaining polyester resin products having desired strength, and mixture used in said method, US Patent 6,333,363.

[22] S. Japon, L. Boogh, Y. Leterrier, J.A.E. Manson, Reactive processing of poly(ethylene terephthalate) modified with multifunctional epoxy based additives, Polymer 41 (2000) 5809.

[23] S. Japon, Y. Leterrier, J.-A.E. Manson, Recycling of poly(ethyleneterephthalate) into closed-cell foams, Polym. Eng. Sci. 40 (2000) 1942.

[24] B.H. Guo, C.M. Chan, Chain extension of poly (butylene terephthalate) by reactive extrusion, J. Appl. Polym. Sci. 71 (1999) 1827.

[25] N.W. Thomas, F.M. Berardinelli, R. Edelman, Polycarbodiimide modification of polyesters for extrusion applications, US Patent: US 4,071,503, 1978.

2015 International Conference on Smart Technologies and Management for Computing, Communication, Controls, Energy and Materials (ICSTM), Vel Tech Rangarajan Dr. Sagunthala R&D Institute of Science and Technology, Chennai, T.N., India. 6 - 8 May 2015. pp.532-537.

A Step Forward in Précising Building Roof Top Areas for Solar PV Installations

Akshaya Tripathi[1], Jasmeen Snadhu[2], Kartik Arunachalam[3] and **Saurabh Biswas[4]**

[1,2]M. Tech, Energy Systems, [3]Research Fellow, R&D
[4]Assistant Professor, Electrical, Power and Energy
University of Petroleum and Energy Studies, Energy Acres, Dehradun, India

***Abstract*— Solar Photo Voltaic (SPV) systems are expected to become one of the most ideal renewable energy resources in India which can be implemented in large scale across different states. This paper presents in-depth investigation of various tools available for the assessment of building rooftops. The gaps in these tools have analyzed in detail. The pressing need of developing a new user friendly tool has been substantiated in this paper. The features and parameters which should be included in the new software/tool have been deliberated in detail. Various formulae and the procedure which need to be programmed in the development of new software have also been discussed in detail. The findings presented in this paper are expected to provide a pathway forward for precise building rooftop area calculations leading to efficient space utilization and subsequent environment benefits.**

***Keywords*— Rooftop Photovoltaic Potential, Accurate building roof area, Geographical Information System, Solar Energy**

I. INTRODUCTION

The rapid increase in population levels and improving living standards has resulted in drastic increase of energy consumption. With swelling environment concerns the need of tapping renewable energy has become extremely important. Slow and steadily renewable energy is shifting from fringe stages to mainstream providing pathways for sustainable development. Renewable energy is gaining importance and getting more recognition than previously; due to its ability of mitigating climate change, creating energy independence from fossil fuels and improving health services by combating air pollution. There is an increasing focus on the progress of solar energy in a developing country like India due to the aggregation of reasons like limited conventional energy reserves, their local environmental and social impacts, energy security, climate change and energy access. As part of the National Action Plan on Climate Change (NAPCC), the Jawaharlal Nehru National Solar Mission (JNNSM) was initiated [1].

There has been a great desire to better understand the maximum potential of clean technologies. Numerous methods and approaches have been developed to make informed decisions. Of all the available resources, methods and approaches the open source software tool for the estimation of photovoltaic solar capacity leads the race. The visual representation of rooftop solar photovoltaic power capacity can be captured in this particular technology. But there have been certain barriers which have prevented this technology to create a revolution due to its non-user friendly format. The common prevailing methods for assessing suitable building rooftop areas can be categorized into three types which area assumption of building roof area ratio per capita, establishment of correlation between the population density and roof area which is also aided by geographic information systems [2].If the solar photo voltaic systems are designed and installed in an efficient manner, it can help reap a heap of environmental benefits [3].

There is an urgent need for developing an open source software bases tool which can evaluate accurate and precise area as per the given coordinates of the boundary itself. The software needs to be designed in such a way that the user can input the area as per the needs rather than depending on the satellite images which are obtained at ten kilometer height levels. The satellite based software is not able to differentiate between concrete area and tin sheet covered area creating an ambiguity in the user's mind. In this application there is inbuilt calculation for obstacle analysis (which is constructed in between the roof) so that exact area can be extracted by subtracting obstacle area and shadow created by that obstacle. This tool shall also be helpful for estimating rooftop solar PV installation potential of the semi-urban or irregular cities.

II. ASSESSMENT OF PREVAILING TOOLS

A. Geographic Information System (GIS) Based Method

Several empirical solar irradiation models have been augmenting by use of geographical information system

Fig. 1. Depiction of TERI's Mapping Tool

tools. The quick processing associated with GIS platforms allows for combination of solar radiation models and additional concern of the effects of topography on incoming solar irradiance. GIS tool helps user to examine the temporal and spatial variability of incident solar irradiance on a landscape level. One of the original GIS-based model is Solar Flux. It was employed in the ARC/INFO platform. Simulation of influence of shadow patterns on direct insolation at specific interval through time is also happened in this tool. It uses the input of a topographic surface with elevation values, latitude, time interval for calculation, and atmospheric conditions. Direct radiation flux, duration of direct radiation, skyview factor and diffuse radiation flux for each surface location is the output of this tool.

GIS-based method is commonly used for the valuation of suitable space for rooftop solar photovoltaics. GIS-based methods involve 3-D models, which help in the identification of solar availability or shadow analysis on buildings. For estimation of total solar energy generation potential, generally 3-D models are used which are generated from orthophotography or Light Detection and Range (LiDAR) data, along with slope, building structure, and orientation data. For the estimation of rooftop solar power potential for solar cities; The Energy and Resource Institute (TERI) is presently developing first-of-kind cloud-based Open Source Web-based -GIS Tool [4]. The importance of this tool is to estimate the rooftop solar photovoltaic power potential for Chandigarh city. The following steps were undertaken in order to assess the solar potential by the TERI authorities.

- Base map preparation
- Building rooftop Data
- Analyze rooftop solar information
- Compute rooftop area
- Estimate Solar Power Potential

The following Figure 1 depicts the above mentioned processes in a nut shell.

B. PV Watts Calculator by NREL

National Renewable Energy Laboratory (NREL) established a web application PVWatts Calculator that estimates the electricity production of a rooftop grid-connected or ground-mounted photovoltaic system based on a few simple inputs. In order to obtain result from this calculator, we need to provide statistics about the system's location, basic design parameters and system economics. PVWatts calculates estimated values for the system's annual and monthly electricity production and detailed cost benefit analysis of electricity. For estimation of energy production and cost of energy of a grid-connected photovoltaic system using

Solar resource data for locations throughout the world PVWatts calculator can be accessed online. This empowers small building owners, homeowners, constructors and installers to develop initial estimates of the cost and performance of potential photo voltaic installations [5].

PVWatts simulations require hourly solar resource data which describe the solar radiation and meteorological conditions at the system location. PVWatts use typical year

weather data files to represent the long-term solar resource at the required location [6]. The calculator automatically identifies appropriate data for the required system based on the address provided by the user for its location [7] [8]. For a system location outside of the United States, PVWatts reads solar resource data from one of the following databases, depending on the location:

- Solar and Wind Energy Resource Assessment Programme (SWERA)
- The ASHRAE International Weather for Energy Calculations Version 1.1 (IWEC)
- Canadian Weather for Energy Calculations (CWEC)

C. Google Earth Method

Building roof area can be calculated using the online available tool of Google Earth. Manual identification of building rooftop and sampling method is included in this study for the estimation of rooftop solar photovoltaic space. The commonly used buildings for sampling are row houses, town houses, high-rise buildings, detached and semi-detached households [9].

D. Gaps in Existing Tools

After reviewing above existing tools we analyze that the GIS base tool could not justify the demand of common user to evaluate the small-scale modeling of the rooftop solar photovoltaics. Tools only provide us with remote geo-referencing satellite images of large areas which are not precise for small areas because of the shadow, cloudy weather, clearness index, etc. The above tool only maps the solar cities which are planned and organized like Chandigarh. Other tool PVWatts only estimates the economic portion, the incentive part, sizing of installation, and preferable technology.

III. NEW TOOL – THE PATHWAY FORWARD

In order to minimize the gaps between the tools and users; open source software bases tool should be made which can be user driven. This tool should be able to accurately and precisely identify area for the building rooftop available using the given coordinates of the boundary by the user itself. In order to minimize and fulfill of these gap between the tools and the user. An open source software base tool should be made which can be user driven. This tool should be able to accurately and precisely identify area for the building rooftop available using the given coordinates of the boundary by the user itself. Utilizing the user's knowledge of building roof; an application needs to be inbuilt for the calculation of obstacle analysis (which is constructed in between the roof) so that exact area can be extracted by subtracting obstacle area and shadow created by that particular obstacle. This tool will be extremely helpful for estimating rooftop solar photovoltaic installation potential of the semi-urban or irregular cities. The following equations and process will help in the estimation of building rooftop solar potential:-

- User's Input of Longitude, Latitude Angle and Altitude of the particular site
- In addition to above inputs the user should also enter the edge points of the building rooftop
- The area shall be extracted from the Google Earth software
- The following parameters need to be analyzed in order to assess the solar potential of the site
  - Declination Angle

    $\delta = (23.45[360/365\ ]*(284+n)])$ (1)

    where, n is the particular day of the year
  - Compute Local Apparent Time(t_s) in hours

    t_s = Standard Time ± 4 (Standard Time Longitude – Longitude of Location) + (Equation of time correction) (2)
  - Computing equation of time (E)

    E=229.18[0.000075 + 0.001868 Cos(B) – 0.032077 Sin(B) – 0.014615 Cos(2B) – 0.04089 Sin(2B)]
  - Where B = (n-1)[360/365] (3)
  - Compute Hour angle

    ω = [ts -12:00]*15 (always +ve) (4)
  - Calculate the Angle of Incidence (θ)

    Cos θ = (Sinδ Sinϕ Cosβ) + (Sinδ Sinβ Cosϕ CosϒY) + (Cosδ Cosϕ Cosω Cosβ) – (Cosδ Sinϕ Sinβ Cosω CosϒY) – (Cosδ Sinω Sinβ SinϒY) (5)

    Where, Φ is Latitude Angle of building roof, ϒ is Azimuth angle, ω is hour angle and β is the slope angle.
  - Work out the day length = [2/15]*(ω) (6)
  - Find Sunrise time = 12 – [1/15 Cos-1(-tanΦ tanδ)]
  - Sunset time = 12 + [1/15 Cos-1(-tanΦ tanδ)] (7)
  - Compute the Air Mass (A.M.) = (1/Cos θ), intensity of light is indirectly affected by air mass
  - Direct radiation(ID) can be calculated through:-
  - ID= 1.353[(1- (Air Density * Altitude)*0.7AM^(0.678)+ (Air Density * Altitude)]

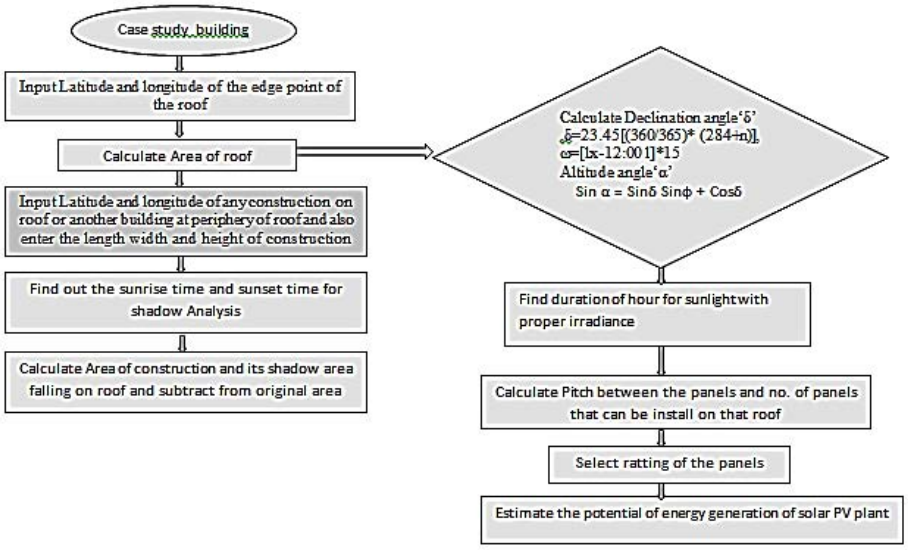

Fig. 2. Flow Chart Depicting the Process of Solar Potential Calculation [1]

- During clear days the diffuse radiation is ten percent of the direct component; therefore global radiation(IG) = 1.1*ID

The above mentioned process has been depicted in the below Figure 2 to have a clear understanding of the process. The Figures 3 and 4 depict the calculation of the building's rooftop area using Google earth via the polygon tool.

IV. Calculate Energy Generation

The main advantage of developing this tool user can estimate the power potential of its own roof. User enters the coordinates of the edge points of the roof so that an polygon is formed between these coordinates.

No. of Coordinates	Latitude	Longitude	Rating of Panels	Total area(m²)	Orientation of roof	Area
4	30.413854	77.970019	300	209.5373	14.84459458	184.3928
	30.413878	77.969914				
	30.414039	77.970066				
	30.414014	77.970161				

Area between the coordinates =209.5373 m^2

Shadow Analysis

User input the coordinates and height of the obstruction if present at periphery of roof or on the roof itself. This tool subtracts the shadow area from the total area of roof.

No. of Obstacle at periphery	Latitude of Obstacle	Longitude of Obstacle	Length of obstacle(m)	width of obstacle(m)	Height of obstacle(m)	Area(m²)	Area Of Shadow by any obstacle on roof periphery(m²)
1	30.413862	77.970013	2	2	10	23.77438	23.77437617
						0	
						0	
No. of Obstacle on roof	**Latitude of Obstacle**	**Longitude of Obstacle**	**Length of obstacle(m)**	**width of obstacle(m)**	**Height of obstacle(m)**	**Area(m²)**	**Area Of Shadow by any obstacle on roof (m²)**
1	30.413972	77.97004	1.1	1.1	1.34	7.06567	7.065670114
						0	

Area of shadow by any obstruction = 23.77 + 7.65

The panels which have to be installed on roof should be facing toward due south so considering that the orientation of the roof should be known to user. This tool has the capability of finding the orientation of roof.

Due to orientation of roof some area can't be utilize by the user.

Orientation percentage reduction in area

0° - 15°	0% - 11%
15° - 30°	11% - 19%
30° - 45°	19% - 25%

Orientation of roof = 14.844°

Reduction in area = 25.14 m^2

After analyzing all factors we can calculate the useful area which is utilized for generating energy.

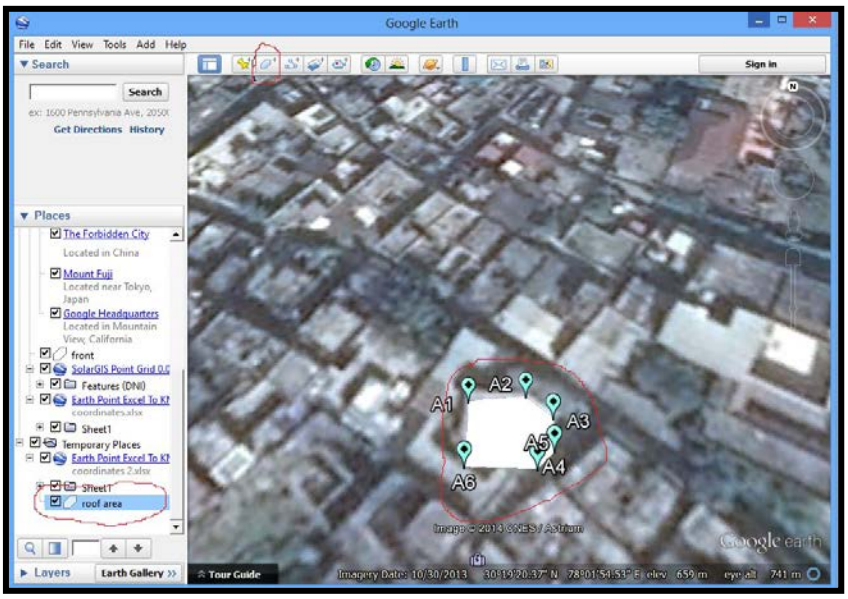

Fig. 4. Google Earth Snapshot for Mapping Building Roof Areas with Different Parameters

Useful Area = 209.5373 – (23.77 + 7.65 +25.12)

= 153.552 m^2

Monthly meteonorm data can be extracted from the METEONORM Software by this tool.

Selection of panel ratting which can be installed on the roof and pitch between the two panels should be calculated so that user came to know about the number of photovoltaic panels used.

Panel Ratting = 300Wp

No. of Panels = 45

Useful Area (m^2)	Monthly Eergy Generation (kWh)	Total Energy Generation (kWh/year)
153.5527878	1253.517861	22446.78646
	1248.077492	
No. of panels	1884.635896	Plant Capacity(KW)
44.18245961	2343.050915	11.60640458
	2716.65017	
	2164.041632	
	1635.62852	
	1765.582144	
	1854.919246	
	2231.207401	
	1857.141459	
	1492.333726	

Using this tool user came to know about the potential of energy can be generated by installing rooftop solar photovoltaic system.

Annual Energy generation = 22446.78 kWh

V. CONCLUSION

An in-depth analysis was carried out in order to investigate the availability of different tools and software for efficient calculation of building rooftop areas. It was found that numerous software's are present but aren't users friendly, thereby substantiating the fact that the development of open source software based tool for rooftop solar photovoltaic installation potential which can be user friendly is a necessity for continuing the rapid development in the field of solar energy sector in India. It should be capable of evaluating the accurate and precise area as coordinate of the boundary shall be fed into the system by user. Expending the user's own knowledge regarding the feasible area on the building roof, the appropriate area available can be easily obtained. Hence this tool is expected to decrease the problem of accuracy for small areas because of shadow, cloudy weather and clearness index. This tool will also be helpful for estimating rooftop solar photovoltaic installation potential of semi-urban and irregular cities. This is expected to empower the user with a self-help tool to assess the installation potential solar photovoltaic on its own rooftop. User can easily understand the application and working of this tool as it is based on geometry rather than mapping.

REFERENCES

[1] G. Shrimali and S. Rohra, "India's solar mission: A review," Renewable and Sustainable Energy Reviews, vol. 16, pp. 6317-6332, 2012.

[2] F. Azadian and M. Radzi, "A general approach toward building integrated photovoltaic systems and its implementation barriers: A review," Renewable and Sustainable Energy Reviews, vol. 22, pp. 527-538, 2013.

[3] J. Peng and L. Lu, "Investigation on the development potential of rooftop PV system in Hong Kong and its environmental benefits," Renewable and Sustainable Energy Reviews, vol. 27, pp. 149-162, 2013.

[4] N. Lukač, D. Žlaus, S. Seme, B. Žalik, and G. Štumberger, "Rating of roofs' surfaces regarding their solar potential and suitability for PV systems, based on LiDAR data," Applied Energy, vol. 102, pp. 803-812, 2013.

[5] B. Marion and M. Anderberg, "PVWATTS-an online performance calculator for grid-connected PV systems," in Proceedings of the Solar Conference, 2000, pp. 119-124.

[6] R. M. a. S. O. J. Melius, "Estimating Rooftop Suitability for PV: A Review of Methods, Patents, and Validation Techniques," December, 2013.

[7] B. Marion, M. Anderberg, R. George, P. Gray-Hann, and D. Heimiller, "PVWATTS version 2–enhanced spatial resolution for calculating grid-connected PV performance," in Proceedings of the 2001 NCPV Program Review Meeting, Lakewood, CO, 2001, pp. 143-144.

[8] P. D. a. R. Margolis, "Supply Curves for Rooftop Solar PV-Generated Electricity for the United States," November, 2008

[9] S. R. Sheppard and P. Cizek, "The ethics of Google Earth: Crossing thresholds from spatial data to landscape visualisation," Journal of environmental management, vol. 90, pp. 2102-2117, 2009.

[10] N. A. Aneta Strzalka, Eric Duminil, Volker Coors, Ursula Eicker, "Large Scale Integration of photovoltaics in Cities".

Particulate Science and Technology, 33: 41–46

ISSN: 0272-6351 print/1548-0046 online
DOI: 10.1080/02726351.2014.933146

Taylor & Francis
Taylor & Francis Group

AC and DC Conductivity Studies on Lead-Free Ceramics: $Sr_{1-x}Ca_xBi_4Ti_4O_{15}(x = 0, 0.2, 0.4, 0.6, 0.8)$

GAGAN ANAND,[1] PIYUSH KUCHHAL,[1] and P. SARAH[2]

[1]*Department of Physics, University of Petroleum and Energy Studies, Dehradun, Uttrakhand, India*
[2]*Research & Development, Vardhaman College of Engineering, Shamshabad, Hyderabad, Andhra Pradesh, India*

$Sr_{1-x}Ca_xBi_4Ti_4O_{15}$ [$x = 0$, 0.2, 0.4, 0.6, 0.8] ceramics are synthesized by solid-state reactive technique. Structural analyses are done by x-ray diffraction data. Morphological studies were carried out by scanning electron microscope, and the data showed plate-like structures. To understand the conductivity mechanism, frequency and temperature dependency of AC and DC conductivity studies are carried out. The conductivity measurements are done using an impedance analyzer (Wayn–Kerr) in the temperature range 100–600°C. The frequency-dependent AC conductivity at different temperatures indicates that the conduction process follows the universal power law, and the hopping frequency shifts toward higher frequency side with increase in temperature, below which the conductivity is frequency independent. The variation of DC conductivity confirms that the ceramics exhibit negative temperature coefficient of resistance behavior at high temperature. DC conductivity values do not show any linearity with doping concentration; for a particular composition SCBT06, the DC conductivity was low.

Keywords: Bismuth, conductivity, ferroelectrics, lead free

1. Introduction

Bismuth layer-structured ferroelectrics (BLSFs) are excellent candidate materials for piezoelectric and pyroelectric sensors requiring a high stability and high operation temperature. This is owing to their high Curie temperatures, low ageing rate, and strong anisotropic electromechanical coupling factors. Due to their promising fatigue-free nature, BLSFs have attracted considerable attention (Park et al. 1999). The BLSFs have a crystal structure containing interleaved bismuth oxide $(Bi_2O_2)^{2+}$ layers and pseudo-perovskite blocks which contain BO_6 octahedron and generally formulated as $(Bi_2O_2)^{2+}(A_{n-1}B_nO_{3n+1})^{2-}$. In this notation, A represents a mono-, bi-, or trivalent ion, B denotes a tetra-, penta-, or hexavalent ion, and n is the number of BO_6 octahedron in each pseudo-perovskite block ($n = 1, 2, 3\ldots$). In literature (Chen et al. 1982; Lee et al. 1992), piezoelectric properties of a number of compounds by replacing the cations having similar structural configurations are reported. Different methods of preparation of the compounds have been suggested, viz. hot forging, hot rolling, hot extrusion, and super-plastic deformation. These methods give ceramics with grain orientations and different densities.

Address correspondence to: Gagan Anand, Assistant Professor Department of Physics, University of Petroleum and Energy Studies, via Bhidoli village, Premnagar, Dehradun, Uttrakhand, India. E-mail: ganand@ddn.upes.ac.in

Color versions of one or more of the figures in the article can be found online at www.tandfonline.com/upst.

The frequency dependence reported for the activation energy in the literature is often contradictory. According to Kuznetkova (1970) and Haberey et al. (1968), for example, the activation energies are frequency dependent, whereas, according to Volger (1954), they are not. Accordingly, the frequency dependence of activation energy poses an interesting question, and a detailed analysis on this aspect is worthwhile. The reason for such a study is that very often one tends to miss any possible dielectric anomalies if the conductivity values were too high. For example, Smolenskii et al. (1959) could not record dielectric anomalies in this compound despite the fact that it was possible to trace hysteresis loops. To understand the conduction mechanism in detail, the AC and DC conductivity studies have been carried out in the present work.

2. Experimental Method

The initial compounds $SrCO_3$, Bi_2O_3, $CaCO_3$, and TiO_2 (Sigma Aldrich Chemicals USA, 99.9% pure, AR grade) were mixed in appropriate ratios for the synthesis of the desired compound. The polycrystalline samples of $Sr_{1-x}Ca_xBi_4Ti_4O_{15}$ [$x = 0$: SBT, 0.2: SCBT02, 0.4: SCBT04, 0.6: SCBT06, 0.8:SCBT08] were prepared by the method of reactive sintering. The standard ceramic fabrication procedure was followed for the preparation. The oxide mixture, weighing 50 g, was subjected to high-energy milling in a planetary ball mill (Fritsch Pulverisette 6) at a speed of 150 rpm for 5 h. A cylindrical tungsten carbide (WC) milling jar, with a usable volume of 250 ml, filled with 50 WC balls, each of 10 mm diameters, was used for the purpose of

milling. Both vial and balls were from Fritsch GmbH Idar-Oberstein, Germany. A total of 50 g of powder was placed in the vial using water as the milling medium. The milling was stopped for 5 min after every 30 min of milling to cool down the system. During each collision, the powder particles get trapped between the colliding balls and between the ball and the inner surface of the vial and lead to smaller particle size. The particle size of the initial materials ranged from 1 to 2 μm. The mixture was stacked in a crucible and calcined in air at 800°C for 4 h and then cooled. The calcined powders were milled for a few minutes to crush any lumps that were formed during the calcinations. The calcined powders were cold isostatically compressed into the form of a cylindrical rod at a pressure of 3,000 Mpa and sintered at 1,175°C for 2 h and then allowed to furnace cool. Pellets having a diameter of 1 cm and thickness of 1 mm were cut from the sintered samples using a low-speed isomet saw. The entire sintering was done in a microprocessor-controlled furnace. The densified pellets were used for all the measurements.

The values of AC conductance were calculated from the admittance data, using the equations:

$$Y = Z^{*^{-1}} = Y' + Y'' \tag{1}$$

$$\sigma' = Y'\left(\frac{d}{A}\right) \tag{2}$$

where σ' is the real part of AC conductance having units of $(\text{ohms} - \text{cm})^{-1}$ $(ohm - cm)^{-1}$ and Y' is the real part of admittance, d being the thickness and A the surface area of the pellet. The sintered samples were used for DC conductivity measurements, conductivity being studied under both static and dynamic conditions at various temperatures varying from room temperature to 800°C using a DC conductivity meter [make marine India electronics].

3. Results and Discussion

3.1 Characterization

X-ray diffraction (XRD) plot is shown in Figure 1. XRD patterns of the compositions SBT, SCBT02, SCBT04, SCBT06, and SCBT08 are shown. The maximum intensity is observed at around 30° corresponding to (119) reflection in all the compositions which is found to be in accordance with the researchers reported earlier (Chen et al. 1982). The SEM micrographs for the compositions SBT, SCBT02, SCBT06, and SCBT08 are shown in Figure 2. The sheet grains are found in the compounds, similar to the typical morphology of BLSF ceramics (Chen et al. 1982). Thus, the strong anisotropic character is demonstrated.

3.2 AC Conductivity

3.2.1 *Variation of AC Conductivity with Temperature*

The log $\sigma_{ac}'s1000/T$ plots shown in the Figures 3(a)–(d) indicate the behavior of the samples with frequency of the applied AC frequency and temperature. At low frequencies, the conductivity increases gradually with temperature but at high frequencies, the conductivity values do not vary appreciably with the temperature up to 225°C 225^0C. Thereafter, the conductivity increases rapidly with the temperature. This is a common feature in many ceramic compounds.

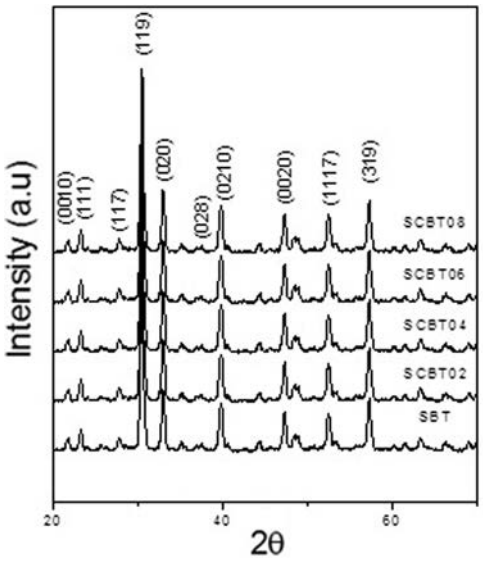

Fig. 1. Room temperature x-ray diffraction patterns for the compositions SBT, SCBT02, SCBT04, SCBT06, and SCBT08.

3.2.2 *Variation of AC Conductivity with Frequency as a Function of Temperature*

Figures 4(a)–(f) shows the AC conductivity plotted for samples SSC00, SSC04, SSC06, and SSC08 at various temperatures, respectively. For the corresponding frequency ranges, the overall values of conductivity appear to be higher by about an order. The conductivity shows an increase with the frequency, and such dependence can be expressed as

$$\sigma' = A\omega^n\sigma' = A\omega^n \tag{3}$$

In this expression, A is a constant, ω is the angular frequency $(= 2\pi f)$ and n is the exponent (Yootarou et al. 1973).

The thermal plots of AC conductivities are fitted to the general conduction activation mechanism given in Equation (7). AC conductivity activation energies for all the samples at different frequencies are reported in Table 1. Activation energies are in accordance with the values reported in the literature. As it can be seen from Table 1, AC conductivity activation energy increases with decrease in the frequency.

Here AC conductivity phenomenon corresponds to the short-range hopping of charge carriers through the trap sites separated by energy barriers of varied heights. The time constant for transition across a lower energy barrier is small compared to that across the higher ones. Therefore, the traps with low activation energy can respond only at high frequencies. At high temperatures, the energy distribution of the traps is more uniform, and the variation of the AC conductivity with frequency is low. This makes the AC conductivity versus frequency curves for different temperatures converge at high frequencies, indicating that at high frequencies the AC conduction becomes almost independent of the temperature (Mamatha et al. 2012).

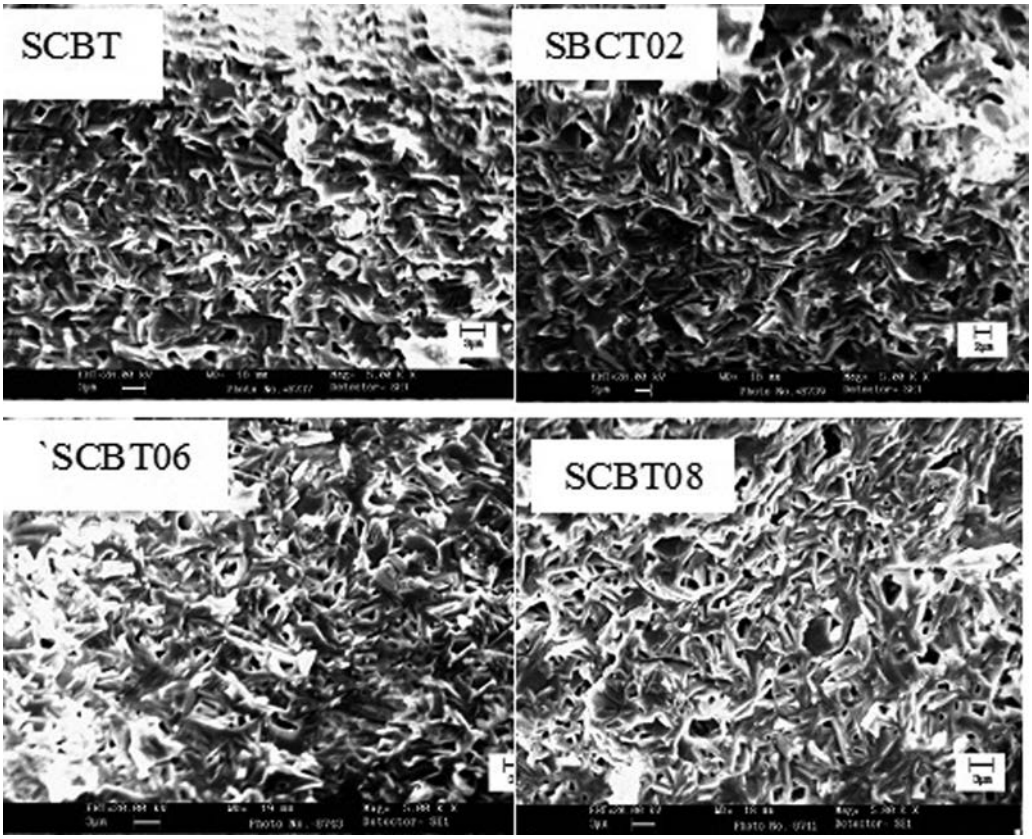

Fig. 2. SEM micrographs for the compositions SBT, SCBT02, SCBT06, and SCBT08.

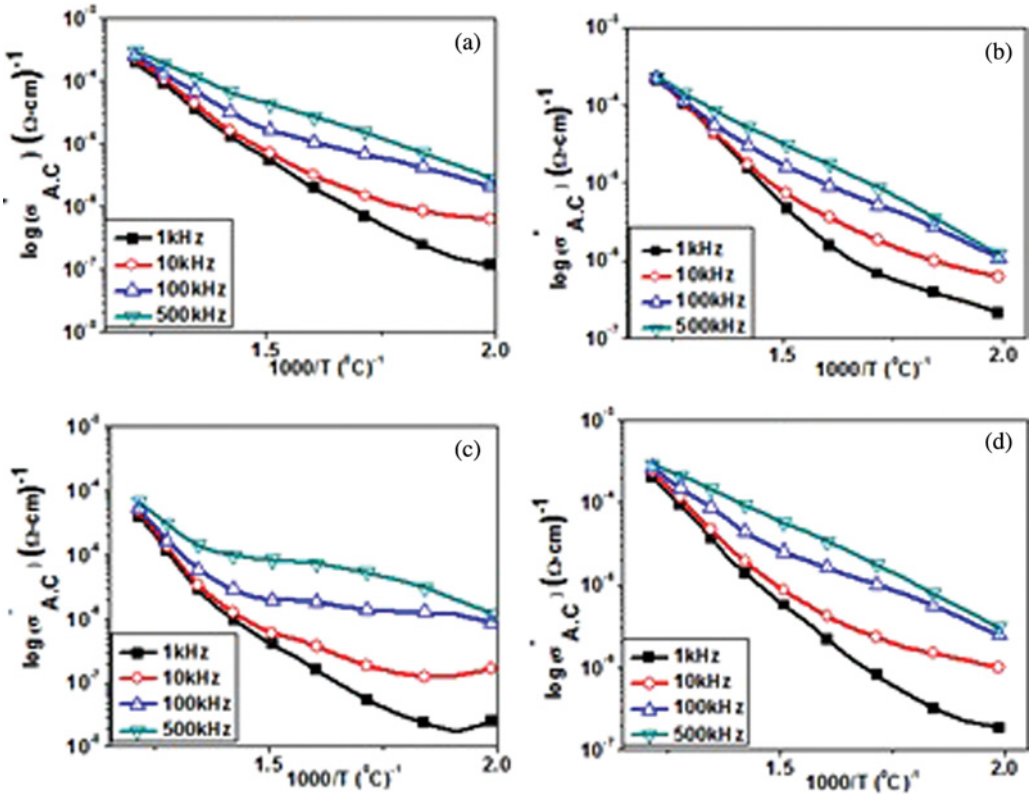

Fig. 3. log σ'_{ac} $1000/T$ for compositions (a) SBT, (b) SCBT02, (c) SCBT06, and (d) SCBT08.

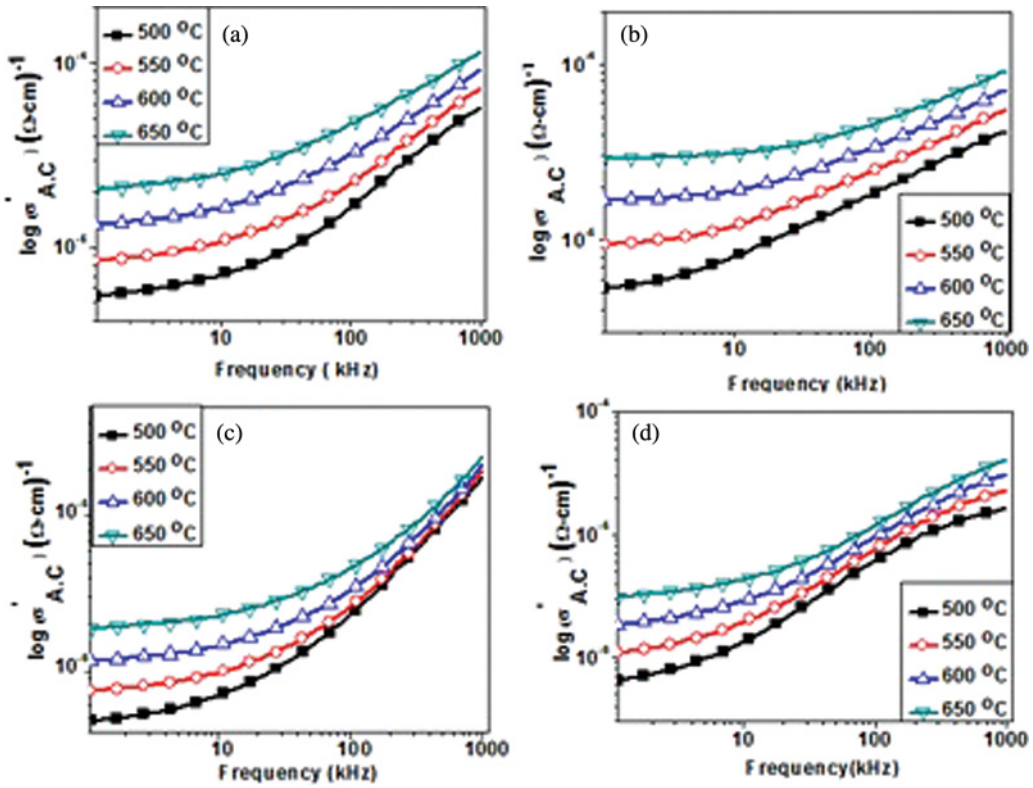

Fig. 4. Variation of function of AC conductivity with frequency at different temperatures for compositions (a) SBT, (b) SCBT04, (c) SCBT06, and (d) SCBT08.

A formalism to investigate the frequency behavior of conductivity in a variety of materials is based on the power relation proposed by Jonscher (1977).

$$\sigma' = \sigma_0 + A\omega^n \sigma' = A\omega^n \tag{4}$$

σ' and σ_0 are the AC and DC conductivities, respectively. The term $A\omega^n$ contains the AC dependence. The exponent n is a function of temperature and frequency and lies between 0 and 1. The polarization process is characterized by the exponent n. Usually, the interaction between the neighboring dipoles decreases with decrease in temperature, and consequently the exponent n increases. The frequency variation of AC conductivity plots is shown in Figures 4(a)–(f). In the higher frequency regions, the electrical conductivity is high. This dispersion in the conductivity values can be explained on the basis of conduction mechanisms in a disordered solid. At high frequencies, the electrical conductivity increases by hopping of the charge carrier at places with high jump probability.

This increase in the electrical conductivity continues as long as the frequency of the applied field is lower than the maximum jump frequency in the solid as reported by Macedoa et al. (2003). As frequency increases, two dispersion regions are found for all temperatures (Mamatha et al. 2013). Here the results do not follow the simple power law. The following power relation is used to explain the frequency dependence of AC conductivity (Barranco et al. 1998).

$$\sigma(\omega) = \sigma_0 + A_1\omega^{n_1} + A_2\omega^{n_2} \tag{5}$$

The term σ_0 corresponding to the translational hopping gives the long-range electrical transport (i.e., DC conductivity) in the long-range limit (Rout et al. 2009). The terms n_1 and n_2 are exponents corresponding to low- and high-frequency region. Similarly A_1 and A_2 are constants corresponding to the low- and high-frequency regions: slopes drawn to the experimental data in the low- and high-frequency region will intersect at a point and the frequency responding to this point is called relaxation frequency.

A small amount of oxygen loss occurs since the compounds have been sintered at high temperatures. According to the Kroger–Vink notation (Kroger et al. 1956)

Table 1. Activation energies for AC and DC conduction in various ceramics

Sample	Activation energy			
	DC (eV)		AC (10 kHz) (eV)	
	350–500°C	500–650°C	350–500°C	500–650°C
SSC00	0.56	0.75	0.41	0.74
SSC01	0.63	0.82	0.56	0.86
SSC02	0.72	0.74	0.62	0.75
SSC04	0.81	0.88	0.53	0.79
SSC06	0.82	1.07	0.49	0.65
SSC08	0.88	1.21	0.65	1.02

$$V_o = V_o' + e' \tag{6a}$$

$$V_o' = V_o'' + e' \tag{6b}$$

where the oxygen vacancy with two effective negative charges is V_o, V_o' is single ionized oxygen vacancy, V_o'' is doubly ionized oxygen vacancy, and e' is the electrons released. The electron released in the above reaction may be captured by Ti ions present in the compounds. The reason for the capture of electrons by Ti is due to its unstable valency ($Ti^{4+} \rightarrow Ti^{3+}$). This polaronic conduction of $3d$ electrons on Ti^{3+} ions takes place at low temperatures (Upadhyaya et al. 1998). Equation (3) describes different contributions to conductivity. The high-frequency dispersion is associated with grains having smaller capacitance value and the low-frequency dispersion is associated with grains boundaries having larger capacitance value (Barramco et al. 1998). The temperature at which the grain boundary resistance dominates over grain resistance is represented by a change in the slope of AC conductivity with the frequency. The frequency at which the slope change takes place is known as the hopping frequency, which corresponds to polaron hopping of charged carriers (Li et al. 2003). The hopping frequency shifts to higher frequency with the temperature. The charged species which are accumulated at the grain boundaries have enough energy to jump over the barrier with rise in temperature and thereby increase the conductivity (Sen et al. 2007; Rout et al. 2009).

3.3 DC Conductivity Measurements

Figure 5 shows the Arrhenius plot for conductivity (DC) measurements in the ranges specified above for the samples SSC00, SSC02, SSC06, and SSC08, respectively. The samples used for this experiment were unpoled one. Initially, the conductivity of the sample decreases from room temperature up to about 170°C, and above that temperature, the conductivity monotonously increases with the temperature. The activation energies have been determined in various temperature regions using the equation.

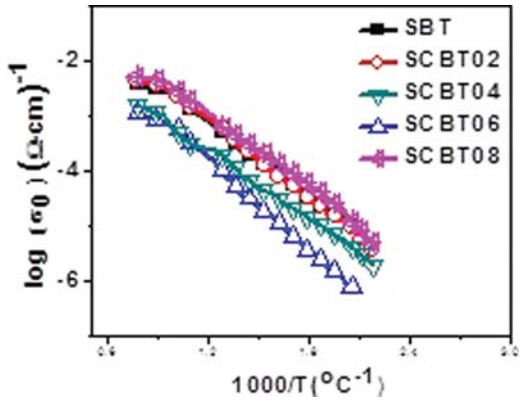

Fig. 5. Variation of DC conductivity as a function of temperature for the compositions SBT, SCBT02, SCBT04, SCBT06, and SCBT08.

$$\sigma = \sigma_0 e^{\frac{-E}{KT}} \tag{7}$$

where σ_0 is the DC conductivity, E is the activation energy, T is the absolute temperature, and K is the Boltzmann constant. The conductivity plot is divided into two region broadly and the activation energy was calculated from the slope of the plot in each region was calculated by the method of least squares. DC conductivity values do not show any linearity with doping concentration. It has been observed that for a particular sample SSC06, the DC conductivity is low.

The conductivity graph shows that change in the slope occurs around 550°C. Probably, this is due to the dielectric transition occurring at this temperature range. The change in the slope of the curve will reflect a change in the conductivity phenomenon in paraelectric and ferroelectric regions. The activation energy values calculated from the slope of Arrhenius plots are listed in Table 1. The change in the activation energy is due to the lattice adjustment at the phase transition from ferroelectric to paraelectric regions. It is observed that the DC activation energy values at lower temperature regions are low compared to the activation energy at higher temperature regions. This may be due to the high energy required to overcome thermal fluctuations by the charge carriers at higher temperatures. At higher temperatures, the increased activation energies increase vacancy concentration as well as the motion of these vacancies. Hence, the conductivity is high at higher temperatures.

It is known that DC conduction is due to the movement of oxygen vacancies in all the layered compounds. In these samples, the conduction is through a–b plane, and the mobility of oxygen vacancies is affected by the distortion of all these planes due to various cations present in this layer. The conductivity at lower temperatures in the sample is due to the loss of oxygen that occurred during the sintering. The difference in activation energies between the two regions could be approximately equal to the energy required for the creation of oxygen vacancies.

4. Conclusions

The polycrystalline $Sr_{1-x}Ca_xBi_4Ti_4O_{15}$($x = 0$, 0.2, 0.4, 0.6, 0.8) ceramics were prepared successfully by high-energy mechanical milling. XRD pattern analysis showed that all the ceramics crystalize in perovskite-type orthorhombic structure. AC conductivity in the above compositions results from the short-range hopping of charge carriers through the trap sites separated by energy barriers of variable heights. The negative temperature coefficient resistance character is revealed for all the ceramics. The temperature-dependent AC conductivity indicates that the conduction process is thermally active process. The activation energies suggest that oxygen vacancies or defects are responsible for long-range transmission of charge carriers. It has been observed that for a particular sample SSC06, the DC conductivity is low.

References

Da-Ren, C., and G. Yan-Yi. 1982. The dielectric and piezoelectric properties of ferroelectric ceramics Bi_4(Pb,Sr)Ti4O_{15} with Bi-layer structure. *Electronic Elements and Materials* 25:1–6.

Haberey, F., and H. P. G. Wijn. 1968. Effect of temperature on the dielectric relaxation in polycrystalline ferrites. *Physica Status Solidi* 26(1): 231–240.

Jonscher, A. K. 1977. The 'universal' dielectric response. *Nature* 267:673–679.

Kroger, F. A., and H. J. Vink. 1956. Relations between the concentrations of imperfections in crystalline solids. *Solid State Physics* 3:307–435.

Kuznetsova. 1970. Frequency dependence of the activation energy for the conductivity in a ferrite. L. A. *Soviet Physics Journal* 2:115–121.

Lee, J. K., C. H. Kim, H. S. Suh, and K. S. Hong. 2002. Correlation between internal stress and fatigue in $Bi_{4-x}La_xTi_3O_{12}$ thin films. *Applied Physics Letters* 80:3593–3598.

Li, Y., M. Liu, J. Gong, Y. Chen, Z. Tang, and Z. Zhang. 2003. Grain-boundary effect in zirconia stabilized with yttria and calcia by electrical measurements. *Materials Science and Engineering: B* 103:108–114.

Macedoa, Z. S., Martinez, A. L., and Hernandes, A. C. 2003. Characterization of $Bi_4Ge_3O_{12}$ single crystal by impedance spectroscopy. *Materials Research* 6(4): 577–581.

Mamatha, B., and P. Sarah. 2012. Dielectric, ferroelectric, piezoelectric and impedance study of lead-free ceramic $SrBI_4Ti_{3.975}Zr_{0.025}O_{15}$. *Journal of Advanced Dielectrics* 2(4): 1250023-(1–9).

Mamatha, B., M. B. Suresh, and P. Sarah. 2013. Frequency and temperature dependence of electrical properties of zirconium and neodymium substituted $SrBi_4Ti_4O_{15}$ ceramics. *Ferroelectrics* 445: 51–66.

Park, B. H., B. S. Kang, S. D. Bu, T. W. Noh, J. Lee, and W. Jo. 1999. Lanthanum-substituted bismuth titanate for use in non-volatile memories. *Nature (London)* 401:682–684.

A. Peláiz-Barranco, A., M. P. Gutiérrez-Amador, A. Huanosta, and R. Valenzuela. 1998. Phase transitions in Ferrimagnetic and ferroelectric ceramics by ac measurements,. *Applied Physics letters* 73(14):2039–2041.

Rout, S. K., A. Hussain, E. Sinha, C. W. Ahn, and I. W. Kim. 2009. Electrical anisotropy in the hot-forged $CaBi_4Ti_4O_{15}$ ceramics. *Solid State Science* 11: 1144–1149.

Sen, S., P. Pramanik, and R. N. P. Choudhary. 2007. Effect of Ca-additions on structural and electrical properties of $Pb(SnTi)O_3$ nano-ceramics. *Ceramics International* 33(4): 579–589.

Smolensky, G. A., V. A. Isupov, and A. I. Agranovskaya. 1959. A new group of ferroelectrics (with layered structure). *Soviet Physics Solid State* 1(1): 149–150.

Upadhyaya, S., A. K. Sahu, D. Kumar, and O. Prakash. 1998. Probing electrical conduction behavior of $BaSnO_3$. *Journal of Applied Physics* 84(2): 828–832.

Volger, G. 1954. Further experimental investigations on some ferromagnetic oxidic compounds of manganese with perovskite structure. *Physica 20*, 1(6): 49–66.

Yootarou, Y., and S. Minorou. 1973. High frequency conductivity in cobalt-iron ferrite. *Japanese Journal of Applied Physics* 12(7): 998–1000.

An Automatic System for the Detection of Optic Disc and Pathologies in Retinal Images

Priyanka Kirsali*, K. Sambasivarao* and Pankaj Badoni†

* II M.Tech(Artificial Intelligence and Artificial Neural Networks),
Centre for Information Technology, University of Petroleum and Energy Studies,
Dehradun, India, Email:k.sambasivarao222@gmail.com
† Assistant Professor, Center for Information Technology,
University of Petroleum and Energy Studies, Dehradun, India, Email:pbadoni@ddn.upes.ac.in

***Abstract*—There are an incredibly large number of undiagnosed Diabetic patients who are unaware of their disease, placing them at a greater risk of Diabetic Retinopathy. As there is no cure or method to prevent it, early detection of symptoms benefits in giving proper treatment. So there is a need for developing a medical system for automatic screening of Diabetic Retinopathy. This paper demonstrates a complete framework for the detection of bright as well as dark lesions in Retinopathy images. The Optic Disc is localized and segmented out from the color fundus images after some pre-processing steps such as filtering and local contrast enhancement. The resulting images are segmented using Fuzzy C-means clustering for the detection of exudates regions. For the detection of hemorrhages, the vascular structure is segmented out from the images following illumination correction. Then the hemorrhages are detected based on background estimation technique. The algorithm was tested and evaluated on two datasets namely DIARETDB0 and MESSIDOR. The proposed methodology illustrated an accuracy percentage of 99.6 for the detection of Optic Disc, 96 for Exudates and 87 for Hemorrhages.**

Keywords: Fuzzy C-means, Optic Disc, Gray-Scale Morphology, Vascular Segmentation, Background Estimation.

I. Introduction

Diabetes has turned in a great health threat worldwide in a brief period. According to the World Health Organization (WHO)[1], the prevalence of diabetes is estimated to increase to 366 million in 2030; it will represent the 4.4 percent of worldwide population. The diabetes may cause abnormalities in the retina (diabetic retinopathy), kidneys (diabetic nefropathy), and nervous system (diabetic neuropathy)[2]. The diabetic retinopathy is a microvascular complication of diabetes, causing abnormalities in the retina, and in the worst case, blindness. About 10,000 diabetic people worldwide lose the vision each year. Typically there are no salient symptoms in the early stages, but the number and severity predominantly increase in time. There is evidence that retinopathy begins its development at least 7 years before the clinical diagnosis of type 2 diabetes. If the diabetic retinopathy is not detected and the patient does not receive appropriated treatment it is very likely that glaucoma will be followed.

The diabetic retinopathy typically begins as small changes in the retinal capillaries. The smallest detectable abnormalities, microaneurysms (MA), appear as small red dots in the retina and are local distensions of the weakened retinal capillary. Due to these damaged capillary walls, the small blood vessels may rupture and cause intraretinal haemorrhages (HA). In the retina, the haemorrhages appear either as small red dots similar to microaneurysms or larger round-shaped blots with irregular outline. The diabetic retinopathy also increase the permeability of the capillary walls which results in retinal oedema and hard exudates (HE). The hard exudates are lipid formations leaking from the weakened blood vessels and appear yellowish with well defined borders. If the local capillary circulation and oxygen support fail due to obstructed blood vessels, pale areas with indistinct margins appear in the retina. These areas are small microinfarcts known as soft exudates (Se). Intraretinal microvascular abnormalities (IRMA) and venopathy are signs of a more severe stage of diabetic retinopathy, where intraretinal microvascular abnormalities appear as dilation in the capillary system and venopathy as shape changes in artery and veins. An extensive lack of oxygen and obstructed capillary in the retina lead to the development of new fragile vessels. These new vessels attempt to grow towards the suffering tissue to supply nutrition and oxygen. However, the new vessels are fragile and tend to grow into the space between the retina and vitreous humour, or directly to the vitreous humour, which can lead to preretinal haemorrhage and a sudden loss of vision. The growth of these new vessels is called neovascularisation. The fundus image showing all the abnormalities are shown in Fig. 1.

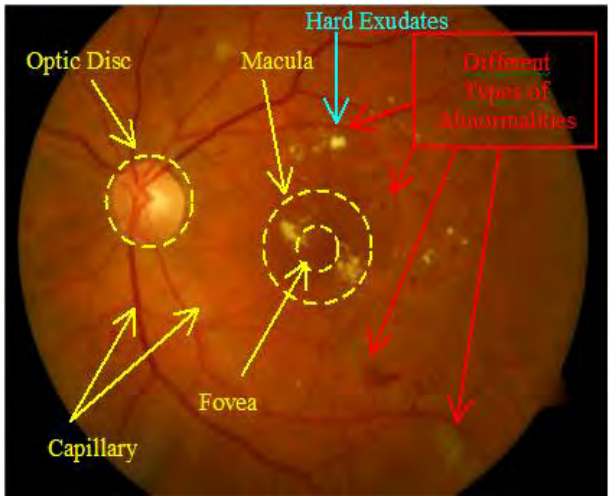

Fig. 1. Retinal fundus image with abnormalities

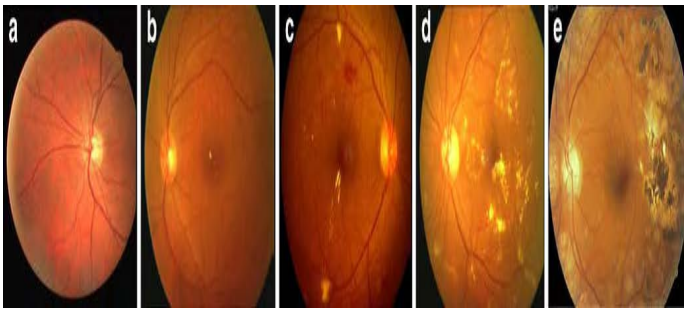

Fig. 2. Typical fundus images: (a) normal (b) mild DR (c) moderate DR (d) severe DR (e) prolific DR

The severity of diabetic retinopathy is divided into two stages: non-proliferative (background retinopathy) and proliferative retinopathy. The nonproliferative DR can be further divided into mild NPDR, moderate NPDR and severe NPDR based on the presence of lesions in retina. The non-proliferative retinopathy indicates the presence of diabetic retinopathy in the eye and consist of microaneurysms, haemorrhages, exudates, retinal oedema, IRMA and venopathy [3]. The microaneurysms and especially hard exudates typically appear in the central vision region (macula) which predicts the presence of macular swelling (macular oedema). If the nonproliferative retinopathy is untreated or undiagnosed it will turn into proliferative retinopathy which is also an eye-sight threatening condition. The proliferative diabetic retinopathy may cause sudden loss in visual acuity or even a permanent blindness due to vitreous haemorrhage or tractional detachment of the central retina. This stage is considered if neovascularisation or vitreous/preretinal haemorrhage is present in the retina [3]. Fig. 2 illustrates various stages of Diabetic Retinopathy.

Retinal Image Analysis is a key element in detecting retinopathies in patients. It assists in the automatic detection of pathologies such as diabetic retinopathy (DR), macular degeneration, and glaucoma. Optic Disc (OD), macula and retinal vasculature are all important anatomical structures in the retina. The OD localization and segmentation is a crucial task in an automated retinal image analysis system. It is required as a prerequisite for the detection of exudates and also helps in macula detection, as macula is the darkest area in the neighborhood of OD. Blood Vessel Detection (BVD) is an essential step in medical diagnosis of fundus images as it aids in the diagnosis of ocular diseases.
In this paper, we have concentrated on detection of both dark and bright lesions in color retinal images. The methodologies for the detection of and extraction of Optic Disc and blood vessels are also presented. The proposed methodology for exudates detection combines computational intelligence and pattern recognition techniques. The preprocessing of retinal images are done completely in RGB color space. The pre-processed images are converted into gray scale for further detection of Optic Disc and lesions. Through this system, we can automate the preliminary analysis and diagnosis of Diabetic Retinopathy.

This paper is organized as follows: In Section II, the related work is discussed. The background knowledge about the problem domain and methodology are provided in Section III. Section IV gives the problem definition and Section V discusses about various techniques used for preprocessing. The methodology for optic disc detection is presented in section VI. Section VII gives brief overview of Fuzzy C-means clustering for detection of exudates and detection of Hemorrhages are presented in section VIII. Results and discussion are shown in section IX. Conclusion and the further possible research directions are discussed in section X.

II. Related Work

Few investigations have been found out in the field of Diabetic Retinopathy for the detection of vasuclar structures as well as lesions in Retinal Images. Sinthanayothin et al used the method of intensity variation for the detection of Optic Disc[4]. The optic discs were localized by identifying the area with the highest variation in intensity of adjacent pixels. A multilayer perceptron neural net is used for the detection of blood vessels, for which the inputs were derived from a principal component analysis (PCA) of the image and edge detection of the first component of PCA. Optic disc segmentation by the method of using level set and Gradient Vector Flow (GVF) based snake was proposed by F.Mendels et al. In GVF, an external force was defined which gave a directional field that accounted for boundary proximity[5]. T. Walter et al. presented watershed segmentation and morphological operations to detect optic disc and blood vessels in retinal images. First optic disc was localized and then the contours of the optic disc is detected by applying the classical watershed transformation. The vascular tree was detected by the application of the morphological top hat transform after preprocessing[6]. Adam Hoover et al proposed a method for optic nerve detection based on fuzzy convergence, which identified the optic nerve as the focal point of the blood vessel network. Fuzzy convergence uses the endpoints of the blood vessel segments to help find the solution. The method used the convergence of the blood vessel network as the primary feature for detection and the brightness of the nerve as a secondary method[7]. Bob Zhang et al. proposed a method for detection of OD in fundus images based on Vessel Direction Matched Filter (VDMF). After finding the OD vessel candidates, VDMF is applied and the pixel with the smallest difference is located as OD center[8]. OD localization in low-resolution fundus images was proposed by Mario Beaulieu et al, in which they used the combination of a Hausdroff-based template matching technique by a pyramidal decomposition for object tracking[9].
Exudates detection was first investigated by R. Phillips et al. In this, Global and local thresholding values were used to segment exudate lesions and reported a sensitivity percentage of 61 and 100 based on 14 images[10]. Gardner et al. proposed a neural network approach to identify the exudates in gray level images. The image was divided into squares of 30 x 30 and 20x20 pixel, based on which feature was being detected for training the ANN[11]. Osareh et al. used fuzzy C-mean for segmenting the color retinal images, followed by classification of segmented regions into exudates and non-exudates using artificial neural network classifier[12]. A Bayesian classifier has also been used to identify candidate red and bright lesions, which were subsequently classified into the right type of lesion using a supervised method[13]. Exudates are found using their high grey level variation, and their contours were determined

by means of morphological reconstruction techniques[14].
Morphological processing algorithms are the most commonly used algorithms for hemorrhage detection. A spot lesion detection algorithm using multiscale morphological processing was proposed by L. Tang et al. The algorithm was tested on 30 retinal images and achieved the sensitivity and predictive value of 84.10 and 89.20 respectively[15]. J. P. Bae et al. proposed a hybrid method for hemorrhage detection which uses a circular shaped template matching with normalized crosscorrelation for hemorrhages detection. Then these were segmented by two methods of region growing: region growing segmentation using the local threshold and adaptive seed region growing segmentation[16]. Ege et al. have made a comparitive study of various techniques for automatic analysis of digital fundus images. In their study, a Bayesian, a Mahalanobis, and a k nearest neighbor classifier were used on 134 retinal images. The Mahalanobis classifier showed the best results: microaneurysms, haemorrhages, exudates, and cotton wool spots were detected with a sensitivity of 69, 83, 99, and 80 percent respectively[17].

III. Background

A. Gray Scale Morphology

The term morphology refers to the description of the properties of shape and structure of any objects. Morphology is mathematically depicted as the operations on sets, but can be performed on two dimensional space. The images in the two dimensional space can be equivalently represented by sets in mathematical morphology. The properties of the image useful for its presentation and description can be extracted by using mathematical morphology. Also morphology is used for preprocessing as well as postprocessing of images. There must be two inputs for any morphological operation: the image to be processed and a structuring element. A structuring element is an arbitrary shaped image which is very small in size than the original image to be processed. The shape of the structuring element can be decided based on the operation to be performed as well as the objects in the original image. This structuring element acts as a moving window which will pass through all the pixels of the image and performs modification to original image based on the operation specified. The origin of the structuring element coincides the pixel of interest in the original image.
Every morphological operation can be defined as a combination of two basic operations: Dilation and Erosion. Let A be the set of pixels of original image to be processed and B be the structuring element. The dilation of image A with the structuring element B is defined as the set of all displacements z, such that B' and A overlap by atleast one element.

$$A \oplus B = \{Z \mid (B')_z \cap A \subseteq A\} \tag{1}$$

Similarly the erosion of original image A by structuring element B is the set of all points z such that B, translated by z is contained in A.

$$A \ominus B = \{Z \mid (B)_z \subseteq A\} \tag{2}$$

Every other operation in morphology is a combination of these two basic operations: Dilation and Erosion. Various operations that can be performed using morphology are Opening, Closing, Convex Hull, Thinning, Thickening etc., Morphological opening of an image A with the structuring element B is nothing but erosion of A by B followed by dilation of A by B. Similarly morphological closing can be viewed as dilation of A followed by erosion of A by the structuring element.

B. Fuzzy C-means Clustering

The main objective of any clustering technique is to divide the data into groups based on similarities among them. A cluster is basically a group of objects that are similar to each other than to the objects in other clusters. These clustering techniques are basically unsupervised methods as they do not use any prior information for categorizing the objects into groups. There are various types of clustering algorithms namely, partitioning, heirarchical, graph-theoritic methods and methods based on objective function. Fuzzy c-means clustering comes under partioning clustering category. The data used for clustering can be numerical, categoric, or a mixture of both. The mostly used similarity index used for clustering is distance norm. Simple clustering methods are based on set theory. In this case, an object can either belongs to a cluster or doesnot belong to that cluster. But in Fuzzy clustering, an object can belong to more than one cluster at a time, with various membership values. As the objects on the boundaries are not forced to come to one cluster, Fuzzy clustering is more natural than simple clustering. In fuzzy c-means clustering, the total objects are divided into c fuzzy clusters.
The objective function of Fuzzy C-means clustering is defined as:

$$J(X, U, V) = \sum_{i=1}^{c} \sum_{k=1}^{N} (\mu_{ik})^m \parallel x_k - v_i \parallel^2 \tag{3}$$

This objective function is also known as C-means functional. The algorithm basically depends on the minimization of this C-means functional. The membership function is used to calculate the membership values of object to all the clusters and is given by

$$\mu_{ik} = \frac{1}{\sum_{j=1}^{c} (D_{ik}/D_{jk})^{2/(m-1)}} \tag{4}$$

and

$$V_i = \frac{\sum_{k=1}^{n} (\mu_{ik})^m x_k}{\sum_{k=1}^{n} (\mu_{ik})^m} \tag{5}$$

This Vi basically indicates the cluster centers. For the first iteration, these values are randomly chosen based on the number of clusters, but later these cluster centers are calculated by taking the weighted mean of all the objects in every cluster, where these weights are nothing but the membership values. The Euclidean distance norm is used for measuring the similarity between two objects.

IV. Problem Definition

Diabetic Retinopathy bacame the most common disease in diabetes affected people, causing severe damage to the retina leading to blindness. Proper diagnosis can be done for diabetic retinopathy if it is detected at early stages. As the symptoms are almost invisible, it cannot be detected easily at the early stages. Many algorithms have been proposed for detecting retinal structures and lesions in fundus images, but few have attained good results. There is a lack of sophisticated screening systems for automatic detection of diabetic retinopathy by analyzing the retinal fundus images. We have developed an automatic system which will detect optic disc as well as lesions with good accuracies. As a part of our work, we have proposed a new methodology for the accurate detection of optic disc with 100 accuracy. The objectives of this work includes:

1) Accurate detection of Optic Disc
2) Detection of exudates in color fundus images
3) Blood vessel extraction and detection of hemorrhages
4) Implementation of algorithm on two different databases
5) Comparison of results with existing algorithms

V. Methodology

Following steps have been proposed to formulate the above said problem:

1) First of all fundus images are collected from two databases namely MESSIDOR database and DIARETDB1 database.
2) Each image is preprocessed using some processing techniques so that the resultant image is more suitable for further steps.
3) Then the optic disc, which is in similar color context with exudates, is detected and segmented out of the image.
4) Then bright lesions known as Exudates are extracted by applying Fuzzy C-means Clustering on the resultant image of step 3.
5) In phase II, images are preprocessed to enhance the illumination of dark regions for detection of hemorrhages.
6) Then the vascular structure is removed from the illumination corrected images.
7) Hemorrhages also known as dark lesions are extracted from the resultant image by using background estimation technique.
8) Testing of proposed algorithms on both the datasets MESSIDOR and DIARETDB1 and calculation of efficiency.

The flow chart which depicts the methodology is shown in Fig. 3.

A. Preprocessing

The color of eye fundus images have so much variation based on the iris color and patient's race. So before proceeding with the detection of optic disc and lesions, we processed the images using some preprocessing techniques to increase the clarity of image. First the image was processed with histogram equalization technique on each individual color components.

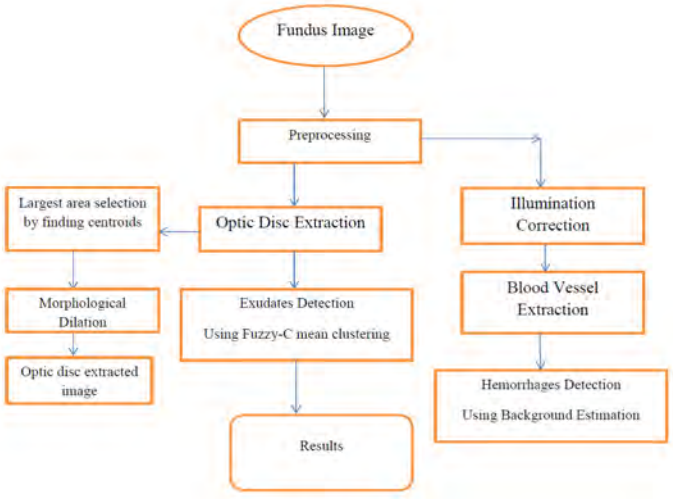

Fig. 3. Proposed Methodology

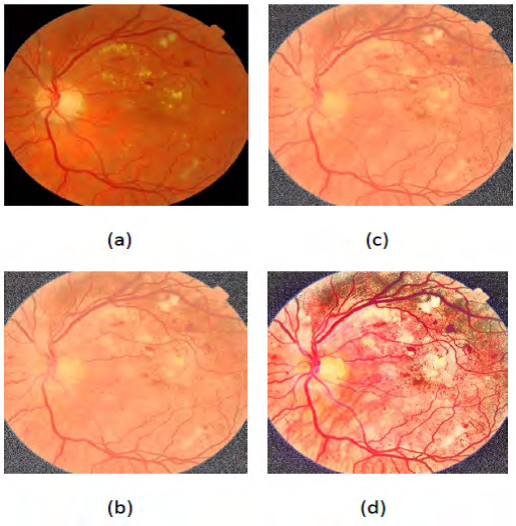

Fig. 4. Preprocessed results: (a)Original Image (b)Histogram equalized image (c)Filtered image (d)Contrast enhanced image

Later the resultant images were filtered using median filter and then the contrast of the images was enhanced. The contrast of the images was enhanced using local contrast enhancement technique for discriminating the exudates from the background. We have applied adaptive histogram equalization technique for contrast enhancement. The resultant images of preprocessing are shown in the Fig. 4.

B. Optic Disc Segmentation

For detection of pathologies in retinal images, we need to detect and extract the optic disc. For detection of bright lesions, optic disc detection plays a prominent role as it matches with the exudates color contrast. So many algorithms have been proposed for detection of optic disc so far. Automatic detection of optic disc center and extraction from the retinal images is a preliminary step for detection of exudates. Optic disc is actually a disc shaped struture in eye which has the similar color characteristics as exudates. In this paper,

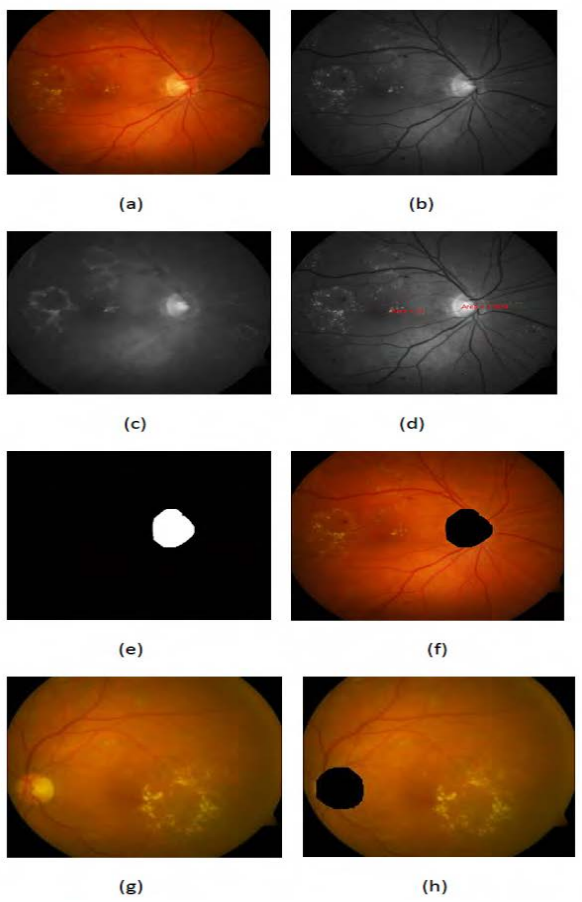

Fig. 5. Optic disc detection results: (a)Original Image (b)Green Channel (c)Result of closing operation (d)Area calculation (e)Largest area component (f)Optic disc eliminated image (g)Original image (h)Optic disc eliminated result

we have proposed an efficient technique for the automatic localization and extraction of optic disc. we have used gray scale morphology along with connected components concept to detect the optic disc. The proposed methodology is described as follows:

1) Consider the green component of the color fundus image and apply morphological closing operation to cover the regions occupied by blood vessels and to form optic disc as a single structure.
2) Convert the image into binary and find out the component which has highest connected components.
3) Calculate the centroid of the connected component to locate the center of optic disc.
4) Calculate the area of each component using regionprops.
5) Return the component with largest area as the Optic disc.

The results for the optic disc extraction are shown below in the Fig. 5. Figures (a) to (f) shows the step by step results of optic disc extraction and figures (g) and (h) shows the optic disc detection result for another image.

C. Exudates Detection using Fuzzy C-means Clustering

There are so many general segmentation algorithms that can be used for multiple variety of data, but there are some specific methods which can be used only for some specific type of data. These specific methods can show better performance then the general methods as these are customized for that particular problem domain. For efficient segmentation of retinal images, various methods have been investigated. As the retinal regions are not always having clear specific boundaries, normal hard segmentation algorithms cannot give sophisticated results. So in this paper, we proposed fuzzy segmentation algorithm for the detection of lesions in retinal images. The resultant optic disc eliminated images are segmented using fuzzy c means clustering to detect the candidate regions for exudates. The optic disc eliminated images are converted into HSI color space and the histograms of each color component are computed. Then these histograms are smoothed by using the Gaussian filter and to detect peaks and valleys.

The initial centers for the clustering are determined by observing the histogram of the Intensity channel of retinal image. The valley locations of the histogram of the intensity channel are the possible cluster centers for the initial stage of clustering. The optimal clustering will result when the local extrema of the objective function is achieved. The high values of membership are assigned to the pixels whose values are close to the centroid and low membership values are assigned to the pixels that are far from the centroid. If we take the derivative of the objective function (3) with respect to the membership function and equating to zero will give the conditions necessary for minimizing the objective function. By using this fuzzy c means clustering, the candidate regions for the exudates are identified. Then the final exudate regions are detected by measuring the similarity between the candidate regions and the optic disc. Euclidean distance is used as the similarity measure for detecting final exudate regions. The detected exudates using the proposed method are shown in the Fig. 6.

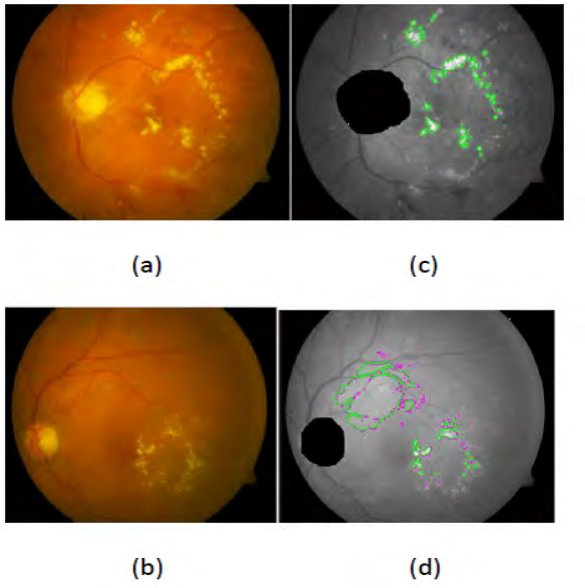

Fig. 6. Exudates detection: (a),(b)Original Images and (c),(d)Detected exudate regions highlighted

D. Blood vessel segmentation and Hemorrhages Detection

Hemorrhages are the dark regions present in the retinal images which are formed in the later stages of Diabetic Retinopathy. The color characteristics of hemorrhages are quite similar to the blood vessels. Therefore for the detection of hemorrhages, we have to detect and eliminate the blood vessels from the retinal images. The methodology for the detection of blood vessel is summarized as below:

1) 2-D Gabor wavelet is applied on the original retinal image to enhance the blood vessels.
2) Then a sharpening filter is applied to sharpen the blood vessel regions.
3) A binary mask is created by detecting the edges from the sharpened image.
4) By using the masking procedure, which assigns 1 to all pixels corresponding to blood vessels and 0 to all other pixels, the blood vessel regions are marked.
5) Morphological dilation is applied on the resultant image to get the final blood vessel portions.
6) The detected blood vessel regions are segmented out from the image by multiplying with the original image.

The results showing the blood vessels extracted are shown in the Fig. 7.

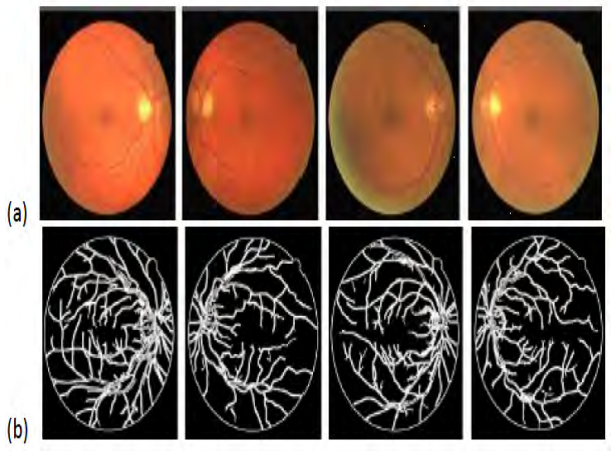

Fig. 7. Blood vessel Extraction: (a)Original Images and (b)Detected blood vessel regions

One of the major step in detecting the dark lesions is preprocessing the image and getting it well suitable for the algorithm to examine with. Here as a part of preprocessing, we tried to enhance the intensity of the image. Firstly, the image is converted into HSI color space and the intensity channel (I) is enhanced. Once the intensity is enhanced, the image is again converted back to RGB color space. For increasing the intensity of the channel, we have used the following formula. The intensity of the image is changed by a considerable factor by taking k=3.

$$I(i,j,k) = \sqrt{(1-(I(i,j,k)-1))^2} \tag{6}$$

As green channel of the image bears maximum information compared to red and blue channels, we used green channel of the image for further processing. The methodology for detection of hemorrhages are:

1) Consider the Green channel of the intensity enhanced image for detection.
2) Fill the holes present in the image by using morphological filling.
3) Then the resultant image is subtracted from the original green channel image to get a gray scale image in which we can differentiate hemorrhages from the background.
4) By applying threshold to that resultant image, we can get the detected hemorrhages.

As the blood vessels and hemorrhages have same intensity profile, we removed the blood vessels from the image before proceeding for detection. The results of hemorrhages detection is as shown in Fig. 8.

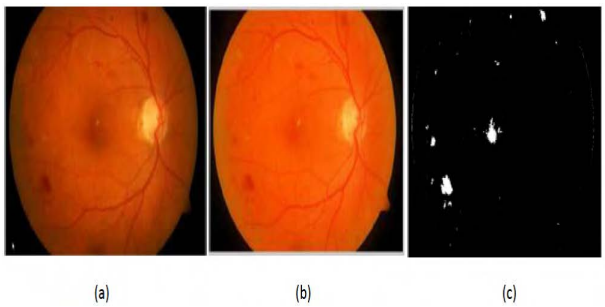

Fig. 8. Blood vessel Extraction: (a)Original Images, (b)Intensity enhanced image and (c)Detected hemorrhages

VI. Conclusion

The automatic feature extraction of optic disc and Detection of Exudates and Hemorrhages of retinal images have been implemented in the project. Optic disc was extracted using morphological operations and selection of largest blob in the retinal image. Proposed method for detecting Exudates is based on Fuzzy-C mean clustering techniques. At last Hemorrhages are detecting using connected component and hole filling technique and back ground estimation technique. The algorithm was tested on two different datasets namely, DIARETDB0 and MESSIDOR to check that the algorithm is not biased for a particular dataset. We were able to perform optic disc extraction with 99 percent accuracy , all Exudates regions were detected by the proposed method with 92 percent accuracy and the hemorrhages are detected with an accuracy percentage of 87.

References

[1] S Wild, G Roglic, A Green, R Sicree, and H King. Global prevalence of diabetes. Diabetes Care, 27(5) 1047−1053, 2004.

[2] Gordon J. Johnson, Darwin C. Minassian, Robert A. Weale, and 2nd Edition Sheila K. West. The Epidemiology Of Eye Disease. Arnold, 2003.

[3] Wilkinson, C. P., Ferris, F. L., Klein, R. E., Lee, P. P., Agardh, C. D., Davis, M., Dills, D., Kampik, A., Pararajasegaram, R., and Verdaguer, J. T. Proposed international clinical diabetic retinopathy and diabetic macular edema disease severity scales. Ophthalmology 110, 9 (September 2003), 1677 1682.

[4] C. Sinthanayothin, J. F. Boyce, H. L. Cook and T. H. Williamson, Automatic localisation of the optic disk, fovea, and retinal blood vessels from digital colour fundus images. vol. 83, no. 8, pp. 902−910, 1999.

[5] F. Mendels, C. Heneghan, and J. P. Thiran, Identification of the optic disk boundary in retinal images using active contours, Irish Machine Vision Image Processing Conf, pp. 103−115, 1999.

[6] T. Walter and J. C. Klein, Segmentation of color fundus images of the human retina: Detection of the optic disc and the vascular tree using morphological techniques, 2nd Int. Symp. Medical Data Analysis, pp. 282−287, 2001.

[7] A. Hoover and M. Goldbaum, Locating the optic nerve in a retinal image using the fuzzy convergence of the blood vessels, IEEE Trans Biomed. Eng, vol. 22, pp. 951−958, 2003.

[8] Bob Zhang and Fakhri Karray, Optic disc detection by multi-scale gaussian filtering with scale production and a vessels directional matched filter, Medical Biometrics Lecture Notes in Computer Science, vol. 6165, pp. 173180, 2010.

[9] Mario Beaulieu Marc Lalonde and Langis Gagnon, Fast and robust optic disc detection using pyramidal decomposition and hausdorff-based template matching, IEEE Transactions on Medical Imaging, vol. 20, no. 11, pp. 11931200, Nov 2001.

[10] R. Phillips, J. Forrester, and P. Sharp, Automated detection and quantification of retinal exudates, Graefes archive for clinical and experimental ophthalmology, vol. 231, no. 2, pp. 9094, 1993.

[11] Gardner, G.; Keating, D.; Williamson, T.; and Elliott, A. Automatic detection of diabetic retinopathy using an artificial neural network: a screening tool, British Journal of Ophthalmology, 80:940−944, (1996).

[12] Osareh, A.; Mirmehdi, M.; Thomas, B.; Markham, R. (2002). Classfication and Localization of Diabetic-Related Eye Disease, A. Heyden et al(EDS).ECCV 2002, LNCS 2353,pp.502−516, (2002) .

[13] H. Wang, W. Hsu, K. G. Goh, and M. L. Lee, An effective approach to detect lesions in color retinal images, in Computer Vision and Pattern Recognition, 2000. Proceedings. IEEE Conference on, vol. 2. IEEE, 2000, pp. 181186.

[14] Walter, T., Massin, P., Erginay, A., Ordonez, R., Jeulin, C., and Klein, J. C., Automatic detection of microaneurysms in color fundus images. Med. Image Anal. 11(6):555566, 2007.

[15] X. Zhang and G. Fan, Retinal spot lesion detection using adaptive multiscale morphological processing, in Advances in Visual Computing. Springer, 2006, pp. 490501.

[16] J. P. Bae, K. G. Kim, H. C. Kang, C. B. Jeong, K. H. Park, and J.-M. Hwang, A study on hemorrhage detection using hybrid method in fundus images, Journal of digital imaging, vol. 24, no. 3, pp. 394404, 2011.

[17] Ege, B. M., Hejlesen, O. K., Larsen, O. V., Mller, K., Jennings, B., Kerr, D., and Cavan, D. A., Screening for diabetic retinopathy using computer based image analysis and statistical classification. Comput. Methods Programs Biomed. 62(3):165175, 2000.

Automated Precise Liquid Transferring System

Meera C S
M.Tech Robotics Engineering
University of Petroleum and Energy Studies,
Dehradun, India
E-mail: meerachitra.s@gmail.com

Pinisetti Swami Sairam
M.Tech Robotics Engineering
University of Petroleum and Energy Studies,
Dehradun, India
E-mail: swami.sairam@gmail.com

Sunil Sunny
M.Tech Robotics Engineering
University of Petroleum and Energy Studies,
Dehradun, India
E-mail: nsunilsunny@gmail.com

Roushan Kumar
Assistant Professor,
University of Petroleum and Energy Studies,
Dehradun, India
E-mail: rkumar@ddn.upea.ac.in

Richa Singh
M.Tech Robotics Engineering
University of Petroleum and Energy Studies,
Dehradun, India
E-mail: richa62@gmail.com

Jubit Emannuel
Project lead
Miranda Automation Pvt. Ltd
E-mail: emmanueljubit@gmail.com

***Abstract*— Nearly all chemical, pharmaceutical, food processing and bio medical industries require large volumes of liquid transfer. With automation technology, the capacity, easiness and efficiency of liquid transferring systems has been greatly enhanced. Precision and accuracy in the volume of liquid dispensed plays a vital role in determining the overall efficiency of the industrial processes. An automated precise liquid transferring system targets replacement of the conventional erratic flow meters and highly expensive flow sensors used in the industries. This non-contact system enhances the overall efficiency of liquid transferring process in a very cost effective manner. The system control was implemented through Unitronics PLC and the noncontact mechanism of liquid dispensing was designed with the help of solenoid valves, relays, FRL and various other devices. The liquid was initially pressurized for a pre-defined time and the precisely dispensed by regulating the opening and closing time of solenoid valves. Provision for liquid transfer to demanded mixture tank is also provided. Flow rate of the liquid and the on- off time for solenoid determines the volume of liquid transferred. Experiment carried out for different volumes of liquid showed an accuracy of 1-2 gm. Using the PLC control and automation, the time required for the entire process of liquid dispensing was brought down to few seconds irrespective of the volume of the liquid dispensed.**

Keywords- Automation, Liquid handling system, Pneumatics, Unitronics PLC & HMI

I. INTRODUCTION

Automation using PLC has set forth a revolution in the industries. This is attributed to the higher production rates, increased output quality, highly efficient usage of raw materials and many other benefits that cannot be claimed even from the high quality workmanship by humans. The earlier developments of automation towards liquid handling were a trademark in areas relating to medical diagnostics and drug industries [1]. Advances in automating liquid handling with various degrees of accuracies were performed mainly for the purpose of protein crystallization [2], [3]. In 1980's automated liquid handling technology was implemented using plurality of pippets and syringes. Later on piezoelectric systems and solenoid based systems were developed to transfer the liquids with good precision and accuracy [4]-[5]. All these systems focused in the replacement of the manual transfer of liquid in a more efficient, accurate and speedy manner.

For industrial applications, quantity of liquid used for different process varies based on demands. In all the dispensing processes precision and repeatability ensures the overall efficiency of the process. Many of the industries resolve this problem by performing time consuming experimental calibration [6]. Recently, flow meters and flow sensors started to be used in the process to ensure the precision and accuracy in liquid dispensing. A pressure feedback loop was employed in enhancing the accuracy by bluebird dispenser in the year 2000[7]. In 2005 MEMS flow sensors were reported to be used for continuous monitoring and ensuring accuracy during liquid dispensing process [8]. Furthermore, in 2005 liquid handling in nano liters, based on embedded fluid actuators were also developed [9].

Later in 2007 and 2009, intelligent control using micro solenoid valve with integrated MEMS sensors were introduced for high precision non -contact type liquid dispensing process [7],[10]. These technologies were mainly useful for liquid dispensing in sub millimeter ranges. But liquid dispensing in food processing industries, integrating such flow meters and flow sensors poses some difficulties where the demand varies from few grams to kilograms. Dispensing the right quantity of liquid, viscous and non-viscous plays a very vital role in determining the product composition. Mostly the flow meters incorporated in the system are sometimes corrosive and mostly do not give

978-1-4799-6046-0/14/$31.00

steady readings resulting in erroneous results affecting the volume of liquid transferred. Integrating highly accurate flow sensors in the system increases the cost of the system to a great extent.

In the paper a cost effective and highly precise liquid transferring system was developed for viscous and non-viscous liquids. The pneumatics based system is fully automated and system control was implemented with PLC. Non-contact type of liquid dispensing was realized using solenoid valves and accuracy in liquid dispensing was ensured using a load cell assembly. The standalone system developed was tested against leakage and was provided with emergency control. A stand-alone system with a dedicated PLC control could replace the use of flow meters and flow sensors in liquid dispensing mainly in food industries. Moreover, the system realized is flexible enough to be incorporated in an already existing liquid transferring system wherein the control can be performed by the existing PLC .The PLC control together with the HMI module makes the system apt to be used in any of the industries performing liquid transferring processes. HMI was designed in a simple and user friendly way that enables will enable easy operation of the system by any individual. Experiments performed to dispense different volumes of liquid showed a maximum deviation of 1-2 gm from the desired volume. The intelligent control of PLC taking continuous feedback from the load cell assembly and thereby modulating the valve open and close time makes the system highly precise and accurate irrespective of liquid nature.

The paper is organized as follows: introduction to liquid transferring system described in first section. In this paper, firstly the system construction is explained in detail. In the second section, implementations of control strategies are presented. Finally experimental results are discussed to demonstrate the accuracy and precision of the system.

II. HARDWARE DESIGN

The automatic precise liquid handling system is classified into four parts: Dispensing unit, Calibration process, liquid filling process and liquid transferring process where in the system construction is explained in detail.

A. Dispensing Unit

The automatic system consists of a dispensing unit and a control unit. The main components constituting the dispensing unit are pneumatically operated solenoid valves for the operations vent, fill, pressure and discharge, an FRL unit, a reservoir tank, a pressurizing tank mounted on load cell and two mixer tanks. The control unit was a PLC incorporated with an HMI module.

HMI and PLC control is chosen to make the make a low cost standalone system. With this system, the price is cut down to a high-extend and the system developed can very precisely transfer the liquid volume to the desired mixer. The system components were appropriately chosen and repeatedly tested to make it a leak proof. For the initial experimental setup, the PLC and HMI module were fixed up on a separate panel and rest of the system was wired to the panel as shown in figure 1.

Fig.1.Experimental setup of automated precise liquid transferring system

B. Calibration Process

Calibration is performed at initial stage to ensure that there is no effect of pressurizing tank or any other components on the load cell such that the load cell can accurately indicate the weight of the fluid coming to the pressurizing tank. In the first stage of the calibration process, zero calibration of the load cell is performed by assuming the total weight of the pressurizing tank mounted over the load cell as zero. This step is proceeded by the span calibration with a known standard weight. After this load cell measure any desired weight with reference to this standard weight. The feedback from the load cell is the input to the PLC that determines the opening and closing time for the solenoid valves.

The 100% accuracy in calibration process is ensured by exact mounting of pressurizing tank over the load cell assembly and ensuring that the external disturbances like air, mounting of the pneumatic tubes affects the strain exerted over the load cell and affects the calibration process. The calibration process designed with HMI is shown in figure 2.

Fig.2. Calibration process in HMI

C. *Liquid Filling Process*

Once the calibration process is performed, the system is designed to run either in manual mode or automatic mode depending on the user selection. With the Auto mode selection the system starts working fully automatically with PLC control as shown in figure 8. Manual mode is designed in such a way that with the user can control the opening and closing of solenoid valves simply by pressing the buttons as shown in figure 3. The HMI design makes the user control through manual mode very simple task. Here, as per the feedback from the HMI interface, the PLC controls the solenoid valves.

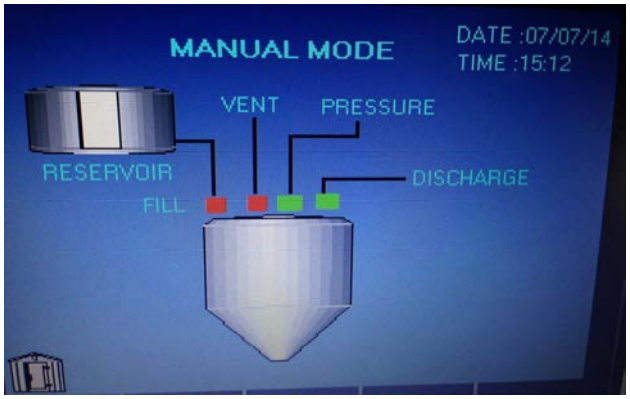

Fig.3. HMI screen of manual mode

The liquid filling process starts with the opening of vent valve so as to evacuate the entrapped gases inside the pressurizing tank. The closing time of the vent valve is determined by the PLC in auto mode depending on the feedback from the load cell. The process is done to ensure that any entrapped gas or unwanted pressure inside the tank do not exert an unwanted strain on the load cell and alter the weight of the liquid when filling process starts.

When the load cell indicates a zero strain, the vent valve is gets close and the fill valve gets open. The fill valve remains open as long as the weight of the liquid filled matches with the weight entered by the user.

D. *Liquid Dispensing Process*

Once the desired quantity of liquid gets filled, pneumatic pressure is developed in the pressure tank. Pressure from the compressor is regulated using an FRL unit, set to the desired pressure for the process and is directed through the pressure valve. For a set time that was experimentally determined, the filled liquid is pressurized and then discharge valve is opened. The discharge tube is made long enough and straight so as to almost touch the bottom of the tank. This is done to ensure the discharge of the liquid that remains at the bottom most portion of the tank. As the discharge valve gets open, the pressurized liquid rushes through the discharge tube to the mixer selected. As determined by repeated experiments pressure was set as 1.5 bars and pressurizing time were set as 5 seconds for the liquid weight ranging from 100 grams to 7 kilograms.

In the system, liquid was dispensed into the two mixer tanks where the selection of the mixer tank can be done by the user. Accurate transferring of the desired liquid volume as needed for the process was ensured by controlling the dispensing time such that the next filling process is initiated only when air starts spraying from the discharge tube. Spraying of air from the outlet of the tube ensures that all the liquid has been transferred and there is only pressurized air is present

III. SOFTWARE DESIGN

This section is divided to two sections: Electro pneumatic system model and Ladder logic control to explain the overall system control taken up to implement the system.

A. *Electro Pneumatic System Model*

A systematic and well defined approach is taken for the control of the entire system so as to obtain very precise results. A dedicated UnitronicsV570 PLC module is programmed in ladder logic using VISILOGIC software [11] -[12]. In case of any error, an alarm signal in both visual and audible form is raised by the controller thereby making the system an efficient one.

Special attention is taken care in making the system error proof. Designing of manual mode in the system was for this purpose. The entire system can be cleaned in case of change of solution from viscous to non-viscous using manual mode. In addition to making the system an error free one, this also ensures the easy maintenance of the system. For user friendliness and easy operation HMI design is made such that the user has to simply press the corresponding button for the valves and perform the operation. Furthermore, load cell calibration option is also provided in HMI. To nullify any errors due to external weight, user can access the calibration option which is linked with the load cell programming. In calibration, initially any additional weight is directly equated to zero, and then calibration with a known weight can be performed with span option as shown in figure 2.

The control of PLC over the valves is implemented using relay card consisting of 8 relays. Considering the feedback and other criterion the valves are opened when a 24V DC signal is passed to the control side of corresponding relay. The system was made with two port solenoid valve. Relay pass on 24V DC signal to energize the solenoid thereby opening the valve. Figure 4.a and 4.b shows the arrangement of relay card and solenoid valves respectively.

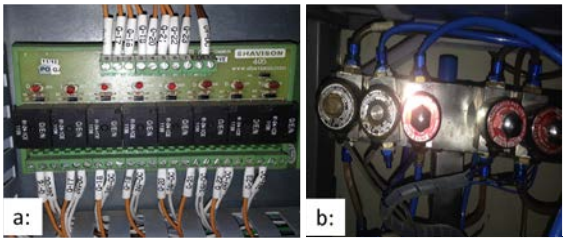

Fig.4. Relay card and solenoid valve arrangement

As the liquid flows into the tank the PLC monitors the tanks weight with the set weight. When the tank weight reaches near to the set weight then the fill valve is shut off according to the tolerance such that no excess liquid flows into the tank. As the discharge process continues, very small amount of solution gets accumulated inside the tank which cannot be taken out. For this dead weight is set such that at the time of discharging, PLC monitors the tank weight to the dead weight. Once the tank weight reaches to the dead weight then the discharge valve is shut down. At the time of filling up process, this excess weight is assumed as zero and process starts. By repeated experiments, dead weight was set as 10gms and tolerance was varied from5 gms-25 gms for weight up to 7 kg of solution.

B. Ladder Logic Control Flow Chart:

The control flow for the automated precise liquid transferring system is shown in figure 5.

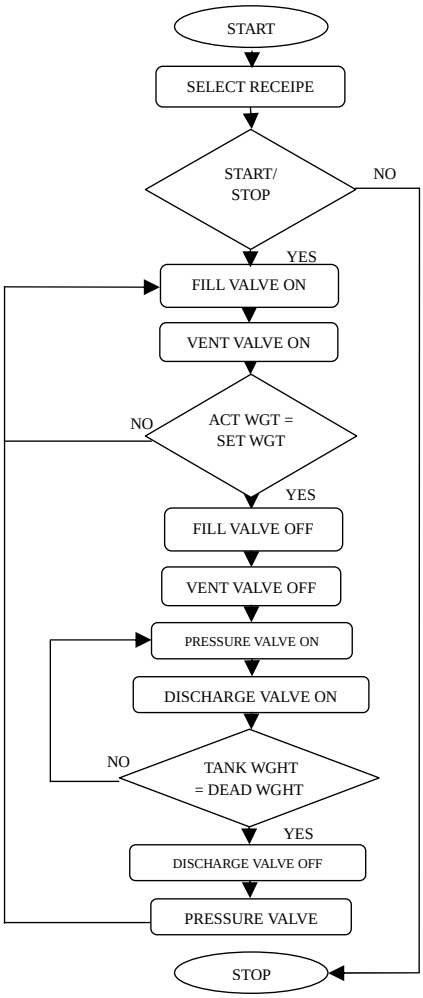

Fig.5. Ladder Logic Control flow chart

IV. RESULTS

Experiments were conducted with non-viscous as well as viscous solutions for 50 times to check the accuracy of the system. Water was used as the non-viscous liquid and sugar solution was used as the viscous solution to conduct the experiments. The comparison between set weight and discharged weight is shown in figure 6. The first figure shows the repeated cycles of measurements taken for non-viscous liquid and second shows with that of viscous solution. It is clear from the figure 6 that the maximum deviation exhibited by the system with viscous and non-viscous solution is ±2gm. The transferred volume to each mixer was measured using a weighing machine.

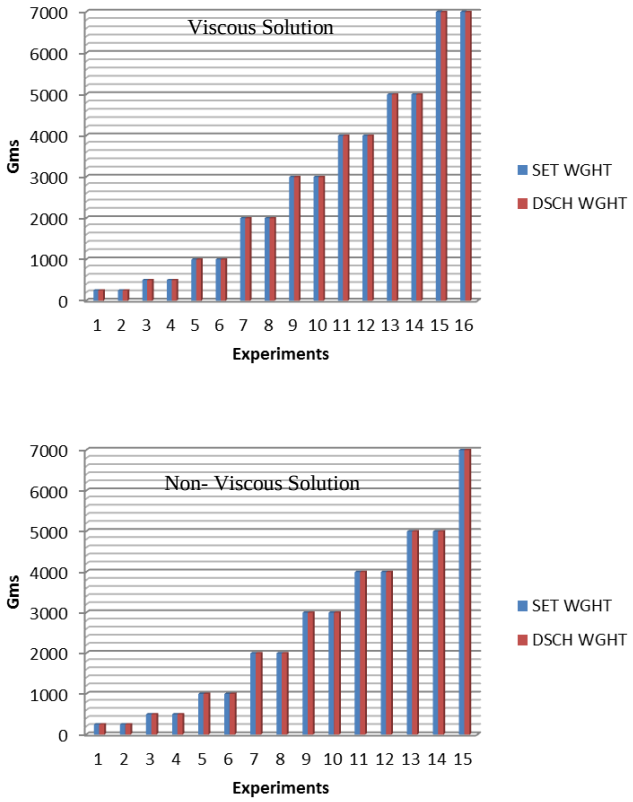

Fig.6. Comparison between set weight and discharge weight for different cycles of experiments

The results show that the control strategies adopted in enhancing the accuracy and precision is highly reliable. After initial calibration, any external weight getting exerted on the system is automatically nullified such that it does not affect the weight of liquid discharged. With this kind of control mechanism, the opening and closing time of the valves are very accurately calculated by the PLC controller with the feedback from load cell assembly. The deviation in discharge is brought down to minimal by closely adjusting the tolerance value. In case of any error, the system raises alarm with an LED indicator and a buzzer which adds to the reliability of the system.

Finally experiments were conducted for 50 times with the same set quantity of 1 kg of solution to check on the repeatability and precision of the system developed. The readings plotted in the figure 8 reveals the steady output

obtained from the system. Moreover, it can be seen that the system indicates high precision and repeatability as the process gets repeated making it apt for the industrial use.

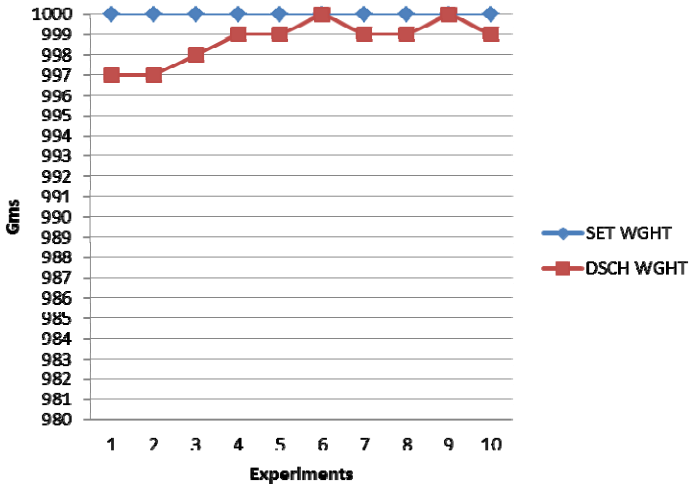

Fig.7. Liquid discharged for different cycles when set weight is 1000 gms

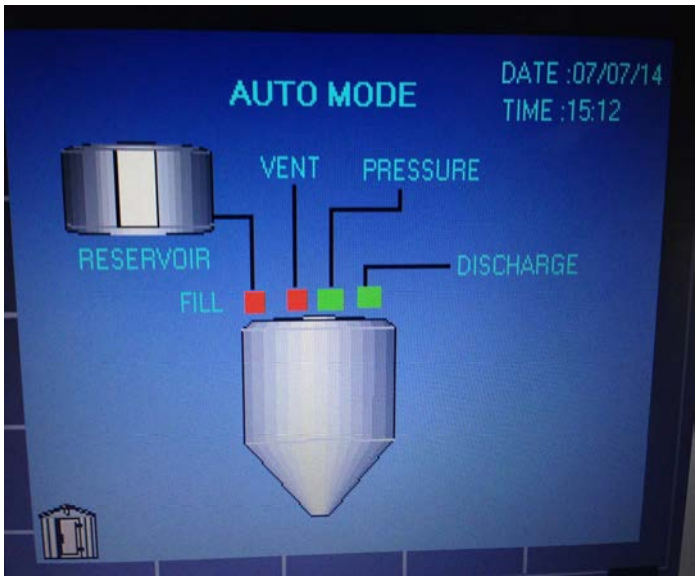

Fig.8. HMI screen in Auto mode

A. Abbreviations and Acronyms

S.NO	Abbreviation	Full Form
1	HMI	Human Machine Interface
2	LED	Light Emitting Diode
3	MEMS	Micro Electro Mechanical Systems
4	PLC	Programmable Logic Control
5	FRL	Filter, Regulator and Lubricator

V. CONCLUSION

The project made satisfies the objective of a highly accurate and precise standalone system that can replace conventional flow meters and expensive flow sensors. The system was mainly developed for food processing industries where the accuracy and precision in dispensing liquid solution is critical. The system can handle solutions from 250gm to 7kg irrespective of viscous or non-viscous nature. The provision for running the system in both auto and manual mode was provided through an HMI interface. The liquid dispensing was performed by careful regulation of opening and closing time of solenoid valves. An emergency stop switch was provided as an additional safety measure. The noncontact liquid system was developed in a very cost effective manner. The system developed could be either used as a standalone one or can be interfaced with an already existing liquid transferring system in place of flow meters or flow sensors. Repetitive experiments were done with different quantities of viscous and non-viscous solutions to check the accuracy of the system. The system showed an accuracy of ±2 gms from the set weight.

VI. ACKNOWLEDGMENT

We extend our sincere thanks to Miranda Automation Private Ltd, Navi Mumbai for their constant guidance and also Electronics, Instrumentation and Control Department of University of Petroleum and Energy Studies for their support.

REFERENCES

[1] Mueller, Lajos Nyarsik, Martin Horn, “Development of a technology for automation and miniaturization of protein crystallization,” Journal of Biotechnology, 2001, vol. 85, pp. 7–14

[2] B. D. Santarsiero, D. T. Yegian. An approach to rapid protein crystallization using Nano droplets. Journal of Applied Crystallography, 2002, pp. 278-281

[3] Raymond Hui, Raymond Hui, “ High-throughput protein crystallization,”Journal of Structural Biology, 2003, vol.142, pp. 154-161

[4] Walter D. Niles, Peter J. Coassin, “Piezo- and Solenoid Valve-Based Liquid Dispensing for Miniaturized Assays, ASSAY and Drug Development Technologies, Volume: 3 Issue 2: May 4, 2005

[5] Daniela Stock, Olga Perisic, Jan Lo¨ we, “Robotic nanolitre protein crystallisation at the MRC Laboratory of Molecular Biology,” Progress in Biophysics and Molecular Biology, 2005, vol. 88, pp. 311–327

[6] Yaxin Liu, Chen Liguo, Lining Sun, Weibin Rong “A Self-adjusted Precise Liquid Handling System”, 2009 IEEE International Conference on Robotics and Automation Kobe International Conference Center Kobe, Japan, May 12-17, 2009

[7] David A.Dunn, llllya Feygin, “Challenges and solutions to ultra-high-throughput screening assay miniaturization: submicroliter fluid handling,” DDT, 2000, vol.5, 84-91

[8] Carsten Haber, Marc Boillat, Bart van der Schoot, “Precise Nanoliter Fluid Handling System with Integrated High-Speed Flow Sensor,” ASSAY and Drug Development Technologies, 2005, vol. 2, 203-212.

[9] Bjom Samel, Volker Nock, Aman Russom, Patrick Grissl and Goran Stemme ‘‘Nanoliter Liquid Handling On A Low Cost Disposable With Embedded Fluid Actuators’’, The 13th International Conference on Solid-State Sensors, Actuators and Microsystems, Seoul, Korea, June 5-9,2005

[10] Yaxin Liu, Liguo Chen, Lining Sun, Automated Precise Liquid Dispensing System for Protein Crystallization, Proceedings of the

2007 IEEE International Conference on Mechatronics and Automation, August 5 - 8, 2007, Harbin, China

[11] Petruzella ,“Programming and logic control”, Tata McGraw-Hill, Third Edition

[12] Hugh Jack ,“Automating Manufacturing Systems with PLCs”, Fourth Edition

Commercial potential and competitiveness of natural fiber composites

1

*J.K. Pandey**, V. Nagarajan†, A.K. Mohanty†, M. Misra†*
*University of Petroleum and Energy Studies, Dehradun, India; †University of Guelph, Guelph, ON, Canada

1.1 Introduction

Use of renewable resource-based materials is increasing in importance with environmental concerns mounting worldwide over the use of nonrenewable resources such as petroleum. Carbon dioxide emissions resulting from human activities have been the constant topic of discussion in the scientific community. In recent years, many industries across various manufacturing sectors have acknowledged the need to adapt environmentally friendly manufacturing technologies and products. Multiple industrial adaptations and explorations of innovative materials are underway to meet the environmental concerns of end users. The scope for composite materials and technologies based on renewable resources is vast; extensive research and laboratory demonstrations have repeatedly proved the technical, environmental, and economical benefits of such innovative materials.

Composite material is a heterogeneous combination of two or more different phase constituents (matrix, load bearing or reinforcement elements, fillers and compatibilizers) (Strong, 2008). Reinforcements and fillers can be long, short, continuous, discontinuous, or spherical particles (Strong, 2008). In this context, natural fibers are of definite interest to fabricate composites. Natural fibers offer numerous advantages; they are discussed in subsequent sections of this chapter. Synergistic combination of natural fibers and plastics can result in a material having favorable level of performance, quality, and cost, and therefore possesses immense potential and prospects for serving different industries and applications. A desirable level of mechanical performance and durability of natural fiber composites (NFCs) with cost competitiveness is the key driver for commercializing these materials for high-volume applications. For the past two decades, comprehensive research has been conducted on NFCs and numerous research articles have been published addressing various challenges in the fabrication of composites where the final goal has always been achieving NFCs with desired level of mechanical performance and cost attributes for certain specific industrial uses. A number of research articles published on natural fibers has reached a new high of 34,385 articles as of March 1, 2015, based on Scifinder resources (http://www.cas.org/products/scifindr/index.html).

Generally, synthetic polymer matrixes are the choice to develop natural fiber-based composites for multiple applications such as automotive, packaging,

Biocomposites: Design and Mechanical Performance. http://dx.doi.org/10.1016/B978-1-78242-373-7.00001-9

flexible electronics, and others. Because petroleum is a depleting resource with fluctuating cost, adding natural fibers to petroleum-based plastics can provide considerable environmental and economic advantages. Natural fibers are available in abundance and are relatively inexpensive. NFCs based on polyolefins such as polypropylene (PP) and polyethylene have been widely researched and are successful in finding applications in the development of interior parts for the automotive industry (Zampaloni et al., 2007; Mohanty et al., 2002; Ellison and McNaught, 2000; Suddell and Rosemaud, 2009). Recently, natural fibers have been explored as reinforcements for engineering thermoplastics such as polycarbonate (PC) in an aim to widen the adaptability window of natural fibers to suit high-performance engineering applications. Mechanical performance of NFCs containing polyolefins and PC as matrix material are discussed in detail in Chapters 9–11.

The environmental aspect concerned with the disposal of composites based on synthetic resins still requires quantitative research. To develop a material with complete environmental compatibility, it is important that every phase of the material possesses the ability to undergo biological degradation. Certain renewable resource-based biopolymers have the potential to be an important component of a continuously emerging new line of low carbon footprint materials. Biopolymers refer to either biodegradable materials, derived from both nonrenewable and renewable resources, or nonbiodegradable materials derived from renewable biological resources (Mohanty et al., 2000). In other words, for a polymer to be called a biopolymer, it has to be either biodegradable, biobased, or both. Biopolymers are often also called bioplastics in many published studies. Combining bioplastics with natural fibers is a strategy to produce advanced composite materials. This strategy enables research scientists to design and engineer materials according to the requirements of the end user while keeping sustainability, economic feasibility, and environmental considerations under the design framework. Chapters 2–7 in this book are dedicated to discussing the mechanical performance of NFCs containing various biopolymers as matrix materials.

1.2 Classification and composition of natural fibers

Natural fibers are mainly classified as vegetable fibers, animal fibers, and mineral fibers (e.g., asbestos) depending on the origin (Mohanty et al., 2000). Vegetable fibers are further classified as wood (soft and hard) fibers and nonwood fibers. Five basic types of nonwood fibers with few representative examples are

- Bast: hemp, flax, jute, kenaf, and ramie
- Leaf: sisal, pineapple, abaca
- Seed/fruit: coir, kapok, coconut
- Straw: wheat, rice, soy, and corn straw
- Grass/reed: switchgrass, miscanthus

Generally, bast fibers are preferred for applications requiring high tensile strength, stiffness, and modulus and they are available in chopped, nonwoven, and mat forms. Bast and leaf fibers find their application in particle boards, fiberboards, automotive components, and products for housing and infrastructure (Anandjiwala and Blouw,

2007). Leaf fibers and coir are employed as cordage materials, cotton in apparel, and jute in carpeting and sacking. Other lignocellulosic residues such as sugarcane bagasse, coffee chaff, and hulls and residues resulting from other agricultural and industrial processing also represent a major fiber source for the development of renewable resource-based biocomposites for industrial applications. Distillers dried grains with solubles (DDGS), a coproduct of the corn ethanol industry, and lignin, a coproduct of the bioethanol and pulp and paper industries are now gaining increased interest for creating new value-added biocomoposite materials (Lamontagne, 2013). Figure 1.1 shows digital photographs of different classes of natural fibers, agricultural residues, and industrial coproducts/byproducts that are being used and researched in the design and engineering of biobased composite materials.

The universe of natural fiber is broad and, even so, the basic chemical structure of many of these fibers is similar in terms of the constituents and varieties in their composition, depending upon the type and origin of the fiber. Natural fiber itself is a

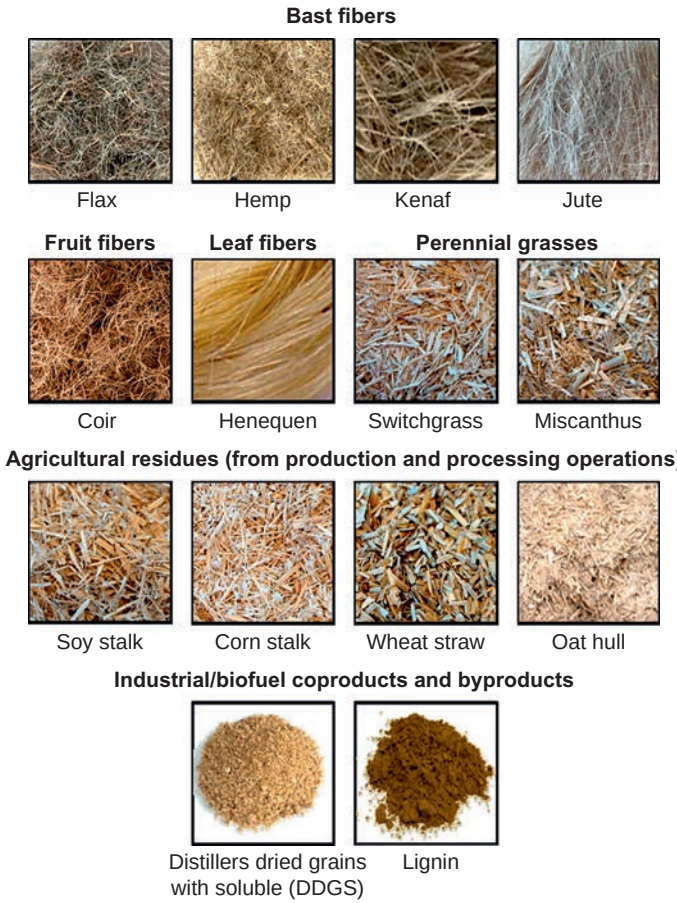

Figure 1.1 Photographs of different classes of natural fibers, agricultural residues, and industrial coproducts/byproducts.

composite by nature as it contains rigid, crystalline cellulose microfibrils in a matrix of lignin and hemicellulose that is amorphous. It also contains pectin, waxes, and some water-soluble compounds. Cellulose is the most abundant organic compound available in earth. Plant cell walls get their strength, stiffness, and stability from this main structural component, cellulose. The amount of cellulose present in a fiber has a significant influence on the properties and performance of the resulting composite materials produced for various applications.

The compositions of various natural fibers have been listed in detail in several review articles and book chapters (Faruk et al., 2012; Calistor et al., 2014). General properties and composition of natural fiber are additionally reviewed in Chapter 5. Figure 1.2 shows the general classification of lignocellulosic natural fibers, surface treatment methods, and challenges, which are discussed in detail in later sections of this chapter. Research and development is directed more toward in situ compatibilization and reactive extrusion techniques for injection molding types of biocomposites.

The mechanical properties of resulting composite materials are highly dependent on the source of natural fiber, mainly because of variation in composition. For example, two composites, made of jute and flax, with similar host matrix and equal concentrations even after identical treatments will not essentially show similar mechanical performance (Mohanty et al., 2000). Nagarajan et al. (2013) investigated the effect of fiber composition and fiber length on biocomposites containing perennial grasses and agricultural residues and concluded that these factors had a complementary effect on the performance of biocomposites.

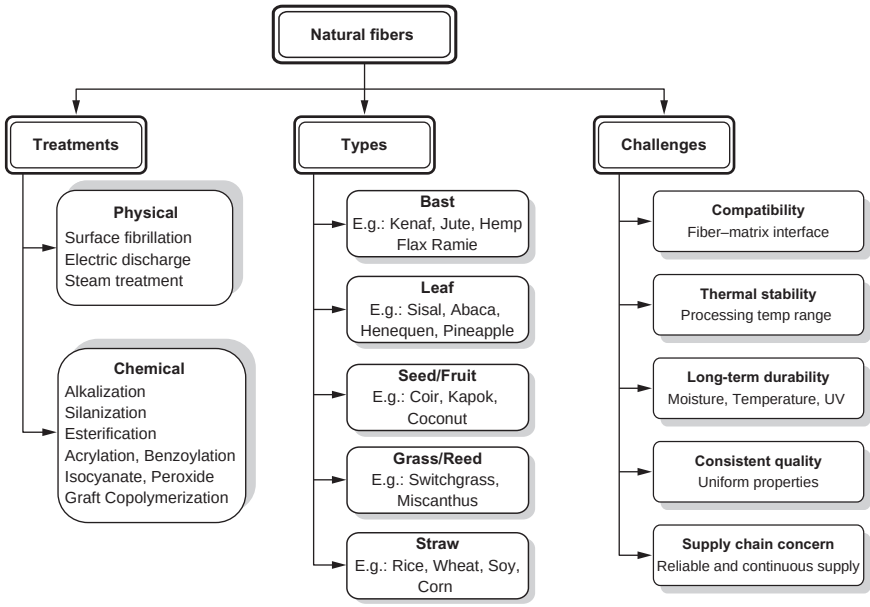

Figure 1.2 Natural fiber types, surface treatment options, and challenges.

1.3 Advantages and attributes of natural fibers

Principal advantages of using natural fibers in fabrication of composites are listed below (Mohanty et al., 2000; Faruk et al., 2012):

- Renewability, biodegradability, and CO_2 neutrality nature of natural fibers makes it environmentally friendly. Carbon sequestration attribute helps in reduction of GHG emissions and, hence, reducing the implications on climate change.
- Reinforcing traditional and biobased polymers with natural fibers can reduce the dependence on petro-based materials, as typically up to 50 wt.% of the matrix can be replaced with natural fibers for several injection-molded applications. Weight percentages of natural fiber in compression-molded composites could be higher than 50% depending on the matrix system and compatibilizers used for certain target applications.
- Natural fibers are available at a lower cost; therefore, they can help in offsetting the cost of matrix materials. Final cost of the parts ends up being cheaper or on par with the synthetic counterparts.
- Natural fibers can be an effective substitute for synthetic fibers such as E-glass fibers in certain applications. This advantage will be well received by industries because several countries have imposed severe restrictions on disposal of products made with glass fibers and the use of asbestos has also been banned in several parts of the world.
- When composites with natural fibers are incinerated for energy recovery process, mainly harmless residues are released without any trace of harmful heavy metals.
- Use of agricultural, lignocellulosic residues for high-volume applications can bring in new source of income for farmers while extending the value chain of the crops. This can help in job creation in rural farming communities.
- Natural fibers have environmentally benign production process and disposal options compared to synthetic fibers. They can be processed in conventional processing equipment; unlike glass fibers, natural fibers are nonabrasive to processing machinery used for manufacturing the composite materials, resulting in overall better efficiency.
- Natural fibers in the bast and leaf fibers category like jute, flax, kenaf, and others have high specific strength and modulus, and low density compared to E-glass fibers. NFCs are lightweight materials compared to glass fiber-filled composites, provided the fiber loading level remains the same; for automotive applications, this translates to a weight saving advantage and improved fuel efficiency.
- Natural fibers exhibit good acoustic and sound abatement properties. They have a relatively safe manufacturing process with reduced dermal and respiratory irritation.

1.4 Challenges encountered in adapting natural fibers for composite applications

Several challenges are encountered while developing composites from natural fibers and they all need to be effectively addressed to elevate the performance and market acceptability of NFCs. The challenges listed below are interconnected, and good control over these factors is important to create composites meeting the desired level of performance set by the industries. Knowledge on physical characteristics of fibers such as fiber architecture, strength, variability, and crystallinity are necessary to design composite formulations with desired performance attributes.

Processing temperature and moisture sensitivity: Most of the traditional polymers are processed between 180 and 200 °C and there are reports on time-dependent degradation of natural fiber at this temperature range. Literature on thermal resistance during processing of certain kind of fibers seems contradictory. For example, processing temperature of 170 °C was reported to affect the thermal stability of jute and flax fibers (Mohanty et al., 2002) whereas, in another study, high temperatures (170–180 °C) (Joshi et al., 2004) did not have any significant effect on the composite tensile properties. However, major damage to flax fiber has been reported at a temperature above 240 °C (Yu et al., 2006). Natural fibers are hydrophilic in nature, which can have adverse effects on the properties of the resulting composites. The moisture content is usually dependent on the composition of noncrystalline parts and the presence of voids on the fiber surface. Appropriate drying methods have to be established before processing the material with polymer matrix. In general, NFCs have higher susceptibility to moisture absorption.

Compatibility: Unfortunately, in most cases the NFC does not possess the same level of performance as glass fiber composites, owing to the incompatibility between hydrophobic polymer matrix and hydrophilic natural fiber. Although this issue can be solved by adequate physical and/or chemical modification, the risk of chain degradation and cost increment is a major thrust area for research. A significant part of Chapter 5 has been dedicated to discussing the effects of the compatibilization techniques explored so far in NFCs based on biodegradable blends as matrix material.

1.5 Supply chain management

Reliable and continuous availability of natural fibers/biomass is extremely important for any successful commercial development of composite materials. Farmers producing biomass for composite applications want to see solid markets and grantees; while on the other hand, industries want to have a guarantee of sustainable biomass supply. Therefore, it is imperative to strike a balance between the needs of farmers and industries. Performance of the supply chain largely depends on the degree of integration and coordination between the individual entities. Seasonal high volumes of agricultural residues available for use in composite applications, could affect the year round production of biocomposite materials. Abundant quantities of biomass are available; however, there is a need to control the fluctuating supply throughout the year. Cost, characteristics, and quality of fibers could vary substantially depending on the harvest conditions. Production patterns affecting the properties of the fibers have to be studied and surveyed over a significant period of time to acquire an understanding of producing fibers with consistent qualities.

One important aspect in the fiber supply chain is logistics. Several studies (Akgul et al., 2010; Yu and Tao, 2009; Sharma et al., 2013) have used mathematical models to assess the complete energy cost involved in the use of biomass along the entire supply chain (development, establishment, production, harvest, storage, and transport to facilities manufacturing the end use products). On the basis of these studies, numerous cost-reduction strategies have been proposed. Reduction in logistics cost could

have a major impact on regional and domestic competitive positioning. Therefore, the presence of an industrial biocomposite manufacturing facility in the vicinity of farmland and agricultural production areas can have great economic advantages. This has been one of the main reasons for the development of small and localized biorefineries demonstrating the concept of regional sustainable manufacturing (Waldron, 2014). This ensures that biomass is locally sourced, as close as possible, to avoid high transportation costs and to keep the feedstock cost to a minimum while increasing the sustainability of the manufacturing process (Waldron, 2014). Another strategy that can effectively address fiber supply concerns is the hybridization of two or more different fibers which can ease the demand on just one fiber type. Hybridization of banana fibers with kenaf (Thiruchitrambalam et al., 2009) and hemp (Idicula et al., 2009) has been researched, and hybridization of agricultural residues (Nyambo et al., 2010) and perennial grasses (Nanda et al., 2012) is being actively explored. Hybridization of natural fibers in combination with coproduct/by-product residues from various industrial operations (Lignin, DDGS) (Sahoo et al., 2004; Vivekanandhan et al., 2013) also offer new avenues.

1.6 Commercial competitiveness, market development, and growth scenario

1.6.1 Factors promoting commercial competiveness

Specific characteristics of some natural fibers are helpful in innovation leading to commercialization of biobased materials. Novel fiber formatting processes can be used to create new biomaterials. NFCs have improved commercial competitiveness because of two major reasons: facilitating mitigation of price fluctuations in the crude oil market and the environmental implications of using nonrenewable materials and products that by definition have a finite supply chain. The annual average (nominal) price for crude oil was in the range of US$15–18 per barrel for most of late 1980s, reaching a maximum of US$20 in 1990 (http://inflationdata.com/Inflation/Inflation_Rate/Historical_Oil_Prices_Table.asp). Prices remained more or less the same: a low of US$12 in 1998 and a high of US$20.50 in 1996. The beginning and early 2000s saw crude prices in the range of US$50/barrel. However, during the past decade, crude prices have steadily increased with a maximum of US$92 in 2008 and 2013 (http://inflationdata.com/Inflation/Inflation_Rate/Historical_Oil_Prices_Table.asp). Although currently a weakening is observed, and they stand at US$89 as of November 2014 (http://inflationdata.com/Inflation/Inflation_Rate/Historical_Oil_Prices_Table.asp), the prices still remain high in terms of historical prices recorded for crude oil. The price of PP has been observed to be tracking the rising prices of crude oil. In the 1980s, the average price of PP was reported to be $803/mt, and $771/mt in the 1990s (FAO Consultation on Natural Fibres, 2007). However, in more recent years the prices for PP seem to have almost doubled with a high of $1367/mt as of September 2013 (Global Petrochemical Prices, 2013); this was when average petroleum prices increased by 2.3% between September 2012 and September 2013 (Global Petrochemical Prices,

2013). A 25% plunge in PP price to $869/mt was recorded as of December 2014 (http://www.platts.com/news-feature/2014/petrochemicals/pgpi/propylene). Such highly volatile prices for traditional plastics are creating scenarios that are favoring the use of alternative materials such as natural fibers that reduce the dependence on fossil fuel based polymers and facilitate steady price offers for longer time periods. The need to spread the environmental advantages of using natural fibers became imperative with fluctuating crude oil prices and oil's depleting nature. However, at the time, the early 1990s, no solid scientific research was being conducted on natural fibers with a view to possible commercialization. That was when the United Nations Conference on Trade and Development and International Jute Organization started addressing the positive environmental attributes of different bast fibers (United Nations Conference on Trade, 1996). Quantitative results demonstrating the environmental advantages of using natural fibers were significantly lacking. van Dam and Bos (2004a) have investigated the environmental impact of natural fibers in industrial applications and have mentioned in their report that "natural fiber production requires less than 10% of the energy originally consumed for the production of PP fibers (around 90 GJ/ton)." In another review, production of China reed fibers was reported to show around 15% lower energy consumption compared to the production of glass fibers (Joshi et al., 2004). The inherent advantages of natural fibers and their characteristics like biodegradability and a low carbon footprint add to the sustainability of the production, distribution, consumption, and disposal of biodegradable/compostable composites for certain specific applications, besides being biobased materials. However, ecological sustainability needs to be addressed in an unambiguous manner through independent studies involving the entire life cycle of natural fibers. Only since the early 2000s have concerted efforts been taken in demonstrating the true environmental benefits through life cycle analysis (LCA). Overall better efficiency is expected with natural fibers compared to synthetic fibers, as revealed through LCA (van Dam and Bos, 2004b). This work laid the groundwork for follow-up actions both in terms of research as well as applied technology. This life cycle perspective could also offer a significant competitive edge for marketing biocomposites based on natural fibers and agricultural residues. LCA can be used to effectively quantify the environmental impacts of natural fibers starting from raw material to processing and to final product disposal; in essence covering the whole life cycle of the fibers (Patel et al., 2005). In this regard, composites containing natural fibers have a distinct advantage in relation to energy consumption, toxicity, emission of effluent, ease of disposal options, and so forth (Patel et al., 2005). Therefore, industries are bound to latch onto NFCs as a promising option to substitute for certain nonrenewable counterparts.

There are also several other factors that contribute toward enhancing the market development and opportunities for natural fibers and biobased products. Production/manufacturing processes, and use of specific consumer goods that are developed with intentions to reduce the environmental damages and cause less hazard are being backed by legislative provisions. Norway is considering tax incentives for biobased polymers and the imposition of new taxes on petro-based CO_2 content in polymers with an aim to increase the market demand for biobased products (Nova-newsletter, 2015). This initiative proposed by Norway is the first of its kind, and is expected to be followed by

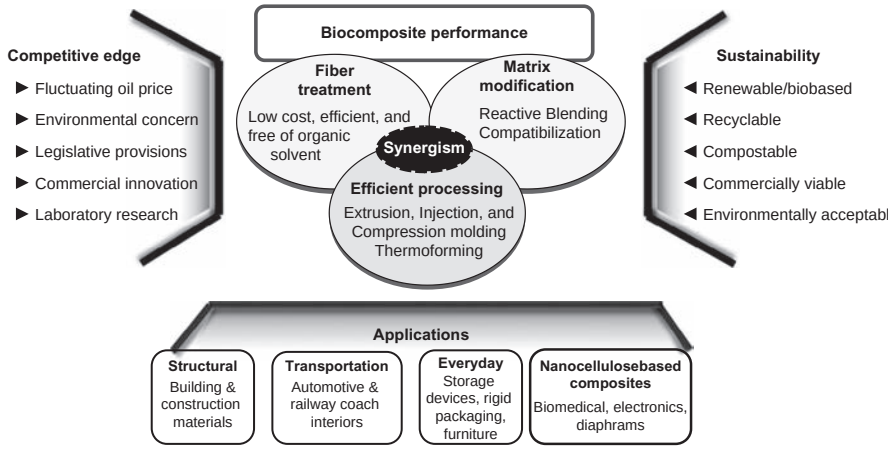

Figure 1.3 Performance, competitiveness, sustainability balance, and applications of biocomposites.

other countries of the world (Nova-newsletter, 2015). The environmental awareness in general has increased tremendously; the importance of natural fibers have been recognized and acknowledged by observing 2009 as the year of natural fibers by the United Nations (www.naturalfibres2009.org/en/). There are now more international platforms available for discussion of current status and market issues being faced in industries based on bioproducts. Examples of a few such organizations include Food and Agriculture Organization of the United Nations (FAO), European Bioplastics, Biotechnology Industry Organization (BIO), Cluster Industrielle Biotechnologie (CLIB) 2021. Aside from all these abovementioned factors, one important player determining the future prospects of NFCs is the research institutions and centers located around the world. These are dedicated to finding the most promising areas of commercial applicability, thereby elevating the status of natural fibers to a new level while considering the balance between performance, economics, and sustainability. Figure 1.3 provides a schematic of a synergistic approach requiring the coactions of efficient natural fiber and matrix treatment, and a suitable processing technique to ensure design and production of biocomposites with the desired level of performance for various applications. Factors influencing competitiveness and sustainability of biocomposites are also represented in the schematic in Figure 1.3.

1.6.2 Market development and growth scenario

According to a report published by Lucintel, TX, on the "Natural Fiber Composites Market Trend and Forecast 2011–2016: Trend, Forecast and Opportunity Analysis" in 2010, total global NFC market reached 430.7 million pounds, valued at US$289.3 million. The predictions forecast that the market will grow to US$531.3 million in 2016 with 11% compound annual growth rate (CAGR) for 2011–2016 (http://www.lucintel.com/reports_details.aspx?RepId=RPT1072). A plastics compounding market report

released by BCC Research, MA, in November 2013 has provided North American market estimates for NFCs (Forman, 2013) through 2018. The proposed CAGR percentage for 2013–2018 is 9.3% for NFCs in construction applications and 15% in nonconstruction applications (Forman, 2013). The market estimate for construction applications in US $ millions was at 2530 and 3924 in 2013 and 2018, respectively. For nonconstruction applications, the estimate was 330 and 664 (US $ million) in 2013 and 2018, respectively (Forman, 2013). This market estimate for NFCs includes wood-fiber composites as well.

Nova Institute, Germany, published "Market study on wood plastic composites (WPC) and NFC" in 2014, giving a comprehensive outlook on the WPC and NFC market in the European Union (Carus et al., 2014). According to this report, production of NFCs in 2012 was 92,000 tons, of which 90,000 tons were for automotive applications. This report has forecasted the production of NFCs in 2020 to go as high as 350,000 tons for automotives and more than 20,000 tons for other applications, provided the strong incentives offered for bioproducts are taken into account; otherwise, the production is forecasted to be 130,000 tons in 2020 (Carus et al., 2014). The most dominant use of natural fibers has been found to be in the automotive industries, for interior trims in doors and dashboards of high-end cars; application in the consumer sector is said to be still at a very early stage (Carus et al., 2014). In 2011, 15.7 million passenger cars and another 2 million motor vehicles such as trucks and motorbikes were manufactured in the EU. Assuming 30,000 tons of natural fibers and 30,000 tons of wood fibers were used in all passenger cars manufactured in 2011, about 1.9 kg of natural fibers and 1.9 kg of wood fibers would be present in every car in the EU (Carus et al., 2014). Technically, however, vehicles containing about 20 kg of natural and wood fibers have also been manufactured (Carus et al., 2014). Leão et al. (2006) estimated the potential use of natural fiber in Brazil to be around 23 kg per automobile, making its use 40,000 tons per annum for the automotive industry alone.

Automotive interior parts applications are currently dominated by NFCs based on synthetic plastics like PP and polyurethane (John and Thomas, 2008; Koronis et al., 2013). However, with rapid developments of biobased and biodegradable polymers, completely biobased/biodegradable NFCs are expected to become prevalent. The global biobased polymer market in terms of production capacity reached 4.67 million metric tons (value of US$13.86 billion) in 2014 and is expected to further rise to 9.77 million metric tons (value of US$23.39 billion) by 2019 with CAGR of 15.91% (Global biobased polymers market, 2015). NFCs based on a combination of polylactic acid/kenaf fibers (Koronis et al., 2013) is being used for making spare tire covers; another such application is tailgate trim, where NFCs based on polybutylene succinate/bamboo fibers are being used (http://www.plastemart.com/upload/Literature/Biopolymers-in-Automotive-Interiors.asp).

There are some promising technological breakthroughs concerning new uses of perennial grasses in biocomposite materials for niche market application. Switchgrass, native to North America (NA), and miscanthus, introduced to NA toward the end of nineteenth century, are the most popular perennial grasses. They can provide high yields

under poor, low-input conditions and are used for forage production, soil conservation, and as ornamental crops. During the last 10 years switchgrass and miscanthus have been developed for energy and fiber applications in North America and, more recently, in Europe (Girouard et al., 1995; Huisman, 1999). These perennial grass fibers may be an interesting reinforcing and filling agent for thermoplastic composites because they provide relatively good quality fibers that can be produced at low cost compared to other agricultural bast fibers, especially for injection molding type applications. Energy use and environmental impacts of growing switchgrass in Ontario have been evaluated through LCA by Kalita (2012). Bioproducts Discovery and Development Centre (BDDC), a research center at the University of Guelph, has been successful in producing NFCs containing perennial grasses (switchgrass and miscanthus) and agricultural residues. The formulations developed at the research center, with the help of collaborating industries, are now being used to make storage bins sold in major Canadian hardware stores (Lamontagne, 2013). The storage bins are said to contain around 25% of perennial grasses. The center has also commercialized NFC formulations that are now being used for manufacturing flowerpots from biobased resins. They contain about 25% miscanthus and are available for purchase from department stores such as Kroger (US) and Lowe's (Canada) (http://www.guelphmercury.com/news-story/4619563-an-eco-friendly-pot-for-your-posies/). Competitive Green Technologies, a biocomposite compounding facility in Ontario, Canada, is the licensed manufacturer for these biobased resins. These NFCs now available on the market have capitalized on the importance of having a local supply of natural fibers to avoid transportation of bulk fibers over long distances, in a way promoting the local economy by acknowledging the supply chain issues.

Another such product that has made it to the market is NCell®, a natural fiber-reinforced composite from GreenCore Composite Inc. The composite contains about 40 wt.% of cellulosic microfibers in PP matrix. This technology has been developed by the University of Toronto and has been exclusively licensed to GreenCore Composites (Lamontagne, 2013). The materials are provided as pellets to be molded as products for desired applications. UPM, a new forest industry company based in Finland has also been successful in producing cellulose fiber-reinforced PP composites. The materials are commercialized under the name UPM ForMi and are available in different grades, in granule forms. A maximum of 50% renewable content has been achieved in certain grades and they are said to offer smooth, reliable, and odorless composite products for a wide range of applications (http://www.upm.com/formi/Pages/default.aspx).

1.7 Future prospects and developments

As discussed throughout this chapter, natural fibers are the suitable material of choice to be used in combination with several polymer matrixes for the development of composites for myriad applications such as automobiles, packaging, flexible electronics, construction, and so on. Abundant availability of natural fibers combined with other

advantageous characteristics, such as being nonabrasive to processing machines, easy processability, and biodegradability, are favoring innovations in designing and manufacturing of NFCs. Rapidly fluctuating price of petroleum-based products combined with strong political and social support to develop ecofriendly materials are expected to drive the growth of NFCs to a greater extent in the future. NFCs are applicable in almost every dimension of life (Suddell and Rosemaud, 2009), ranging from commodity to engineering applications. Because natural fibers possess low density compared to glass fibers, it is possible to achieve weight reduction in automotive parts by adapting natural fibers, provided the substitution is at same volume percentage. According to an estimate, achieving 25% reduction in weight of an automobile could save 250 million barrels of crude oil, which in turn could result in reduction of CO_2 emissions to the tune of 220 billion pounds per year (Mair, 2000; Kamath et al., 2005). It has been demonstrated that a reduction in CO_2 emission, about 3 t CO_2/t of the material, is possible when glass fibers are substituted with hemp fibers at same volume percentage, resulting in saving 1.16 m^3 of crude oil (Pervaiz and Sain, 2003).

Qualities, such as the ability to achieve specific orientation under magnetic field, and possibilities of desirable surface modifications, have directed intense research efforts in the area of cellulose nanofiber-based composites to develop optical devices, magnetic strips, and biosensors (Pandey and Takagi, 2011). Their application in the development of conducting composites with future of flexible and biodegradable electronics is another impressive area for natural fiber material. Cellulose nanofibers may also have a decisive role for development of lightweight, high-strength composites as they are optically active, such property can be utilized in fabricating colored films (Nishio et al., 1998). Such films can find application in bank notes, electoral cards, security papers and certificates, passports, and visas. Cellulose whiskers and semiconducting polymers have also been used recently to produce conductive composites (van den Berg et al., 2007).

Further, NFCs developed for structural applications such as infrastructure and housing applications, including decking, windows, doors, fencing, and construction of bridges, will have significant market share in the future. It is important to mention that although complete substitution of traditional, synthetic fibers with natural fibers are not anticipated or intended, NFCs will continue to find their own success in niche markets. Mass uses of NFCs are also envisaged for high-volume applications such as automobiles, provided that such products are commercially competitive through improved efficiency of processes and techniques.

Acknowledgments

The authors would like to acknowledge the funding support from (i) Ontario Ministry of Agriculture, Food and Rural Affairs, (OMAFRA)–University of Guelph Bioeconomy–Industrial Uses Theme; (ii) OMAFRA–New Directions Research program; (iii) the Ontario Ministry of Economic Development and Innovation (MEDI), Ontario Research Fund, Research Excellence Round 4 program (ORF–RE04); (iv) the Natural Sciences and Engineering Research Council (NSERC) Canada Discovery grant (Mohanty) and Network of Centres of Excellence (NCE)

AUTO21 program; (v) the Canadian foundation for Innovation's Leaders Opportunity Fund (CFI–LOF); (vi) Ontario Agri-Food Technologies (OAFT); (vii) Federal Economic Development Agency (FedDev #509260), Southern Ontario; (viii) Grain Farmers Ontario (GFO); and (ix) Hannam Soybean Utilization Fund (HSUF).

References

Akgul, O., Zamboni, A., Bezzo, F., Shah, N., Papageorgiou, L.G., 2010. Optimization-based approaches for bioethanol supply chains. Ind. Eng. Chem. Res. 50 (9), 4927–4938.

Anandjiwala, R.D., Blouw, S., 2007. Composites from bast fibres—prospects and potential in the changing market environment. J. Nat. Fibers 4 (2), 91–109.

Calistor, N., Nagarajan, V., Mohanty, A.K., Misra, M., 2014. Natural fiber composites from agricultural by-products: an overview. In: Netravali, A.N., Pastore, C.M. (Eds.), Sustainable Composites: Fibers, Resins and Applications. DEStech Publications, Inc. Lancaster, Pennsylvania, USA.

Carus, M., Eder, A., Dammer, L., Korte, H., Scholz, L., Essel, R., Breitmayer, E., 2014. Wood–plastic composites (WPC) and natural fibre composites (NFC): European and Global Markets 2012 and future trends. Nova Institute, Germany. www.nova-institut.de/download/market_study_wpc_nfc_short_version (last accessed March, 2015).

Ellison, G.C., McNaught, R., 2000. The use of natural fibres in nonwoven structures for applications as automotive component substrates. Research and development report, Ministry of Agriculture Fisheries and Food Agri-Industrial Materials, UK. www.maff.gov.uk/farm/acu/acu.htm, February.

FAO Consultation on Natural Fibres, 2007. The co-movement of jute and hard fibres prices with the prices of polypropylene and crude oil. FAO Consultation on Natural Fibres, Rome, 31 January–1 February.

Faruk, O., Bledzki, A.K., Fink, H.P., Sain, M., 2012. Biocomposites reinforced with natural fibers: 2000–2010. Prog. Polym. Sci. 37 (11), 1552–1596.

Forman, C., 2013. The plastics compounding market. Report by BCC research, November. http://www.bccresearch.com/market-research/plastics/plastics-compounding-market-pls018d.html (last accessed March, 2015).

Girouard, P., Henning, J.C., Samson, R., 1995. Economic assessment of short rotation forestry and switchgrass plantations for energy production in central Canada. In: The Canadian Energy Plantation Workshop, Ottawa, Canada. pp. 11–16.

Global biobased polymers market, 2015–2019. Market report by Technavia analysis.

Global Petrochemical Prices, September 2013. http://www.platts.com/news-feature/2013/petrochemicals/pgpi/index (last accessed March, 2015).

Huisman, W., 1999. Harvesting and handling of *Miscanthus giganteus*, *Phalaris arundinacea* and *Arundo donax* in Europe. In: Proceedings of the Fourth Biomass Conference of the Americas. Elsevier Science, Oxford, pp. 327–333.

Idicula, M., Sreekumar, P.A., Joseph, K., Thomas, S., 2009. Natural fiber hybrid composites – a comparison between compression molding and resin transfer molding. Polym. Compos. 30, 1417–1425.

John, M.J., Thomas, S., 2008. Biofibres and biocomposites. Carbohydr. Polym. 71 (3), 343–364.

Joshi, S.V., Drzal, L.T., Mohanty, A.K., Arora, S., 2004. Are natural fiber composites environmentally superior to glass fiber reinforced composites? Compos. Part A: Appl. Sci. Manuf. 35 (3), 371–376.

Kalita, B., 2012. Life cycle assessment of switchgrass (*Panicum virgatum* L.) biomass production in Ontario. Master of Science, University of Guelph, Guelph, Canada.

Kamath, M.G., Bhat, G.S., Parikh, D.V., Mueller, D., 2005. Cotton fiber nonwovens for automotive composites. Int. Nonwovens J. 14 (1), 34–40.

Koronis, G., Silva, A., Fontul, M., 2013. Green composites: a review of adequate materials for automotive applications. Compos. Part B: Eng. 44 (1), 120–127.

Lamontagne, N.D., 2013. New natural-fiber composites find their roles. Plastics Engineering (June). http://www.nxtbook.com/nxtbooks/wiley/pe_201306/index.php?startid=22 (last accessed March, 2015).

Leão, A., Sartor, S.M., Caraschi, J.C., 2006. Natural fibers based composites – technical and social issues. Mol. Cryst. Liq. Cryst. 448 (1), 161–763.

Mair, R.L., 2000. Tomorrow's plastic cars. ATSE focus no. 113, July/August.

Mohanty, A.K., Misra, M., Hinrichsen, G., 2000. Biofibres, biodegradable polymers and biocomposites: an overview. Macromol. Mater. Eng. 276–277, 1–24.

Mohanty, A.K., Misra, M., Drzal, L.T., 2002. Sustainable biocomposites from renewable resources: opportunities and challenges in the green materials world. J. Polym. Environ. 10, 19–26.

Nagarajan, V., Mohanty, A.K., Misra, M., 2013. Sustainable green composites: value addition to agricultural residues and perennial grasses. ACS Sustain. Chem. Eng. 1 (3), 325–333.

Nanda, M.R., Misra, M., Mohanty, A.K., 2012. Performance evaluation of biofibers and their hybrids as reinforcements in bioplastic composites. Macromol. Mater. Eng. 298, 779–788.

Nishio, Y., Kai, T., Kimura, N., Oshima, K., Suzuki, H., 1998. Controlling the selective light reflection of a cholesteric liquid crystal of (hydroxypropyl) cellulose by electrical stimulation. Macromolecules 31 (7), 2384–2386.

Nova-newsletter, 2015. From http://news.bio-based.eu/ (last accessed March, 2015).

Nyambo, C., Mohanty, A.K., Misra, M., 2010. Polylactide-based renewable green composites from agricultural residues and their hybrids. Biomacromolecules 11 (6), 1654–1660.

Pandey, J.K., Takagi, H., 2011. Self healing potential of green nanocomposites from crystalline cellulose. Int. J. Mod. Phys. B 25 (31), 4216–4219.

Patel, M., Bastioli, C., Marini, L., Würdinger, E., 2005. Life-cycle assessment of bio-based polymers and natural fiber composites. Biopolymers Online.

Pervaiz, M., Sain, M.M., 2003. Carbon storage potential in natural fiber composites. Resour. Conserv. Recycl. 39 (4), 325–340.

Sahoo, S., Misra, M., Mohanty, A.K., 2004. Biocomposites from switchgrass and lignin hybrid and poly(butylene succinate) bioplastic: studies on reactive compatibilization and performance evaluation. Macromol. Mater. Eng. 299 (2), 178–189.

Sharma, B., Ingalls, R.G., Jones, C.L., Khanchi, A., 2013. Biomass supply chain design and analysis: basis, overview, modeling, challenges, and future. Renew. Sustain. Energy Rev. 24, 608–627.

Strong, A.B., 2008. Fundamentals of Composites Manufacturing: Materials, Methods and Applications. Society of Manufacturing Engineers, Dearborn, MI.

Suddell, B.C., Rosemaud, A., 2009. Industrial fibres: recent and current developments. In: Proceedings of the Symposium on Natural Fibres, pp. 71–82. ftp://ftp.fao.org/docrep/fao/011/i0709e/i0709e10.pdf (last accessed March, 2015).

Thiruchitrambalam, M., Alavudeen, A., Athijayamani, A., Venkateshwaran, N., Perumal, A.E., 2009. Improving mechanical properties of banana/kenaf polyester hybrid composites using sodium lauryl sulfate treatment. Mater. Phys. Mech. 8, 165–173.

United Nations Conference on Trade and Development, 1996. Jute and hard fibres: overview of major current issues. http://www.unctad.info/upload/Infocomm/Docs/Jute/docs/unctadcom71.en.pdf (last accessed March, 2015).

van Dam, J.E.G., Bos, H.L., 2004. Consultation on natural fibres: the environmental impact of hard fibres and jute in non-textile industrial applications. ESC-fibres consultation no. 04/4, Rome, 15–16 December.

van Dam, J.E., Bos, H.L., 2004. The environmental impact of fibre crops in industrial applications. Hintergrundpapier zu, van Dam, JEG.

van den Berg, O., Schroeter, M., Capadona, J.R., Weder, C., 2007. Nanocomposites based on cellulose whiskers and (semi) conducting conjugated polymers. J. Mater. Chem. 17 (26), 2746–2753.

Vivekanandhan, S., Zarrinbakhsh, N., Misra, M., Mohanty, A.K., 2013. Coproducts of biofuel industries in value-added biomaterials uses: a move towards a sustainable bioeconomy. In: Fang, Z. (Ed.), Liquid, Gaseous and Solid Biofuels – Conversion Techniques. INTECH Open Access Publisher, Rijeka, Croatia.

Waldron, K.W., 2014. Advances in Biorefineries: Biomass and Waste Supply Chain Exploitation. Woodhead Publishing, Swaston, Cambridge, UK.

Yu, S., Tao, J., 2009. Economic, energy and environmental evaluations of biomass-based fuel ethanol projects based on life cycle assessment and simulation. Appl. Energy 86, S178–S188.

Yu, L., Dean, K., Li, L., 2006. Polymer blends and composites from renewable resources. Prog. Polym. Sci. 31 (6), 576–602.

Zampaloni, M., Pourboghrat, F., Yankovich, S.A., Rodgers, B.N., Moore, J., Drzal, L.T., Mohanty, A.K., Misra, M., 2007. Kenaf natural fiber reinforced polypropylene composites: a discussion on manufacturing problems and solutions. Compos. Part A 38, 1569–1580.

DEVELOPMENT OF POSITION TRACKING AND GUIDANCE SYSTEM FOR UNMANNED POWERED PARAFOIL AERIAL VEHICLE

Vindhya Devalla[*], Amit Kumar Mondal[§], A J Arun Jeya Prakash[*], Om Prakash[*]
[*]*Department of Aerospace Engineering,* [§]*Department of Electronics, Instrumentation and Control*
University of Petroleum and Energy Studies, Dehradun, India

***Abstract*— An experimental Unmanned Powered Parafoil Aerial Vehicle (UPPAV) was developed to gather aerial data. Certain characteristics like low-speed, low-cost, and high stability makes the powered Parafoil a versatile and promising platform for surveillance and imaging applications. UPPAVs are easy to operate, robust and safe and have high flight duration. The developed UPPAV has a chassis fitted with a high torque Brushless DC motor, Servo motor and a Parafoil wing. This paper describes development of the position tracking and guidance system using the GPS unit placed on the chassis. It focuses on the extraction and transmission of the specific GPS values like longitude, Latitude and Altitude from the bulk values obtained. The GPS navigation system will provide continuous position of the system. These obtained values can be used by the pilot to maneuver the system to the desired location. The developed system mounted on the chassis consists of Microcontrollers, GPS, and 433 MHz trans-receivers.**

***Index Terms*—Unmanned Power Parafoil Aerial Vehicle (UPPAV), GPS, RS232, PAV Mathematical Modeling**

I. INTRODUCTION

The introduction part can be divided into two parts focusing unmanned aerial vehicles and unmanned powered Parafoil aerial vehicles

A. Unmanned Aerial Vehicles

The U.S Department of Defense (DOD) defines an unmanned aircraft as follows [1]:
A powered vehicle that does not carry a human operator, can be operated remotely or autonomously, can be expendable or recoverable and can carry a lethal or non-lethal payload. Ballistic or semi ballistic vehicle, cruise missiles, artillery projectiles, torpedoes, mines, satellites and unattended sensors are not considered unmanned vehicles. Unmanned vehicles are the primary component of an unmanned system.

This definition covers multiple forms of unmanned systems including Unmanned Air Systems (UASs), unmanned ground vehicles (UGV), unmanned surface vehicles (USVs), and unmanned underwater vehicles (UUVs).

The first remote controlled UAV was developed for military use and was called drone. UAV generally consist two systems namely, Unmanned Aircraft and Control Station. There is a wide range of UAVs available from small vehicles with less than 0.8kg (e.g. Sensefly) to very large vehicles with the flight weight more than 900kg (e.g. B-Hunter). The different types of UAVs can be classified as: multi-rotor, fixed wing and Parafoil UAV [2]. The classification can be done on weight, height and construction. Depending upon the above mentioned categories the unmanned aerial vehicles can be divided in three types namely glider type, multi- copter types and Parafoil aerial vehicle types. Certain characteristics like low-speed, low-cost, and high stability makes the powered Parafoil a versatile and promising platform for surveillance and imaging applications. Unmanned powered Parafoil aerial vehicles are easy to operate, robust and safe and have good flight duration.

B. Unmanned Powered Parafoil Aerial Vehicles

The Powered Parafoil (PPC) is an aircraft which derives lift from a ram-air inflated canopy, under which the fuselage is suspended. The Parafoil is inflated by the dynamic pressure of the air flowing into the canopy which has a cross section in the shape of an airfoil [3]. This process helps the vehicle to create lift.

Fig 1: ParaPlane Corporation first model [1]

This feature differentiates these Parafoils from conventional Parafoils which are used to simply create drag. Powered Parafoils have been utilized mostly for recreation activities, but some of the special properties make them a suitable platform for unmanned aerial vehicle (UAV) and remote sensing applications. Powered Parafoils have existed since 1981[1]. The concept was introduced at the Sun & Fun aviation event by the ParaPlane Corporation. They represent aircraft that are somewhere between balloons and fixed wing aircraft when control is considered as shown in figure 1. The direction of a powered Parafoil is controlled by the pilot pushing on either a left or right steering bar that pulls down on a line attached to the trailing edge of the canopy. The increased drag causes the aircraft to turn.

978-1-4673-7231-2/15/$31.00 ©2015 IEEE

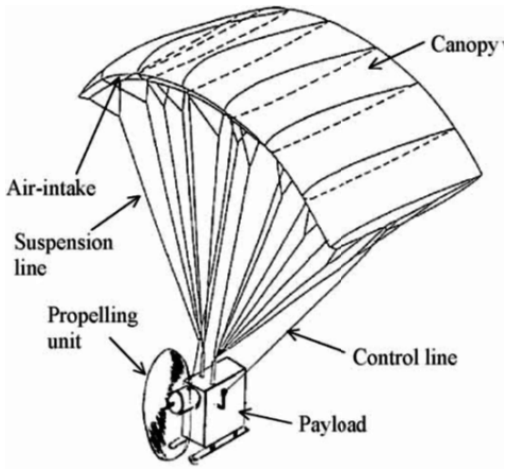

Fig 2: Control Surfaces of Powered Parafoil UAV [3, 4]

The control lines connected to the canopy are pulled down together, which will drop both trailing ends of the canopy at a time and cause a sudden increase in lift. This maneuver is done during landing, when the pilot wants a smooth touchdown. A different steering configuration which is used on some small-scale aircraft is known as a "fly-bar." In this design, the Parafoil is connected to the ends of a bar, as seen in figure 2.

This bar can be pulled either side of the aircraft, changing the direction of the lift and making the aircraft turn. Aircraft using each of the two steering systems behave identically in response to thrust inputs. Powered Parafoils have the tendency to fly at a constant airspeed [4]. A powered Parafoils will climb, cruise and descend somewhere around the speed of 26 – 32 MPH. These Aircrafts have pendulum stability and oscillations as shown in the figure 3, because of the mass of the airframe suspended significantly below the canopy. This feature allows the aircraft to achieve directional control rather than rolling motion [2]. These platforms are very stable and must only get disturbed with gusts that would change the flight trajectory.

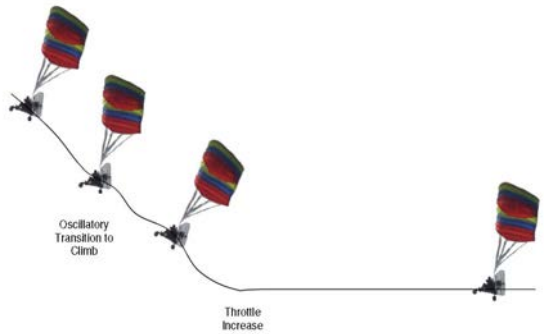

Fig 3: Oscillations in Powered Parafoil while takeoff [5]

The addition of a propelling unit makes the paraglider an Unmanned Aerial Vehicle (UAV). The applications of powered Parafoil in surveillance and imaging has benefit of a low-speed, low-cost, and stable platform which is capable of lifting payloads of up to 600 lbs. Generally these vehicles are operated remotely with a pilot. In case of surveillance, the pilot is unsure about the locations. This paper presents a technique and algorithm for tracking the location of UPPAV which will help the pilot for precise surveillance. The paper follows with hardware and software design of the position and tracking system giving a brief overview about the components used. This paper also gives the detailed description of the algorithm developed and the testing results of the system developed and installed on the developed UPPAV.

II. NINE DEGREES OF FREEDOM MODEL OF UPPAV

A 9 DOF dynamical model of the Parafoil was created to assist in the development of the pipeline monitoring in oil and gas using powered Parafoil aerial vehicle project. It is an important component of the Parafoil simulation and is essential for the creation of the control and guidance systems. The Powered Parafoil (PPC) is an aircraft which derives lift from a ram-air inflated canopy, under which the fuselage is suspended. The Parafoil is inflated by the dynamic pressure of the air flowing into the canopy which has a cross section in the shape of an airfoil. This process helps the vehicle to create lift. This feature differentiates these Parafoils from conventional Parafoils which are used to simply create drag. Powered Parafoils have been utilized mostly for recreation activities, but some of the special properties make them a suitable platform for unmanned aerial vehicle (UAV) and remote sensing applications [6]. The canopy is considered to be a stable system once inflated completely. Since, there are no traditional control surfaces as that of an airplane the powered Parafoil is controlled in a unique way. The direction of a powered Parafoil is controlled by the pilot pushing on either a left or right steering bar that pulls down on a line attached to the trailing edge of the canopy. The increased drag causes the aircraft to turn. The 9 DOF model is given as in equation 1. The Parafoil payload model is modeled as two body system consisting of canopy mass and payload mass suspended below the canopy using the suspension lines. The steering configuration used is known as a "fly-bar." In this design, the Parafoil is connected to the ends of the flybar. This bar can be pulled either side of the aircraft, changing the direction of the lift and making the aircraft turn. This type of Parafoil, payload model uses 9 DOF model [1]. The separation between the Aerodynamic center of the canopy and the payload center of gravity produces a swinging motion. In the 9 DOF model two masses m_b and m_p are connected at point C. R_b and R_p are two rigid mass less links that connects Parafoil and payload at joint C. the two bodies are free to rotate about the Joint C [7]. In this model the spring damper modeling of relative yawing motion in Parafoil and payload due to the lines has been employed. In this model the payload tries to re-orient itself when Parafoil yaws during a turn. Three reference frames have been used namely Parafoil reference frame, body reference frame and the Join C reference frame. Three types of forces acting on the Parafoil has been modeled as, Aerodynamic force, Gravitational force and internal force due to joint C. Similarly for payload four forces acting modeled as, Aerodynamic force, Gravitational force, Thrust force and internal force due to joint C [8, 9]. Aerodynamic moment is modeled for the Parafoil. The rotational spring-damper is modeled as M_c. figure 4, gives the 9DOF model and figure 2 describes the canopy tilt angle in direction control model [6]. Collecting Parafoil translational and rotational motion equations, Payload translational and rotational motion equations we get nine

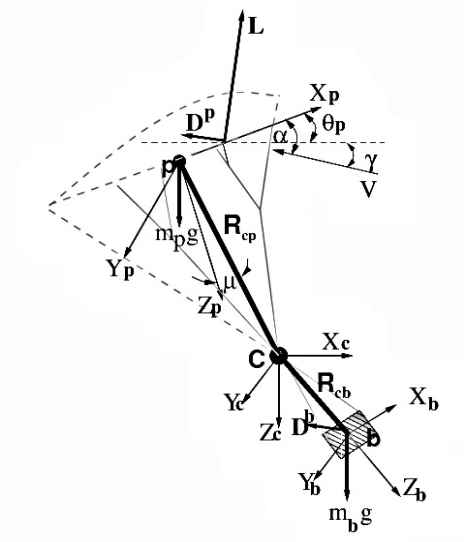

Fig 4. 9DOF Model [6]

degrees of freedom equations of motion of combines Parafoil payload system in concatenated matrix form as:

$$\begin{bmatrix} -M_b R_{cb} & 0 & -M_b T_b & T_b \\ 0 & -(M_p + M_F)R_{cp} & -(M_p + M_F)T_p & -T_b \\ I_b & 0 & 0 & -R_{cb}T_b \\ 0 & I_p + I_M & 0 & R_{cp}T_p \end{bmatrix} \begin{bmatrix} \dot{\Omega}_b \\ \dot{\Omega}_p \\ V_c \\ F_c \end{bmatrix} = \begin{bmatrix} B_1 \\ B_2 \\ B_3 \\ B_4 \end{bmatrix} \tag{1}$$

$$\begin{aligned} B_1 &= F_b^A + F_b^G + F_b^T - \Omega_b \times M_b \Omega_b \times R_{cb} \\ B_2 &= F_p^A + F_p^G - \Omega \times (M_p + M_F)\Omega_p \times R_{cp} \\ &\quad + M_F \Omega_p \times T_p V_c - \Omega_p \times M_F T_p V_c \\ B_3 &= -\Omega_b \times I_b \omega_b \\ B_4 &= M_p^A - \Omega_p \times (I_p + I_M)\Omega_p \end{aligned} \tag{2}$$

The kinematic equations for the trajectory of point C and the Euler angles of the Parafoil and the payload are:

$$\begin{Bmatrix} \dot{x}_C \\ \dot{y}_C \\ \dot{z}_C \end{Bmatrix} = \begin{Bmatrix} u_C \\ v_C \\ w_C \end{Bmatrix}$$

$$\begin{Bmatrix} \dot{\phi}_b \\ \dot{\theta}_b \\ \dot{\psi}_b \end{Bmatrix} = \begin{bmatrix} 1 & S\phi_b t\theta_b & C\phi_b t\theta_b \\ 0 & C\phi_b & -S\phi_b \\ 0 & \frac{S\phi_b}{C\theta_b} & \frac{C\phi_b}{C\theta_b} \end{bmatrix} \begin{Bmatrix} p_b \\ q_b \\ r_b \end{Bmatrix}$$

$$\begin{Bmatrix} \dot{\phi}_p \\ \dot{\theta}_p \\ \dot{\psi}_p \end{Bmatrix} = \begin{bmatrix} 1 & S\phi_p t\theta_p & C\phi_p t\theta_p \\ 0 & C\phi_p & -S\phi_p \\ 0 & \frac{S\phi_p}{C\theta_p} & \frac{C\phi_p}{C\theta_p} \end{bmatrix} \begin{Bmatrix} p_p \\ q_p \\ r_p \end{Bmatrix} \tag{3}$$

III. GPS TRACKING

In this mode, the GPS is supposed to track the location of the UPPAV. The tracking algorithm has been developed and the developed system is installed in the UPPAV so that it can continuously send the UPPAV location to the pilot who would maneuver the UPPAV according to the desired path for this purpose, 9 DOF model has been used to predict the GPS locations of the UPPAV from start point to end point.

Using the 9 DOF model the following graph in figure 5 has been plotted for the distance covered by the UPPAV in 10seconds with the tilt angle of 20 degrees.

Using the initial Latitude and longitude (as shown in figure 6) values the end point is determined by the following formula.

The GPS values are predicted using the following equations:

$$\begin{aligned} latitude &= lat\_0 + (180/pi) \times (y_c / R) \\ longitude &= lon\_0 + (180/pi) / \sin(lat \times pi/180) \times (x_c / R) \end{aligned} \tag{4}$$

The initial latitude and longitude values are taken as

Lat_0 = 3024.9837 N

Lon_0=7758.1379 E

The radius of earth R is 6378.1 Km

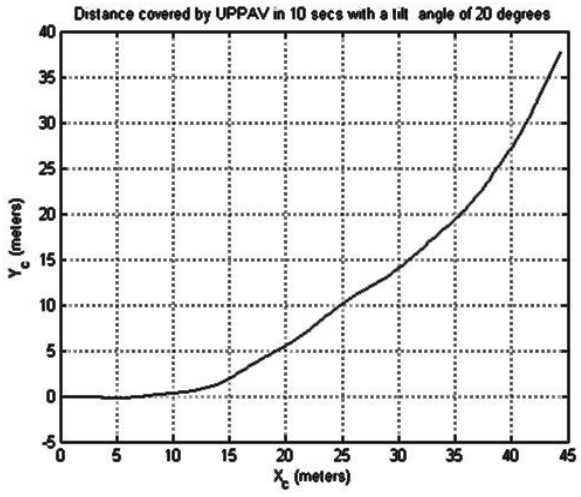

Fig 5. Distance covered by UPPAV

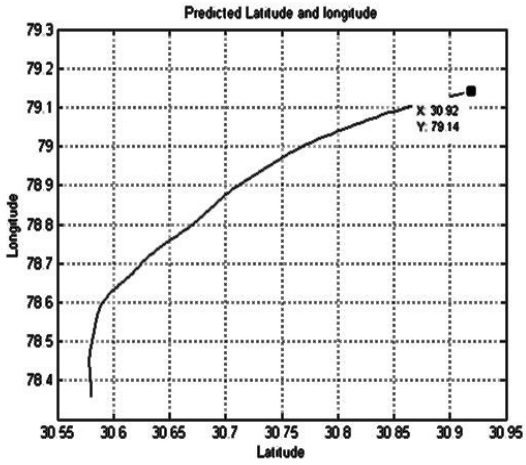

Fig 6. Latitude Longitude of UPPAV

IV. HARDWARE DEVELOPMENT

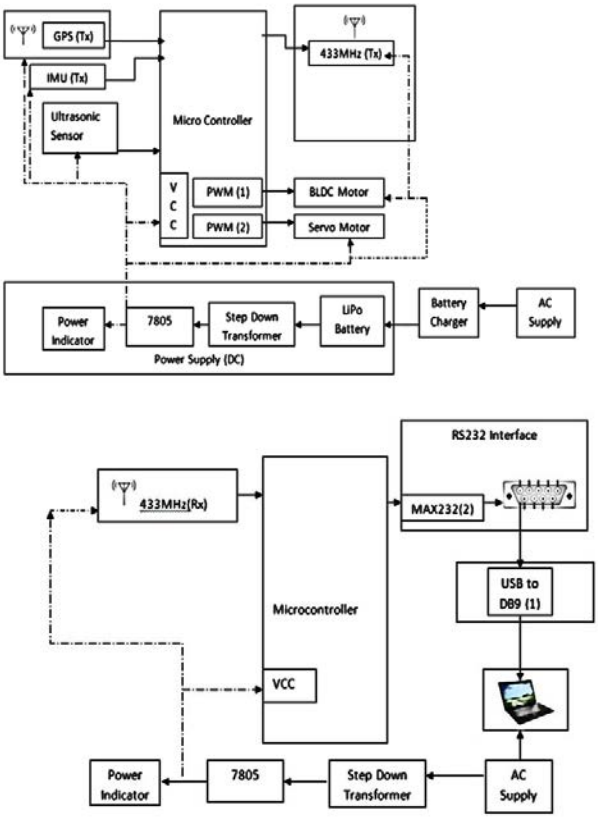

Fig 7: Block diagrams of the hardware module both on board and the ground station

The methodology followed for achieving the above mentioned target is to develop embedded system (Hardware Model). The hardware model is divided into two parts, which are, onboard embedded system design and ground station design the communication between the onboard embedded system and the ground station is done using 433MHz trans-receivers, as shown above in figure 7.

The hardware system on board and ground station has the following systems:

- GPS
- Microcontroller
- Power Supply
- 433MHz Trans-receivers
- MAX 232
- DB9

A. GPS

The GPS module has 4 pins. VCC, GND, Rx, Tx. The module continuously send the NMEA [10, 11] data which include $GPGGA, $GPGSA, $GPGSV and $GPRMC.

The GPGGA provides the current Latitude, Longitude and Altitude position of the Parafoil Aerial Vehicle.

The GPGGA data format is given as

$GPGGA,hhmmss.ss,llll.ll,a,yyyyy.yy,a,x,xx,x.x,x.x,M,x.x,M,x.x,xxxx*hh (shown in figure 9)

- hhmmss.ss = UTC of position
- llll.ll = latitude of position
- a = N or S
- yyyyy.yy = Longitude of position
- a = E or W
- x = GPS Quality indicator (0=no fix, 1=GPS fix, 2=Dif. GPS fix)
- xx = number of satellites in use
- x.x = horizontal dilution of precision
- x.x = Antenna altitude above mean-sea-level
- M = units of antenna altitude, meters
- x.x = Geoidal separation
- M = units of geoidal separation, meters
- x.x = Age of Differential GPS data (seconds)
- xxxx = Differential reference station ID

Out of all the data we are interested in Lat, Long and Alt values. These lat long and alt values are extracted using AVR Software interrupts, which discussed in detail in further sections.

B. Microcontroller

The Microcontroller used here is ATMEGA 16 [12] (AVR Series). The Latitude, Longitude and Altitude values are read using software interrupts [13] (discussed in detail in section III) and data is transmitted to 433 MHz Trans-receivers [14].

C. Powers Supply

The power supply unit takes in the 12V supply form the battery and gives out 5V for the microcontroller, GPS and the 433 MHz Trans-receivers.

D. MAX 232

The conversion of TTL logic to CMOS logic is done by MAX232 [6]. This IC is basically used for the creating communication between micro-controller and the PC (Personal Computer). The controller operates at TTL logic Level (0-5V) and the PC works on CMOS logic (-25V to 25V) [13]. Since the logic levels of both systems are different it becomes difficult to setup a communication link between the two systems. This link is provided by MAX232. This IC includes a capacitive voltage generator that supplies RS232 voltage levels using 5V supply. The receivers in MAX232 can accept -30V to +30V and the transmitters convert this input to RS232 level [15]. MAX232 needs four external capacitors whose value range from 1µF to 22µF.

V. ALGORITHM

A GPGGA_Extract algorithm is developed for determining the position of UPPAV. Once the GPS ia attached to the Microcontroller's reciever terminal the whole NMEA data is received by the controller using interrupt serviece routine (ISR). The controller then The developed algorithm is coded in Embedded C programming language for ATMEGA 16 microcontroller. The algorithm starts with enabling AVR input output ports, delay function and interrupts. checks for the GPGGA String. If the string is matched then the controller checks for '$', followed by End of Line and Next line. Once it recognizes this data the latittude, logitude and altitude values are extracted using their position in the string. The Algorithm for UPPAV is as shown below:

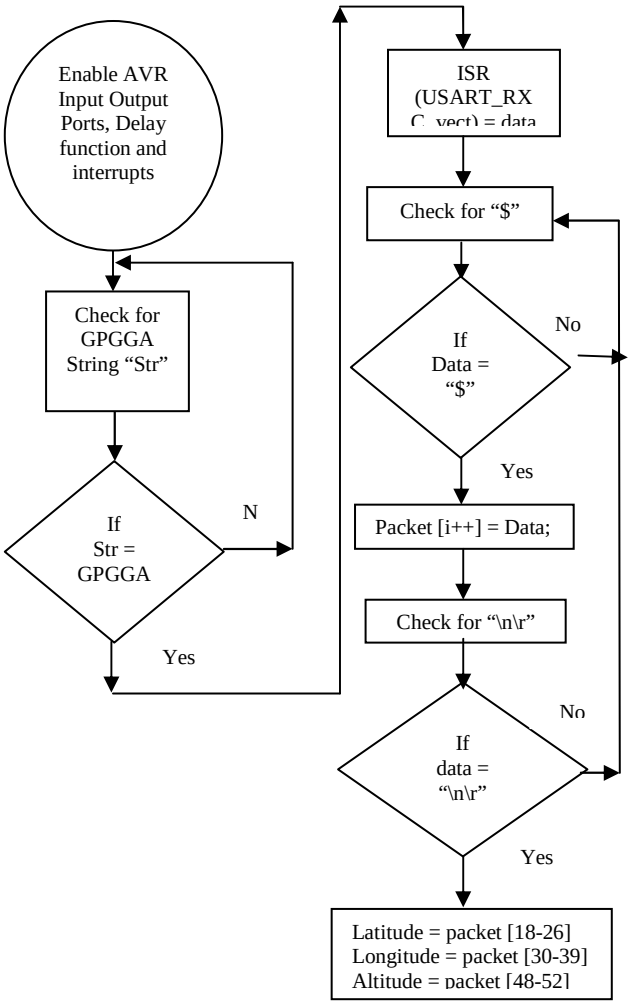

VI. Results and Conclusion

The simulation of the designed system is made in Proteus Software for checking the working of the system. Proteus is a software for designing Printed Circuit Boards, by Labcenter electronics. Figure 8 shows the schematic diagram of the hardware module designed. It has ATMEGA 16 microcontroller to read in the GPS values from COM Port and a 16X4 LCD with help of USART.

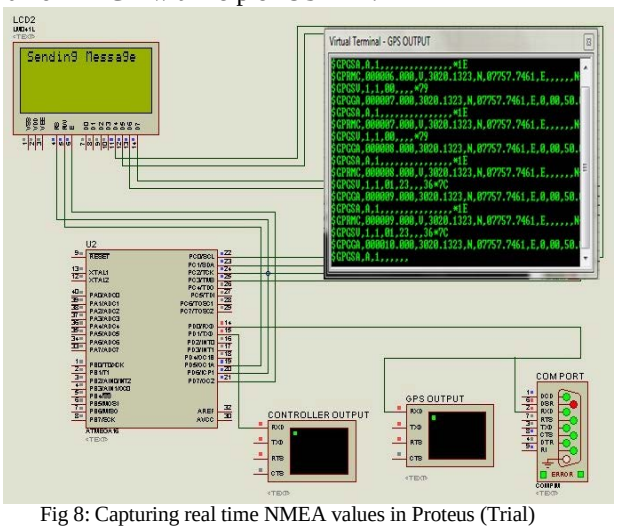

Fig 8: Capturing real time NMEA values in Proteus (Trial)

The Developed GPS module has been successfully developed and installed on the UPPAV. The data is logged successfully in the ground station which was used by the pilot to maneuver the vehicle to the desired location

The path followed by the UPPAV with about a 20 degrees tilt on the fly bar has been modeled successfully and the X, Y path has been traced for about 10 seconds. The traced path has been further converted into latitude and longitude values (as shown in figure 9) by taking the initial value measured from the developed GPS module. The values are captured in the ground station and are vaildated with google earth as shown in figure 11, altitude, pressure and temperature data obtained by the flight test are shown in figures through 12 to 15. The recorded test flight data are provided in Annexure 1. Because of the low speed of UPPAV the values obtained are accurate and precise.

The GPGGA value obtained in the Virtual terminal are extracted using GPGGA_Extract algorithm as discussed in section V. This module developed can be incorporated in any type of unmanned aerial vehicle.

This developed system can be useful to model the closed loop control system for a powered Parafoil aerial vehicle, so that the vehicle can be made completely autonomous.

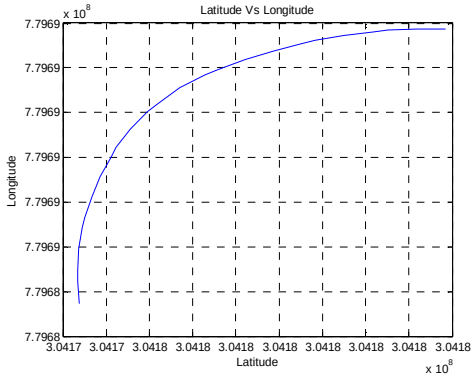

Fig 9. Aerial Distance Covered by UPPAV

VII. Future Scope

There are number of applications where the PAV would provide a unique capability that is not adequately satisfied by other devices currently available. The PAV is superior in terms of cost, ruggedness/durability, ease of use, portability, time to activate and reusability when compared with the competing technologies in variety of mission scenarios. There are number of military uses for developed PAV which include airdrop guidance, battle damage assessment, and communication in the rugged terrain. Civilian application include; an aid in search and rescue efforts, evaluating plant health by farmers and land management workers, and as a communications and observation device for forestry firefighting crews. Future work will involve in guidance navigation and control using waypoints, achieving an autonomous flight.

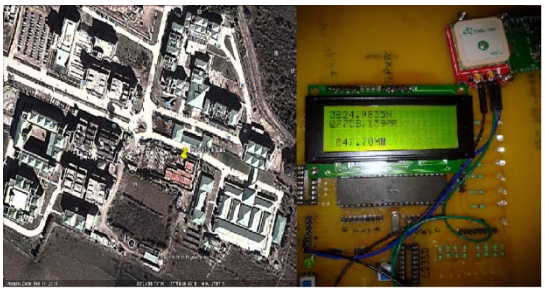

Fig 11: Validating the acquired GPS values with Google Earth

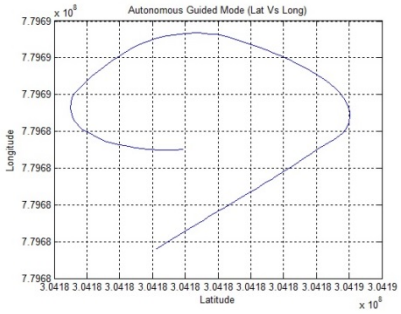

Fig 12. Path Covered by UPPAV

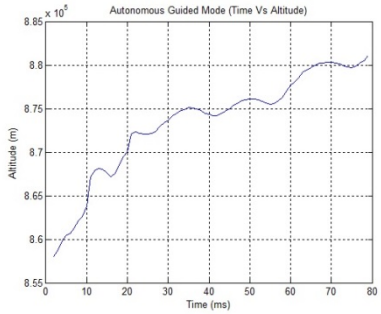

Fig 13. Altitude covered by UPPAV

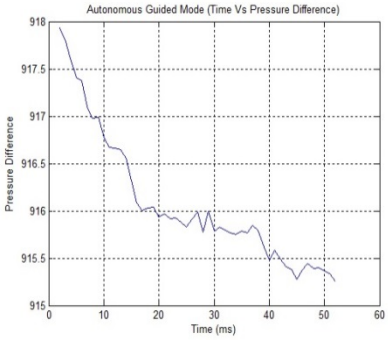

Fig 14. Pressure Difference with time during Take-off

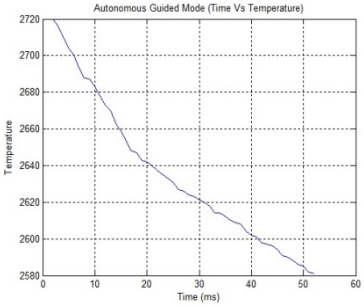

`` Fig 15. Decrease in Temperature with time during Take-off

REFERENCES

[1] Toohey, D., *Development of a small parafoil vehicle for precision delivery*, 2005, Massachusetts Institute of Technology.

[2] Hans-Peter Thamm, T.L., Christian Reuter. *Design of a process model for unmanned aerial systems (UAS) in emergencies*. in *10th International ISCRAM Conference*. 2013. Baden- Baden, Germany.

[3] Devalla, V. and O. Prakash, *Developments in unmanned powered parachute aerial vehicle: A review*. Aerospace and Electronic Systems Magazine, IEEE, 2014. **29**(11): p. 6-20.

[4] Dietro, P., *History of Paraplane*, in *Adirondack Chapter Newsletter*2012, EAA Spirit of Aviation.

[5] Chambers, J.R., *Longitudinal Dynamic Modeling and Control of Powered Parafoil*, in *Department of Mechanical Engineering*, Rochester Institute of Technology: New York.

[6] Devalla, V., O. Prakash, and A.K. Mondal. *Angle of Attack, Pitch Angle and Glide Angle Modeling at Various Thrust Inputs for a Powered Parachute Aerial Vehicle*. in *Book of Abstracts*. 2014. Department of Aerospace Engineering, IIT Kanpur.

[7] Akasaka T., B.G., Azuma A.,, *An investigation of the paraglider's turn mechanism.* Journal of the Japan Society for Aeronautical and Space Science., 1999. **47**(540): p. 1999.

[8] Slegers, N.J., *Effects of canopy-payload relative motion on control of autonomous parafoils.* Journal of guidance, control, and dynamics, 2010. **33**(1): p. 116-125.

[9] Wise, K. *Dynamics of a UAV with Parafoil under Powered Flight*. in *AIAA Guidance, Navigation, and Control Conference and Exhibit, Keystone, CO, AIAA*. 2006.

[10] Rhydolabz. *GPS*. [cited 2013 12, June]; Available from: http://www.rhydolabz.com/index.php?main_page=product_info&cPath=184_186&products_id=475.

[11] NMEA. *NMEA data*. 2015; Available from: http://www.nmea.org/.

[12] Datasheet, A., *AVR Atmega16, Atmega16L Datasheet.* Atmel Corporation, 2004.

[13] Mazidi, M.A., S. Naimi, and S. Naimi, *AVR Microcontroller and Embedded Systems: Using Assembly and C*2010: Prentice Hall Press.

[14] Baronti, P., et al., *Wireless sensor networks: A survey on the state of the art and the 802.15. 4 and ZigBee standards.* Computer communications, 2007. **30**(7): p. 1655-1695.

[15] Amit Kumar Mondal, V.D., Vivek Kaundal, Kamal Bansal, *Development of a Damper control system for combined cycle thermal gas power plant*, in *ASME Gas Turbine India 2014 Conference*2014, ASME: New Delhi, India.

PART IV

NANOADSORBENTS AND NANOFILTRATION

13

ADVANCED OXIDATION PROCESSES, NANOFILTRATION, AND APPLICATION OF BUBBLE COLUMN REACTOR

SUKANCHAN PALIT
Department of Chemical Engineering, University of Petroleum and Energy Studies, Dehradun, India

13.1 INTRODUCTION

Environmental engineering is moving toward the next generation of science and technology. The advanced oxidation process (AOP) is a major water treatment and waste treatment procedure. Due to strict and stringent environmental restrictions and regulations, scientists are keen on discovering newer and novel environmental engineering procedures. So, AOPs or membrane separation procedures are opening up new windows of innovation in this age of green technology. The world of imagination has brought the scientific age to a new reality. Integration of various AOPs for wastewater treatment has opened up exciting and exhilarating insights for the scientific community. Our aim in this chapter is to outline in a far-reaching review and experimental validation the importance of various AOPs, the potential of nanofiltration, and the applications of a visionary tool—the bubble column reactor. Our basic aim is to outline the importance of AOPs and nanofiltration of dye wastewater and integrate them with applications of a bubble column reactor.

13.2 VISION OF AOP

The vision of a scientist is versatile and inspiring. Research, scientific vision, and scientific steadfastness has compelled scientists to strive further. The world of chemical engineering and environmental engineering is ushering in a new global era, and a new world of scientific research is emerging. The scientific vision and immense scientific understanding of advanced oxidation processes (AOPs), nanofiltration, and bubble column reactors is awesome, ever-growing, and far-reaching. The basic advantages of a bubble column reactor are that it has feasible hydrodynamics and excellent heat and mass transfer characteristics. Extensive research work is being undertaken by scientists, researchers, and the learned scientific community. The world of the unknown is opening up to a new age and a new vision. Environmental restrictions and stringent regulations are the forerunners of this scientific vision.

AOPs comprise a promising and challenging technology for the treatment of wastewaters containing organic compounds that are not easily removable. All AOPs are designed to produce hydroxyl radicals, which act with high efficiency to destroy organic compounds. AOPs combine ozone(O_3), ultraviolet (UV), hydrogen peroxide (H_2O_2), and/or a catalyst to offer a powerful water treatment solution for the reduction and/or removal of residual organic compounds as measured by chemical oxygen demand (COD), biological oxygen demand (BOD), or total organic carbon (TOC). This chapter delineates in detail a general review of

Nanomaterials for Environmental Protection, First Edition. Edited by Boris I. Kharisov, Oxana V. Kharissova, and H. V. Rasika Dias.

efficient AOPs developed to decolorize and/or degrade organic pollutants for environment protection. The fundamentals involved in the main applications of typical methods such as Fenton, electro-Fenton, photo-Fenton, ozonation, and UV methods are deliberated and discussed in great detail. Various combinations of these processes and their industrial applications are outlined in this study.

13.3 VISION OF NANOFILTRATION AND THE WIDE DOMAIN OF MEMBRANE SCIENCE AND ITS IMPACT ON SCIENTIFIC RESEARCH PURSUIT

It is urgent and imperative to review and discuss the past to provide a compelling vision for the future. The research domain of membrane science and nanofiltration is undergoing rapid and spontaneous changes. The scientist's vision has widened and the emerging scientific imagination is compelling. The purpose of this chapter is to review the history of development of membranes and membrane processes particularly nanofiltration for water production in general and seawater desalination in particular. We want to highlight some new trends in the following areas: membrane development, membrane characterization, membrane transport, and membrane system design. The future prospects in the four areas are discussed in minute detail. Membrane development deals with recent progress in the development of reverse osmosis (RO) membranes used for desalination. There are two different approaches, both based on in situ polycondensation. One is to develop membranes for desalination of brackish water operable at ultralow pressure and the other is to develop membranes operable at high pressures to achieve high pure water recovery in seawater desalination. In the membrane characterization section, atomic force microscopy (AFM) is featured as a new tool to investigate the nature of membrane surfaces. The effects of surface roughness, which can be measured by AFM, on membrane productivity and membrane fouling are outlined.

An in-depth insight into the drawbacks of nanofiltration is presented by Van der Bruggen et al. [1]. According to their definition, nanofiltration was defined as "a process intermediate between reverse osmosis and ultrafiltration that rejects molecules which have a size in the order of one nanometer." They have reviewed every aspect of the subject of nanofiltration. Nanofiltration was introduced in the late 1980s, mainly aiming at combined softening and organics removal. Since then, the applications of nanofiltration have extended tremendously. An insight into the branch of nanofiltration showed the giant steps science has taken for the well-being of mankind.

The review delineates six challenging areas for nanofiltration where solutions and remedies are still scarce: (i) avoiding membrane fouling, and the possibility of remediation; (ii) improving the separation between solutes that can be achieved; (iii) further treatment of concentrates and an increase in the efficiency of separation; (iv) chemical resistance and limited/short life span of membranes; (v) insufficient and low rejection of pollutants in water treatment; and (iv) the urgent need for modeling and simulation tools. This chapter gives a holistic idea of the state of the art in this field and what the scientific fraternity should aim at as well as its vision. All six thrust areas or domains are interlinked and could possibly reach out in a greater way to bring about remedies and solutions.

Nanofiltration has new possibilities such as in drinking water production, arsenic removal, the removal of pesticides, the production of endocrine disruptors and chemicals, and partial desalination.

Matsuura [2] dealt with progress in membrane science and technology for seawater desalination in a phenomenal and visionary review paper. This review outlines some new trends in the following four areas: membrane development, membrane characterization, membrane transport, and membrane system design. Future targets, vision, and prospects in these four areas are delineated. The review deals with membrane development highlighting recent progress in the development of RO membranes used for desalination. There are two different approaches, both based on in situ polycondensation. One is to develop and devise membranes used for desalination of brackish water operable at ultralow pressures, and the other is to develop and devise membranes operable at high pressures to achieve high pure water recovery in seawater desalination. In the membrane characterization section, the application of AFM in investigating and discovering the science behind membrane surfaces is discussed. Also, the review paper by Matsuura (2001) deals with transport models made primarily for charged membranes. Membrane transport deals with transport models made primarily for charged membranes. Hybrid systems for seawater desalination in which membrane processes are incorporated are discussed. According to the Conclusion section in this review paper, there is an enormous and sizable potential to reduce desalination costs by combining membrane processes with novel separation techniques/unit operations.

Sidek et al. [3] reviewed a phenomenal paper on the factors governing the nanofiltration membrane separation process. The main objectives of this paper are to review the performance of nanofiltration membranes in removing unwanted particles from a solution by evaluating the factors, such as Donnan and steric interaction and transmembrane pressure (TMP), that influence rejection by the membrane. The right combination of membrane pore size (steric effect) and its effective charge density (Donnan effect) leads to optimum separation performance. However, the effect of TMP on nanofiltration rejection is not consistent. At high TMP, rejection can be either increased or decreased, depending on other operating parameters such as pH, ionic strength, the presence of salt. pH and feed concentration (ionic strength) play a significant role in nanofiltration membrane separation.

They outlined membrane characteristics governing factors. Trans membrane pressure drop (TMP) is outlined in major detail. The delineated features are effects of TMP on flow rate and rejection. They described in detail the physics behind the effects of TMP on flux rate. The effects of the TMP on the permeate flux at different solute concentrations can be observed by keeping the operating temperature and pH constant. The permeate flux at the steady state increases, with the applied pressure at all concentrations. An increase in flux was noted with an increase in the operating pressure. Since nanofiltration is basically a pressure-driven filtration process, flux is supposed to increase with pressure. The phenomenon can be mathematically explained.

Hong et al. [4] delineated the chemical and physical aspects of natural organic matter (NOM) fouling of nanofiltration membranes. The role of chemical and physical interactions in NOM fouling of nanofiltration membranes is systematically investigated. Results of fouling experiments with three basic acids demonstrate that membrane fouling increases with increasing electrolyte (NaCl) concentration, decreasing solution pH, and addition of divalent cations (Ca^{2+}). At fixed solution ionic strength, the presence of calcium ions, at concentrations typical of those found in natural waters, has a marked effect on membrane fouling. Divalent cations interact specifically with carboxyl functional groups and thus substantially reduce charge and the electrostatic repulsion between humic macromolecules.

In recent years, membrane filtration has emerged as a viable treatment alternative to comply with existing and pending water quality regulations. Of particular interest is the use of nanofiltration as a treatment alternative for the removal of NOM, a precursor of disinfection by-products, in anticipation of more stringent regulations. Nanofiltration technology also offers a versatile approach to meeting multiple water quality objectives, such as the control of organic, inorganic, and microbial contaminants.

Successful application of nanofiltration technology, however, requires efficient control of membrane fouling. Fouling, often associated with the accumulation of substances on the membrane surface or within the membrane pore structure, worsens membrane performance and ultimately shortens membrane life.

Hilal et al. [5] reviewed research work on using AFM toward improvement in nanofiltration membrane properties for desalination pretreatment.

Seawater is characterized by having a high degree of hardness, varying turbidity and bacterial contacts, and high total dissolved solids (TDS). These properties give rise to major problems such as scaling, fouling, high energy requirements, and the requirement of high-quality construction materials. To solve seawater desalination problems and to minimize their effect on productivity and water cost of conventional plants, a new approach using nanofiltration as pretreatment to both RO and thermal processes has been shown to enhance the production of desalted water and reduce the cost, yet it is an environmentally friendly process.

The following areas were covered:

a. Development of high-performance nanofiltration membranes
b. Development of accurate and practical characterization methods
c. Development of a good predictive modeling technique

The use of AFM in membrane studies was also outlined in detail.

Hilal et al. [6] attempted a comprehensive review of nanofiltration membranes and dealt with its treatment, pretreatment, modeling, and AFM. This review addresses the application of AFM in studying the morphology of membrane surfaces as part of nanofiltration membrane characterization.

A comprehensive review of nanofiltration in water treatments is presented including a review of the applications of nanofiltration in treating water as well as in the pretreatment process for desalination; the mechanism as well as minimization of nanofiltration membrane fouling problems; and the theories for modeling and transport of salt and charged and noncharged organic compounds in nanofiltration membranes.

Ashaghi et al. [7] dealt with nanofiltration in detail in their research review on ceramic ultrafiltration and nanofiltration membranes for oilfield-produced water treatment. Produced water is any fossil water that is brought to the surface along with crude oil or natural gas. By far, produced water is the largest by-product or waste stream by volume associated with oil and gas production. The volume of produced water is dependent upon the state of maturation of the field. There is an urgent need for new technologies for produced water treatment due to increased focus on water conservation and environmental regulation. Ceramic ultrafiltration and nanofiltration membranes represent a relatively new class of materials available for the treatment of produced water. According to their research, the issues needing to be addressed are the prevention of membrane fouling during operation and the provision of an expedient, cost-effective, and nonhazardous means of cleaning fouled membranes. The researchers embarked on the present study because there are not enough existing studies related to the treatment of oilfield-produced water using ceramic membranes. Ceramic membrane systems under nanofiltration and ultrafiltration conditions have proven to be economically attractive for the treatment of produced waters with elevated concentrations of oils and low to medium diameters of the particles.

No research review is complete unless the mechanisms of membrane science or nanofiltration are not taken into account.

Wijmans et al. [8] dealt with the solution–diffusion model in their review. The solution–diffusion model has emerged over the past 20 years as the most widely accepted explanation for transport in dialysis, RO, gas permeation, and pervaporation. In this review paper they dealt with the phenomenological equations for transport in these processes using the solution–diffusion model and derived the equations starting from the fundamental statement that flux is proportional to a gradient in chemical potential. The direct and indirect evidence for the model's validity is presented, together with a brief discussion of the transition between a solution–diffusion membrane and a pore-flow membrane seen in nanofiltration membranes and some gas-permeation membranes. The principal property of membranes used in separation applications is the ability to control the permeation of different species. Two models are used to describe this permeation process. The first is the solution–diffusion model, in which permeants dissolve in the membrane material and then diffuse through the membrane down a concentration gradient. A separation is achieved between different permeants because of differences in the amount of material that dissolves in the membrane and the rate at which the material diffuses through the membrane. The second is the pore flow model in which permeants are separated by pressure-driven convective flow through tiny pores.

Nghiem et al. [9] delineated the removal of natural hormones by nanofiltration membranes with measuring, modeling, and mechanisms. The removal of four natural steroid hormones—estradiol, estrone, testosterone, and progesterone—by nanofiltration membranes was investigated. Two nanofiltration membranes with quite different salt retention characteristics were utilized.

Renou et al. [10] reviewed the opportunities in landfill leachate treatment. In most countries, sanitary landfilling is nowadays the most common way to eliminate municipal solid wastes (MSW). In spite of many advantages, the generation of heavily polluted leachates, with significant variations in both volumetric flow and chemical composition, constitutes a major drawback. Year after year, the recognition of landfill leachate effect on the environment has forced authorities to fix more and more stringent requirements for pollution control. This paper is a review of landfill leachate treatments. The advantages and drawbacks of the various treatments are discussed under the following topics: (i) leachate transfer, (ii) biodegradation, (iii) chemical and physical methods, and (iv) membrane processes.

Childress et al. [11] related nanofiltration membrane performance to membrane charge (electrokinetic) characteristics. The performance (i.e., water flux and solute rejection) of a thin-film composite (TFC) aromatic polyamide nanofiltration membrane and its relation to membrane surface charge (electrokinetic) characteristics was studied.

Properties of nanofiltration membranes, model development, and industrial applications have been delineated in a dissertation by Johannes Martinus Koen Timmer [12]. The dissertation deals with industrial membrane processes and aspects of nanofiltration. It also deals with the transport of lactic acid through RO and nanofiltration membranes. A model for mass transport is described. In the pursuit of excellence, they delineated and described the entire pressure-driven membrane process. Their research encompassed the dairy industry and the applications of nanofiltration.

Water engineering or environmental engineering is a boost to this research pursuit when we consider the work done by Xia et al. [13] for arsenic removal by nanofiltration and its application in China. According to their study, arsenic contamination of groundwater and the associated health risks have been reported in many parts of China. Nanofiltration is a promising technology for arsenic removal since it requires less energy than traditional RO membranes. In this study, the removal of arsenic from synthetic waters by nanofiltration membranes was investigated. Arsenic rejection experiments included variation of arsenic feed concentration, pH, and existence of other ionic compounds. The possible influence of NOM on As(V) rejection by nanofiltration membranes was also explored.

Orecki and Tomaszewska [14] did a fundamental research on oily wastewater treatment using nanofiltration process. The authors lucidly and intensely dealt with a positive objective on the domain of oily wastewater treatment using the formidable intellectual challenge of the application area of nanofiltration. The nanofiltration studies were carried out with a permeate obtained from ultrafiltration (UF) (used for the treatment of the oily wastewater from metal industry). The influence of transmembrane pressure on a permeate flux, the degree of rejection of oil and inorganic compounds were investigated with great precision. The studies on the nanofiltration treatment of oil wastewater demonstrated a high effectiveness of the rejection of oil and inorganic compounds. The permeate obtained from the treatment was free of oil. The nanofiltration process was carried out in a pilot plant equipped with a tubular module with the AFC 30 membrane (PCI)—(the working area equal to 0.9 m^2) and a spiral wound module (with the nanofiltration 270-2540 membrane (Film Tec—the working area equal to 2.6 m^2). The studies earlier predicted and performed showed that the membranes differed in molecular weight cut-off (MWCO). The MWCO of the membranes were found out to be equal to 250 g/mol for nanofiltration 270-2540 and nanofiltration AFC30, respectively. The results and discussion showed a remarkable pattern. The raw oily wastewater used in these studies was collected from metal treatment industry. Apart from oil, the wastewater contained a lot of other contaminants, including solid state, lubricants, metal fines and sometimes dissolved metals. Although the UF membranes rejected oil in 90%, the permeate still contained different solutes. The authors performed an integrated ultrafiltration and nanofiltration technique. The conclusions in this study were affirmative. As a result of nanofiltration used as a second stage of oily waste water treatment the removal of organic compounds (TOC) for the studied membranes (nanofiltration 270-2540 and nanofiltration AFC 30) exceeded 65%. Moreover the cations are

rejected by 75% and the sulfates were rejected by 95%. The permeate did not contain oil. Orecki and Tomaszewska [14] established a theory of the effectiveness of integrated ultrafiltration—nanofiltration process. Hilal et al. [15] dealt with nanofiltration of highly concentrated salt solutions approaching seawater salinity. Nanofiltration membranes have been employed in pretreatment unit operations in both thermal and membrane seawater desalination processes. This has resulted in reduction of chemicals used in pretreatment processes as well as lowering the energy consumption and water production cost and therefore has led to a more environmentally friendly process. In order to predict nanofiltration membrane performance, a systematic study on the filtration performance of selected commercial nanofiltration membranes against brackish water and seawater is required. In this study, three commercial nanofiltration membranes (NF90, NF270, NF30) have been used to treat highly concentrated (NaCl) salt solutions up to 25,000 ppm, a salinity level similar to that of seawater.

A phenomenal review on cotton textile processing, its waste generation, and effluent treatment was undertaken by Babu et al. [16]. This review discusses cotton textile processing and methods of treating effluents in the textile industry. This area of research combines a discussion of waste production from textile processes, such as desizing, mercerizing, bleaching, dyeing, finishing, and printing with a discussion of advanced methods of effluent treatment, such as electrooxidation, biotreatment, and photochemical and membrane processes.

Ning [17] undertook research work on arsenic removal by RO. A short review on the RO process and applications was dealt with by Garud et al. [18]. The short review discusses the applicability of an RO system for treating effluents from the beverage industry, distillery spent wash, groundwater treatment, the recovery of phenol compounds and the reclamation of wastewater, and seawater RO (SWRO) treatment indicating the efficiency and applicability of RO technology.

13.4 FURTHER RESEARCH ENDEAVOR IN THE FIELD OF NANOFILTRATION

Nanofiltration presents vast and challenging opportunities for knowledge advancement in the field of desalination technology. The world of environmental engineering will usher in a new era in the field of membrane science with immense challenges and vision. Our endeavor encompasses research on AOPs and the application of a bubble column reactor. The challenges that lie ahead are significant and far-reaching. Desalination technology and nanofiltration have a close umbilical relationship. These two branches of engineering will definitely solve the intricate problems of water technology. Man's scientific vision will be enhanced and emphasized if the hurdles are overcome and frontiers scaled. The world of environmental engineering and nanofiltration will surely be a challenge to the drinking water problems of the suffering millions.

13.5 RESEARCH THRUST AREAS IN THE FIELD OF AOPs AND THE VISION TOWARD EFFECTIVE OZONATION PROCEDURES

Palit et al. [19] dealt with membrane separation processes and RO in a detailed review. The application area and thrust was on wastewater treatment. The author has widely described the scope of RO and its potential applications.

Stasinakis [20] in an insightful review dealt with immense depth on the use of selected advanced oxidation processes for wastewater treatment. The purpose and the aim of the study was to review the use of titanium dioxide/UV light process, hydrogen peroxide/UV light process and Fenton's reactions in wastewater treatment. The main reactions and the operating parameters (initial concentration of the target compounds, amount of oxidation agents and catalysts, nature of the wastewater etc) affecting these processes are reported, while several recent applications to wastewater treatment are presented.

Koch et al. [21] dealt with immense details on ozonation of hydrolyzed azo dye reactive yellow 84(CI). According to scientific innovation and immense scientific understanding, the combination of chemical and biological water treatment processes is a promising technique to reduce recalcitrant wastewater loads. Ozonation has been applied to many fields in water and wastewater treatment. Especially for textile mill effluents ozonation can achieve high color removal, enhance biodegradability, destroy phenols and reduce chemical oxygen demand (COD). This work unfolds the reaction intermediates and products formed during ozonation. The work mainly deals with the degradation of hydrolyzed Reactive Yellow 84 (Color Index), a widely used azo dye in textile finishing processes with two monochlorotriazine anchor groups. The authors have investigated the formation of intermediate products and the reaction kinetics of the entire procedure of ozonation. A general review on AOPs for wastewater treatment was done by Sharma et al. [22]. Efficient AOPs developed to decolorize and/or degrade organic pollutants for environmental protection were covered. The fundamentals and main applications of typical methods such as Fenton, electro-Fenton, photo-Fenton, ozonation, and UV radiation were discussed. Various combinations of these processes and their industrial applications are the visionary aspects of this study.

Research on AOPs for the treatment of textile and dye wastewater was attempted by Kalra et al. [23]. Their paper reviews different AOPs like ozonation, hydrogen peroxide, UV radiation, and their combination for comparison of treatment efficiencies for remediation of textile wastewater. This paper reveals that the treatment efficiencies depend on the characteristics of wastewater to be treated.

The use of AOP in an ozone+ hydrogen peroxide system for the removal of cyanide from water was dealt with by Kepa et al. [24]. The results of laboratory tests are presented in this paper, which indicate that AOPs can be used for the removal of cyanide from water. A comparative analysis was carried out for the processes of ozonation, oxidation with hydrogen peroxide, and advanced oxidation in the O_3+H_2O_2 system.

Zhou et al. [25] wrote a review paper on advanced technologies in water and wastewater treatment. They dealt with three emerging treatment technologies including membrane filtration, AOPs, and UV irradiation that hold great promise to provide alternatives for greater protection of human health and environment.

Kdasi et al. [26] provided a clear picture of the treatment of textile wastewater by AOPs in a review. An overview of basic treatment efficiency for different AOPs is considered and presented based on specific features. The review covers a lucid introduction, textile wastewater characteristics, a description of AOPs, application areas of a UV lamp, ozone, O_3/UV, H_2O_2, O_3/H_2O_2, O_3/H_2O_2 (peroxane), O_3/H_2O_2/UV, and a broad conclusion.

Palit et al. [27] touched upon membrane separation processes and AOPs for dyes in a bubble column reactor in a keen and far-reaching overview. Topics covered included the dependence of rate constant, order of reaction, and subsequently rate of reaction on the pH and oxidation–reduction potential associated with the ozonation of dye.

Gogate et al. [28] dealt with imperative technologies for wastewater treatment with emphasis on oxidation technologies at ambient conditions in a review. This work highlights the basis of the different oxidation processes including the operation parameters for the reactor design with a complete overview of the various applications for wastewater treatment in the recent years.

Chiron et al. [29] explained in a review the state of the art of pesticide chemical oxidation. This review reveals a general lack of data on kinetics of formation and disappearance of the major by-products. The efficiency of AOPs has scarcely been investigated at the industrial scale, that is, in presence of a mixture of active ingredients together with their formulating agents and at concentration levels above 10 mg/l.

Kos et al. [30] dealt with the subject of decoloration of real textile wastewater with AOPs. The efficiency rates of AOPs for the decoloration of different types of textile wastewater from textile plants in Lodz, Poland, were compared on the basis of the results obtained. AOPs with the use of ozone, gamma radiation, hydrogen peroxide, and UV radiation gave good decoloration results.

Suty et al. [31] described the applications of AOPs with emphasis on the present and future aspects. The use of AOPs to remove pollutants in various water treatment applications has been the subject of study for around 30 years. Most of the available AOPs have been investigated in depth, and a considerable body of knowledge has been built up about the reactivity of many pollutants. Nevertheless, it is difficult to obtain an accurate picture of the use of AOPs, and their applications for a range of water treatment processes have not been determined to date. The purpose of this overview is to discuss these processes and provide an indication of future trends and prospects.

Abdelmalek et al. [32] dealt in the area of removal of pharmaceutical and personal care products (PPCPs) from RO retentate using AOPs. Studies focusing on pharmaceutical and PPCPs have raised questions concerning their concentrations in the RO retentate. AOPs are alternatives for destroying these compounds in retentate that contains high concentration of effluent organic matter (EFOM) and other inorganic constituents.

Huber et al. [33] dealt with oxidation of pharmaceuticals during ozonation and AOP applications in drinking water treatment. It was shown that the second-order rate constants determined in pure aqueous solutions could be applied to predict the behavior of pharmaceuticals dissolved in natural water. Overall, it can be concluded that ozonation and AOPs are promising processes for efficient removal of pharmaceuticals in drinking water.

Huber et al. [34] explained decolorization of process waters in deinking mills and similar applications in a review. Process waters in deinking mills often feature a strong coloration, due to dyes and pigments released from the recovered paper. This can usually be remediated by pulp bleaching treatment with appropriate chemicals. In this review, the available technologies for process water decolorization are discussed (chemical methods, physicochemical methods, and biological treatments).

13.6 MAN'S SCIENTIFIC MIND TOWARD NOVEL ENVIRONMENTAL ENGINEERING PROCEDURES

Man's scientific vision is targeted toward improving the lot of the suffering millions and toward tackling drinking water issues. The hidden scientific truth and scientific vision is targeted in every step towards progress of purposeful and definitive research pursuit. The aim of this chapter is to delineate the intricacies of wastewater treatment and bring before the scientific community

rigorous scientific inquiry. The greatness of the past and present will frame the future. So the aim and mission towards a better and congenial human society is ushering in hope and insightful destiny.

13.7 APPLICATION OF A BUBBLE COLUMN REACTOR AND VISION OF INNOVATIVE IDEAS

The bubble column reactor is a visionary tool for its application in AOPs. Challenges lie ahead in the integration of nanofiltration and the bubble column reactor. Excellent heat and mass transfer characteristics urges the scientific community to declare it as a challenging and visionary tool. The world of environmental engineering and the domain of wastewater treatment will usher in a new era with the application of bubble column reactor.

Bubble column reactors are intensively used as multiphase reactors and contactors in the chemical, biological, and pharmaceutical domains. They provide several advantages during operation and maintenance such as high heat and mass transfer characteristics, compactness, and low operating and maintenance costs. Three-phase bubble column reactors are widely used in chemical reaction engineering, that is, in the presence of catalysts, and also in biochemical applications where microorganisms are utilized as solid suspensions in order to manufacture industrially valuable bioproducts. Investigation of design parameters characterizing the operation and transport phenomena of bubble columns has led to a better understanding of hydrodynamic properties, heat and mass transfer characteristics, and flow regime mechanisms at work during the operation. The review [35] also targets and focuses on bubble column reactors, their description, design and operation, application areas, fluid dynamics, and regime analysis encountered.

The application of bubble column reactors has had a tremendous impact in recent years in the field of environmental engineering. The world of unknown in the areas of AOPs and nanofiltration will open up new windows of innovation and intuition in the years to come. Bubble column reactors have new applications with regard to AOPs. The vision is clear-cut with the frontiers of environmental science and engineering expanding to unprecedented levels. The grit and determination of the scientist's vision is inspiring and immense. The common man's problems in the field of desalination will mostly be solved by the science of nanofiltration. Research areas will slowly grow to visionary proportions.

13.8 DOCTRINE OF HEAT AND MASS TRANSFER CHARACTERISTICS OF A BUBBLE COLUMN REACTOR

Heat and mass transfer predictabilities are the major targets of the operation of bubble column reactor. Theoretically, a scientist's vision is toward better operation and maintenance of this visionary tool. The aim is to achieve better hydrodynamics as well as better reactivity, heat, and mass transfer.

13.9 DOCTRINE OF HYDRODYNAMICS OF BUBBLE COLUMN REACTOR AND MULTIPHASE FLOW

The importance of hydrodynamics of bubble column and the associated regime of multiphase flow is targeted toward efficient reactivity and linked to heat and mass transfer characteristics.

Bubble column reactors belong to the general class of multiphase reactors that include mainly three categories, that is, trickle bed reactors (fixed or packed bed), fluidized bed reactor, and bubble column reactor [36–39].

13.10 HIDDEN TRUTH IN THE DOMAIN OF ENVIRONMENTAL ENGINEERING AND NANOFILTRATION

Hurdles and unsurpassed barriers shapes the future and the scientific rigor is a vibrant witness. The greatness of environmental engineering tools are unraveled and the human society aims at a sustainable future. The Loeb–Sourirajan model has revolutionized the entire field of membrane science. Principles of membrane science have been established through scientific research. Newer and novel methods of water treatment and desalination are shaping and reshaping scientific intuition. Environmental engineering will usher in a new dawn in science and technology. The backbone of this unending scientific endeavor is strict and stringent environmental regulations. Developed and developing nations are gearing up toward new challenges to embrace the far-reaching environmental engineering frontier.

13.11 FUTURE VISION AND FUTURE FLOW OF THOUGHTS

Nanofiltration has been found to be extremely effective and visionary and will be very much in demand in the years to come [36–39]. Vision, opportunity, and diligent truth will propel the scientist's vision toward a new scientific generation. The greatness and the faults of the technology are envisioned in its application. Bubble column reactors and AOPs are also pillars of the ongoing review. Their applications in the field of environmental engineering are extremely purposeful, intricate, and far-reaching. Man's scientific vision and scientific endeavor is powered by a determination—the determination to serve the suffering millions. The problem of drinking water is immense, and stringent hurdles need to be overcome in both developed and developing countries. So the ultimate target and vision is to make technology accessible to the common masses and venture out to heal the wounds of science and technology. Nanofiltration, AOPs, and the application of bubble column reactors is just a beginning. The application areas of nanofiltration are absolutely far-reaching and visionary. The world will face new challenges in these scientific domains in years to come.

ACKNOWLEDGMENT

The author wishes to acknowledge Dr. Bhaskar Sengupta of Queen's University, Belfast, United Kingdom, under whose guidance he did research work on ozonation of dyes in a bubble column reactor. The author gratefully acknowledges the contributions of past and present teachers of Jadavpur University, Kolkata, India. Also, the contribution of staff, students, teachers, and management of University of Petroleum and Energy Studies, Dehradun, India, needs to be mentioned.

REFERENCES

[1] Bruggen V, Manttari M, Nystrom M. Drawbacks of applying nanofiltration and how to avoid them: a review. Sep Purif Technol 2008;63:251–263.

[2] Matsuura T. Progress in membrane science and technology for seawater desalination—a review. Desalination 2001;134:47–54.

[3] Sidek NM, Ali N, Fauzi SAA. The governing factors of nanofiltration membrane separation process performance: a review, UMTAS, Empowering Science Technology and Innovation towards a Better Tomorrow; 2011, 241–248.

[4] Hong S, Elimelech M. Chemical and physical aspects of natural organic matter (NOM) fouling of nanofiltration membranes. J Membr Sci 1997;132:159–181.

[5] Hilal N, Mohammad AW, Atkin B, Darwish NA. Using atomic force microscopy towards improvement in nanofiltration membranes properties for desalination pretreatment—a review. Desalination 2003;157:137–144.

[6] Hilal N, Al-Zoubi H, Darwish NA, Mohammad AW, Abu Arabi M. A comprehensive review of nanofiltration membranes: treatment, pretreatment, modeling and atomic force microscopy. Desalination 2004;170:281–308.

[7] Ashaghi KS, Ebrahimi M, Czermak P. Ceramic ultrafiltration and nanofiltration membranes for oilfield produced water treatment: a mini review. Open Environ J 2007;1:1–8.

[8] Wijmanns JG, Baker RW. The solution–diffusion model—a review. J Membr Sci 1995;107:1–21.

[9] Nghiem LD, Schafer AI, Elimelech M. Removal of natural hormones by nanofiltration membranes: measurement, modeling and mechanisms. Environ Sci Technol 2004;38:1888–1896.

[10] Renou S, Givaudan JG, Poulain S, Dirassouyan F, Moulin P. Landfill leachate treatment: review and opportunity. J Hazard Mater 2008;150:468–493.

[11] Childress A, Elimelech M. Relating nanofiltration membrane performance to membrane charge (electrokinetic) characteristics. Environ Sci Technol 2000;34:3710–3716.

[12] Timmer JMK. Properties of nanofiltration membranes; model development and industrial application [PhD thesis]. Eindhoven: Technische Universiteit; 2001.

[13] Xia S, Dong B, Zhang Q, Xu B, Gao N, Causseranda C. Study of arsenic removal by nanofiltration and its application in China. Desalination 2007;204:374–379.

[14] Orecki A, Tomaszewska M. The oily wastewater treatment using the nanofiltration process. Pol J Chem Technol 2007; 9 (4):40–42.

[15] Hilal N, Al-Zoubi H, Mohammad AW, Darwish N. Nanofiltration of highly concentrated salt solutions up to seawater salinity. Desalination 2005;184:315–326.

[16] Babu RB, Parande AK, Raghu S, Prem Kumar T. Cotton textile processing: waste generation and effluent treatment. J Cotton Sci 2007;11:141–153.

[17] Ning RY. Arsenic removal by reverse osmosis. Desalination 2002;143:237–241.

[18] Garud RM, Kore SV, Kore VS, Kulkarni GS. A short review on process and applications of reverse osmosis. Univ J Environ Res Technol 2011;1 (3):233–238.

[19] Palit S. A short review of applications of reverse osmosis and other membrane separation procedures. Int J Chem Sci Appl 2012;3 (2):302–305.

[20] Stasinakis AS. Use of selected advanced oxidation processes (AOPs) for wastewater treatment: a mini review. Global NEST J. 2008;10 (3): 376–385.

[21] Koch M. Yediler A, Lienert D, Insel G, Kettrup A. Ozonation of hydrolyzed azo dye reactive yellow 84(CI). Chemosphere 2002;46:109–113.

[22] Sharma S, Ruparelia JP, Patel ML. A general review on advanced oxidation processes for waste water treatment. International Conference on Current Trends in Technology (NUiCONE-2011). Institute of Technology, Nirma University, Ahmedabad, India; December 8–10, 2011.

[23] Kalra SS, Mohan S, Sinha A, Singh G. Advanced oxidation processes for treatment of textile and dye wastewater: a review. 2nd International conference on environmental science and development IPCBEE 2011, Vol. 4. Singapore: IACSIT Press.

[24] Kepa U, Stanczyk-Mazanek E, Stepniak L. The use of advanced oxidation process in the ozone+ hydrogen peroxide system for the removal of cyanide from water. Desalination 2008;223:187–193.

[25] Zhou H, Smith DW. Advanced technologies in water and wastewater treatment. J Environ Eng Sci 2002;1:247–264.

[26] Al-Kdasi A, Idris A, Saed K, Guan CT. Treatment of textile wastewater by advanced oxidation processes: a review. Global Nest Int J 2004;6 (3):222–230.

[27] Palit S. Membrane separation processes and advanced oxidation processes of dyes in bubble column reactor-a keen and far reaching overview. Int J ChemTech Res 2012;4 (3):862–866.

[28] Gogate PR, Pandit AB. A review of imperative technologies for wastewater treatment I: oxidation technologies at ambient conditions. Adv Environ Res 2004;8:500–551.

[29] Chiron S, Fernandez-Alba A, Rodriguez A, Garcia-Calvo E. Pesticide chemical oxidation: state of the art. Water Res 2000;34 (2):366–377.

[30] Kos L, Perkowski J. Decolouration of real textile wastewater with advanced oxidation processes. Fibres Text East Eur 2003;11 (4):43.

[31] Suty H, De Traversay C, Cost M. Applications of advanced oxidation processes: present and future. Water Sci Technol 2004;49 (4):227–233.

[32] Abdelmelek SB, Greaves J, Ishida KP, Cooper WJ, Song W. Removal of pharmaceutical and personal care products from reverse osmosis retentate using advanced oxidation processes. Environ Sci Technol 2011;45:3665–3671.

[33] Huber MM, Canonica S, Park GY, Gunten UV. Oxidation of pharmaceuticals during ozonation and advanced oxidation processes. Environ Sci Technol 2003;37:1016–1024.

[34] Huber P, Carre B. Decolorization of process waters in deinking mills and similar applications: a review. BioResources 2012;7 (1):1366.

[35] Kantarci N, Borak F, Ulgen KO. Bubble column reactors. Process Biochem 2005;40:2263–2283.

[36] Sukanchan P. Progress in membrane separation processes, ozonation and other advanced oxidation processes-a review. Int J Chem Anal Sci 2012;3 (1):1290–1292.

[37] Sukanchan P. Ozone treatment as an effective advanced oxidation process for the degradation of textile dye-effluents. Int J Chem Anal Sci 2012;3 (1):1293–1295.

[38] Palit S. Ozonation of direct red—23 dye in a fixed bed batch bubble column reactor. Ind J of Sci Technol 2009;2 (10).

[39] Palit S. Ozonation associated with nanofiltration as an effective procedure in treating dye effluents from textile industries with the help of a bubble column: a review. Int J Chem Chem Eng 2011;1 (1):53–60.

Evaluation and Analysis of Knowledge Management Best Practices in Software Process Improvement A multicase Experience

MITALI CHUGH
Department of Computer Science
Tula's Institute
Dehradun, India
mitalichugh21@yahoo.co.in

NEERAJ CHUGH
Department of CIT
UPES, Bidholi
Dehradun, India
neeraj_chugh77@yahoo.co.in

DEVENDRA KUMAR PUNIA
JK Lakshmipant University,
Jaipur, India
devendra.punia@gmail.com

***Abstract*— Software is important for our day-to-day lives and its impact is rising constantly. The quality of the developed software is straightforwardly dependent on the quality of the development process, researchers and practitioners primarily focus on improvement of the software process. Software Process Improvement (SPI) is a systematic and well-organized approach for development of the capabilities of software organizations and it is done through the evaluation of the existing practices of the organization and development of the software processes based on the competencies and experiences of the practitioners of the organization. There are a number of studies that focus on the practical use of KM in SPI. In this research work it has been explored though multicase analysis how KM can be significant and supports SPI.**

***Keywords*—software development; software quality; SDLC models; SPI; knowledge management; software engineering.**

I. IMPORTANCE OF SOFTWARE

Software is a significant component of individual's day-to-day life. It is hidden in the products that we use in our daily activities. Cars, airplanes, factories, mobile phones, travel agencies, military, banks, games etc. are depended or controlled by software [1]. The software plays an important role than ever and its significance is increasing continuously. The controlling software for the products should be efficient and reliable i.e. it should be of high quality. The versions and functionalities of software have increased greatly along with the significance of quality of software. Software Development Organizations aim to produce high quality software, which is developed by software engineers or innovative employees who will efficiently develop and use an organization's knowledge and expertise. But much cited Standish report on software projects shows, "a staggering 31.1% of projects will be cancelled before they ever get completed. Further results indicate 52.7% of projects will cost 189% of their original estimates. The cost of these failures and overruns are just the tip of the proverbial iceberg. The lost opportunity costs are not measurable, but could easily be in the trillions of dollars..." [2] The ongoing changes in technology and increasing demand of software affect the software processes and practices in such a way that they are no longer static in nature. Moreover, the quality of the developed software is directly dependent on the quality of the development process, researchers and practitioners mainly focus on improvement of the software process [3]. Software Process Improvement (SPI) is a methodical and efficient approach for developing the capabilities of software organizations and it is done through the evaluation of the existing practices of the organization and development of the software processes based on the competencies and experiences of the practitioners of the organization. One of the major challenges is to frame the strategies and mechanisms in order to manage the relevant and updated knowledge about the software development and maintenance. Insights from the knowledge management field are thus potentially helpful in software process improvement for facilitating the creation, amendment, and collaboration of software processes in an organization proceedings. A number of studies have emphasized and illustrated the usefulness of applying KM to SPI. However, a lot more has to be done for further exploring the practical use of KM in the context of SPI. In this research work focus is on the practical use of KM in SPI and explores the answers for the following questions: 1) How SPI is carried in practice? 2) How does KM support SPI? 3) What are the practical issues/challenges that are to be addressed for managing knowledge in SPI?

II. SOFTWARE PROCESS IMPROVEMENT

A number of studies have emphasized and illustrated the usefulness of applying KM to SPI. However, a lot more has to be done for further exploring the practical use of KM in the context of SPI. In this research work focus is on the practical use of KM in SPI and explores the answers for the following questions: 1) How SPI is carried in practice? 2) How does KM support SPI? 3) What are the practical issues/challenges that are to be addressed for managing knowledge in SPI? In 1970s, software development teams rarely developed applications within due constraints of time and budget. The applications developed often did not meet requirements of their customers and systems. The similar trend continued during the 1980s and

978-1-4799-1734-1/15 $31.00 © 2015 IEEE
DOI 10.1109/ICACCE.2015.76

1990s. Today, delivery of software systems is still delayed; they cost more than what has been estimated, and contain a number of defects. To overcome these inadequacies, there are a number of software process standards, such as the IS0 9001 [4], CMM [5], BOOTSTRAP [6], SPICE [7], IDEAL [8] which have been implemented by the software development organizations. These software process standards advise organizations what has to be done for developing quality software. According to [9] SPI concentrates on three primary concerns: the management of SPI activities, the approach taken to guide the SPI programs, and the perspective used to focus attention on the SPI goal(s). The management of SPI activities are based on three ideas: 1) the activities of SPI are planned in a dynamic way, 2) all improvement activities are cautiously planned, and3) It is ensured that the feedback is taken for the software engineering practices that are followed. Finally, the perception of SPI is focused on three ideas: 1) SPI is based on software processes, 2) the competencies of practitioners' are considered as the key resource, and 3) SPI focuses to change the context of the software operation to generate sustainable support for the practitioners' involved. [9][10].

III. KNOWLEDGE MANAGEMENT (KM)

Survival and success of any organization depends on organization's adaptability to the changing business environment. The competitive environment is no longer predictable and it is changing rapidly in terms of complexity and uncertainty. In consequence knowledge Management (KM) has been recognized as a source for enhancing organization's capabilities resulting in success of the organization. For understanding knowledge Management it is important to distinguish knowledge from information. Thus we can say: 1) Information consists of facts and data describing a problem and knowledge covers truths and beliefs, concepts and Know-how.2) Information relates to description or definition while knowledge comprises of strategy, practice, method or approach. We cannot consider data and information as knowledge until we grill the facts and values from it. In the hierarchy knowledge is at the highest level, information at the middle level and data at the lowest level. We initially started with data processing in 1960s moved on to information age in 1980s and finally reached knowledge age in 1990s where knowledge has to be managed. Knowledge management is difficult concept to define as it is a multifaceted concept for different circumstances and for different people. The American Productivity and Quality Center defines knowledge management as "the strategies and processes of identifying, capturing and leveraging knowledge"[10]. Management is an emerging framework of four process sets involved in knowledge creation, knowledge collection, knowledge organization, Knowledge refinement and knowledge dissemination [11]. Another way to perceive Knowledge management is as management of organizational memory, assisted by an organizational memory information system (OMIS) that supports the fundamental activities leading to organizational effectiveness [12].In KM, focus is on "Doing the right thing" rather than "doing things right" so that core competencies do not become core rigidities in future [13]. IBM and Lotus defined knowledge management when entering into the knowledge management arena: ''a discipline that systematically leverages content and expertise to provide innovation, responsiveness, competency, and efficiency'' [14]. While Microsoft states that ''Knowledge management is nothing more than managing information flow; getting the right information to the people who need it so they can act on it quickly" [15]. There are a number of ways for perceiving KM. However each definition agrees on certain viewpoints as:

a) Knowledge is embedded in processes, products and services.

b) Knowledge is represented in database and documents.

c) Knowledge is transferred and shared in the organization.

d) Knowledge can be accessed by outsourcing. Successful KM gives access to better information needed to do a job; although it does not provide answer to the problem it facilitates the learning of the answer [16].

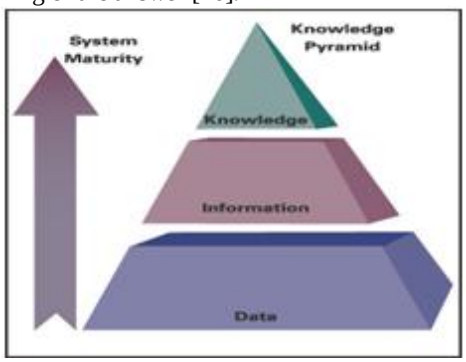

Fig. 1. Data Information Knowledge Pyramid

IV. KM AND SPI

In this day and age business environment for software development project is getting more composite and multifaceted, the dependence on the knowledge processes to resolve issues is vital. A number of researchers have reported that software development is knowledge intensive activity [17][18][19]. Mathiassen, Nielsen and Pries-Heje declared in their analysis that right management of organizational knowledge is quiet significant in SPI efforts and it is a key factor for survival and success [20]. Mathiassen and Pourkomeylian (2003) stated KM and SPI are very close related, in their study based on practical usage of KM to support improvement in a software organization [21]. These studies have created a substantial concern that how organization can effectively cope up with dynamic environment or agile environment. Organization agility characteristic has been explained as "the ability to manage and apply knowledge effectively, so that an organization has the potential to thrive in a continuously changing and unpredictable business environment" [22]. According to this definition software organizations should have appropriate Knowledge Management process. Kess and Haapasalo also support software process as knowledge processes and structured within a KM framework. Hence, KM has been used in software organization for software process initiatives [23].

Software process is not standardized for all software projects and, it must be customized to cope with dynamic environment [24]. The lessons learned from a project process should be shared and effective Knowledge Management is essential for supporting software process initiatives [25]. In a study on software process in three small software development organizations it has been argued that KM is heart to software process improvement model [26]. The process requires KM activities as knowledge creation, sharing and storage. Mathiassen et al., (2002) and, Bjornson and Dingsoyr (2008) have supported the view that knowledge creation and sharing are among the main principles that must be adopted by the organizations in order to succeed in SPI[27-28].

V. CASE STUDY

In this section a description and analysis of the SPI projects has been specified. The studies are selected based on relevance to research area in the present study. The research is organized as a multiple case study [29] and each case description is accompanied by a discussion of the results achieved and conclusions drawn from each project.

A. Knowledge creation in Improving a Software Organisation [30]

This study was carried out at AstraZeneca- one of the world's top pharmaceutical companies. The organization manufactures a wide of range of products designed to fight disease in different areas of medical need. AstraZeneca is a research-driven organization. AstraZeneca has a software organization having four departments that provide global IT services to the entire organization: one in the UK, one in the USA, one in Sweden and one to provide IT support for research and development for the entire organization. This research started before the merger between the two companies in an IS organization called Clinical Research and Information Management (CRIM) at the former Astra Hassle in Sweden and continued later in the new IS organization, which then changed its name to Development IS (DevIS). As a software organization in the pharmaceutical business, DevIS must address many quality requirements. The software development activities took place in two forms: a) Development of new software products (software development). b) Changing the existing software products (software maintenance).

The outcomes of a problem analysis carried out in 1999 within DevIS were not as expected and required and there was a need for improving software project. An improvement project was initiated, organized, planned, by Director of DevIS called Software Process Improvement at DevIS (SPID). The main objective of SPID was to understand and improve software processes.

1) *The Research Approach:* A collaborative research approach has been used in which action research has been combined with field experiment and practice study with an objective of changing practice. The field experiments were set up to test the created software processes in and practice studies were used to learn about the existing maturity level of the organization. The key process areas included were: Software project planning, Requirement Management, software quality assurance, software configuration management. Project managers and developers from the selected projects answered the CMM based questionnaire and the data collected was analyzed statistically.

2) *Lessons learned:* The software improvement project has been analyzed from an organizational knowledge creation point of view using a structure based on Nonaka and Takeuchi (1995) organizational knowledge creation process.

a) Lesson one: Two related knowledge domains (Software Process Improvement (SPI)-, and Software Engineering (SE)-knowledge) are involved in the knowledge creation process in an SPI project.

b) Lesson two: a: The project manager of the SPI project, software managers, and assisting consultants are the key actors involved in the creation of SPI-knowledge (Knowledge creation process).

c) Lesson two: b: The software engineers and the SPI project manager are the key actors involved in the creation of SE-knowledge.

d) Lesson three: a: The knowledge creation process in the case of SPI-knowledge happens mostly on the individual level and sometimes on the group level.

e) Lesson three: b: The knowledge creation process in the case of SE-knowledge happens mostly on the group level and sometimes on the organizational level.

B. Knowledge sharing in Improving a Software Organisation [30]

The SPI unit of Astra Zeneca adopted Knowledge management strategy based on codification and personalization to support knowledge sharing within and outside SPI unit. An IT based solution had been developed so that codified knowledge was accessible to all practitioners in the organization and some by networking there is sharing of personalized knowledge between the practitioners. Moreover, for further improvement of knowledge sharing in SPI unit a survey was conducted of the organization's experience with a number of networks that were active from past few years. The results of the survey and insights from the literature on networks were combined in the study and the following has been proposed: 1) Both structured and non-structured networks should be developed to support knowledge sharing within and outside SPI unit. 2) Knowledge sharing should become an integrated part of SPI unit's daily work. The primary motive is to provide guidelines for improving applied personalized strategy in SPI unit. The analysis includes seven networks that stay alive in the organization for more than three years.

1) *Challenges:* a) There is a requirement of dedicated network leader who can co-ordinate meetings on a regular basis. b) The networks are not able to function well as network members and network coordinators do not have sufficient amount of time for conducting meetings. Moreover there is lack of commitment from the participants. There are some members who do not participate in discussion and are only spectators. c) Some members felt that they cannot participate

in networks because of their day-today work. Moreover, they also felt management should provide resources for creation and transfer of knowledge in the organization. d) There must be a networking strategy to support creation and sharing of knowledge.

2) Critical Success factors: a) The practitioners considered it significant to have a network consisting of both experienced and inexperienced persons. This facilitates creation and transfer of knowledge. b) The seven networks function on individual level s well as organizational level. c) The number of participants should be kept 10-15 so as to initiate discussions at the meetings. d) Another factor that was considered critical was a committed network leader with ample amount of time and optimum resources. e) Management should provide time and tools to facilitate networking activities.

3) Discussion:

a) Formalization: The meetings at Astra Zeneca should be more formal (as preferred by people) due to the fact that networks have been initiated by the participants and there is no support from management to facilitate knowledge sharing. Externalization: At Astra Zeneca due to less active involvement of management the seven networks under study do not have external orientation and there is no network leader to facilitate networking.

*b)*Purpose: Practitioners do not have a clear understanding the existence of network; this is due to absence of networking strategy. A networking strategy that addresses communication role and responsibility.

*c)*Commitment: Another challenge i.e. lack of commitment for networking efforts from members as well as network coordinators is due to lack of dedicated time for networking and their participation is also limited up to a certain extent. A well designed networking strategy can reduce such a problem.

*d)*Co-ordination: According to the finding from the interviews conducted, a coordinator is essential not only for initiation of network but also for its continuation.

*e)*Critical Mass: The size of the network as specified by most of the practitioners during interview is that it should be around 10-15 persons i.e. it should not be huge. While others specify no upper limit.

4) *Improving Knowledge Sharing in SPI unit:* The primary goal in the SPI unit is knowledge management about SPI at Astra Zeneca. For sharing of codified knowledge in and outside SPI unit EPL (Electronic Process Library) is used. The SPI unit needs to further develop a number of structured and non-structured networking facilities to implement KM strategy.

C. *Creating SPI Knowledge and methods as knowledge enablers[31]*

1) *Case Companies: GAMMA (ALIAS):* Gamma Company is a unit/part of a large telecommunication group (Epsilon). The company primarily develops software for management systems of mobile phone networks and telephony and data communication switches. The organization is geographically distributed in SWEDEN having business units. In a business there are nearly 20-30 employees and it works with 2-3 products. In the year 1997 Gamma initiated a Knowledge Management project with an aim to develop knowledge Management System (KMS). The development of KMS was carried out to support collection and reuse of software experiences of Gamma's software Engineers.The management system is based on experience factory and its experience base is designed to collect, analyze, generalize and store experiences from software development project of Gamma. The Knowledge Management project is named as KNOWIT and experience base is named as EXPBASE. By the use of traditional codification for Knowledge Management design for EXPBASE was initialized and more than 1,000 person hours software projects. Thus the flow of knowledge, its distribution and what type of knowledge software project members should possess and use was tracked and described. The members of KNOWIT conducted a number of interviews with project managers and members with a concern to find out how knowledge was sought and exchanged among the projects. One more fact-finding was conducted using observation for software project leaders and members. Based on the results of the interviews and observations the development of EXPBASE was not carried further as the studies showed major discrepancies between knowledge seeking and knowledge transfer of the people and knowledge seeking and transfer by EXPBASE. In the next step based on the studies of the exchange of knowledge between firm's software developers and project leaders design and development of Knowledge Management System was reconsidered on the basis of networking approach, a people centered approach. The experience engine can be characterized as personalization strategy to Knowledge Management. In the redirected KM initiative there are experience broker and Experience communicator. The Experience broker should have a well developed network and is responsible for capturing knowledge from meetings and moving between teams. The experience communicator transfers knowledge and experiences to software developer, so as to help in specific problem solving.

a) Discussion: KNOWIT and EXPBASE missed two important dimensions - Lack of physical spaces for knowledge exchanges.EXPBASE did not seem to be a proper way for handling spontaneous and adhoc needs for knowledge.

2) Theta and Omega(Alias): In this case study a snapshot has been presented for two software development organizations, in which role of methods-a common SPI approach used as knowledge enablers has been adopted for improving a software process. The firms used methods for project management and Software Engineering process. These methods are based on international standard from ISO, IEEE and TICK IT. The extent of methods implementation varied significantly in the organization. Omega, the smaller organization had a set of methods that were known to the

people in organization in common, although the knowledge about methods varied from person to person. As compared to Omega, Theta had more number of methods and Knowledge about methods varied largely between the various units of the organization. The project members that had a long working experience with the organization had less knowledge about the methods. They have more or less personalized the methods. On the other hand less experienced were more proficient about methods as they wanted to enhance their knowledge about the working of the organization. In both the companies' theta and omega the methods used were customized but the extent of customization varied. It is worth mentioning that from the SPI perspective, feedback from practice to method developers related to customization was quiet low. This was limitation for process improvement. Methods had associated terminology section that was important with regard to knowledge enablers. The terminology section contains key concepts about the methods. The terminology is of extra importance in Theta project where there are geographically distributed sub-projects. The terminology glossary is a facilitator for knowledge sharing over national and cultural boundaries.

*a) Discussion and lessons learned:*Software development methods are vital knowledge enablers in the software development process. If an organization does not have an implemented common method then it is quiet difficult to capture the experiences. It is evident from the study that methods are of great value to naïve employees as they can grasp the knowledge about the organization. Flexible methods are essential in dynamic environment of software development. The methods were being customized in THETA and OMEGA as each development project is unique and requires customization of methods for supporting specific task. The complexity of product and software development process emphasizes the requirement of Knowledge Management and KM enablers (methods).This results in improvement in knowledge re-use and learning. From the cases it can be learned that in the process of software development methods are key knowledge enablers for SPI initiative and effort.

VI. COMPARATIVE ANALYSIS

In this research paper three organizational SPI projects have been analyzed from the perspective of organizational knowledge creation, knowledge sharing and methods that are used as KM enablers. The study has been organized as multicase analysis. From the first case study carried out at ASTRA ZENECA knowledge creation issues and knowledge sharing issues have been addressed. The knowledge sharing efforts were guided by different strategies depending on different types of SPI services to support codified as well as personalized knowledge. In the study different natures of IDEAL model and CMM are considered and it has been suggested that they are personalized approach whereas maintenance and dispersal of process and procedures are open approaches and these are codified. Moreover the main idea in the study was not to reach a particular level of CMM instead it focused on learning SPI, improving and implementing software processes in the organization and on increasing practitioner's understanding about organization's quality rules and requirements. In the third case the two organizations studied are quite different from each other but they both show that software development is a knowledge intensive process. The methods are used as the knowledge enablers. Software development methods are vital knowledge enablers in the software development process.

TABLE I. OVERVIEW OF STUDIES

KM activity for SPI	***Research Approach***	***Key Process Areas***	***Inference Drawn***
Knowledge Creation	Collaborative and Action research. Assessments SPI-meetings SPI-workshops Customization meetings (Training sessions)	Software project planning, Requirement Management, software quality assurance, software configuration management.	1. SPI and SE knowledge are involved in the knowledge creation process in an SPI project. 2. The project manager of the SPI project, software managers, and assisting consultants are the key actors involved in the creation of SPI-knowledge creation process. 3.The knowledge creation process in the case of SPI-knowledge happens mostly on the individual level and on the group level. The knowledge creation process in the case of SE-knowledge happens mostly on the group level and sometimes on the organizational level.
Knowledge Sharing	SPI-meetings group & department meetings IT-based solutions Networking facilities Customizatio n meetings Training sessions	Structure of networking, problems with networking, critical success factors in networking	1.Recognition of additional external networking facilities. 2.Development of structures for gathering, analyzing and evaluating feedback from structured and non-structured networking facilities. 3. Internal development of etworks to support creation of nowledge through the lessons learned in software projects. 4 Utilization of IT-based media and EPL for sharing of knowledge.
Creating SPI knowledge & methods as Knowledge enablers	Practice study and Action Research	SPM and Software Engineering process	1. Software development methods are vital knowledge enablers in the software development process. 2. The complexity of product and software development process emphasizes the requirement of KM and KM enablers (methods). The methods facilitate the process of Communication. 3. In the process of software development methods are key knowledge enablers for SPI initiative and effort.

VII. CONCLUSION

The software development is a complex process due to the numerous amendments in technologies, processes and multicultural arrangements. For such frequently varying

process of software development preformatted packaged solutions or standard approaches are helpful only to a certain extent [32]. From the study it has been found that the SPI projects should focus on SPI and KM concepts rather than model based recommendations like those of CMM. In addition to this another finding is that SPI project should have plans, resources, roles deliverables and an overall KM strategy. Methods provide structure to the development process and support communication between the projects and create a structure for capturing process related experiences and with structured feedback loops. They play a major role in the learning software organization. It has been thus concluded in the study that methods as knowledge enablers play an important role in SPI.A method should also be used as a mechanism for learning and knowledge creation in the process of software development. KM is useful in SPI.

REFERENCES

[1] K. Schneider, "Experience and Knowledge Management in Software Engineering," in *Springer*, Verlag, Berlin, 2009.

[2] Dennis, "Chaos," The Standish Group , Massachusetts, 1995.

[3] A. Fuggetta, "Software Process: A Roadmap," in The Future of Software Engineering,ICSE'2000, Limerick, Ireland, 2000.

[4] Y.-H. Yao and H.-K. Lee, "APPLYING ISO 9001 AND CMMI IN QUALITY-ORIENTED KNOWLEDGE," International Journal of Electronic Business Management , vol. 2, no. 2, pp. 140-151, 2004.

[5] M. C. Paulk, C.V.Weber, B.Curtis and M. B.Chrissis, The Capability Maturity Model: Guidelines for Improving the Software Process, Addison-Wesley, 1994.

[6] P.Kuvaja and A.Bicego, BOOTSTRAP - a European assessment methodology. Software Quality Journal, vol. 3, pp. 117-127, 1994

[7] M.Paulk, "Effective CMM-Based Process Improvement, 6th International conference on Software Quality," Ottawa, Canada, 1996.

[8] B.McFeeley, IDEAL. A User's Guide for Software Process Improvement. The Software Engineering Institute, Carnegie Mellon University, Pittsburgh: Handbook CMU/SEI-96-HB-001, 1996.

[9] I.Aaen, J.Arent, L.Mathiassen and ,. V. O.Ngwenyama, " A Conceptual MAP of Software Process Improvement," Scandinavian Journal of Information Systems, Special Issue on Trends in the Research on Software Process Improvement in Scandinavia, vol. 13, pp. 123-146, 2001.

[10] S.Atefeh, L. McCamble, C. Moorchead and S. H. Gitters, "Knowledge management: the new challenge for the 21 century," Journal of Knowledge Management, vol. 3, no. 3, pp. 172-179., 1999.

[11] M. Leidner and D. Alavi, "Review: knowledge management and knowledge management systems: conceptual foundations and research issues," MIS Quarterly, vol. 25, no. 1, pp. 107-6, 2001.

[12] E.W. Stein and V. Zwass, "Actualizing Organizational Memory with Information Systems," Information Systems Research, vol. 6, no. 2, pp. 85-117, 1995.

[13] M. T. Hansen, N. Nohria and T. Tierney, "What's Your Strategy for Managing Knowledge," Harvard Business Reviews, vol. 77, no. 2, pp. 106-118, 1999.

[14] W. Pohs, Practical Knowledge Management: the Lotus Discovery System, 1st ed., Double Oak, TX: IBM Press, 2001.

[15] B. Gates, Business @ the Speed of Thought: Using a Digital Nervous System, New York: Warner Books, 1999.

[16] C. Dean, ""Knowledge management - not rocket science",," *Journal of Knowledge Management*, vol. 9, no. 2, p. 19 – 30, 2005.

[17] P. Pourkomeylian, "Doctoral Dissertation Software Practice Improvement," Göteborg University, 2002.

[18] A.Aurum, F. Daneshgar and J.Ward, "Investigating Knowledge Management practices in software development organisations – An Australian experience',," Information and Software Technology,, vol. 50, no. 6, pp. 511-533, 2008.

[19] T. Dingsøyr, H. Djarraya and E.Royrvik, "Practical knowledge management tool use in a software consulting company," Communications of the ACM, vol. 48, no. 12, p. 97–103., 2005.

[20] P. Robillard, "The role of knowledge in software development," *Communications of the ACM*, vol. 42, no. 1, p. 87–94, 1999.

[21] F. Bjornson and T. Dingsoyr, "A Study of a Mentoring Program for Knowledge Transfer in a Small Software Consultancy Company," in Springer, Berlin / Heidelberg, 2005.

[22] I. Aaen, A. Börjesson and L. Mathiassen, "SPI agility: How to navigate improvement projects," Software Process: Improvement and Practice, vol. 12, no. 3, pp. 267-281, 2007.

[23] K. Sirvio, A. Mantyniemi and V. Seppanen, "Toward a practical solution for capturing knowledge for software projects," Software IEEE, vol. 19, no. 3, pp. 60-62, 2002.

[24] P. Kess and H. Haapasalo, "Knowledge creation through a project review process in software production," International Journal of Production Economics, vol. 80, no. 1, pp. 49-55, 2002.

[25] R.Dove, Response Ability - The Language, Structure, and Culture of the Agile Enterprise, New York: Wiley, 2001.

[26] Y. Maholtra, "Knowledge Management Lessons Learned: What Works and What Doesn't," Information Today Inc. (American Society for Information Science and Technology Monograph Series), 2000.

[27] B. Meehan and I. Richardson, "Identification of Software Process Knowledge Management," *Software Process: Improvement and Practice* , vol. 7, no. 2, pp. 47-55, 2002.

[28] L.Mathiassen and J. P.-H. P.A.Nielsen, Learning SPI in Practice in Improving Software Organization : From Principle to Practice, Addision Wesley, 2002.

[29] S. Carlsson and A. S. Mikael, "Software Process Improvement Through Knowledge Management at http://www2.warwick.ac.uk/fac/soc/wbs/conf/olkc/archive/oklc4/papers/oklc2003_carlsson.pdf," [Online]. [Accessed july 2013].

[30] G. Pérez-Bustamante, "Knowledge management in agile innovative organisation," Journal of Knowledge Management, vol. 3, no. 1, pp. 6-17, 1999.

[31] I. Nonaka and H. Takeuchi, The Knowledge-Creating Company, Oxford University Press, 1995.

[32] M. Chugh, N. Chugh and D. K. Punia, "Knowledge Management A Facilitator for Software Process Improvement," International Journal of Computer Applications (0975 – 8887), vol. 87, no. 18, pp. 13-19, 2014.

2015 International Conference on Smart Technologies and Management for Computing, Communication, Controls, Energy and Materials (ICSTM), Vel Tech Rangarajan Dr. Sagunthala R&D Institute of Science and Technology, Chennai, T.N., India. 6 - 8 May 2015. pp.499-503.

GRIHA Norm Evaluation – A Field Study in Uttarakhand, India

Jasmeen Sandhu[1], Akshaya Tripathi[2], Kartik Arunachala[3] and **Madhu Sharma[4]**

[1,2]M. Tech, Energy Systems, [3]Research Fellow, R&D, [4]Assistant Professor, Electrical, Power and Energy
University of Petroleum and Energy Studies, Energy Acres, Dehradun, India

***Abstract*— Enormously growing demands for urban fabricated spaces have caused enormous rise in the construction of buildings. In addition to this the increasing population of India has also resulted in constructing of numerous schools, colleges and universities. The need of the present hour is that these developments should occur in a sustainable manner causing minimal or no harm to the environment. This field study was undertaken in order to gain a comprehensive understanding of the developing construction sector of India. The aim was to assess the importance of educational institutions in the promotion of green buildings. This paper gives a preview of various green building rating systems available in India along with their salient features. An educational institution was assessed by means of GRIHA (Green Rating for Integrated Habitat Assessment) evaluation system. During the course of field survey all the criterions were assessed. The findings and the possible star rating which can be achieved by the educational establishment has been described in this paper.**

***Keywords*— GRIHA, Smart City, Green Buildings, Greenhouse Gas, Climate Zones, Sewage Treatment Plant, Volatile Organic Compound (VOC)**

I. INTRODUCTION

The level of urban development in India is and will continue to be exceedingly enormous driven by rapid pecuniary and population growth. The constructions and use of buildings let it be either educational institutions, offices or large malls and hotels are being driven by rapid urban expansion which is likely impose incredible pressure on the natural environment. India's ability to decouple resource consumption from the economic growth shall be directly affected by the investments done at present in the infrastructure sector. Even though urbanization is happening at a rapid rate in India the techniques used for appropriate urbanization are less advanced as compared to those used in various other developing countries. The promotion of green building which has been initiated in India offers the one of best ways to approach towards development by least damage to the environment. It is anticipated that India will have sixty eight cities with a population of more than one million, thirteen cities with more than four million people and six megacities with population greater than ten million with New Delhi and Mumbai being among the world's largest cities in the world by 2030 [1]. The construction sector in India is alone responsible for 23.6% of the national greenhouse gas emissions and buildings are responsible for nearly forty percent of the material flow [2].

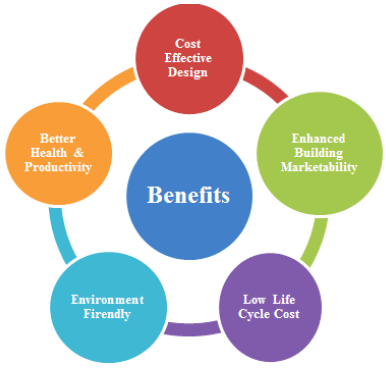

Fig. 1. (a) Benefits of Green Buildings

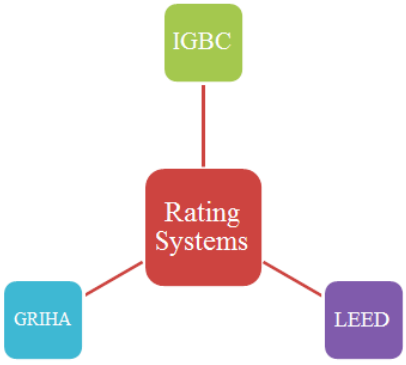

Fig. 2. (b) Different Rating Systems in India

Dehradun the capital of Uttarakhand is expected to be a smart city and one of the sixty eight cities with a population of more than one million. The majority of this population shall be youngsters ranging from the age of 6 years to 28 years as Dehradun is considered to be educational hub with

lots of educational institutions right from deemed universities, government colleges, training institutes, boarding schools and day schools. Lots learning establishments are being constructed in addition to the already existing ones. The rapid development is bound to impose tremendous pressure on the natural environment especially due to the hilly terrains and mountains in the vicinity of Dehradun. The carbon footprint which occurs and is bound to happen during the construction, sitting, operation and extraction of buildings is extremely huge. Keeping these issues into consideration educational institutions as green buildings is the way forward in Dehradun which would set an example for other towns of Uttarakhand. A sustainable building having minimal impacts on the environment throughout its life shall be termed as 'Green Building'. This shall be understood as the means of construction making efficient energy use of available resources in each and every aspect. This comprises fabrication of construction materials, design use and subsequent flattening of a structure in any sector at all phases. The benefits of a green building have been depicted in a snapshot in Fig 1. Figure 2 portrays the different existing green building rating methods in India.

II. ASSESSMENT OF GREEN BUILDING RATINGS PREVAILING IN INDIA

As a result of numerous measures and initiatives taken by the Indian government to promote green buildings; several ratings have been developed and are followed at present. Certain ratings and schemes followed in India are Indian Green Building Council (IGBC), Green Rating for Integrated Habitat Assessment (GRIHA), National Building Code (NBC), Energy Conservation Building Codes (ECBC) and Bureau of Energy Efficiency (BEE). IGBC is the adapted form of LEED (Leader in Energy and Environment Design) designed by the United States Green Building Council (USGBC). Separate sets of ratings are available for factories, homes, townships, special economic zones and green backdrops under the IGBC guidelines [3]. Energy star rating of the appliances was introduced by the BEE, in which the appliances are tested and given appropriate star ratings as per the energy consumption patterns. The higher the number of stars an appliance gets, the better its energy consumption. ECBC was also brought into application by the BEE based on the NBC. ECBC is extremely comprehensive and measures each and every characteristic of a building and offers several rating procedures depending upon the area [4]. The Energy and Resources Institute (TERI) developed Indian specific green rating system title as GRIHA which was officially accepted and brought into practice in the year 2007 by the Indian Government. To initiate the process of evaluation and certification of contenders aiming for GRIHA rating an Association for Development and Research for Sustainable Habitats (ADARSH) was formed. In this paper we have assessed an educational institution in Dehradun area on the basis of GRIHA rating [5]. We chose such an institution which had both established buildings and the buildings in progress in order to evaluate majority of the GRIHA parameters.

III. ELUCIDATION OF GRIHA AND DEHRADUN

The provisions of the National Building Code 2005 and Energy Conservation Building Code 2007 along with other IS codes is taken into account in the GRIHA Rating system. The rating system based on the accepted environmental and energy principles aims to strike the balance between the established practices and evolving concepts at both the national and international level [6] [7]. This system holistically evaluates the environmental performance of the building over its entire life cycle.

The system looks into the following parameters in an integrated manner:-

- Site Planning
- Building System Design
- Building Envelope Design
- Water Management
- Waste Management
- Tapping of Renewable Energy for On-site purposes
- Assortment of Environmentally Appropriate materials
- Maintenance of appropriate indoor environmental quality

Points are obtained for meeting the design and performance intended criteria in this performance oriented system which also acts as the source of guide. There are a total of 34 criterions in the GRIHA evaluation system which is broadly classified in two categories known as the 'applicable' and 'selectively applicable' ones. The former is further subdivided into two more categories termed as 'mandatory' and 'non-mandatory' norms. Due to technical restrictions and limited environmental benefits the 'selectively applicable' criterions shall not be applied to the project. These criterions shall only be decided during the registration process. The criterions numbers two, three, nineteen, twenty, twenty four and a part of twenty one fall outside the cadre of applicable criterions [8].

Dehradun falls under Composite Climate zone, which is one of the five climatic zones of India. Its latitude lies between 29°58'N & 31°2'N and longitude is between 77°34'E &

78°. The city experiences high temperatures during summers and extremely dry cold in the winters. The humidity level rises up during the monsoon season. The city faces high direct solar radiations in every season except monsoons when most of the radiations are in diffused form [9].

IV. Field Study

This field study was carried out in order to evaluate the compliance of an educational institution with the GRIHA norms. This study was carried over the duration of two weeks in order to cover each and every corner of the construction site and the establishments. The results of the study help an independent assessment before the applying for GRIHA ratings [10]. Results of the field survey have been discussed in this section.

A. Reduction of Air Pollution During Construction

This criterion aims at ensuring appropriate screening, covering of bricks, stockpiles and tons of dust materials in addition to water spraying facility wheel-washing facilities. It also intends at reducing air pollution during construction. As per the prescribed norms a total of two points can be achieved by fulfilling this particular criterion. Submission of tender documents substantiating the air pollution prevention measures is extremely mandatory by the contractor. Photographs taken at the site should also be submitted as proof. In our field of study this criterion was fulfilled, the snap shots of barricading at various parts of the side have been depicted in Figure 2 (a) and (b). This criterion helps in mitigating possible respiratory problems to the workers and laborers due the air pollutants and dust generation on site.

Fig. 2. (a) Barricading Near the Path Way

Fig. 2. (b) Barricading at Construction Site

B. Waste Water Treatment

The objective of criterion twenty is to promote the treatment of waste water. The facility should provide an area dedicated for the treatment of waste water generated from the establishment and have dedicated channels for safe disposal of by-products. The organization should mention the entire details of the waste water treatment process and indicate the possible quantum of treated water along with steps to be undertaken for safe disposal. The sampling plan of the treatment plant along with quality checking frequency should also be clearly specified. The water testing of parameters should be carried out as prescribed in the Pollution Control Acts, Rules and Notifications (CPCB, 1998). This criterion is applicable only if the generated waster is less than ten kilo-liters in a day. The organization's efforts in creating the Sewage Treatment Plant (STP) have been shown in Figure 3(a) and (b).

Fig. 3. (a) Construction of STP

There is an optional clause under this criterion which allows the institute to gain two more points if the treated water meets the disposable application standards.

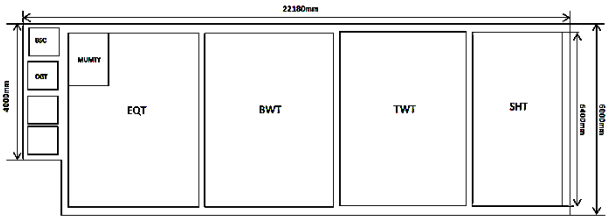

Fig. 3. (b) Diagram of STP

C. Facilities for Differently Abled Students

Fig. 4. (a) Rest Room Facility

Fig. 4. (b) Pathyway Facility

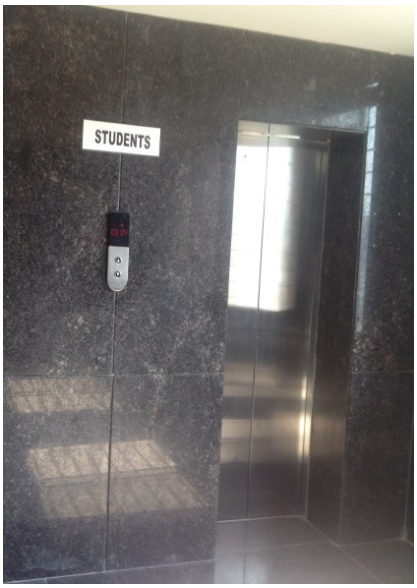

Fig. 4. (c) Lift Facility

During the establishment of GRIHA rating system special care was taken regarding the accessibility in a building for the differently abled people. Criterion thirty one states the necessity of providing basic levels of accessibility for differently abled persons. Care should be taken to ensure hindrance free accessibility and usability of the building and the available facilities by the differently abled visitors, employees and clients. This results in gaining of one point for the organization and making things easier for the differently abled people. The organization has taken the much needed care for the differently abled students. Separate rest rooms and pathways have been constructed for the differently abled students in addition to lifts for their easy access within the establishment boundary as depicted in Figure 4 (a), (b) and (c).

D. Low use of Low VOC Paints/Sealants/Adhesives

The criterion number twenty six aims at promoting the users to select and use paints, sealants and adhesives with minimum concentrations of chemical substances and volatile organic compounds such as formaldehyde etc. Maximum of three points can be achieved depending on the clause satisfaction. Figure 5 (a) and (b) depict no usage of paints for decorative purposes in the corridors of the educational institute.

V. Conclusion

The field study was conducted in the Dehradun region which is considered as the educational-hub of the country substantiates the fact that the educational institutions can play a big role in the promotion of green buildings and

Fig. 5. (a) Walls with Proper Finishing

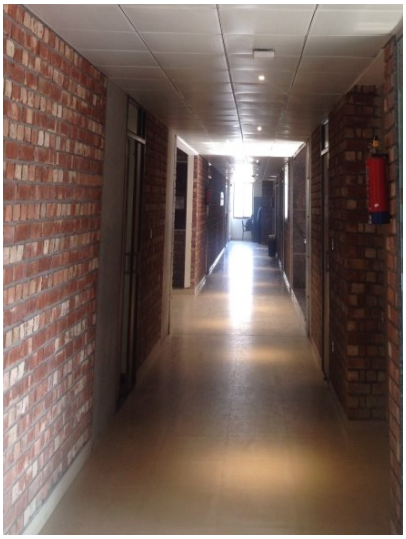

Fig. 5. (b) Corridor with No Paints

subsequently GRIHA. The field study was conducted in such a manner that all the criterions were evaluated and few are highlighted in this paper which includes Reduction of Air Pollution during Construction, Waste Water Treatment, facilities for Differently Abled Students and minimum use of Low VOC paints/sealants/adhesives. This paper presents these highlighted criterions along with their portraits. As per the evaluation, this building can receive high star rating. This type of analysis provides a distinctive method of green building evaluation too. This will help educational institution set benchmarks for other organizations and companies in the region.

REFERENCES

[1] S. Sankhe, I. Vittal, R. Dobbs, A. Mohan, and A. Gulati, "Indiaâ s urban awakening: Building inclusive cities sustaining economic growth," 2010.

[2] P. Commission, "Interim report of the expert group on low carbon strategies for inclusive growth," Planning Commission, Government of India, New Delhi, India. Available online at http://planningcommission. nic. In/reports/genrep/Inter_Exp. pdf, 2011.

[3] L. India. Summary of LEED.

[4] C. I. Team and C. U. Team, "Building Energy Benchmarking in India: an Action Plan for Advancing the State-of-the-Art," Centre for Building Research and Development, June 2014

[5] S. Korkmaz, D. Erten, M. Syal, and V. Potbhare, "A review of green building movement timelines in developed and developing countries to build an international adoption framework," in Proceedings of Fifth International Conference on Construction in the 21st Century: Collaboration and Integration in Engineering, Management and Technology, 2009, pp. 20-22.

[6] V. Singh, "Analysis Methods for Post Occupancy Evaluation of Energy-Use in High Performance Buildings Using Short-Term Monitoring," Arizona State University, 2011.

[7] National Building Code of India 2005

[8] K. WaidyaseNara, M. De Silva, and R. Rameezdeen, "Comparative Study of Green Building Rating Systems: in Terms of Water Efficiency and Conservation," The Second World Construction Symposium 2013: Socio-Economic Sustainability in Construction, June 2013

[9] I. R. G. USAID ECO-III Project, "Energy Conservation Building Code ", http://beeindia.in/schemes/documents/ecbc/eco3/ecbc/ ECBC-User-Guide (Public).pdf July, 2009.

[10] M. o. N. a. R. E. TERI, Government of India "Introduction to National Rating System - GRIHA," ed. http://www.grihaindia.org/files/Manual_VolI.pdf.

EPJ Web of Conferences **86**, 00046 (2015)
DOI: 10.1051/epjconf/ 20158600046

Incomplete fusion reactions in ^{16}O+^{159}Tb system: Spin distribution measurements

Vijay R. Sharma[1,a], Abhishek Yadav[2], Devendra P. Singh[3], Pushpendra P. Singh[4], Sunita Gupta[5], Manoj K. Sharma[6], Indu Bala[2], R. Kumar[2], S. Muralithar[2], R. P. Singh[2], B. P. Singh[1,b], R. Prasad[1], and R. K. Bhowmik[2]

[1] *Department of Physics, Aligarh Muslim University, Aligarh 202 002, India*
[2] *NP-Group, Inter University Accelerator Centre, New Delhi - 110 067, India*
[3] *Department of Physics, CoE, University of Petroleum & Energy Studies, Dehradun - 248 007, India*
[4] *Department of Physics, Indian Institute of Technology Ropar, Punjab 140 001, India,*
[5] *Physics Department, Agra College, Agra- 282 001, India*
[6] *Physics Department, S. V. College, Aligarh - 202 001, India*

Abstract. In order to explore the reaction modes on the basis of their entry state spin population, an experiment has been done by employing particle-γ coincidence technique carried out at the Inter University Accelerator Centre, New Delhi. The preliminary analysis conclusively demonstrates, spin distribution for some reaction products populated via complete and/or incomplete fusion of ^{16}O with ^{159}Tb system found to be distinctly different. Further, the existence of incomplete fusion at low bombarding energies indicates the possibility to populate high spin states.

1 Introduction

The study of incomplete fusion (ICF) of heavy ions with different projectile-targets combination has been a topic of renewed interest at energies near and above the Coulomb barrier [1, 2]. Observations show that at the presently studied energies ($\approx$ 4-7MeV/A), the dominant nuclear reaction mechanisms are complete fusion (CF) and the ICF [3–6]. Efforts are still in progress to gain better understanding of ICF processes. Britt and Quinton [7] were the first to observe the production of forward-peaked fast α particles in the breakup of the ^{12}C, ^{14}N and ^{16}O projectiles at energy $\approx$ 10.5 MeV/A. Advances in the understanding of ICF dynamics were made after the charged particle-γ coincidence measurements by Inamura et al. [8]. On the basis of semi-classical theory of heavy ion (HI) reactions, the CF and ICF processes are broadly categorized on the basis of driving input angular momentum ℓ imparted into the system. In the CF process the driving input angular momentum $0 \leq \ell \leq \ell_{crit}$, in accordance with a sharp cutoff approximation and may be understood in the following way. In case of CF, the attractive nuclear potential overcomes the repulsive Coulomb and centrifugal potentials in central and near-central collisions. Hence, CF process takes place at a small values of impact parameter at which the formation of fully equilibrated compound nucleus (CN) takes place. On the other hand, at relatively higher values of impact parameter, a competition between repulsive centrifugal and attractive nuclear potential results in the breakup of the projectile. Therefore, an incompletely fused composite system comprising of a part of the projectile and the target appears in the exit channel that leads to the ICF process, wherein the involvement of driving input angular momentum ℓ is relatively larger than that needed for the CF process to take place. Quantitatively, the driving input angular momentum exceeds the critical limit (ℓ_{crit}) for CF and hence, no fusion can occur unless a part of the projectile is emitted to release the excess driving input angular momentum. As such, prompt emission of a part of the projectile (predominantly α clusters) takes place to provide sustainable input angular momenta to the system (e.g., ^{16}O breaks into ^{12}C and α particle). After such an emission, the resulting angular momenta carried by the remnant projectile is less than or equal to its own critical angular momentum limit for fusion to occur with the target nucleus. Hence, in case of ICF the residual nuclei produced is therefore assumed to be associated with ℓ values above ℓ_{crit} for CF. It may be relevant to mention here that, Tserruya et al. [9] showed that ICF processes may contribute significantly below and above input angular momentum limits and there is no sharp cutoff limit of input angular momentum.

Further, the ICF reaction studies by charged particle-γ coincidence technique have been carried out with low-Z (Z $\leq$ 10) projectile-induced reactions on heavy targets (A $>$ 150). However, such information is scarce for medium mass target nuclei. Several models [4] have been used to fit the experimental data obtained at energies well above the Coulomb barrier (i.e., $E_{lab} \geq$ 10.5 MeV/A) but have shown certain failings in their ability to explain ICF data at relatively low bombarding energies (i.e.,$\approx$ 3-7 MeV/A.

[a] e-mail: phy.vijayraj@gmail.com
[b] e-mail: bpsinghamu@gmail.com

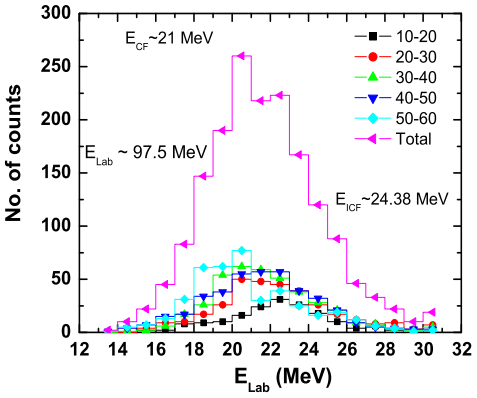

Figure 1. (Color online) Fusion-evaporation (CF) α-energy profile for forward (F) zone (10^0-60^0) at projectile energy E = 97.5 ± 1.5 MeV in the ^{16}O + ^{159}Tb system predicated by PACE4. Different angular slices from 10^0 to 60^0 are also shown in this figure.

Hence, the study of ICF dynamics is still an active area of investigation.

Recent studies on spin distributions for the system ^{16}O + ^{169}Tm at ≈ 90 MeV beam energy show significantly different patterns in the spin distributions for the reaction products produced by CF and ICF processes [10, 11]. To get more information about input angular momentum involved for various degrees of ICF dynamics, a particle-γ coincidence experiment has been performed for the system ^{16}O + ^{159}Tb at ≈ 4-7MeV/A projectile energy. In this paper, spin distributions for various evaporation residues (ERs) have been identified and are reported. This paper explains our preliminary results of spin distribution measurements for CF and ICF residues in ^{16}O+^{159}Tb system at ≈ 97.5 ± 1.5 MeV beam energy.

2 Experimental Setup and Data Reduction Methodology

Aiming to investigate the high ℓ values in successively opened ICF channels and to test the possibility of populating high-spin states in final reaction products via ICF, a particle-γ coincidence experiment was performed at the Inter-University Accelerator Center (IUAC), New Delhi, India. In the present work, spin distributions of CF and ICF products has been measured at 99 MeV beam energy. An isotopically pure Terbium (^{159}Tb, abundance ≈ 100%) target of thickness 1.79 mg/cm^2 was bombarded by ^{16}O^{6+} with beam current ≈ 30-35 nA. Target thickness was measured by an α-transmission method. This technique is based on the measurement of the energy loss per unit path length by ≈ 5.487 MeV α particles obtained from a standard ^{241}Am source, while passing through the target material. In the present section brief details of experimental setup and data reduction methodology are discussed.

2.1 Experimental Setup

In the present work, coincidences are recorded using the γ-detector array (GDA) along with an array of charged particle detectors (CPDs) to identify the different reaction channels. The GDA consists of 12 Compton-suppressed high resolution high-purity germanium (HPGe) γ spectrometers arranged at three angles with respect to the beam axis, i.e., 45^0, 99^0, and 153^0, and four detectors installed at each of these angles. The array of CPDs is an assembly of 14-phoswich detectors arranged in two truncated hexagonal pyramids, the bases of these pyramids lie in a horizontal plane with each having a trapezoidal shape. The top and bottom spaces are filled by two hexagonal detectors that, together with trapezoids, cover ≈ 90% of the total solid angle. In order to employ different gating conditions and to detect particles (Z = 1, 2) in coincidence with prompt γ rays at various angles, the array of CPDs was divided into three angular zones (i) forward (F) 10^0-60^0, (ii) sideways (S) 60^0-120^0, and (iii) backward (B) 120^0-170^0. The coincidences were demanded between particles (Z = 1, 2) and prompt-γ rays by employing three gating conditions corresponding to the given angular zones for each value of Z. Depending on the fast and slow components of the CPDs, particles (a sum of protons and α's) and α's in each angular zone were detected in coincidence with prompt-γ rays. As a matter of fact, the CPDs at forward (F) angles (10^0-60^0) are expected to detect both slow and fast α components; i.e., (i) slow α component: fusion-evaporation (CF) α particles, and (ii) fast α component: direct α particles associated with ICF. The energy profile of slow α particles (emitted from fully equilibrated CN) was generated by the theoretical model code PACE4 [12] (see Fig. 1). This code is based on the statistical approach of CN de-excitation by Monte Carlo procedure and was extensively used for CN-related calculations in past years. Similar input parameters, as in Ref. [11], are used for this calculation. As can be seen in Fig. 1, the theoretically estimated most probable energy of slow α particles (E_α^{CF}) is found to be ≈ 21 MeV at 97.5 ± 1.5 MeV beam energy. However, the energy of the fast α component (E_α^{ICF}) can be calculated as projectile energy times ejectile-projectile mass ratio, and comes out to be ≈ 24.37 MeV at 97.5 ± 1.5 MeV for the ^{16}O beam. As such, the gating condition i.e. backward α-gated spectra is subtracted from the forward α-gated spectra were used, so that only fast α component in the forward cone can be detected.Further, an Al absorbers of appropriate thickness (estimated by the SRIM08 code [13] based on the range-energy formulation) were used to stop the elastic scattering from ^{16}O beam. Multiparameter, particle-γ-coincidence data are recorded in the list mode, which includes different gating conditions such as particle(s)/α detected in backward (B), forward (F), and sideways (S) angles. Singles data were collected to identify xn channels predominantly populated via CF.

2.2 Data Analysis

Off-line data analysis was performed in steps using the nuclear physics data analysis software INGAsort [14]. In the

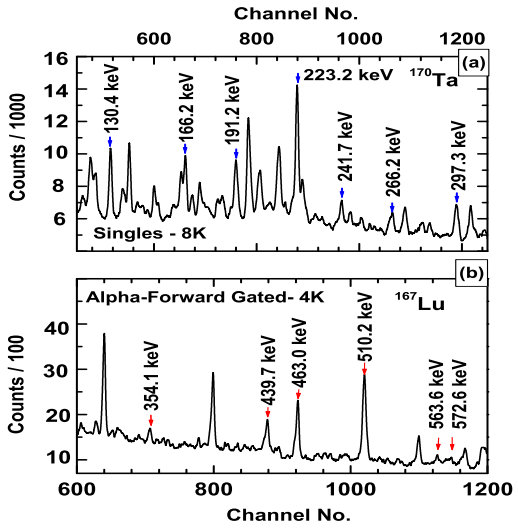

Figure 2. (Color online) Typical γ-spectrum for the ^{16}O + ^{159}Tb interaction at 97.5 ± 1.5 MeV, where γ-lines are assigned to the bands identified for the CF and/or IF residues. (a) Singles (b) forwarded alpha-gated spectra.

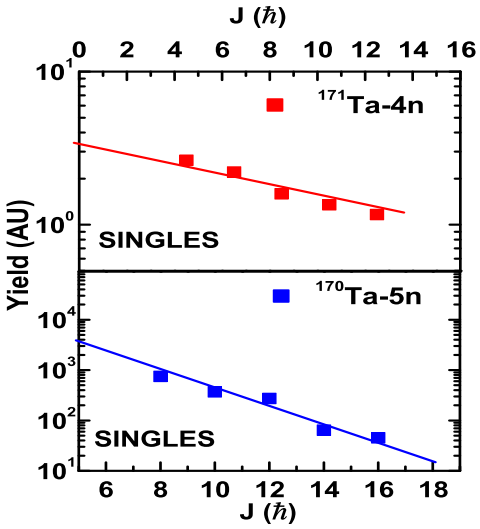

Figure 3. (Color online) Experimentally measured spin distributions for CF-4n, 5n channel (identified from singles spectra). Reaction products are labeled by self-explanatory notations and emission cascades. Lines through the data points are drawn to guide the eyes.

first step, the energy calibration and gain matching of the HPGe detectors were carried out by counting standard radioactive γ source (^{152}Eu) before and after the experiment precisely at the target position. In the second step, particle-γ-coincidence spectra were generated to identify different reaction channels. Various gating conditions are projected onto the γ spectra to generate particle-gated spectra for each angular zone. Assuming isotropic γ emission, all gated spectra for a particular gating condition are summed up to improve the event statistics. The different reaction products populated via CF and/or ICF are identified on the basis of their characteristic γ lines by looking into the particle gated and/or singles spectra. The xn channel are identified from singles spectra recorded by two coaxial HPGe detectors. In order to identify pxn channels populated via CF, backward (B)-α gated spectra are subtracted from backward (B) particle-gated spectra to generate pure backward (B)-proton-gated spectra. The CF αxn channels (consisting of slow α component) are identified from the backward (B)-α-gated spectra. Further, as expected in ICF, the direct α particles (associated with ICF) are supposed to be concentrated only in the forward (F) cone. It may further be pointed out that the slow α component (associated with CF) coming from the de-excitation of CN may also be emitted in the forward cone due to the isotropic nature of the particle emission in CN reactions. As was already mentioned in the previous section, the slow α component is filtered out by putting an Al absorber on forward cone CPDs. However, to remove any contamination from the slow α component in the forward (F) cone, backward (B)-α-gated spectra are subtracted from the forward (F)-α-gated spectra. The ICF channels are identified from forward (F)-α-gated spectra (corrected for slow α-component). The relative production yield of the identified reaction products are deduced from the intensity of the photopeak of characteristic prompt γ transitions assigned to a particular reaction product. Spectroscopic data, such as prompt γ energies and their intensities, are taken from the NNDC and RADWARE level scheme directory [15, 16]. Further, it may be pointed out that the relative number of statistical and "yrast"-like transitions depend on the entry state angular momenta and the available excitation energy (E*). The CF reaction products are formed at high E* and low angular momenta leading to more statistical transitions, where "yrast" states are expected to be fed by statistical γ transitions. However, the ICF reaction products may achieve low E* (due to the involvement of partial degrees of excitations) and high angular momenta (relatively higher values of impact parameters contribute to the high-spin states) at a given projectile energy. In such a case, the number of "yrast"-like transitions are expected to be much larger than that of the statistical ones, where less or no feeding is expected. Therefore, the spin distributions of CF and ICF products are expected to be entirely different in nature and can be used as a sensitive tool to probe reaction dynamics by looking into the entry state spin population [17]. As such, to have an insight into the decay patterns of CF and ICF reaction products, spin distributions of different reaction products were generated.

3 Results and Discussion

As has already been discussed that events were collected with particle-γ coincidences given by the HPGe Compton suppressed detectors and Phoswich detectors. The CF channels ^{171,170}Ta were identified from the background suppressed singles spectra. In order to increase the statistics, the gain matched γ-ray spectra of HPGe detectors

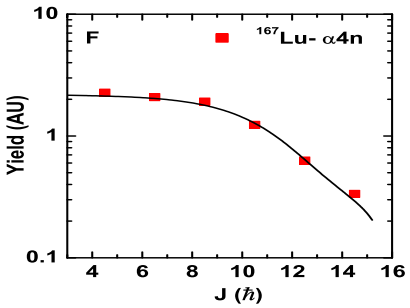

Figure 4. (Color online) Experimentally measured spin distributions for ICF-α4n channel (identified from forward α-gated spectra). Reaction products are labeled by self-explanatory notations and emission cascades. Lines through the data points are drawn to guide the eyes.

were summed up. As a representative case, Fig. 2(a and b) shows the typical singles and forwarded alpha-gated spectra. The selection of the rotational band for ^{170}Ta residues has been obtained from the level scheme [18] and the peaks are assigned for the characteristics γ-lines in Fig. 2(a). Relative production yields as a function of experimentally observed spin (J) for ^{170}Ta alongwith ^{171}Ta populated via CF only are plotted in Fig 3. The errors have not been shown in the figures as they have been estimated to be $\leq 10\%$ and the inclusion of these errors is not likely to modify the present analysis. The measured spin distribution profile for ICF residues ^{167}Lu (α4n channel) is plotted in the Fig.4, where, the selection of the band for this channel has been obtained from the level scheme [19]. It may be mentioned that Figs. 3 and 4 show the experimentally measured relative production yield as a function of spins (J) which is termed as 'spin distribution' [11].

The nomenclature 'F' used in Fig.4 indicates the involved reaction dynamics for ICF-channel i.e., identified from forward(F)-α-gated spectra. As can be observed from the figures 3 and 4, in general, there is a strikingly different behavior of the spin-distribution patterns for different channels which indicates the involvement of entirely different reaction dynamics in the production of these reaction products. The intensity of xn(singles) (populated via CF only) falls off rather quickly with observed spin (J), indicating strong feeding and/or broad spin population during the de-excitation of CN. However, for αxn-F-channels (expected to be populated via ICF), the intensity appears to be almost constant up to a certain value of J, and then decreases towards high angular momentum. This indicates the absence of feeding to the lowest members of the 'yrast' band and/or the members of the 'yrast' band and/or the population of low spin states are strongly hindered in the ICF channels.

4 Summary

This paper gives the recent preliminary experimental results for the particle-γ coincidence experiment. The identified xn (populated via CF) and αxn (populated via ICF) channels indicate the different de-excitation patterns on the basis of entry state spin. In order to understand the magnitude of mean driving angular momenta (ℓ-values), and to examine the possibility to populate high spin states via ICF, mean driving angular momenta involved in CF and ICF channels will be deduced from the analysis of spin-distributions.

Acknowledgements

The authors thank to the Chairman, D/o Physics, AMU, Aligarh & the Director, IUAC, New Delhi, for providing all the necessary facilities to carry out this work. RP, BPS, DPS and VRS thanks to the DST: SR/S2/HEP-30/2012 for providing financial support.

References

[1] P. R. S. Gomes *et al.*, Phys. Lett. B **601**, 20 (2004).
[2] M. Dasgupta *et al.*, Nucl. Phys. A **787**, 144 (2007).
[3] A. Yadav *et al.*, Phys. Rev. C **86**, 014603 (2012); ibid **85**, 034614 (2012); ibid **85**, 064617 (2012) and references therein.
[4] Vijay R. Sharma *et al.*, Phys. Rev. C **89**, 024608 (2014), ibid., **84**, 014612 (2011).
[5] Devendra P. Singh *et al.*, Phys. Rev. C **89**, 024612 (2014).
[6] M. Cavinato *et al.*, Phys. Rev. C **52**, 2577 (1995).
[7] H. C. Britt and A. R. Quinton, Phys. Rev. **124**, 877 (1961).
[8] T. Inamura *et al.*, Phys. Lett. B **68**, 51 (1977).
[9] I. Tserruya *et al.*, Phys. Rev. Lett. **60**, 14 (1988).
[10] P. P. Singh *et al.*, Phys. Rev. C **78**, 017602 (2008).
[11] P. P. Singh *et al.*, Phys. Lett. B **671**, 20 (2009).
[12] O. B. Tarasov and D. Bazin, Nucl. Instrum. Methods Phys. Res., Sect. B **204**, 174 (2003).
[13] SRIM06; [http://www.srim.org/].
[14] R. K. Bhowmik, S. Muralithar, and R. P. Singh, DAE-Nucl. Phys. Symp. **44B**, 422 (2001); **44B**, 382 (2001) (private communication).
[15] http://www.nndc.bnl.gov/
[16] RADWARE, the level scheme directory on http://radware. phy.ornl.gov/agsdir1.html.
[17] G. J. Lane, G. D. Dracoulis, A. P. Byrne, A. R. Poletti, and T.R. McGoram, Phys. Rev. C **60**, 067301 (1999), and references therein.
[18] Y. H. Zhang *et al.*, Phys. Rev. C **60**, 044311 (1999).
[19] C. H. Yu *et al.*, Nucl. Phys. A **511**, 157 (1990).

Innovative Road Map for Leveraging ICT Enabled Tools for Energy Efficiency – From Awareness to Adoption

Neelu J. Ahuja[1]
neelu@ddn.upes.ac.in
Centre for Information Technology,
College of Engineering Studies,
University of Petroleum and Energy Studies, Dehradun.

Inder Singh[2]
inder@ddn.upes.ac.in
Centre for Information Technology,
College of Engineering Studies,
University of Petroleum and Energy Studies, Dehradun.

Abstract

Educating the energy efficiency measures at grass root levels, ranging from awareness to adoption, is the need of the hour and a very significant step towards energy security. The present work proposes a project-oriented approach based roadmap for the same. The approach initiates with a pre-survey of energy users, in terms of understanding their awareness level, current energy consumption patterns, and ascertaining their proposed adoption level towards innovative energy efficiency measures. It also assesses their interest towards different IT tools and mechanisms including their interface design preferences. Material designed, custom-tailored as per the needs of the users, is proposed to be delivered through identified IT methods. A post-survey done after an active IT intervention period proposes to bring out the variation from the pre-survey. Finally, use of analytical tools in concluding phase adjudges the interventions' effectiveness in terms of awareness generation, technology adoption level, change in energy consumption patterns, and energy savings.

Keywords - Web-based Applications, Mobile applications, Computer Based Training, ICT adoption, Energy Efficiency.

I. INTRODUCTION

India has one of the world's fastest growing energy markets and is expected to be the second largest contributor to global energy demand increases by 2035, accounting for 18% of the rise in global energy consumption. India's has growing energy demands but limited fossil fuel reserves. Due to this limitation of resources India needs to be energy efficient. For being an energy efficient country, there is a need for greater degree of planning and update of measures in a systematic manner for better application and implications.

The gap between demand and supply of Energy resources has widened today. This has increased pressure on energy resources. Energy resources should be used efficiently as they play a critical role in the development of an economy. Moreover consumers are not aware of the energy efficiency measures. The problem lies in awareness and popularization of energy efficiency measures both at domestic level and industrial level using IT intervention. Formulated plans and identified measures need to reach larger audience in order to achieve significant energy savings.

Popularization of energy efficiency measures is of prime importance in the current context, considering the amount of energy loss that can be prevented through it. This warrants a compelling need to adopt Information Technology (IT) tools and services to this effect. The existence of an appropriate information dissemination and popularization methodology is as important as creation of such information.
ICT being a tool with maximized reach facilitates, the dissemination of energy efficiency related information with emphasized impact, and also ascertains the adoption level by the end users though analytical approach towards pre and post ICT intervention.

978-1-4799-1734-1/15 $31.00 © 2015 IEEE
DOI 10.1109/ICACCE.2015.45

Innovative IT methods, such as web portals, applications, facilitate a very wide extent of information delivery. Technological advancements in IT aid information, to be appropriately tailored, specifically aligned towards identified target groups and delivered using varied communication channels.

A systematic approach is called for with crisp objectives supported by concrete implementation plan. Primary objective is to determine the awareness level of consumers sector-wise, with sectors being identified as offices of public sector undertakings or of private industries and limited companies, or collection of informal domestic users. The scope of the present work is to develop web portal for popularization of energy efficiency measures among consumers of identified sectors. Next most significant segment of the approach is quantification and measurement of adoption level of these measures post ICT intervention for the consumers of identified sectors.

II. RELATED WORK

The section below summarizes work done so far concerning ICT intervention with respect to energy efficiency. Use of Information Technology in popularization, awareness generation and change implementation is a long known phenomenon. TERI (The Energy and Resources Institute) has been active to take the call of the hour to design and implement a variety of innovative energy savings solutions promoting safe and secure tomorrow. Available web-portal reveals education to youth for sustainable development as the key to their operations [1].

USAID – India (US Agency for International Development) funded project ECO-III 2010, exclusively focused upon the energy efficient buildings through conservation building code implementation framework [2,3]. The complete workflow is IT driven and implemented using IT tools. "Energy Services Company" concept is catching up in India with more and more entrepreneurs joining the wagon. The thought ahead as mentioned in an article of Bulletin of Energy efficiency (BEE) is to educate the top management on the implications of energy cost reduction, its influence on profits, competition, pricing, etc. Before they consider the ESCO option, they will have to appreciate that energy savings will result in profit improvement, and energy saving is the easiest option to improve profits compared to all other options. Further, use of IT for demonstration projects pertaining to various industrial sectors and utilities in addition to the present promotional demonstration project for government buildings, has been identified as action area, with continuous thrust by government.

Ministry of New and Renewable Energy (MNRE), of Govt of India, has "Information & Public Awareness Programme" with objective to disseminate information on new and renewable sources of energy (NRSE) systems/devices through variety of media like electronic, print & exhibition as well as outdoor media, thereby popularizing and creating awareness about such systems and devices [4]. It also brings to the fore benefits, technological developments and promotional activities taking place in the renewable energy arena from time to time. The role of this program, for inculcating the importance of renewable energy amongst masses has been assuming increasing significance in recent times. The Programme is implemented mainly through IT-Enabled integration of State Nodal Agencies, Directorate of Advertising & Visual Publicity (DAVP), Doordarshan, All India Radio (AIR), and Department of Posts, etc.

UNDP's project in partnership with ministry of railways has been functional since 2011, with prime focus on institutional capacity development, technical training, implementation of energy-efficient technologies and sharing knowledge on best practices [5,6]. IT has been extensively put to use for this purpose. Project to be continued until 2017, has following accomplishments so far: Web portal 'railsaver.gov.in' on energy efficiency management system (launched-15 April 2014). The portal is educative and additionally contains energy data for the Indian railways. Center of Excellence (COE) established at the Indian Railways Institute for Electrical Engineers (IRIEEN), Nasik imparts training to the Indian

Railways staff on energy efficiency. Technology Information Resource and Facilitation Desk (TIRFAD) established at the Research Design & Standards Organization (RDSO), Lucknow, Uttar Pradesh further work, towards energy efficiency goal [6].

III. Materials and Methods

Uttarakhand is a gifted state in terms of availability of natural resources primarily the solar energy to support itself in the times of energy crisis and to overcome the problem of limited fossil fuel resources. This tremendous potential is being actively tapped for energy from new and renewable sources. But an extravagant and un-economical usage of energy, would lead to defeat of the whole purpose. Hence, it is a compelling and enthralling call to the state to churn out significant energy savings.

There is a need to take concrete steps for conventional energy conservation measures in domestic sectors, and industries and commercial establishments, proliferate in the state. There is a marked need to evolve suitable alternatives to meet the burgeoning energy demand. Information dissemination and public awareness through training programs, publications, exhibitions, seminars and conferences, has been identified by Strategic Energy Conservation Action Plan report of UREDA [7].

Web portal, energy calculator tool and android applications to disseminate information on energy efficiency measures are the primary anticipated deliverables from this project-based approach. Further processes and features proposed to be interleaved with the above are blogs, games (to elicit attention and interest of different groups), animations and animated favorite characters to deliver message, photo-sharing, latest trends in energy domain, relevant government notifications, less known but relevant interesting facts, energy (consumer) efficient product descriptions, video shares, performance benchmarks, encouragement certificates (individual/firm) and awards such as star performer of day/week/month, idea-owner of the day, best article/poster, best photo, and many similar interest generating features, with overall goal to save energy.

IV. Detailed Methodology

The section below presents a step-wise mechanism envisioned for ensuring the implementation of the proposed approach.

A. Pre-survey

First step of the process encompasses, pre-survey of users. The objective being primarily to understand general awareness, energy consumption pattern and the adoption level of the users towards ICT intervention in the area of energy efficiency. Additionally, the objective is to understand, the applicability of mobile applications, for users. Essential aspect is, to obtain user-interface preferences that reduce anxiety of users. It is very crucial at this stage to get a feel of their interest towards innovative IT methods and approaches. This becomes a precursor to analysis of IT infrastructural requirements such as bandwidth, storage, bulk-SMS, free-email ids as per the user base. Complete pre-requisite list for the subsequent operations is to be finalized based on this survey output.

B. Web-hosting, Platforms and Tools used

List of IT tools identified is: web-site/portal, android application, mobile applications and the like. For web-site development, a domain is needed to be provisioned, preferably of type '.org' as the purpose is awareness generation and knowledge dissemination and not for profit earning.

Web-hosting mechanism being identified is J2EE because it is platform independent and consists of a set of services, APIs and protocols that provides functionality for developing multi-tiered web-based applications. Provision for bulk-SMS facility is essential to be used along with the web portal. An android application developed for calculating the energy consumption, also is another essential artifact of

the web portal. It is a smart tool for users to monitor their energy consumption, and check out energy saving statistics before and after awareness campaigns. Mobile applications developed and distributed through web-portal and web applications are likely to ensure reach to large user base.

Web-site and database design are based on survey inputs. User-Interface design is of prime importance in terms of ensuring maximum user-friendliness and bilingual approach for maximum reach. Filling up of the registration form is mandatory in the web-site, to capture information about users, their occupations, sectors etc.

Database in MySQL server as backend for storing data from web-site is proposed to ensure smooth storage management.

Web-site development is proposed to be based on, software-engineering approach. Beta-version launch shall ensure testing the web-site and all the other tools developed. Testing is for bugs, denial of services, vulnerability and security checks. Agile and iterative methodologies are proposed to be used to refine the prototype model for better outcomes.

Filled-in registration forms from database repositories shall be analyzed using SPSS/similar statistical tools for categorization /segmentation of users based on demographic profile, age-wise profile, gender-wise profile, sectorial profile. Finally, identified sectors will be considered for further process.

Guest lectures, events, competitions, campaigns will be planned and scheduled. Energy Efficiency CBT (Computer Based Training) kits are proposed to be prepared for distribution.

Web-site and mobile applications shall be actively made available for usage. Other awareness tools such as Guest-lectures, kit distributions, events, poster presentations, campaigns etc will be actively implemented. Advertisement and promotion activities will be done using social and other media right from the process of web launch, until after successful implementation.

C. Post survey

Post-survey will be done along the same lines as pre-survey. Targeted sectors will be exclusively revisited for specific inputs with focus to capture information regarding the change in the energy consumption pattern and achieved energy saving, in addition to quantification of adoption level towards ICT intervention.

D. Data Analysis

Data collected and analytical tools such as SPSS applied over are proposed to present comparative study of the pre-and post-survey results. Findings interpreted in terms of efficacy of the awareness campaigns are the expected deliverables. An additional output is the finding concerning impact of this study on energy conservation.

The components sequenced in the roadmap have been graphically represented in Fig. 1 given below:

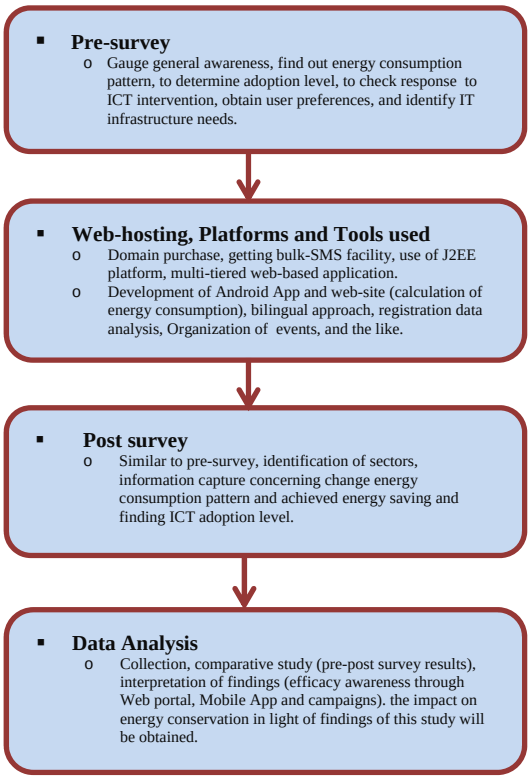

Fig. 1. Components of Road Map

In effort to further crystallize the fore-thought and planning the envisioned activities have been outlined in a tabulated form. Also a detailed timeline spread over 24 months period has been presented in this work.
Presented in the section below in Table 1 is the proposed time line facilitating implementation by specific agencies, further offering a concrete line of action.

Activities	Time Line (in Months)
Platform and tools- Phase 1	2
Website design, modules- Phase 1 (Energy calculator- Phase 1 & Content and registration form-- Phase 1)	3
Website development- Phase 2	2
Beta version, test run, feedbacks- Phase 2	1
Launch of Website and classification of sectors	1
Awareness campaign, activities, social media, bulk messages	4
Post User Survey	3
Difference in Pre and Post Consumer Awareness and impact on energy consumption , Number of hits using SPSS	4
Draft Report and Communication with users	4

Table 1. Implementation Timeline

Fig. 2 presents graphical chart of the same.

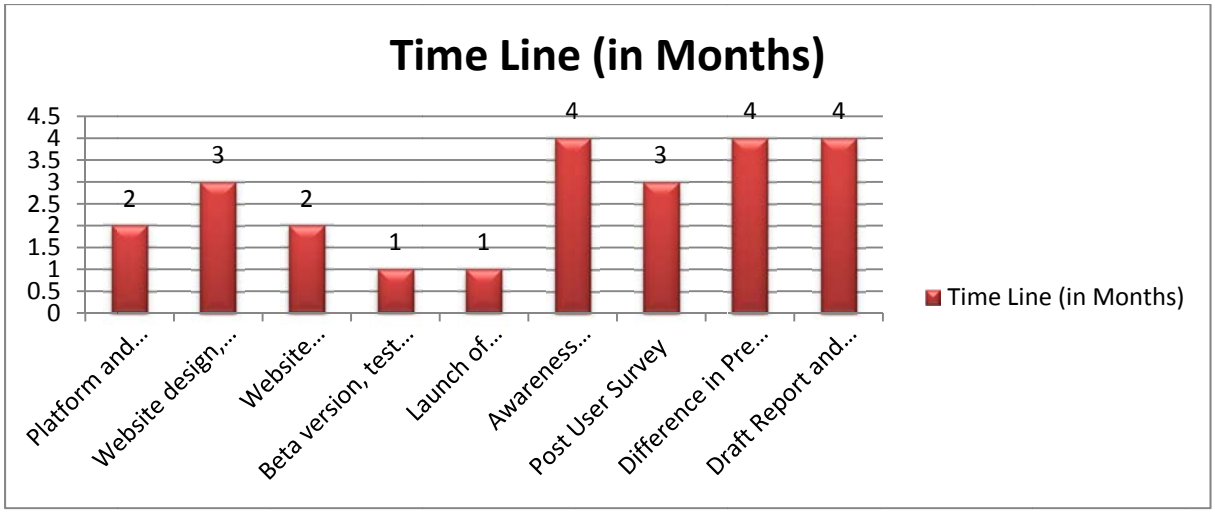

Fig. 2. Graphical Chart Representation of the timeline.

V. DISCUSSION

The socio-economic relevance of the roadmap being presented is manifold in the sense that energy efficiency awareness promotes saving energy resources reciprocates increase in GDP. It further initiates creation of ecological environment by using renewable energy resources, raising awareness among society towards saving energy. Moreover it will have wider implication on economy of India by fulfilling the demand and supply gap.

VI. CONCLUSION

The present work proposes an innovative, inventive roadmap for IT intervention in spreading awareness towards energy saving through energy efficiency measures. It enables a forethought process towards a national cause, facilitating a participatory approach in a very coordinated, well-beaded manner, ranging from awareness to adoption, in built with analytics to adjudge adoption levels.

REFERENCES

[1] The Energy and Resources Institute. [Online]. http://www.teriin.org/

[2] (2014, December) United States Agency for International Development programs and activities in India. [Online]. http://www.usaid.gov/india

[3] United States Agency for International Development (USAID/ India). [Online]. http://www.eco3.org/usaid

[4] (2015, January) Ministry of New and Renewable Energy - Support Programs. [Online]. http://mnre.gov.in/schemes/support-programmes/

[5] (2014, October) United Nations Development Programme in India. [Online]. http://www.in.undp.org/

[6] (2014, July) Improving Energy Efficiency in the Indian Railways System. Web Site - http://www.in.undp.org/content/india/en/home/operations/projects/environment_and_energy/improving_energyefficiencyintheindianrailwaysystem.html.

[7] "Strategic Energy Conservation Action Plan," UTTARAKHAND RENEWABLE ENERGY DEVELOPMENT AGENCY, UK, Association Of Energy Conservation & Environment Protection 01/UREDA/VCTAS/2008 -09, 2009.

EPJ Web of Conferences **86**, 00064 (2015)
DOI: 10.1051/epjconf/ 20158600064

Low energy incomplete fusion and its relevance to the synthesis of super heavy elements

Abhishek Yadav[1,a], P Kumar[2], A Raghav[2], Mohd Shuaib[2], V R Sharma[2], D P Singh[3], P P Singh[4], Sunita Gupta[5], U Gupta[2], M K Sharma[6], Indu Bala[1], R Kumar[1], S Muralithar[1], R P Singh[1], B P Singh[2], and R Prasad[2]

[1]*NP Group: Inter-University Accelerator Centre, Aruna Asaf Ali Marg, New Delhi-110 067, Delhi, India*
[2]*Department of Physics, Aligarh Muslim University, Aligarh-202 002, Uttar Pradesh, India*
[3]*Department of Physics, University of Petroleum and Energy Studies, Dehradoon-248 007, Uttrakhand, India*
[4]*Department of Physics, Indian Institute of Technology Ropar, Roopnagar-140 001, Punjab, India*
[5]*Department of Physics, Agra College, Agra-282 001, Uttar Pradesh, India*
[6]*Department of Physics, S. V. College, Aligarh-202 001, Uttar Pradesh, India*

Abstract. To study the presence of incomplete fusion at energies around the Coulomb-barrier and to understand its dependence on various entrance-channel parameters, the incomplete fusion fractions have been deduced (*i*) from excitation function measurements for ^{18}O,^{13,12}C+^{159}Tb, and (*ii*) from forward recoil range measurements for ^{12}C+^{159}Tb systems, at low energies (<7MeV/A). The data have been analyzed within the framework of compound nucleus decay, which suggests the production of *xn*/p*xn*-channels via complete fusion, as these are found to be well reproduced by PACE4 predictions, while, a significant enhancement in the excitation functions of α-emitting channels has been observed over the theoretical ones, which has been attributed due to the incomplete fusion processes. Further, the incomplete fusion events observed in case of forward recoil ranges have been explained on the basis of the breakup fusion model, where these events may be attributed to the fusion of ^{8}Be and/or ^{4}He from ^{12}C projectile to the target nucleus. For better insight into the underlying dynamics, the deduced fractions of incomplete fusion have been compared with other nearby systems as a function of various entrance channel parameters. The incomplete fusion has been found to be sensitive to the projectile's energy and alpha-Q-value of the projectile.

1 Introduction

In super-heavy element (SHE) production laboratories, considerable efforts are being employed to synthesize the SHE using heavy-ion induced complete fusion (CF) reactions with low excitation energy [1]. In addition to the fission and quasi-fission, the existence of incomplete fusion (ICF) at low incident energies (i.e., ≈ 4-7 MeV/A) may add complexity to the synthesis of SHEs. In general, at these energies, CF is supposed to be the sole contributor to the total fusion cross section [2]. However, in recent years a large fraction of ICF has been observed at energies as low as ≈ 4-7 MeV/A [3–7]. The onset of ICF at near barrier energies triggered the resurgent interest to understand the ICF reaction dynamics. In ICF reactions the incident projectile is assumed to break up into its fragments, as a consequence of excess input angular momentum, and one of the breakup fragments fuses with the target nucleus [8]. It is customary to disentangle CF and ICF on the basis of driving angular momenta (ℓ-values) [8]. At central and/or near-central interactions for ℓ-window $0 \leq \ell \leq \ell_{crit}$, the CF is expected to be the dominant process, where intimate contact and transient amalgamation of entire projectile and target nucleus leads to the formation of an excited compound nucleus with pre-determined charge/mass and excitation energy. However, for peripheral collisions or at sufficiently higher energies, ℓ-values may be higher than ℓ_{crit}. As a consequence fusion of entire projectile may be hindered and gives way to the ICF. This forms an incompletely fused composite (IFC) system, and direct projectile-like-fragments (PLFs) found to be centered in the forward cone. This IFC have relatively less mass/charge and excitation energy (due to partial fusion of projectile), but have high angular-momenta (imparted due to non-central interactions) as compared to the CN formed via CF [8]. The additional break-up degrees of freedom make the fusion process more complicated and the possible reaction processes may be; *i*) the non-capture break-up, when none of the breakup fragments is captured, *ii*) ICF, when one of the breakup fragments is captured, *iii*) sequential complete fusion (SCF), the successive capture of all fragments by the target nucleus. Experimentally, it is not possible to disentangle the cross-sections for direct (σ_{DCF}) and sequential (σ_{SCF}) complete fusion, because both channels lead to the same final reaction residues. Hence, the CF cross-section (σ_{CF}) is taken as the sum of σ_{DCF} and σ_{SCF}, whereas the sum of σ_{CF} and incomplete

[a]e-mail: abhishekyadav117@gmail.com

fusion cross-section (σ_{ICF}) may be referred to as the total fusion cross-section ($\sigma_{TF} = \sigma_{CF}+\sigma_{ICF}$). After the first experimental observation of "fast α-particles" at energies $\approx$ 10.5 MeV/A [9], a variety of experimental and theoretical studies have been devoted to understand ICF-reactions. Some of these studies are summarized in an outstanding review by Gerschel [10]. It may, however, be pointed out that the existing models/theories fairly explain ICF data obtained at energies E $\geq$ 10.5 MeV/A or so, but there is no theoretical model available to predict ICF at lower energies. Due to the unavailability of reliable theoretical model to predict low energy ICF, the experimental study of underlying dynamics is still an active area of investigation.

In view of the above, we have undertaken a programme to study the ICF-reaction dynamics in different projectile-target combinations at low energies. The onset of ICF at slightly above barrier energies has been emphasized in the excitation function (EFs) measurements [5, 6], however, a clear existence of ICF at low energies has been demonstrated by measuring more than one linear momentum transfer components in the forward recoil ranges [7]. In addition to this, the unclear or ambiguous dependences of ICF on various entrance channel parameters have also been explored and contradicting dependences of the fraction of incomplete fusion have been reported [11–13]. Morgenstern *et al*. [13]correlated the ICF fraction with entrance channel mass asymmetry (μ_A). Recently, Singh *et al*. [5] introduced the importance of projectile structure in ProMass-systematics. Hence, in order to explore the low-energy incomplete fusion and to find a consistent general systematics for low energy ICF reactions, which may support the SHE formation, measurements of excitation function for ^{18}O,^{13,12}C+^{159}Tb systems at energies $\approx$ 4-7MeV/A and forward recoil ranges for ^{12}C+^{159}Tb at three above barrier-energies have been performed.

2 Experiments

In order to ascertain above aspects, two kinds of experiments have been performed by our group at the Inter-University Accelerator Center (IUAC), New Delhi; (*i*) the experiments to measure "*the excitation functions*" of radio-nuclides populated during the interaction of ^{18}O,^{13,12}C+^{159}Tb systems at energies $\approx$ 4-7MeV/A, and (*ii*) the experiments to measure "*the forward recoil ranges*" of residues populated during the interaction of ^{12}C+^{159}Tb at three widely different above barrier energies. Here, brief experimental details are given for the ready reference; however, the details are given in refs [5, 6]. In these experiments the activation technique has been used. The irradiation of the samples have been carried out in the General Purpose Scattering Chamber having an in-vacuum transfer facility, which has been used to minimize the lapse time between the stop of the irradiation and beginning of the counting of the activity induced in the target-catcher assembly. The activities induced in the samples were recorded by counting each target along with the catcher foil, using a pre-calibrated HPGe γ-ray spectrometer. A 50Hz pulser was used to determine the dead time. The detector-sample separation was adjusted to keep the dead-time below 10% during the counting so as to minimize the pile up effects. The efficiency calibration of the detector in the specified geometry was carried out using a standard ^{152}Eu source of known strength at various source-detector separations. The characteristic γ-lines have been used to identify reaction products. Further, the decay curves of the identified reaction products have also been analyzed to confirm the identification. Nuclear data on radio-nuclides, such as the corresponding γ-ray abundances and half-lives were taken from ref [14]. The production cross sections of the reaction products have been determined using the standard formulation [5, 6]. It may be pointed out that the errors in the measured production cross sections may arise due to (*i*) the nonuniformity of target foils, (*ii*) fluctuations in the beam current, (*iii*) the uncertainty in geometry dependent efficiency of HPGe detector, and (*iv*) due to the dead time of the spectrometer. Detailed discussion on the error analysis is given elsewhere [5, 6]. The overall errors including statistical errors are estimated to be $\geq$15%, excluding the uncertainty in branching ratio, decay constant, etc.

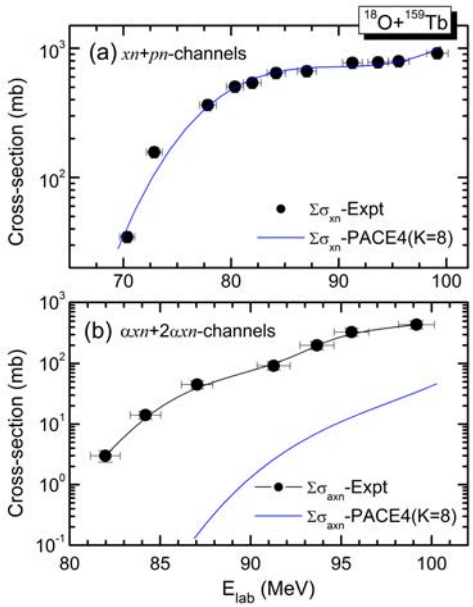

Figure 1. The experimentally measured and theoretically calculated EFs for (a) xn+pxn, and (b) αxn+2αxn-channels populated in ^{18}O+^{159}Tb interactions (for details see the text).

3 Interpretation of results

3.1 Excitation Functions (EFs)

To understand the formation mechanism of reaction products, the experimentally measured excitation functions have been analyzed within the framework of statistical model code PACE4 [15] based on equilibrated CN-decay of Hauser-Feshbach theory. It may, however, be pointed out that the ICF and pre-equilibrium-emission (PEE) are not taken into consideration in this code. In this code, level density parameter (a=A/K) is an important input parameter which affects the CF cross-sections and may be varied to match the experimental cross-sections. In the present

system at studied energy range the parameter "a=A/8" has been found to reproduce satisfactorily, the experimental data for both the *xn* and *pxn*-channels, which shows the production of these residues via CF processes. As a representative case, in Fig.1 (a) the sum of cross-sections for all experimentally measured *xn* & *pxn*-channels for ^{18}O+^{159}Tb system have been compared with that of corresponding theoretical calculations with physical justified set of parameters. The same set of parameters has been retained and used to check the production mechanism of α-emitting channels, also. In Fig.1 (b), the sum of measured αxn and $2\alpha xn$-channels for same system has been plotted and compared with theoretical calculations. As shown in Fig.1 (b), the measured cross-sections for α-emitting channels are found to be significantly enhanced than theoretical predictions. The enhanced cross-section in case of α-emitting channels point towards some physical effects which are not included in this code. It has already been mentioned that PACE4 do not take ICF, PEE into account and hence, this enhancement may be attributed as the contribution due to ICF-reaction mechanism.

3.2 Forward Recoil Range Distributions (FRRDs)

In heavy-ion interactions, the CF & ICF processes may lead to the characteristic velocity distribution of the reaction products on the basis of linear momentum transfer from projectile to the target nucleus. As such, the distribution of measured yields of the populated reaction residues as a function of velocity and/or the range of residue in a stopping medium may give an insight into the reaction mechanism. Though the differences in the velocity and ranges of CF and ICF reaction products are not so significant, by using very thin catcher foils ($\approx\mu$g/cm^2), it is possible to separate both kind of residues. Hence, in order to demonstrate the presence of ICF reactions in ^{12}C+^{159}Tb, the recoil ranges of residues have also been measured at three above barrier energies. The resulting normalized yields of different reaction products have been plotted against cumulative catcher foil thicknesses to obtain the differential recoil range distributions for the residues viz., ^{168}Lu ($3n$), ^{167}Lu ($4n$), ^{165}Lu ($6n$), ^{167}Yb ($p3n$), ^{165}Tm ($\alpha 2n$), ^{163}Tm ($\alpha 4n$), ^{161}Ho ($2\alpha 2n$), ^{160}Ho^g ($2\alpha 3n$) and ^{160}Ho^m ($2\alpha 3n$). In this paper, as a representative case to show different linear momentum transfer components in various CF and ICF processes the FRRDs for ^{167}Lu($4n$) and ^{165}Tm($\alpha 2n$) residues have been presented and shown in Figs.2(a-f). These figures clearly show the different momentum transfer components, depending on the fused mass of the projectile with the target nucleus. In the case of $4n$-channel (Fig.2(a-c)), the measured FRRDs show only a single peak, at all the three bombarding energies, indicating only single linear momentum transfer component (a characteristic of the CF process) involved in the production of ^{167}Lu residues. Similarly, in case of α-emitting channels, the residues ^{165}Tm, ^{163}Tm, ^{161}Ho, ^{160}Ho^g and ^{160}Ho^m are populated, respectively via $\alpha 2n$, $\alpha 4n$, $2\alpha 2n$ and $2\alpha 3n$ channels. The observed FRRDs were resolved into more than one Gaussian peaks. As a representative case, the FRRDs for the residues, ^{165}Tm ($\alpha 2n$), have been plotted at

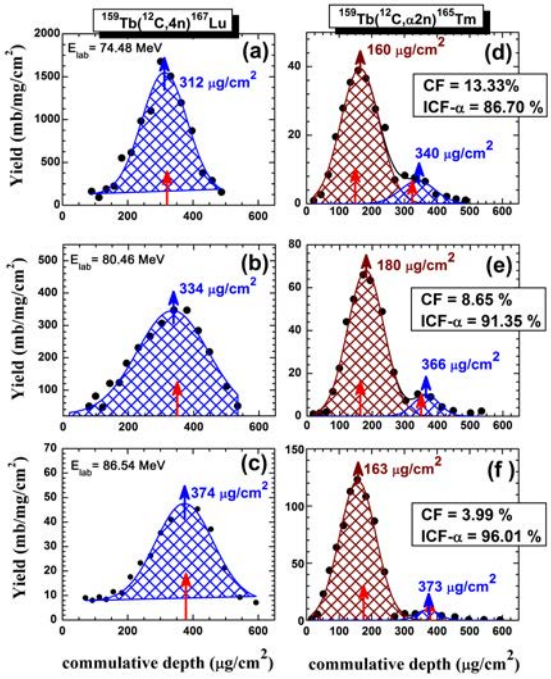

Figure 2. Typical FRRDs for ^{167}Lu and ^{165}Tm populated via $4n$ and $\alpha 2n$-channel, respectively. The red arrows are the theoretical most probabble ranges (for detail see text).

three different energies in Fig.2(d-f). As can be seen from this figure, the FRRDs may be fitted with two Gaussian peaks, one at 340±32, 366±60 and 373±65 μg/cm^2 for three beam energies, indicating the complete momentum transfer events, however, another peak at lower cumulative depths correspond to the fusion of ^{8}Be (if ^{12}C is assumed to break-up into ^{8}Be $+\alpha$) with ^{159}Tb target nucleus. Similarly, the FRRDs for other α-emitting channels indicating the presence of more than one linear momentum transfer component. It may be pointed out that, the neutron emission from the recoiling residues may change the energy/momentum of the recoiling nucleus, depending on the direction of emitted particles. This is reflected in the width (FWHM) of the experimentally measured recoil range distributions. The width may also arise because of the contribution from straggling effects. The most probable recoil ranges (R_{theo}) have also been theoretically calculated (shown in Fig.2 by red arrows); assuming that in the case of CF, the incoming ion completely fuses with the target nucleus and transfers its total linear momentum to the fused system, which recoils to conserve the input linear momentum. The theoretically calculated and experimentally measured recoil ranges are found to agree reasonably well within the experimental errors (for details see ref. [6]).

3.3 Incomplete fusion fraction

It is evident from the analysis of EFs and FRRDs measurements that ICF-reactions contribute significantly to the production cross-section of α-emitting channels at studied energies. Nevertheless, both the measurements of FRRDs and the EFs give nearly same F_{ICF} values for same system

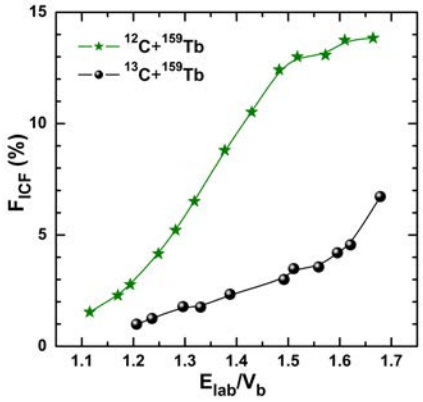

Figure 3. The comparison of F_{ICF} for $^{13}C+^{159}Tb$ and $^{12}C+^{159}Tb$ systems at constant v_{rel}=0.053c.

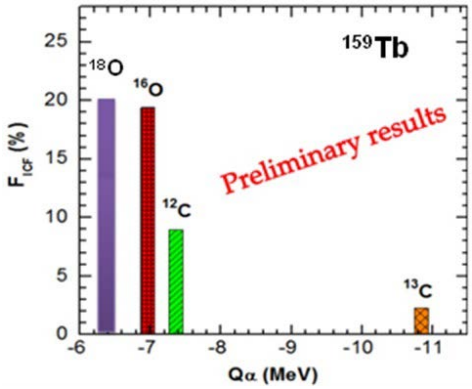

Figure 4. The comparison of incomplete fusion fraction for the studied systems ^{18}O,$^{13,12}C+^{159}Tb$ with $^{16}O+^{159}Tb$ [5].

which strengthen the measurements and indicate the self-consistency of the data [6]. Further, the ICF contribution for all studied systems have been deduced using the prescription of Gomes *et al.*, [4]. The ICF-contribution for individual channels has been deduced by subtracting CF cross-sections ($\Sigma\sigma_{CF}$) from the experimentally measured total fusion cross sections (σ_{TF}) at each studied energy. It is not out of place to mention that the σ_{TF} has been corrected for the missing channels (which could not be measured experimentally) by their PACE4 values. Hence, the $\Sigma\sigma_{ICF}$ may be taken at least as the lower limit of ICF-contribution. The percentage F_{ICF}, which is the measure of relative strength of ICF contribution to the total fusion, may be defined as, F_{ICF} %= $(\Sigma\sigma_{ICF}/\sigma_{TF}) \times 100$ have been deduced and the comparison of F_{ICF} for ^{12}C and 13C interactions with ^{159}Tb target have been shown in Fig.3, where ^{12}C projectile having more ICF as compared to ^{13}C projectile, which shows a clear projectile dependency on ICF reactions.

4 Remarks on the effect of projectile type

In order to understand the effect of projectile on ICF-reactions, the F_{ICF} for $^{18,16}O$,$^{13,12}C+^{159}Tb$ systems at a constant relative velocity (v_{rel} = 0.053) have been plotted as a function of Q_α-value of the projectile in Fig.4. This comparison of F_{ICF} for different projectiles on same target reveals a strong projectile dependence of low-energy incomplete fusion. It is clear from this figure, that the F_{ICF} is $\approx$ 18% larger for ^{18}O than ^{13}C as projectile on the same target ^{159}Tb, which can be understood by recently proposed alpha-Q-value systematics [6]. The more-negative Q_α-value for ^{13}C translates into the smaller breakup probability into constituent α clusters, resulting in a smaller ICF-fraction than for ^{18}O induced reactions. The present work strengthens the recently observed alpha-Q-value systematics [6] for strongly bound projectiles. It may, however, be pointed out that the systems studied in the present work are rather light, which may not cater to the requirement of synthesizing super heavy elements. However, a rich data set from medium to heavy targets may help to develop some systematics to understand the probability of involved reaction processes at these energies, which may be useful in the super heavy element research.

Acknowledgements

The authors thank to the Director, IUAC, New Delhi, India, for providing all the necessary facilities to carry out this work. One of authors A.Y. thanks the DST for providing support through Young Scientist Scheme under start-up research grant.BPS, RP and DPS thank to DST and UGC for providing financial support.

References

[1] Yu. Ts. Oganessian *et al.*, Nature (London) **400**, 242 (1999), and references therein.
[2] M. Dasgupta *et al.*, Nucl. Phys. A **787**, 144-149 (2007).
[3] A. Diaz-Torres and I. J. Thompson, Phys. Rev. C **65**, 024606 (2002); Phys. Rev. Lett. **98**, 152701 (2007).
[4] P. R. S. Gomes *et al*, Phys. Rev. C **73**, 064606 (2006); Phys. Lett. B **601**, 20 (2004).
[5] Pushpendra P. Singh *et al.*, Phys. Rev. C **77**, 014607 (2008); Euro. Phys. J. A **34**, 29-39 (2007).
[6] Abhishek Yadav *et al.*, Phys. Rev. C **85**, 034614 (2012); *ibid* **85**, 064617 (2012); *ibid* **86**, 014603 (2012) and references therein.
[7] D. P. Singh *et al.*, Phys. Rev. C **81**, 054607 (2010).
[8] T. Inamura *et al.*, Phys. Lett. B **68**, 51 (1977); Phys. Lett. B **84**, 71 (1982); Phys. Rev. C **32**, 1539 (1985).
[9] H. C. Britt and A. R. Quinton, Phys. Rev. **124**, 877 (1961).
[10] C. Gerschel, Nucl. Phys. A **387**, 297 (1982).
[11] L. F. Canto *et al.*, Phys. Rev. C **58**, 1107 (1998).
[12] M. Dasgupta *et al.*, Phys. Rev. C **70**, 024606 (2004).
[13] H. M. Morgenstern *et al.*, Phys. Rev. Lett. **52**, 1104 (1984); Z. Phys. A **313**, 39 (1983).
[14] E. Browne and R. B. Firestone, Table of Radioactive Isotopes (Wiley, New York, 1986).
[15] A. Gavron, Phys. Rev. C **21**, 230 (1980).

Neural Network based Decision Support System for Optimal Incinerator Control

Prakash G L*, Samson Saju†, Snehil Mitra† and Vedant Sharma†

* Assistant Professor, Department of Computer Science and Engineering, UPES, Dehradun, Email:glprakash78@gmail.com
†M.Tech, Artificial Intelligence and Artificial Neural Network, Department of Computer science and Engineering, UPES, Dehradun, Email:samsonsaju@gmail.com

Abstract*—In recent years there has been a significant increase in the use of AI based techniques in the field of industrial control. Different Intelligent techniques like Fuzzy Logic, Artificial Neural Network and other Hybrids have been successfully implemented for various control problems. Waste gases generated in refineries from different processes like the Claus process, cannot be directly released into the atmosphere as it has sulfur compounds and other harmful compounds. These waste gases are incinerated before discharging to make them harmless. The incineration process uses fuel gas for oxidizing waste gases, thus incinerator needs to be optimized to use minimum fuel gas and maximum oxidization. In this paper a neural network is modeled for optimal control of incinerator in Sulfur Recovery Block of refineries. Optimal control is achieved by means of an Artificial Neural Network based Inverse Plant model. The Neural Network model was developed by using the neural network tool box in MATLAB.

Keywords: Artificial Neural Networks, SRU, Incinerator

I. INTRODUCTION

Petroleum Oil refineries are very important as they convert the crude oil into useful daily products such as petrol, diesel, kerosene, Liquefied Petroleum Gas (LPG) and other useful products. Sulfur is one of the major byproduct of refining crude oil. This sulfur is recovered by means of Sulfur recovery units. In sulfur recovery units (SRU), a stream of waste gas is produced from the Modified Claus process, known as tail gas which contains sulfur compounds thus cannot be introduced into the atmosphere without any treatment. The harmful compounds present in the tail gas can be destroyed with the help of incineration process. Incinerators are employed in sulfur recovery units for the treatment of tail gas before releasing the waste gas to the atmosphere.

The incinerator system burns all the sulfur compounds in the tail gas to SO_2 and then at a high elevation the gas is discharged to the atmosphere. The incinerator is designed to limit total SO_2 emission consistently within 0.1 percent of unrecovered sulfur and to limit H_2S stack emissions to less than 10 ppmv.

The incinerator system includes four sections- incinerator, reduction furnace, waste heat boiler and vent stack. In the thermal oxidizer burner, fuel gas is burned with excess air to a temperature over 1650^oC. The temperature is sufficient to heat the tail gas from Tail Gas Treatment Unit to $\sim 761^oC$ in the thermal oxidizer mixing chamber and to oxidize the residual H_2S and sulfur compound to SO_2, while minimize SO_3 formation. Reduction furnace is used to minimize NO_x formation. NH_3 rich sour water stripper gas along with required amount of air and fuel is fed to the burner to destroy NH_3 to N_2. The hot gas is routed to the incinerator. Figure 1, shows the schematic representation of the incinerator in SRU.

The hot flue gas from thermal oxidizer mixing chamber is passed through incinerator waste heat boiler to recover heat from the gas. Steam is generated. The flue gas from incinerator waste heat boiler at 325^oC is discharged to the incinerator stack. The stack height of 80 meters is set to ensure dispersion of SO_2 and to meet ground level concentration limits. Besides the oxidation of hydrocarbons to carbon dioxide and water, other oxidation reactions in the incinerator are as follows:

$$H_2S + 3/2O_2 \longrightarrow SO_2 + H_2O$$
$$2COS + 3O_2 \longrightarrow 2CO_2 + 2SO_2$$
$$CO + O_2 \longrightarrow CO_2$$
$$CS_2 + 3O_2 \longrightarrow 2SO_2 + CO_2$$
$$Sn + nO_2 \longrightarrow nSO_2$$

The incinerator effluent temperature controls the flow rate of fuel gas and it is maintained at desired operating temperature of $\sim 761^oC$. The incinerator is refractory lined with an external thermal shroud to control the shell temperature. Skin thermocouples are provided to monitor the shell temperature. The shell temperature is maintained between 149 to 350^oC.The incinerator air blower is designed to ensure a minimum of 2 percent excess O_2 in the flue gas at the stack and flue gas temperature of $\sim 761^oC$ from the incinerator. Ambient air is drawn through the inlet filter to remove solid debris and to protect against water during heavy rainfall.

The reaction in the reduction furnace is as follows:

$$2NH_3 + 3/2O_2 \longrightarrow N_2 + 3H_2O$$

The destruction of ammonia to nitrogen is ensured by adjusting air and fuel flow. Excess air causes formation of NO_x. The combustion air to the reduction furnace is drawn from the same incinerator air blower. The hot gas from the

reduction furnace is routed to the incinerator. The hot flue gas from incinerator is cooled by incinerator waste heat boiler. Incinerator WHB is used to recover heat from the flue gas and to generate MP steam. The flue gas at $\sim 325^oC$ is vented to the atmosphere through the vent stack. SO_2, O_2, NO_x and CO analyzers are provided in the stack to measure the SO_2, O_2, NO_x and CO in the effluent gas.

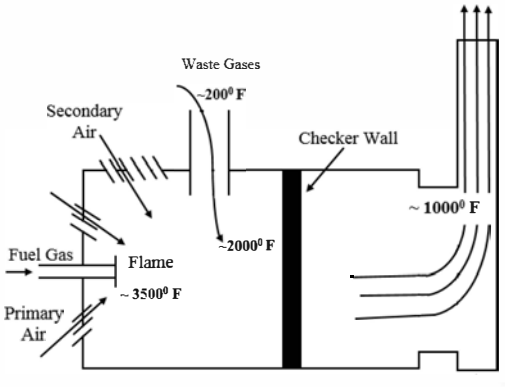

Fig. 1. Schematic Representation of the Incinerator

Suppose we know an input output relationship as described in equation (1). The inverse model is a function that produces the vector x for an input vector d. Equation (2) is the inverse model of equation (1). In an inverse plant model we construct a neural network approximation of $f^{-1}(\cdot)$ by using the data procured from the actual plant. The inverse plant model is shown in Figure 2.

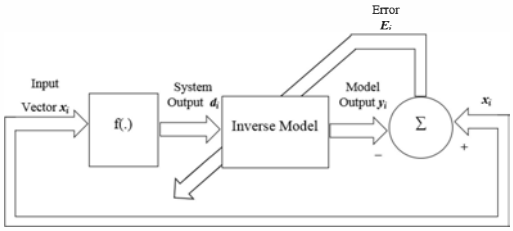

Fig. 2. Block Diagram of Inverse Plant Model

$$d = f(x) \tag{1}$$

$$x = f^{-1}(d) \tag{2}$$

This paper is organized as follows: In Section II, the related work is discussed. The Neural network models and architectures are discussed in Section III. Section IV gives the problem definition and Section V discusses about the proposed methodology including preparation of training data and training the ANN. The performance analysis is discussed in Section VI. Conclusion and the further possible research directions are discussed in section VII.

II. RELATED WORK

In 1973, studies were initiated to determine if it was necessary for the incinerator to consume large volumes of fuel gas to assure protection of the environment. Many laboratory and field investigations were carried out by Western Research on the optimal use of fuel gas in incinerators. The result of these studies are shown in previous works [1] - [3]. From these studies it was concluded that for a given incinerator there exists certain operating condition which requires minimum fuel consumption and yet provide satisfactory oxidization of harmful sulfur compounds. It was also found out in the studies that up to 40 percent of the fuel gas could be saved by operating the incinerators in these optimal operating range. There exists different works which propose different methodologies and techniques for increasing the efficiency of incinerators by use of effective catalysts [4], modified design for tail gas cleanup process for Claus process [5][6].

Recently artificial neural networks has been found to be very promising for adaptive control of nonlinear systems. The ability of neural networks to model arbitrary nonlinear functions and their inverses is shown in [7] - [12]. The generalizing capability of artificial neural networks avoids the requirement of a true analytical inverse [9] - [11]. Various algorithms have been used for training neural networks and Levenberg Marquardt algorithm is found to be very efficient algorithm. It is considered to be the combination of steepest descent and the Gauss Newton method [13]. Levenberg Marquardt is a standard iterative technique for non linear least squares problems [14][15].

III. ARCHITECTURE

Perceptron is one of the simplest forms of artificial neuron used in artificial neural networks. Perceptron is built around McCulloch Pitts model of neuron. An input vector is given into the perceptron which is multiplied with the weight vector and linearly combined with the bias and is applied to the thresholding function which determines whether the output of the neuron. The model of a perceptron is shown in figure 3.

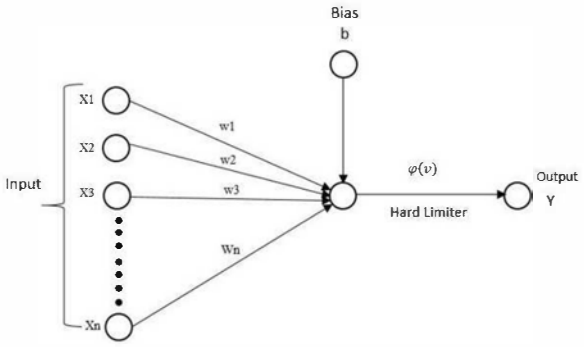

Fig. 3. Representation of Perceptron

$$v = \Sigma^m{}_{i=1} w_i x_i + b \tag{3}$$

$$y = \varphi(v) \tag{4}$$

Where x_i is the i^{th} input and w_i is the i^{th} weight and b is the bias. v is the output of the linear combiner. $\varphi(.)$ is the activation function. A single layer perceptron is an artificial neural network made of single layer of neurons. To overcome some practical limitations another model known as the multilayer perceptron is used which has an input layers, n number of hidden layers and an output layer. Figure 4, shows a structure of a multilayer perceptron. In this paper we used a multilayer perceptron to model the inverse plant.

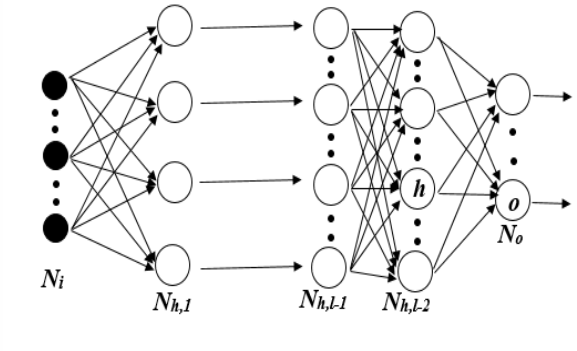

Fig. 4. Multilayer Perceptron

The initial weights for the model were found out by performing different runs using Bayesian regulation backpropagation. These initial weights obtained by the trial and error method are provided to the Levenberg Marquard algorithm .

For training a neural network, Levenberg Marquardt (LM) algorithm is considered to be one of the best. This algorithm identifies the minimum of a function that is specified as the sum of squares of nonlinear functions. The combination of steepest descent and the Gauss Newton method is considered to be the Levenberg Marquardt algorithm. In this algorithm, the calculation of Hessian matrix is not required. Although in the case of Gauss Newton method the Hessian matrix is calculated. The Hessian matrix is approximated as the square of the Jacobian matrix which is given by the equation:

$$H = J^T J \tag{5}$$

The gradient of the error function is given by the equation:

$$g = J^T e \tag{6}$$

Here J is the Jacobian matrix that contains first derivatives of the network errors with respect to the weights and biases and e is a vector of network errors. The standard backpropagation algorithm can be used for computing Jacobian matrix, instead of computing the Hessian matrix. Computation of Jacobian matrix using backpropagation is much more simpler. This approximation is used for the updation which is shown by the equation:

$$X_{k+1} = X_k[J^T J + I]^1 J^T e \tag{7}$$

When the current value of the solution is not at all close to the correct solution, the Levenberg Marquardt algorithm acts like steepest descent method. When the current value of the solution is close to the correct one, the Levenberg Marquardt algorithm acts more like Gauss Newtons method. Thus the behavior of Levenberg Marquardt algorithm depends on the type of solution.The parameters of three layer perceptron artificial neural network developed for this project is shown in Figure 5.

S.No	Paramaters	Values
1	Number of Layers	3
2	Neurons in input layers	4
3	Number of Neurons in first hidden layer	9
4	Number of Neurons in second hidden layer	13
5	Number of Neurons in output layer	3
6	Activation Function of input and hidden layers	Logsig
7	Activation Function of input and hidden layers	Linear
8	Training Algorithm	Levenberg Marquardt

Fig. 5. Parameters used in the model

IV. PROBLEM DEFINITION

The waste gases stream from a modified Claus Sulfur Recovery Unit (SRU) contains a number of sulfur compounds that cannot be directly released into the atmosphere environment. The usual method of destroying these compounds is incineration. Since the concentration of combustible compounds in waste gas are too low to support combustion alone, it is necessary to add fuel gas to the incinerator to attain a temperature necessary for the oxidation of the compounds. The fuel gas being a costly resource needs to be optimally used to maximize the profits of the organization. Certain studies have shown that optimal incinerator control can lead upto 40 percent savings on fuel gas [1] thus decision support system is required to optimize the use of fuel gas and increase the efficiency of

the incineration process. The output of the incinerator depends upon the various factors such as oxygen concentration, air flow rate, fuel gas flow rate etc. Thus for the optimal control of the incinerator, an inverse plant is modeled with the help of neural network.

V. METHODOLOGY

The Following steps have been proposed to formulate the above said problem:

1) Data points of modified Claus plant tail gas incinerator were collected.
2) The Data points collected were plotted to visually understand the data.
3) The optimal operating range of modified Claus plant tail gas incinerator was identified.
4) A training data set was prepared over different optimal operating ranges of the incinerator.
5) MLPNN can be used to create a model which predicts the input parameters for optimal operation of the incinerator to meet the expected output. System can be simulated with the help of MATLAB/ SIMULINK.
6) Building a Multilayer Perceptron Neural Network where the operator enters the required plant output and the model predicts the input to the plant to meet the expected output.
7) The error histogram of the model is obtained to analyze the accuracy of the predictions.
8) The regression plot of the model is analyzed to understand the system performance.

A. Preperation of Training Data

Using a simulator data points of modified Claus plant tail gas incinerator were collected. These data points where graphically represented to understand the data. Figure 6, shows the relationship between the adiabatic stack temperature and fuel gas consumption. From figure 6, it is observed that the the curve is parabolic in nature. The curve shows that for optimal operation of the incinerator (less fuel more temperature) the data points should lie to the right of the curve.

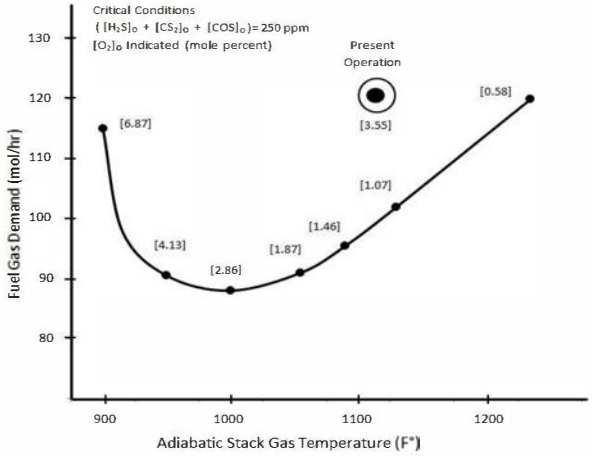

Fig. 6. Critical curve for incinerator operation

B. Neural Network Model

The proposed artificial neural network model have been simulated using neural networks toolbox in MATLAB. The model takes four inputs Vent O_2 concentration, SO_2 concentration, Temperature to be maintained in the incinerator, total flow rate of tail gas input into the incinerator. The Outputs of the network are control parameters of the process they are Fuel gas flowrate, Air flowrate and Oxygen concentration in the input air. The developed model is shown in figure 7. Figure 8, shows the GUI where the operator enters the required plant output and the model predicts the input to the plant to meet the expected output.

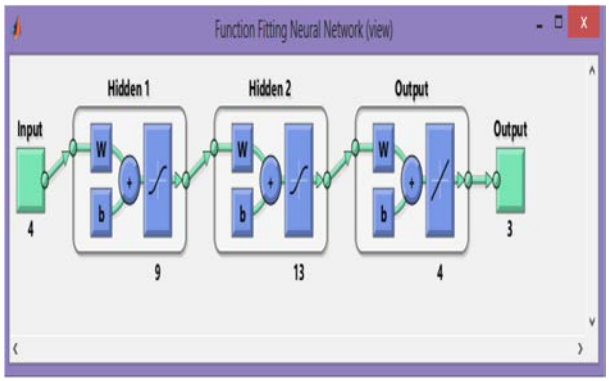

Fig. 7. Inverse Plant Model

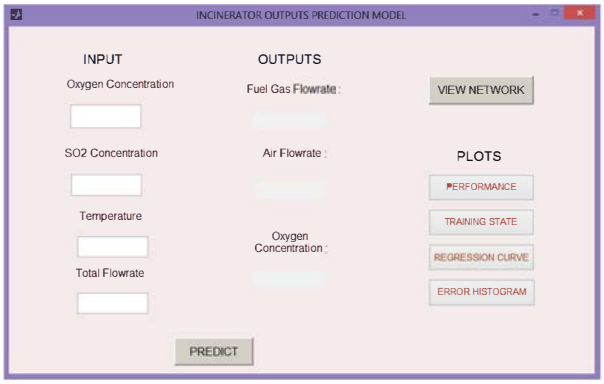

Fig. 8. GUI of the developed application

C. Training of Neural Network

Many training algorithms have been developed for training of neural networks. All the training algorithm play a relevant and crucial role for the convergence of any perticular problem. In this paper, Levenberg Marquardt Algorithm is used for training our multilayer perceptron. The Levenberg Marquardt algorithm was developed by Kenneth Levenberg and Donald Marquardt. The Levenberg Marquardt method is a iterative technique used to solve nonlinear least squares problems and minimizes a nonlinear function. When the function is non linear in the parameters nonlinear least squares problem

is occurred. The Levenberg Marquardt method involve an iterative improvement to parameter values. Thus the sum of the squares of the errors between the function and the measured data points is reduced.

The Levenberg Marquardt is a curve fitting method, which is actually a combination of two methods. It combines the gradient descent method and the Gauss Newton method. The fast convergence of Gauss Newton algorithm is combined with the stability of gradient descent algorithm. In gradient descent method, the parameters are updated to reduce the sum of the squared errors. The updation of the parameters is done in the direction of the greatest reduction of the least squares objective. In Gauss Newton method, the least squares function is assumed to be locally quadratic and the minimum of the quadratic is obtained. This assumption is made to reduce the sum of the squared errors. When the parameters are far from their optimal value the Levenberg Marquardt method behaves as gradient descent method. When the parameters are close to their optimal value the Levenberg Marquardt method behaves as Gauss Newton method. This algorithm is better and simpler than Gauss Newton, as the computation of hessian matrix is not required. It can solve the problems with error surface more than the quadratic approximation. Levenberg algorithm is superior to gradient decent algorithm as it converges the solution faster. The flow chart of the Levenberg Marquardt algorithm is shown in figure 9.

The training process using Levenberg Marquardt algorithm is as follows:

1) The initial weights are randomly generated to evaluate the Mean Square Error.
2) Use Weight updation formula to update and adjust the weights.
3) With the help new updated weights, again evaluate the Mean Square Error.
4) Due to weight updation, if the Mean Square Error is increased, reset the weight vectors and increase the coefficient by some factor. Repeat weight updation as per step 2.
5) Due to weight updation, if the Mean Square Error is decreased, accept the new weight vector and decrease the coefficient by the same factor as in step 4.
6) Repeat the same procedure from step 2 with new updated weights after every iteration until the current total error is smaller than the threshold limit value.

VI. PERFORMANCE ANALYSIS

A neural network was modeled to predict the input parameters for modified Claus plant tail gas incinerator. The predicted parameters are Fuel gas flowrate, Air flowrate and Oxygen concentration in the input air. Figure 10 shows the error histogram of the trained model. From the error histogram it can be the error range in readings are between -6.1 and 3.65. Figure 11 shows the regression plot. It can be

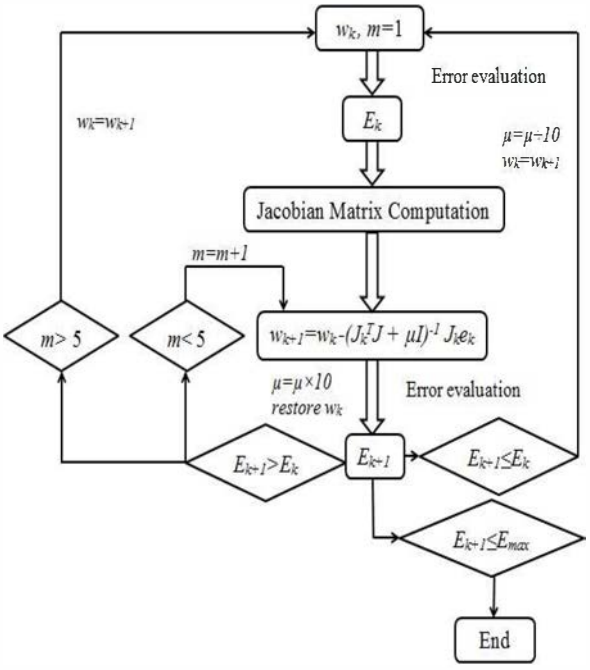

Fig. 9. Levenberg Marquardt algorithm

observed that model has fit the data well as as all the points lie on the line inclined line.

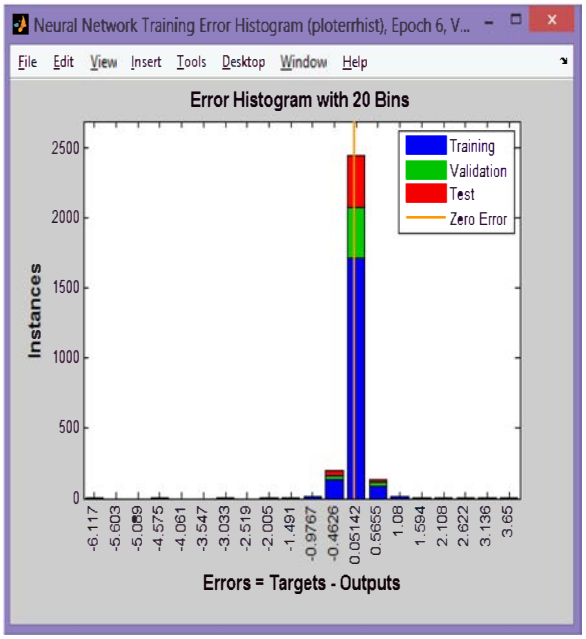

Fig. 10. Error histogram

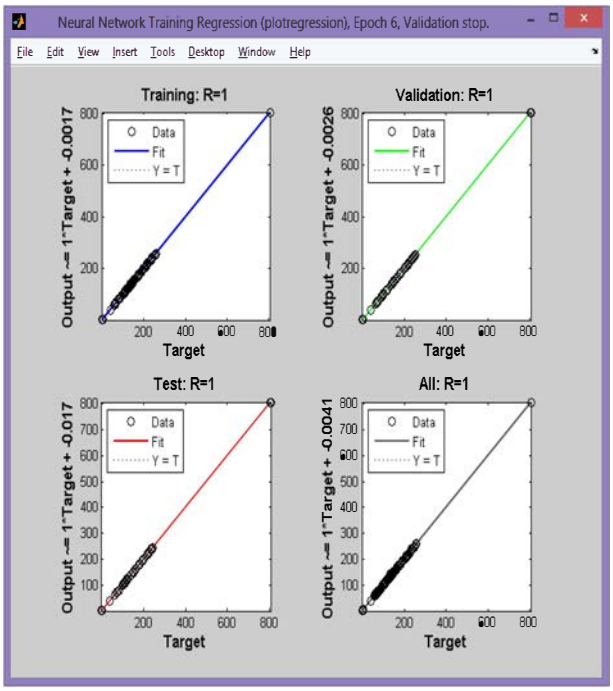

Fig. 11. Regression plot

VII. CONCLUSIONS

In this paper, a Neural Network approach is shown for for the optimal incinerator control. The main contribution of this paper is to propose a decision support system by using an inverse plant model. The proposed model is built in MATLAB Simulink environment. It has been found that the model is able to successfully approximate the training data and generate the inputs for the plant for its optimal operation. The system can be extended by means of an Expert system so as to help the operator to make better decisions for optimal overall plant control.

REFERENCES

[1] Harold G. Paskall and John A.Sames, *Sulfur Recovery*, 14^{th} Edition.

[2] R.K. Kert, H.G. Paskall and L.C. Biswanger, *Sulphur Plant Waste Gases- Incineration Kinetics and Fuel Consumption, Energy Processing*, Canada, March-April, 32-40, 1976.

[3] Western Research and Development Ltd., *A Study Of Incineration of Sulphur Plant Waste Gases,* Report TS-DS-1-74 to the Government of the Province Of Alberta, Department of the Environment, May, 197).

[4] Christophe Ndez, Jean-Louis Ray, *A new Claus Catalyst to Reduce Atmospheric Pollution,* ELSEVIER Catalysis Today, Volume 27, Issues 12, 29 January 1996, Pages 4953, 1st World Conference Environmental Catalysis For a Better World and Life.

[5] Nicuor Vatachi, *Modified Claus Process Applied To Natural Gas For Sulfur Recovery*, Dunrea de Jos University of Galati, 2009, ISSN 1221-4558.

[6] Yasser F. Al Wahedi, *Optimization of Temperature Swing Adsorption Systems for the Purpose of Claus Tail Gas Clean Up*, Master of science thesis submitted to the faculty of the graduate school of the University of Minnesota, June 2012.

[7] K.J.Hunt, D.Sbarbaro, *Neural Networks for Nonlinear Internal Model Control*, In IEEE Proceedings of Control Theory and Applications, Volume:138, Issue: 5.

[8] B.Widrow, M.Bilello, *Adaptive inverse control, Intelligent Control,* In Proceedings of the IEEE International Symposium on 25-27 Aug 1993.

[9] M.A. Hussain, L.S. Kershenbaum, *Implementation of an Inverse-Model-Based Control Strategy Using Neural Networks on a Partially Simulated Exothermic Reactor*, ELSEVIER Chemical Engineering Research and Design, Volume 78, Issue 2, March 2000, Pages 299311.

[10] D.H. Rao, M.M Gupta and H.C Wood, *Adaptive Inverse Control of Nonlinear Systems Using Dynamic Neural Networks*, Intelligent System Research Laboratory, College of Engineering University, Saskatoon, Canada.

[11] Jaroslava ilkov, Jaroslav Timko, Peter Girovsk, *Nonlinear System Control Using Neural Networks*, Department of Electrical Drives and Mechatronics Technical University of Koice Letn, Slovak Republic, 2006.

[12] Haider A. F. Almurib, *Direct Neural Network Control via Inverse Modelling*, Department of Electrical and Electronic Engineering, The University of Nottingham Malaysia Campus Semenyih, 43500.

[13] Manolis I. A. Lourakis, *A Brief Description of the Levenberg-Marquardt Algorithm,* Institute of Computer Science Foundation for Research and Technology - Hellas (FORTH), February 11, 2005.

[14] Henri P. Gavin, *The Levenberg-Marquardt Method for Nonlinear Least Squares Curve-tting Problems*, Department of Civil and Environmental Engineering Duke University October 9, 2013.

[15] Vijayashree, *Training the Neural Network using Levenberg-Marquardts Algorithm to Optimize the Evacuation Time in an Automotive Vacuum Pump,* International Journal of Advanced Research in Engineering and Technology (IJARET), April 3, 2013

EPJ Web of Conferences **86**, 00050 (2015)
DOI: 10.1051/epjconf/ 20158600050

Observation of incomplete fusion at low angular momenta

Devendra P. Singh[1,a], Abhishek Yadav[2], Indu Bala[2], Anubhav Raghav[3], Mohd. Shuaib[3], Prabhat Kumar[3], Pushpendra P. Singh[4], Unnati[3], M. K. Sharma[5], Vijay R. Sharma[3], R. Kumar[2], R. K. Gupta[1], B. P. Singh[3], and R. Prasad[3]

[1] *Department of Physics, University of Petroleum and Energy Studies, Dehradunn-248 007, Uttrakhand, India*
[2] *NP Group: Inter-University Accelerator Centre, Aruna Asaf Ali Marg, New Delhi-110 067, Delhi, India*
[3] *Department of Physics, Aligarh Muslim University, Aligarh-202 002, Uttar Pradesh, India*
[4] *Department of Physics, Indian Institute of Technology Ropar, Roopnagar-140 001, Punjab, India*
[5] *Department of Physics, S. V. College, Aligarh-202 001, Uttar Pradesh, India*

Abstract. Present work deals with experimental studies of incomplete fusion reaction dynamics using off-line γ-ray spectrometry at energies as low as ≈3-6 MeV/nucleon. Excitation functions for five reaction products populated via complete and/or incomplete fusion processes in ^{16}O+^{130}Te system have been measured and compared with the predictions of the statistical model code PACE4. A significant enhancement in the measured excitation functions compared to theoretical predictions for α-emitting channels has been observed and is attributed to incomplete fusion processes. The relative strength of incomplete fusion has been found to increase with projectile energy. Results show that incomplete fusion is associated even for angular momenta lesser than the critical angular momentum for complete fusion and also reveals importance of incomplete fusion even at energies as low as ≈3-6 MeV/nucleon.

1 Introduction

In recent years, incomplete fusion (ICF) processes in heavy-ion interactions around the Coulomb barrier have been a topic of interest for exploring the nuclear structure and reaction dynamics [1–6]. In the ICF processes, direct α-particles have been observed in the forward cone with nearly the same velocity as that of the incident ion [7]. It may be pointed out that, at 3-6 MeV/nucleon complete fusion (CF) is supposed to be the sole contributor to the total fusion cross-section [2, 8]. Interestingly, α-emitting channels at energies ≈3-6 MeV/nucleon are found to show enhancement of cross-sections over the statistical model predictions, which may be due to the projectile breakup processes in these reactions. At higher projectile energies (≈10 MeV/nucleon), Wilczynski et al. [9] have well explained the cross-sections for ICF reactions based on partial statistical equilibrium and on the idea of a generalized concept of angular momentum. However, on the basis of the above prescription, ICF reactions could not be explained at lower projectile energies, where the maximum angular momentum values (ℓ_{max}) are less than the critical angular momentum ($\ell_{critical}$). The γ-multiplicity measurements by Wilczynski et al. [9], Inamura et al. [10], Gerschel et al. [11], and Trautmann et al. [12] also indicate that such breakup fusion, in general, involves $\ell \geq \ell_{critical}$. However, studies [13] on spherical targets showed involvement of ℓ-values in ICF lower than $\ell_{critical}$ as well, giving rise to conflicting reports on the dependence of ICF on the angular momentum. Further, it may be pointed out that the available theoretical models [9, 14–17] satisfactorily predict the magnitude of ICF contribution, to some extent, in some cases at energies ≈10 MeV/nucleon, but none of these models is able to successfully explain such data at low energies. In view of the above, a clear picture of the mechanism of ICF has yet to emerge, particularly at energies ≈3-5 MeV/nucleon.

2 Experiments

A beam of $^{16}O^{7+}$ obtained from the 15-UD Pelletron accelerator of the Inter-University Accelerator Centre, New Delhi, India, has been used to irradiate ^{130}Te target samples (enrichment ≈61%), prepared using vacuum evaporation on Al foils of thickness ≈6.75 mg/cm^2. The thickness of sample deposition (≈1.8 mg/cm^2) in each target was determined by the α-transmission method. Two stacks, containing two ^{130}Te samples each, followed by Al catchers, were irradiated at 85 and 90 MeV, respectively, in the General Purpose Scattering Chamber (having in-vacuum transfer facility) with a constant beam current (≈3 pnA) for ≈8 h duration. The irradiated samples along with the catchers were taken to a high-purity Ge detector for γ counting. The resolution of the detector system was ≈2 keV FWHM for the 1332.0 keV γ-line of ^{60}Co. The reaction residues of interest have been identified by their measured half-lives ($T_{1/2}$) and characteristic γ-ray energies. A critical evaluation of the uncertainties in the

[a] e-mail: dpsingh19@gmail.com

measured cross-sections has been considered. The errors in the measured production cross sections may arise due to (*i*) the nonuniformity of target foils, (*ii*) fluctuations in the beam current, (*iii*) the uncertainty in geometry dependent efficiency of HPGe detector, and (*iv*) due to the dead time of the spectrometer. Detailed discussion on the error analysis is given elsewhere [4–6]. The overall errors including statistical errors are estimated to be ≥15%, excluding the uncertainty in branching ratio, decay constant, etc.

3 Measurements and analysis

The cross-sections for (5n)^{141}Nd, (α3n)^{139}Ce, (3αn)^{133}Xe^{m}, (3αn)^{133}Xe^{g}, and (3α3n)^{131}Xe^{m} residues have been measured in the energy range of ≈60-90 MeV. In the present work, 5n channel residues [^{141}Nd ($t_{1/2}$ = 2.49 h)] could be identified by the characteristic γ-ray of 1127 keV and also by measuring its half-life using decay curve analysis. Further, the ^{139}Ce residues may be formed by the CF of ^{16}O and ^{130}Te, forming the composite system ^{146}Nd*, which may decay by the evaporation of an α-particle and three neutrons. ^{139}Ce residues may also be produced if the fragment ^{12}C (if ^{16}O undergoes breakup into an α particle and ^{12}C fragments) fuses with the ^{130}Te target nucleus followed by the evaporation of three neutrons. In the same way, ^{133}Xe^{g,m} and ^{131}Xe^{m} residues may also be formed by CF as well as ICF processes. Theoretical calculations of cross-sections for the residues populated via CF and/or ICF channels have also been done using the code PACE4 [18]. This model follows the correct procedure for angular momentum coupling at each stage of de-excitation. The angular momentum conservation is explicitly taken into account at each step. In this code the fusion cross-section was calculated using the Bass formula. The details of this model are given in our earlier work [4]. In this model the most important parameter is level density parameter (LDP). The LDP (a = A/K), where A is the atomic mass of the compound nucleus (CN) and K is a free parameter. It is not out of place to mentioned that in this code ICF of the incident ion is not taken into consideration, so any enhancement in the measured cross-section compared to PACE4 code predictions may be attributed to breakup fusion channels. The α3n channel gives rise to the population of ^{139}Ce. The isomeric state of ^{139}Ce ($t_{1/2}$ ≈56s) decays completely via transition to the ground state of ^{139}Ce. Therefore, the measured activity of ^{139}Ce^{g} may be taken as the sum of the metastable and ground states of ^{139}Ce. In order to determine the ICF contribution to the measured α-emitting channels, the measured $\Sigma\sigma_{exp}(\alpha)$ (sum of cross-sections of all measured α-emitting channels) has been compared with the corresponding calculated values based on CF calculations, i.e., $\Sigma\sigma_{Th}(\alpha)$. In Fig. 1(a), a comparison of $\Sigma\sigma_{exp}(\alpha)$ has been made with corresponding $\Sigma\sigma_{Th}(\alpha)$ calculated using PACE4. It may be observed from Fig. 1(a) that the $\Sigma\sigma_{Th}(\alpha)$ obtained from PACE4 predictions are significantly lower than the $\Sigma\sigma_{exp}(\alpha)$ in the entire energy

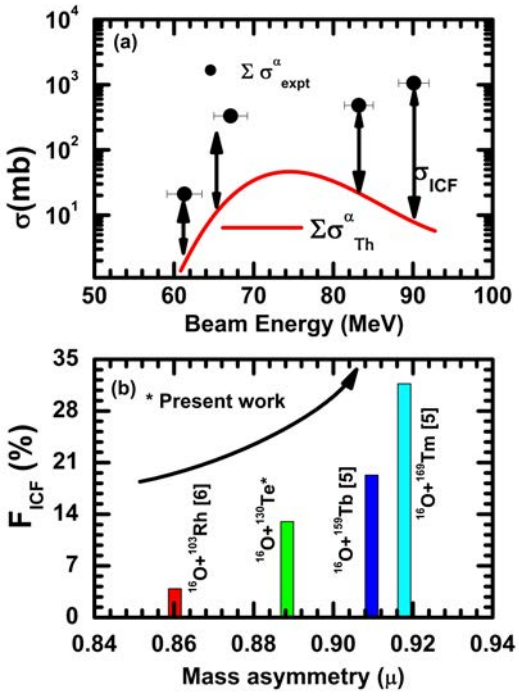

Figure 1. (a) Comparison of the sum of the measured cross-sections for α-emitting channels and calculated values. The increasing difference between the experimental and calculated values with energy indicates the dominance of ICF processes with energy. (b) The ICF fraction (F_{ICF}) as a function of mass asymmetry at a constant relative velocity (β = 0.055c) for the presently studied system along with results from the literature [5, 6].

range. The enhancement of the experimental values compared to the theoretical predictions may be due to the ICF processes and has been denoted by σ_{ICF}. It may also be noted that the difference between $\Sigma\sigma_{exp}(\alpha)$ and $\Sigma\sigma_{Th}(\alpha)$ increases with energy throughout the entire energy region of interest, indicating the dominance of ICF with a maximum ICF contribution at the highest studied energy.

Further, the isomeric cross-section ratios (ICRs) for the residues in the reaction ^{130}Te(^{16}O,3αn)^{133}Xe produced via CF and/or ICF channels are also found to increase with energy, in general. Since the ICF reactions are considered to take place in peripheral collisions, a relatively large amount of angular momentum may be transferred and this may increase with energy. The increase in isomeric population with energy shows that a part of the input angular momentum may get converted to the nuclear spin and the isomeric population may increase. Thus, the ICR may depend strongly on the relative spins of metastable and ground states and also on the energy difference between the levels. In order to understand how the ICF fraction varies with the entrance channel mass asymmetry (μ), the value of F_{ICF}(%) for the ^{16}O + ^{130}Te system has been compared with those found in the literature [9, 10] at a constant relative velocity (β = 0.055c). As can be seen from Fig. 1(b) the F_{ICF} is found to increase with mass asymmetry (μ) for the ^{16}O projectile with different

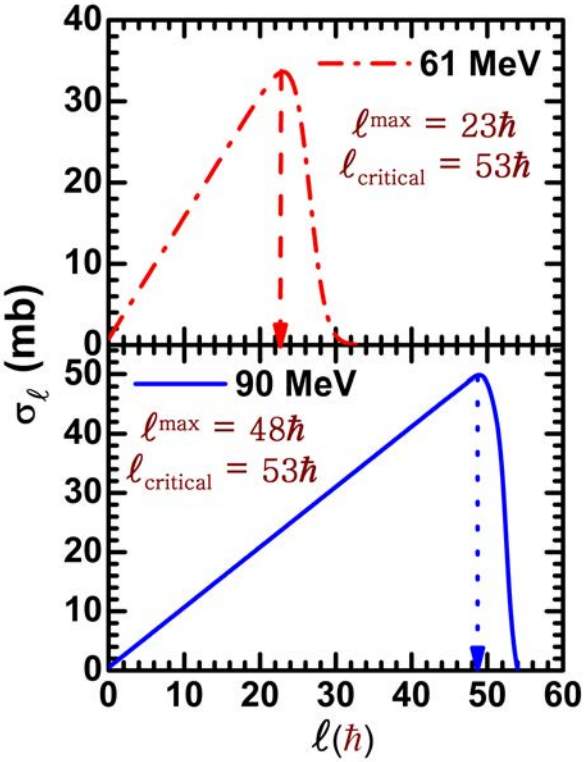

Figure 2. Typical Fusion ℓ-distributions calculated by using the code CCFULL for the ^{16}O + ^{130}Te system at E_{lab} ≈61 and 90 MeV.

targets. As inferred from this figure, the ICF probability is higher for more mass-asymmetric systems, which is in accordance with the Morgenstern mass-asymmetry systematics [19].

Further, it is possible to calculate the cross-sections for CF and ICF channels separately using the 'sumrule' model [20, 21], based on the idea of a generalized concept of critical angular momentum following partial statistical equilibrium. The underlying assumption in the 'sumrule' model is that the ICF channels open up only for those partial waves which have ℓ values greater than $\ell_{critical}$ (i.e., $\ell \geq \ell_{critical}$). On the other hand, partial waves with $\ell \leq \ell_{critical}$ contribute to CF. The present findings indicate that a diffused boundary in ℓ space may penetrate close to the barrier, such that fusion may take place even for $\ell < \ell_{critical}$. In order to ascertain the above in the ℓ distribution for the ^{16}O + ^{130}Te system, the $\ell_{critical}$ value has been calculated [9] and is found to be 53$\hbar$. Fig. 2 shows the fusion ℓ distributions for the ^{16}O + ^{130}Te system calculated using the code CCFULL [22] at two extreme energies 61 and 90 MeV, respectively. The values of ℓ_{max} at two energies (61 and 90 MeV) are found to be ≈23$\hbar$ and 48$\hbar$, respectively which are less than the $\ell_{critical}$ value (53$\hbar$) for fusion for this system. From Fig. 2, it may also be seen that, even at the highest studied energy, the maxima of ℓ values are not as high as $\ell_{critical}$ for fusion for both the studied energies. Thus, the ICF contributions are expected to be negligible at these energies. However, the present measurements for ICF channels suggest that a significant number of partial waves below $\ell_{critical}$ may contribute to ICF channels. The present observations clearly indicate a diffused boundary for ℓ-values, contrary to the sharp cut-off model, that may penetrate close to the barrier.

4 Summary

In the present work, for α-emitting channels, enhancement in cross-sections over the predictions of statistical model calculations has been observed and may be attributed to the prompt break-up of the projectile, leading to ICF processes. A comparison of data for ICF contribution for the same projectile with different targets indicates a strong and increasing trend of incomplete fusion fraction with target mass number and showing a strong mass asymmetry dependence. The 'sumrule' model calculations highly underestimate the ICF cross-sections, indicating the limitation of the model assumption that a substantial contribution to ICF comes from collision trajectories with $\ell > \ell_{critical}$. In the energy range of the present study, calculations indicate that ℓ_{max} is less than $\ell_{critical}$, thus, significant cross-sections for ICF channels at these beam energies indicate the contribution from collision trajectories with $\ell < \ell_{critical}$ as well.

Acknowledgements

The authors thank the Director of IUAC, New Delhi, India, and to the Dean, CoES, UPES, Dehradun for providing facilities to carry out the work. RP and BPS thank to UGC and DST, New Delhi, India, for providing financial support. DPS and AY thank to the DST for providing financial support through Project No. SR/FTP/PS-025/2011 and SB/FTP/PS-194/2013, respectively, under the Fast Track Scheme for Young Scientists.

References

[1] P. R. S. Gomes *et al.*, Phys. Rev. C **73** (2006); Phys. Lett. B **601**, 20 (2004).
[2] M. Das Gupta *et al.*, Nucl. Phys. A **787**, 144 (2007) ; Phys. Rev. C **70**, 024606 (2004).
[3] Abhishek Yadav *et al.*, Phys. Rev. C **85**, 034614 (2012); *ibid* **85**, 064617 (2012); *ibid* **86**, 014603 (2012) and references therein.
[4] D. P. Singh *et al.*, Phys. Rev. C **80**, 014601 (2009) ; Phys. Rev. C **81**, 054607 (2010).
[5] P. P. Singh *et al.*, Phys. Rev. C **77**, 014607 (2008) ; Phys. Lett. B **671**, 20 (2009).
[6] Unnati *et al.*, Nucl. Phys. A **811**, 77 (2008).
[7] H. C. Britt and A. R. Quinton, Phys. Rev. C **124**, 877 (1961).

[8] L. F. Canto *et al*., Phys. Rev. C **58**, 1107 (1998).
[9] J. Wilczynski *et al*., Phys. Rev. Lett. **45**, 606 (1980).
[10] T. Inamura *et al*., Phys. Lett. B **68**, 51 (1977) and Phys. Lett. B **84**, 71 (1979).
[11] C. Gerschel *et al*., Nucl. Phys. A **387**, 297 (1982).
[12] W. Trautmann *et al*., Phys. Rev. Lett. **53**, 1630 (1984).
[13] I. Tserruya *et al*., Phys. Rev. Lett. **60**, 14 (1988).
[14] T. Udagawa and T. Tamura, Phys. Rev. Lett. **45**, 1311 (1980).
[15] J. P. Bondrof *et al*., Nucl. Phys. A **333**, 285 (1980).
[16] R. Weiner *et al*., Nucl. Phys. A **286**, 282 (1977).
[17] V. I. Zagrebaev *et al*., Ann. Phys. (NY) **197**, 33 (1990).
[18] O. B. Tarasov and D. Bazin, Nucl. Instrum. Methods Phys. Res., Sect. B **204**, 174 (2003).
[19] H. Mogenstern *et al*., Phys. Lett. B **113**, 463 (1982); Z. Phys. A **324**, 443 (1986).
[20] J. Wilczynski *et al*., Nucl. Phys. A **373**, 109 (1982).
[21] K. Siwek-Wilczynska *et al*., Phys. Rev. Lett. **42**, 1599 (1979).
[22] K. Hagino *et al*., Comput. Phys. Commun. **123**, 143 (1999).

Conceptual Design of an Automatic Fluid Level Controller for Aerospace Applications

Abhishesh Pal
Department of Mechatronics Engineering, University of Petroleum & Energy Studies
Dehradun - 248007, Uttarakhand, India
abhishesh.pal6@gmail.com

Roushan Kumar
Department of Electronics Engineering
University of Petroleum & Energy Studies,
Dehradun - 248007, Uttarakhand, India

V.R.Sanal Kumar
Department of Aeronautical Engineering
Kumaraguru College of Technology
Coimbatore – 641 049, Tamil Nadu, India
vr_sanalkumar@yahoo.co.in

Abstract— **In this paper an attempt has been made for the conceptual design of an automatic fluid level controller for cryogenic tank lucratively for aerospace applications. An ideal design technique of the low temperature multi-phase fluid level control system for estimating the boil-off rate and/or the flow rate to facilitating the estimation of the total quantity of effective fluid available for completing the mission based on the use of microcontroller has been presented. The proposed control system model is mainly composed of microcontroller, level sensor, temperature sensors, pump and relay. This system could estimate the actual fluid volume of the low temperature cryogenic fluid for the evaluation of the effective propulsive efficiency of the entire aerospace vehicle. The preliminary sea level test results, using water as the base fluid, show that the system model being proposed is able to monitor the liquid level very effectively and accurately for estimating the total volume of the fuel and oxidiser for estimating the operating time of the aerospace vehicle lucratively.**

Keywords- microcontrollers, fluid level indicaters, boil-off rate, rocket engine, sensors

I. INTRODUCTION

The design of an automatic fluid level controller for cryogenic tank is of topical interest. There are many liquid level measurement techniques available in the industry, viz., continuous level measurement, superconducting wire level device, capacitive level measuring systems, transmission line system, discrete level measurement, ultrasonic level measurement, hydrostatic (head) level measurement, liquid-vapor detectors (resistive, superconducting), acoustic "dip stick" method, mass measurement (gauging) for various aerospace applications.

Liquid level sensing at cryogenic temperatures is required for many critical aerospace applications, but it is extremely difficult. There are a wealth of problems for cryogenic sensor devices, which include the extreme cold, which makes many sensors inoperable due to freeze-out of conduction carriers, mechanical stress and strain which impacts reliability, undesirable device heat generation in the vessel, and a host of others. In addition, consideration of sensor wiring and vessel penetration is required. In principle, acoustic devices can successfully operate to extremely low temperatures without any serious performance degradation.

In particular, Surface Acoustic Wave (SAW) devices operate as sensors, and certain embodiments are passive, wireless, and coded for multi-sensor applications. However, few results are reported on SAW devices for cryogenic applications. Research has been performed on the use of SAW devices for operation as liquid level sensors. The initial application is for a level sensor to be used by NASA in its cryogenic liquid fuel tanks, for both ground and space vessels. The results of previous studies conducted by various investigators concluded that under proper conditions, SAW devices can be used as liquid sensors at cryogenic temperatures.

In this conceptual study we dealt with water as our experimental fluid to design a lucrative, cost effective controller with multi-fold objectives. Water level controller prevents overflow and dry running of the water pump, thus saves water, electricity and manpower. Once we install this system the end user can relax enjoy auto-working of the pump. In the case of cryogenic tanks with the use of fluid level indicators space scientist can estimate the boil off rate and the remaining fluid available in the tank. This is very critical in the case of delayed launching of aerospace vehicles after filling the cryogenic fuel in the rocket tanks. Accurate fluid level estimation can help the mission director to take a thoughtful decision for refilling the tank before its launch.

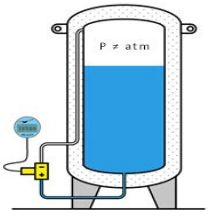

(a) Typical cryogenic tank

978-1-4799-1753-2/15/$31.00 ©2015 IEEE

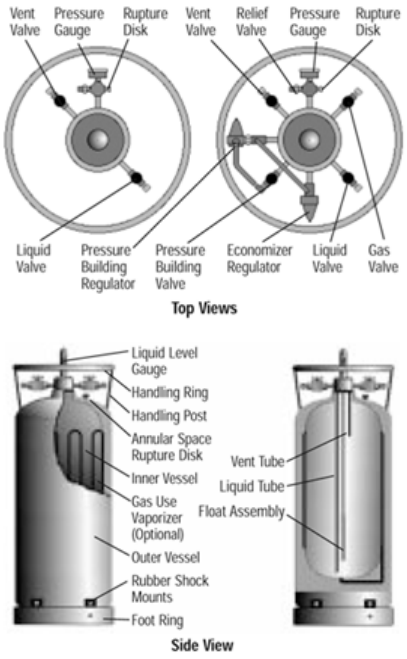

(b) Two views of cryogenic cylinders

Fig. 1 (a-b) Typical Liquid Cryogenic Cylinders

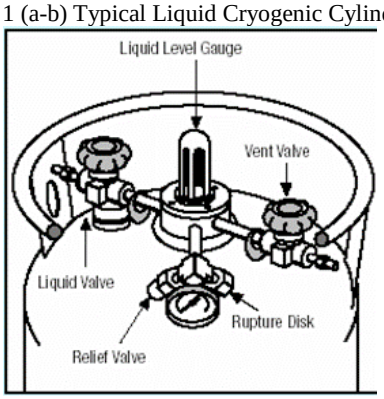

Fig. 2 Illustration of Typical Gauge and Valve Configuration of Cryogenic Tank.

Note that the refilling time of cryogenic tank might lead to an altered launch window and other trajectory prediction complications. Therefore an accurate measurement of the cryogenic fluid level is inevitable for any mission. Figure 1 shows the illustration of cryogenic tanks, gauge and its valve configurations. The liquid level control systems are widely used for monitoring of liquid levels, reservoirs, silos, and dams etc. But cryogenic sensors are very critical in design. Usually, liquid level control kind of systems provides visual multi level as well as continuous level indication. Audio visual alarms at desired levels and automatic control of pumps based on user's requirements can be included in this management system. Proper monitoring is needed to ensure water sustainability is actually being reached, with disbursement linked to sensing and automation. Such programmatic approach entails microcontroller based automated water level sensing and controlling.

The automatic controlling of water level in storage tank is an old concept but the technology adopted to do so is advancing continuously. Various methods were used to sense the water level in the storage tanks which includes mechanical float ball attached to an electrical limit switch, plastic moulded reed relay arrangement, direct sensing of low voltage DC electrical signals, etc. All of them had one or the other disadvantages or needed periodical maintenance to keep the system working. This even affected the reliability of the Level Controller systems.

The most advanced yet cost effective method of level sensing, known as AC SIGNAL SENSING is being developed. This is based on the principle of conduction through water wherein signal will be sent to the water, and the sent signal will be received through the level sensors set at desired levels. This type of sensing will not result in any corrosion or sulphating of sensors and deposition of salt on the surface of sensors. This will have an advantage that sensors need not be periodically cleaned or changed. As there are no moving parts, the dirt in the water will not affect the performance. The sensors which are used will have life more than a decade and absolutely does not need any maintenance. Of late, control systems have been widely applied to many industrial systems, particularly in the field of the process control that requires the critical control performance such as, high accuracy, high speed and good linearity. The parameters which are commonly considered in most of the indicators are pressure, temperature, and fluid level. The proposed control system model is mainly composed of microcontroller, level sensor, temperature sensors, pump and relay. This system could detect the actual fluid volume of the low temperature cryogenic fluid for the estimation of the effective propulsive efficiency of the entire aerospace vehicle.

II. LITERATURE REVIEW

Literature review reveals that the innovators at NASA's Marshall Space Flight Center have developed a unique prototype for measuring the liquid level in a tank, employing a novel process. The technology can operate in a wide range of environments, including high and low temperatures and pressures, and is simpler and less expensive than other optical sensing techniques. The instrument also provides far greater accuracy and faster results in cryogenic conditions than typical cryogenic liquid metering methods. It is ideal for cryogenic and non-cryogenic ground tank metering applications, and zero-gravity systems that include stratification or settling techniques [1]-[19].

Literature review further reveals that it is versatile, which operates at high and low temperatures and pressures, functions in corrosive environments, and provides highly accurate metering for both cryogenic and non-cryogenic liquids. It allows accurate liquid level measurements to 0.1% of the optical fiber length. It is safe and avoids an explosion hazard—requires no electrical signals in the tank cryogenic and non-cryogenic optical liquid level instrument for stratified conditions. It offers a very rapid response time (up to

gigahertz data rates), enabling measurement of rapidly changing fluid levels or sloshing liquids. It is flexible and accommodates snaking through access ports or shaping to fit tank contours. It is lucrative and incorporates directly into a plastic tank, reducing cost and eliminating the need for holes in the tank in some applications. According to the previous studies automatic water controllers are designed using: Level Transducer, Pressure Transducer, which are briefly described in the subsequent session.

A. Level Transducer

In the past few years, control systems have been widely applied to many industrial systems. Level control is commonly used in almost every process system. The level control system must be controlled by the proper controller. Actual systems and controllers are widely implemented in the discrete time domain since they employ microprocessors or computers in general. Recently, a variable structure control in the discrete-time domain has much received the attention. The objective of the controller in the level control is to maintain a level at a given set point and be able to accept new set point values dynamically. The aim of this work is to present an ideal design technique of the liquid level control system based on the use of the commercially available microcontroller Atmega 16. The proposed control system model is composed of microcontroller Atmega 16, level sensor and solenoid valve. Experimental results show that the system model being proposed is able to control the liquid level very effectively and provide a good response. Moreover the benefit obtained from this system is to be able to employ as an educational tool for demonstrating in an educational project and the control engineering laboratory. Furthermore, it is to be expected as this control system for collecting and controlling the physical data such as pressure, temperature etc.

The water level controller designed in this work is a reliable circuit. It takes over the task of indicating and controlling the water level in the overhead water tanks. The level of the water is displayed through the LED. The graphite probes are used to sense the water level. The probes are inserted into the water tank whose level of water is to be monitored. This water-level Controller-cum-alarm circuit is configured around the well-known Atmega16 Microcontroller. It continuously monitors the overhead water level and displays it. It also switches off the solenoid valve when the tank is full and automatically switches it on when the water level is low.

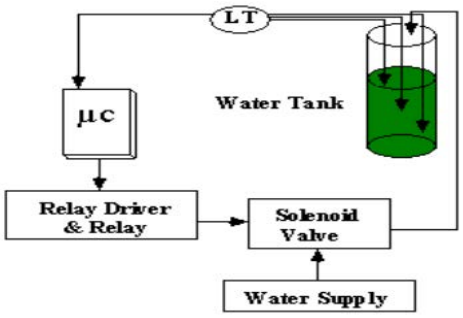

Figure 3 Proposed liquid level controller configuration (LT = Level Transmitter).

Figure 3 shows the configuration of the proposed microcontroller-based control scheme, which is applied to control the level of the liquid. It mainly contains a microcontroller, level transducers (LTs) and solenoid valve named SV. The Embedded C programming is used in the microcontroller to control the level and also displaying the data through LED from microcontroller.

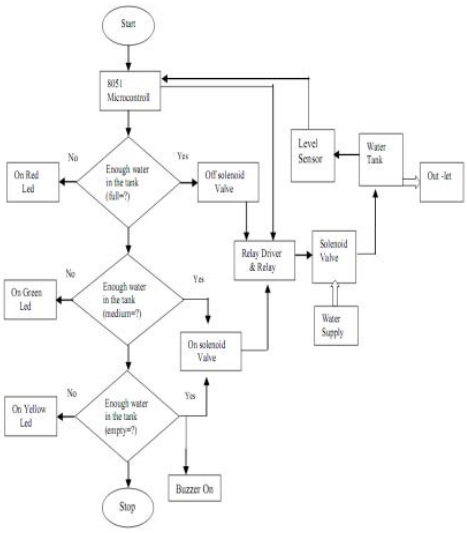

Figure 4 The operation performed by the programming using LT.

In this designing, the LT's principal task is to produce electrical signal that is directly proportional to the level in the tank. With this transducer liquid level will be transmitted to the microcontroller (µC) and afterwards, microcontroller software checks for the condition of the output voltage at each three points and then directs the solenoid valve to operate the control valve inside the solenoid valve. In addition, the water supply is provided in the tank through the solenoid valve
In the software design, the Embedded C language programming for Atmega16 microcontroller is used. The operation is performed by the programming described by the flowchart in Fig. 4.

The alternative technique in which the solenoid valve and microcontroller are applied for controlling the liquid level system is proposed. The proposed control system provides many attractive features, such as, can be applied to the level transducer for sensing the liquid level in the tank, can display data on LED via microcontroller interfacing. Experimental results show that the system operation agrees very well with expectations.

B. Pressure Transducer

This work presents a design technique for the implementation of the liquid level control system by based on the use of a

single-chip microcontroller. The proposed model system offers the following attractive features:
(i) Application of the pressure transducer for sensing the height of liquid in tank
(ii) Using the obtained liquid level for defining on-off condition of the water pump
(iii) The liquid values were controlled by using stepping motors for controlling.
(iv) Can set up by using manual control or automatic control.
(v) Can monitor and display the process status either on microcontroller-based control board or on the computer via RS232 serial-port.

Experimental results have been employed to show the effectiveness of the system operation. It is a well known fact that the digital control system can offer high accuracy and high-speed response. These are the reasons that cause a strong motivation to design and implement the automatic control system based on the digital controller. Actual systems and controllers are widely implemented in the discrete- time domain since they employ microprocessors or computers in general. Recently, a variable structure control in the discrete-time domain has much received the attention. Therefore, this work presents an alternative technique to implement the modelling of the liquid level control system based on the use of the commercially available microcontroller (µC) in conjunction with the personal computer (PC). The system model is designed around the personal computer, a popular commercial microcontroller Atmega16, stepping motors and some pressure transducers. The implementation and experimental results are shown to demonstrate the usefulness of the proposed control scheme. Furthermore, it is to be expected as this control system can be modified to other actual systems for collecting and controlling the physical data, such as, pressure, temperature and etc.

C. Proposed Control Scheme

Figure 5 shows the configuration of the proposed microcontroller-based control scheme, which is applied to control the level of the liquid system. It mainly contains a personal computer (PC), a microcontroller (µC), pressure transducers (PTs) and stepping motors named M1, M2 and M3. The feature of the PC is used for programming data into the µC and also displaying data from the µC. In this designing, the PT principal task is to produce an electrical signal that is directly proportional to the pressure in the tank. With this transducer, the output electrical signal corresponding to the liquid's level will transmit to the µC. The output voltage signals from transducers PT1 and PT2 in liquid Tank No.1 and Tank No.2, respectively, are amplified by instrumentation amplifiers shown in Fig. 5, and converted to digital signals at Level1 and Level 2 terminals by an analog-to-digital converter (ADC) inbuilt feature in µC control board. After that the software checks for the condition of the output voltage at each point and then responses the stepping motor named M1, M2 in order to operate the control values V1 and V2 In addition, the stepping motor M3 and the water pump P are provided circulating the mixed-liquid in the Tank No.3 back into Tanks No.1 and Tank No.2 again. The computer program flowchart for initializing process is shown in Fig.6.

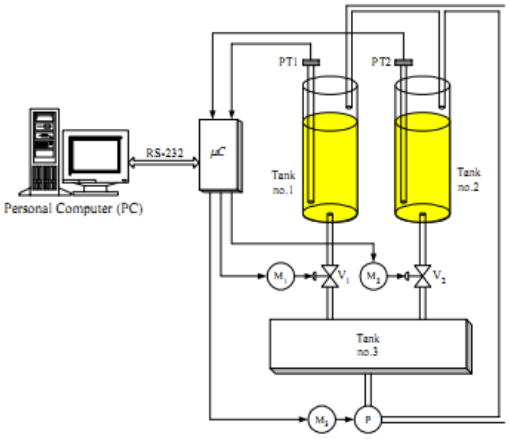

Fig. 5. Proposed liquid-level controller configuration (V = control value; M = stepping motor; P = water pump; PT = pressure transducer)

D. Implementation and Experimental Results

In this experiment, the proposed level control system is designed based on the PC with the Embedded C programming language implementing the computer software, and plugged directly into a commercial microcontroller Atmega16 by serial interface devices. Each function menu can be explained as follows.

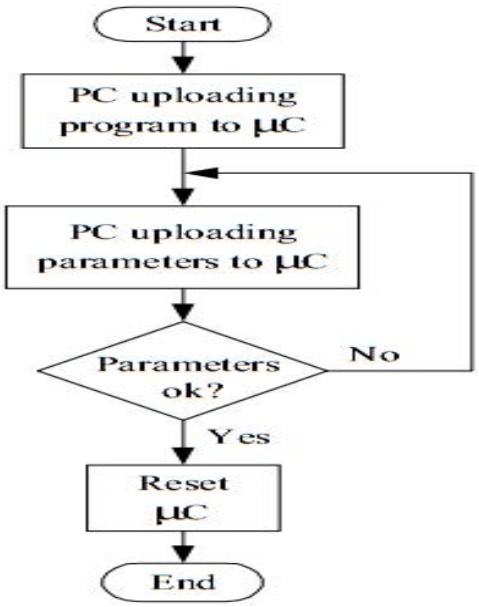

Fig. 6. The computer program flowchart for initializing process.

Level 1 Control and Level 2 Control: The user can set up the liquid's level in Tank No.1 and Tank No.2 by using these

menus. The setting conditions from the user will be controlled the water pump as required.

Speed Control: This menu is provided for controlling direction and speed of the mixer in Tank No.3.

Value Position Control: In this menu, the control values V1 and V2 are controlled within the limits.

Pump Control: Water pumps of the system are set up in this menu corresponding to conditions that set in the Level 1 and Level 2 Control Menus.

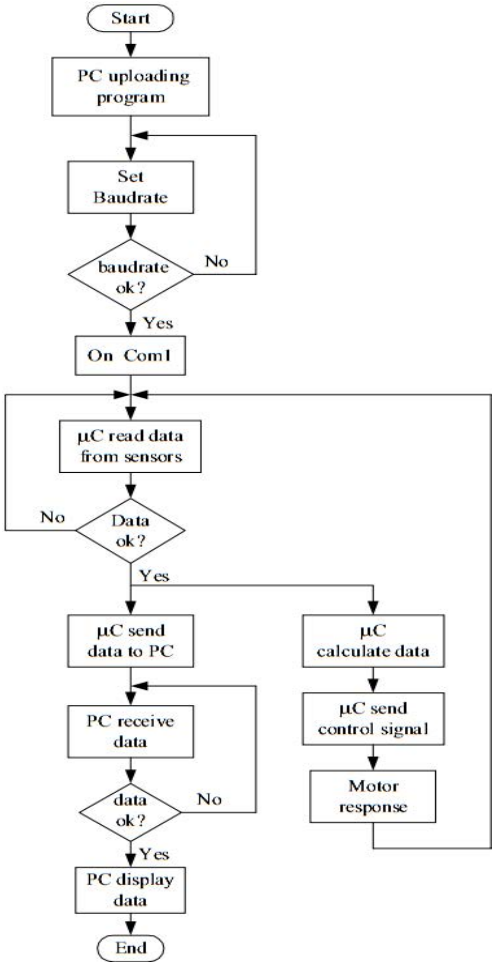

Fig. 7 The computer and microcontroller operation flowchart for data processing.

Atmega16 status: The Atmega16 status will show in this menu in order to indicate the connection between microcontroller and computer. For the experimental results, the errors of the output signals are depended on the hardware restrictions, for example the accuracy of the A/D and the D/A converters.

The proposed control system provides many attractive features, such as, can be applied the pressure transducer for sensing the liquid level in tank, can be displayed the process data either on control board or on microcomputer via RS232 serial-port. Experimental results have been employed to show the effectiveness of the system operation. Figure 7 shows the computer and microcontroller operation flowchart for data processing.

E. Problem Definition

Sustainability of available water resource in many reason of the world is now a dominant issue. This problem is quietly related to poor water allocation, inefficient use, and lack of adequate and integrated water management. Water is commonly used for agriculture, industry, and domestic consumption. Therefore, efficient use and water monitoring are potential constraint for home or office water management system.

Measuring water level is an essential task for government and residence perspective. In this way, it would be possible to track the actual implementation of such initiatives with integration of various controlling activities. Therefore, water controlling system implementation makes potential significance in home applications. The existing automated method of level detection is described and that can be used to make a device on/off. Moreover, the common method of level control for home appliance is simply to start the feed pump at a low level and allow it to run until a higher water level is reached in the water tank. This is not properly supported for adequate controlling system. Besides this, liquid level control systems are widely used for monitoring of liquid levels, reservoirs, silos, and dams etc. Usually, this kind of systems provides visual multi level as well as continuous level indication. Audio visual alarms at desired levels and automatic control of pumps based on user's requirements can be included in this management system. Proper monitoring is needed to ensure water sustainability is actually being reached, with disbursement linked to sensing and automation. Such programmatic approach entails microcontroller based automated water level sensing and controlling.

The Liquid Level Control systems are used to accomplish five different functions: (i) Water Make-Up, (ii) High Water Alarm, (iii) Low Water Alarm, (iv) High Water Cut-off, and (v) Low Water Cut-off. The most common application of a water level control system is water makeup. The system regulates the amount of water in the tower basin and keeps it within normal operating levels. This makeup system is used to control a water pump. When the water level drops below a prescribed, preset level, the water pump starts to fill the basin to its proper level.

High and low water alarms can be utilized to give warnings associated with abnormal operating water levels. To provide indication of these types of alerts, the control system provides dry contacts to interface with various digital control systems or can be connected to user supplied alarm indicators to signal when corrective action is required. Low-water cut-offs are commonly used to protect pumps from operating without sufficient water. When used in unattended operating environments, the low-water cut-off is configured to shut the pump off, thus preventing costly repairs. Dry contacts can be wired directly in series with pilot duty controls or to digital control systems to initiate the shutdown of protected equipment during low-water situations.

The water level control system consists of special purpose liquid sensing relays on one or more individual circuit cards connected to a probe assembly located in the water basin. Each circuit card contains one relay and external signalling is provided by each of these special purpose cards. The individual relay provides a "Form C" normally open and normally closed dry contact. The circuit card activates the relay using "through the water" continuity by way of the senor probes located in the water basin.

Utilizing water's ability to conduct electricity, a circuit path can be established between one probe tip and the other. Current conducts through the water across probes of dissimilar length. One common or reference probe is present in all systems and is shared by all functions of the system. This probe can be identified by its length. It is the longest probe in the system and extends the deepest into the basin. The current path is routed between all other probe tips and this one "common". When the water level reaches the shorter probe, the circuit is completed and the relay responds, opening or closing relay contacts corresponding to a fixed level. For low-level control, the ground reference probe and a slightly shorter probe provide the circuit. When the water level drops below this tip, the continuity between this probe and the reference probe is interrupted and the relay contacts transfer. The distance from the tip of the low probe to the floor of the basin determines the minimum water level that is allowed before an alarm is produced or pump operation is interrupted. The number of additional probes is determined by the individual application. As an example, in a "water makeup" system there are three probes, viz., one reference and two standard or short-tipped probes. The tip of the reference probe is normally positioned slightly above the basin floor with the additional probe tips positioned at different heights dictated by their specific function.

The Makeup system would have one probe at a height to begin or start filling the basin and another positioned higher to complete or stop filling. A probe for a High Alarm or High Cut-off would be positioned at a level to activate when the basin water exceeds its normal operating level and logically a Low Alarm or Low Cut-off would be positioned to detect a low water level nearer the bottom of the basin. Again, signalling is achieved in two ways. High Level and Makeup cards react when the water provides a completed circuit or continuity between its sensor and the reference probe. The second type of signal is for Low Level detection. The Low Level cards react when the water is not present and opens the circuit or disrupts the current flow between its probe and the reference.

A water level control system can be configured to meet various combination requirements. Since one individual circuit card is responsible for each function, the size and circuitry varies in proportion to the number of operations desired. For example, a water level makeup control will require a control panel with one circuit relay card and three probes. A system configured for water makeup that includes a high alarm and a low alarm, will require three circuit cards and five probes—one circuit card for the water makeup option, one for high operation and one for low.

III. MODEL CONSTRUCTION AND SOLUTION

For experiment this design we have been using a 16 bit microcontroller, a reserve tank, water tank and water pump. Water pump has been controlled using water level sensor. Four homemade water level sensors are used to detect the water level. Inverted sensor data used to pass as the input of microcontroller.

A. System Architecture

At the first stage of design a water level sensor is been made for sensing water level accurately. Microcontroller is used to control the overall system automatically that reduces the design and control complexity. Microcontroller takes input from the sensor unit which senses the water level. After processing input variables, resultant output decides the water pump's action (on/off) with respect to current water status of the tank.

B. Sensor Unit

Water level sensor unit consist two parts, one sensor is used in reserve tank and other four sensors placed inside water tanks. Moreover, sensors are composed with rod, nozzles, inducting rubber etc. Rod is made by iron and steel / Graphite, that is connected with ground. Nozzles are connected with +5v. Iron/Graphite rod and nozzles are binding together via a rubber. Rubber is used to make the electrical connection of iron rod and nozzles separate. Due to water conductivity 10kΩ resistance has been used. The basic operation is, when one nozzle of the sensor is drawn into water, nozzle and rod becomes connected due to water conductivity. Then nozzle gets ground signal (0v) which is connected with input of the inverter. The output of inverter is connected as the input of microcontroller which makes LEDs on/off, acts as user display unit.

C. Control Unit

The basic operation of control unit is the controlling water pump by microcontroller which is defined by particular program. Water pump is connected with an output pin of microcontroller via a relay circuit which is connected with a transistor. The collector of this transistor is connected with the relay circuit and the emitter is grounded. In the relay circuit, one diode is used for sending signal in one direction and one inductor is to opposing the change of current flow respectively. The output of relay circuit is connected with motor pump's cable as a negative. The other side of motor's cable is connected with AC 220V as positive voltage.
Control unit performs following actions:

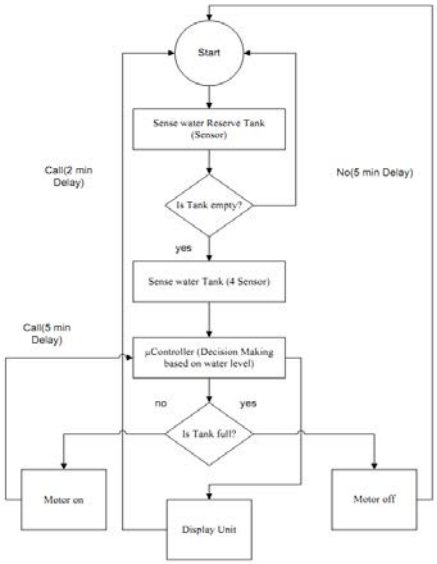

Fig. 8 The computer and microcontroller operation flowchart for data processing.

1) **Off operation**: When the microcontroller sends 0 volt to the base of the transistor then it becomes off and its emitter and collector becomes open. Then no ground signal (0v) is collected in the relay circuit. So, the negative side in the cable of motor pumps getting positive signal (+5v). Therefore, the motor pump will be OFF due to getting positive signal (+5v) at one side and 220v ac at the other end.

2) **On operation**: Transistor becomes on when the microcontroller sends positive signal (+5v) and its emitter and collector become short. Relay circuit and motor pump will get ground signal (0v) and for this reason the motor pump will be ON due to getting ground at negative side and 220V AC to the other side. In addition, the current is changed up to positive signal (+5v) to ground or its reverse then the inductor can tolerate some resistance. For this reason we should use a diode. An on/off switch is used to control the motor driver circuit manually.

The computer and microcontroller operation flowchart for data processing is shown in Fig.8 and experimental results are depicted in Table-1.

TABLE I
EXPERIMENTAL RESULT OF WATER LEVEL SENSING UNIT, MOTOR AND VISIBLE LEVEL DESCRIPTION FOR USER BY LED LIGHT

Inverted Input From Water Sensor		Output						
Res. Tank	Water Tank	LED 1	LED 2	LED 3	LED 4	Motor	Tank	Reserve Tank
0	0000	OFF	OFF	OFF	OFF	OFF	Empty	Empty
1	0000	ON	OFF	OFF	OFF	ON	Empty	Water Exist
1	1000	ON	ON	OFF	OFF	NO OP.	1/4	Water Exist
1	1100	ON	ON	ON	OFF	NO OP.	2/4	Water Exist
1	1110	ON	ON	ON	ON	NO OP.	3/4	Water Exist
1	1111	ON	ON	ON	ON	ON	Full	Water Exist

E. Programming Description

The program we used to control the entire process is written in Atmega16 microcontroller's C language. All the codes have been tested and simulated using AVR software which is provided by MICROCHIP. When the system powered up, microcontroller took the input from the water sensor through the inverter. Inputs from C3, C4, C5 and C6 of microcontroller are loaded by register and its combination is being checked.

The combination checking was done in the following way. (i) When microcontroller gets the first pin signal then it loads the signal to its register. After that it checks the next pin signal and then loads it to its register. Other pin signals operation also done respectively in the same way. Finally it loads all (four) required pin's signal to the register. By using these four signal combinations it decides an output and sends that signal to the output pin. (ii) The whole operation makes a cycle or repeats itself with respect to the input signals.

IV. RESULTS AND DISUCSSION

Though we have carried out the conceptual design of an automatic fluid level controller for low temperature fluid level estimation using water as the base fluid, many more works need to be carried out in two-phase flow environment owing to the fast that cryogen will evaporate quickly and invite level estimation errors using the conventional approach. Admittedly, huge amount of cryogenic fuel is being wasted during its industries uses due to lack of proper level estimation and control. We tried to overcome these problems using this conceptual study by implementing an efficient automated fluid level monitoring using suitable sensors as has been described using water as the base fluid. This research work was done with a motive to establish a flexible, economical and easy configurable system for low temperature fluid level estimation in a canister, which can be solved most of our industrial problems. Figure 9 shows the circuit description of automatic fluid (water) level controller.

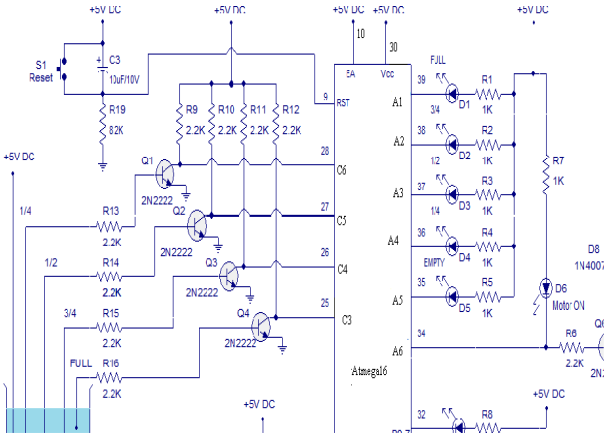

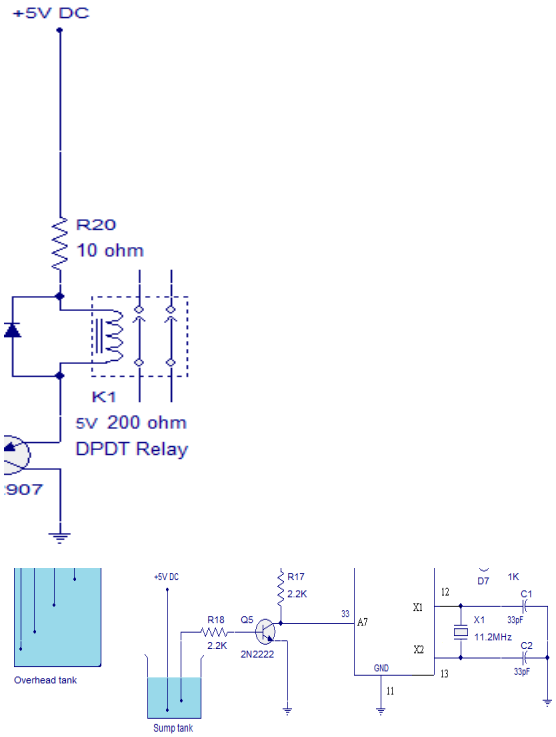

Fig. 9 Circuit description of automatic fluid level controller.

A low cost Atmega16 microcontroller is used in this system which is the key point to reduce. The proposed system guarantees to cut down the wasting of fluid. This monitoring and controlling system uses daily life device like laptop or mobile phone. Due to the fact of controlling remotely, a useful wireless automated controlling system can be introduced. This proposed web based monitoring and controlling network can work with the existing fluid controlling system successfully.

The experience gained through this study leads to say that the proposed system could detect the actual fluid volume of the low temperature cryogenic fluid for the estimation of the effective propulsive efficiency of the entire aerospace vehicle. The preliminary sea level test results, using water as the base fluid, shows that the system model being proposed is able to monitor the liquid level very effectively and accurately for estimating the total volume of the fuel and oxidiser for estimating the operating time of the aerospace vehicle lucratively. This small work is a pointer towards for the accurate evaluation of the cryogenic fluid volume during the mission of the aerospace vehicles.

ACKNOWLEDGMENT

The authors would like to thank Anchal Gupta of University of Petroleum & Energy Studies, Dehradun India for her extensive support of this research work.

REFERENCES

[1] Fisher, B.H. Liquid Sensing Using SAW Devices, Frequency Control Symposium, 2007 Joint with the 21st European Frequency and Time Forum. IEEE InternationalMay 29 2007-June 1 2007, ISBN: 978-1-4244-0646-3.

[2] Rodd, M. G. and Deravi. F. "Communication Systems for Industrial automation" Prentice Hall, 1989.

[3] Kuo. B. C. "Digital control system" Holt-Saunders International Editions, 1980.

[4] Gao,W.Wang. Y. and Homaifa, "A Discrete-time structure control system" IEEE Transaction on Industrial Electronics. 42, 2 (1995): 117-122.

[5] Pan, Y. and Furuta, K. "Discrete time VSS controller design." International Journal of Robust and Nonlinear Control. 7 (1997): 373-386.

[6] Hung, J.Y., Gao, W. and Hung, J.C. "Variable Structure Control: A Survey" IEEE Transactions on Industrial Electronics. 40, 1 (1993): 2-22.

[7] Barnett, R. H. The 8051 family of Micro-controllers. Prentice-Hall, 1995.

[8] G.Betta, L. Ippolito, A. Pietrosanto, and A.Scaglieone, "An optical fiber based technique for continuous level sensing" IEEE Trans. Instrum.Meas, Vol.44,pp. 686-689, June 1995.

[9] G.Betta, A. Pietrosanto, and A.Scaglieone, "Microcontroller based performance enhancement of an optical fiber level transducer" IEEE Trans. Instrum.Meas, Vol.47,pp. 489-493, April 1998.

[10] R.E. Shaffer, S.L. Rose-Pehrsson, R.A. McGill, A comparison study of chemical sensor array pattern recognition algorithms, Anal. Chim.Acta 384 (1999) 305–317.

[11] T. S. Aye, and Z M. Lwin, "Microcontroller Based Electric Expansion Valve Controller for Air conditioning System", World Academy of Science, Engineering and Technology, 2008

[12] E.J. Cho and F.V. Bright, Integrated chemical sensor array platform based on light emitting diode, xerogel-derived sensor elements, and high-speed pin printing, AnalyticaChimicaActa, vol. 470, pp. 101-110, 2002.

[13] P. Dietz, W. Yerazunis, D. Leigh, Very Low-Cost Sensing and Communication Using Bidirectional LEDs, UbiComp 2003: Proceedings, vol. 2864, pp. 175-191,2003.

[14] M. Javanmard, K.A. Abbas and F. Arvin, "A Microcontroller-Based Monitoring System for Batch Tea Dryer", CCSE Journal of Agricultural Science, Vol. 1, No. 2, December 2009.

[15] Roderick L. Shepherd, William S. Yerazunis and Senior Member, "Low-Cost surface Mount LED Gas Sensor", IEEE King Tong Lau and Dermot Diamond, Sensors-00997, 2005.

[16] MOTOROLA Sensor Device. 3rd ed. MOTOROLA Inc. (TMOS), 1995.

[17] L. Byrne, K.T. Lau, and D. Diamond, Monitoring of headspace total volatile basic nitrogen from selected fish species using reflectance spectroscopic measurements of pH sensitive filmsî, The Analyst, vol. 127, pp. 1338-1341, 2002.

[18] V.R.Sanal Kumar,V.R. et al., *"A Classical Evaluation of the Thermophysical Properties of Insulators for Cryogenic Rockets,"* 41st AIAA/ASME/SAE/ASEE Joint Propulsion Conference & Exhibit, 10-13 July 2005, Arizona, USA, Paper No. AIAA 2005 – 4085.

[19] V.R.Sanal Kumar et al., *"Insulation Qualification Studies for Cryogenic Rockets,"* 41st AIAA/ASME/SAE/ASEE Joint Propulsion Conference & Exhibit, 10-13 July 2005, Arizona, USA, Paper No. AIAA 2005-3849.

Operating temperature of PV module modified with surface cooling unit in real time condition

Madhu Sharma, Kamal Bansal
Electrical, Power and Energy
University of Petroleum and Energy Studies
Dehradun, India
madhusharma@ddn.upes.ac.in

Dharam Buddhi
SelaQui Institute of Engineering and Technology
Selaqui
Dehradun, India

***Abstract*—** High operating temperature decreases photo voltaic module efficiency. Normal Operating Cell Temperature, NOCT of silicon crystalline is about 49^{o}C as reported. A cooling unit with reverse flow water circulation is designed, fabricated and applied on PV back surface to partially avoid undesirable effect of its temperature increase. This modified module with cooling unit and similar non-cooled modules are installed outdoor identically at University of Petroleum and Energy Studies campus, Dehradun. Installed Normal Operating Cell Temperature, INOCT of both the modules are determined and compared by varying water flow rate from cooling unit. And also water flow rate is optimized to maintain minimum possible operating temperature.

***Index Terms*—** INOCT, optimum mass flow rate, passive surface cooling unit, PV module

I. INTRODUCTION

Out of total energy produced, electrical output is only one component with typical ideal conversion efficiency in the range of 15% from PV module [1]. Remaining produced energy is heat. As this heat energy is neither utilized nor captured, increases PV module temperature which actually influence their overall performance.

In Ras AL Khaimah, at CSEM – UAE Innovation Centre outdoor testing facility for PV module was installed on the roof. 165 Wp multi-crystalline silicon module had been selected for experiment and was mounted at 30^{o} of fixed tilt angle facing true south. Day star I-V curve tracer and CSEM-UAE AMCU flyer unit gave I-V characteristics under varying load of selected module at different solar radiation in outdoor condition. Global radiation, module surface temperature, ambient temperature, current and voltage readings of PV module were recorded for analysis. Experimental results showed that module efficiency varies between 8-10%, which was differing 3-4 % from STC specified efficiency. And this efficiency drop is the results of high operating surface temperature (50-60^{o}C) of PV module [2].

During 2009 at Malaysia temperature dependence coefficient of crystalline silicon PV modules and amorphous silicon module have been obtained using linear regression techniques. Three modules a-Si, multi crystalline and mono-crystalline were installed in field with data monitoring using data logger. It was found that multi crystalline PV module is highly temperature sensitive among three types [3].

The photon rate of PV cell increases with the temperature and hence reverse saturation current. This results in the change of current and voltage, which means marginal changes in current but major changes in voltage [4].

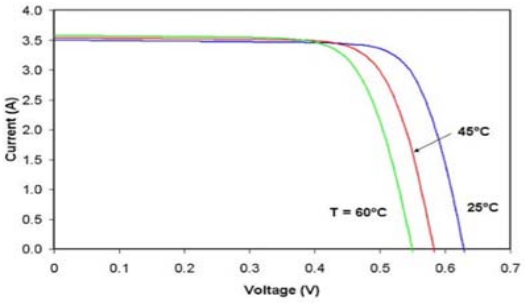

Figure1. Shows how the I-V curve varies with varying temperature [4]

IV curve define the PV cell performance [5] for a given solar radiation. PV cell has two limiting parameters short circuit current (I_{sc}) when V=0, and open circuit voltage V_{oc} when I=0 with rise in temperature of PV cell I_{sc} increases slightly while V_{oc} drop significantly. Open circuit voltage drops 2mV/^{o}C rise of temperature for silicon materials. In solar modules operation, temperature is an important issue as temperature rise significantly reduces electrical output, increases thermal stress and degradation rates. Author suggested that with appropriate cooling system with air or water, electrical efficiency can significantly enhance. Combining both technologies, photovoltaic & thermal as hybrid PVT to

978-1-4799-6046-0/14/$31.00 ©2014 IEEE

generate electricity and heat water in a house for instance is another way to handle heat issue [5].

There is more than 25 % performance reduction of PV module, as modules operate over 50°C above ambient temperature commonly. To make significant gains in PV system performance, its operating temperature can be lowered by dissipating heat from the module and this heat can be utilized for practical heating purposes [1].

Traditional linear expression for PV electrical efficiency is

$$\eta_c = \eta_{Tref} [1 - \beta_{ref} (T_c - T_{ref})]$$

Where η_{Tref} and T_{ref} is cell efficiency and cell temperature at Standard Test Condition (STC – 1000 W/m^2, 25°C) and $\boldsymbol{\beta_{ref}}$ is temperature coefficient (°C^{-1}).

In this paper, we present basic design consideration to modify commercially available polycrystalline module. The method of finding Installed normal operating temperature is discussed. And INOCT of non-cooled module and with cooling module are determined and presented.

II. EXPERIMENTS AND STANDARDS

To install photovoltaic module, system designer and inventor consider data sheet of modules to make choice of module type and brand. Data sheet include few primary characteristics like module peak power and efficiency at STC (standard test condition), temperature coefficient of power, open circuit voltage, short circuit current and sometimes low light behavior as STC rarely met in real time condition [6].

In STC, measurements are taken using a solar simulator under laboratory conditions and it is controversial as standard condition can never be found in real time. Climate parameters like solar insolation, ambient temp, wind speed etc., are the locality dependent variable on which the performance of PV module depends. For effective design of PV system, device rating measurements at the site of is desirable and this allows actual power output prediction. In the outdoor environment, PV efficiency as a complex function of micro climatic parameters and working temperature of PV module plays a crucial role in rating determining. High radiance and high temperature combination leads lower efficiency compared to low radiance and low temp combination [7].

Operating temperature of the module depends on the radiation absorption properties, thermal dissipation, module encapsulating materials, module functioning and also depends on insolation, ambient temp, accurate installation status and wind speed. Module parameters like voltage, current, power and efficiency greatly influence by the module operating temperature and thus, it is very important to perform a quantitative analysis under real operating condition. Author investigated the temperature influence on PV parameters of amorphous- silicon (a-Si) and copper indium deselinide (CIS) thin film modules at Patras, Greece (latitude 38°) where at Patras peak sun hours over 4.2 per day and working temp of the module between 16 to 60°C. V_{oc} percentage reduction with temperature increase is greater of CIS than a-Si modules. CIS short circuit current temperature coefficient in position at low and medium temperature, and at entire working temperature range approximately constant with slight tendency to reduce. In case of CIS maximum power as a function of temperature decreases linearly. Annual behavior indicated that CIS module efficiency decreases with temperature and a-Si module was not severely affected [8].

Difference between junction temperature of PV module and ambient temperature is a consequence of continuous solar radiation and the accumulation of thermal energy in the interior of modules lead to serious performance deterioration. Author found this temperature difference will increase linearly with radiation intensity rise, even if ambient temperature changes [9].

As a module temperature indicative NOCT (Normal Operating Cell Temperature) is commonly use. NOCT is mean solar junction temperature in Standard Reference Environment (SRE) with in an open rack mounted module. SRE includes total irradiance 800W/m^2, wind speed 1m/s, ambient temperature 20°C, tilt angle - at normal incidence to the direct solar beam at local solar noon and nil electrical loads. NOCT is a reference of how the module will work in real condition therefore is an important characteristic. To calculate NOCT there are several intimation standards EN-61215 for crystalline PV module, EN-61646 for thin film PV module, ASTM E1036M or both (non - concentrator terrestrial PV modules and arrays)[10].

Fact on which all above standards are based is that T_m-T_a (module temp - ambient temp) difference is essentially linear to irradiance and largely independent of wind speed.

INOCT i.e. Installed Nominal Operation Cell temperature is the cell temperature of installed module connected to load and also mounting configuration of the module is taking into account. In open rack case it is recommended that one use a value of INOCT 3°C less than NOCT value [11].

Gail-Angee Migan reported that NOCT of a typical module is 48°C whereas; best operates at 33°C and worst at 58°C [4].

III. SYSTEM DESCRIPTION AND OUTDOOR TESTING

To reduce the operating temp of PV module, a PV surface cooling system is designed, developed and experiment set up is installed. Multi crystalline silicon PV module of 75 Wp is modified by applying cooling system underneath. Cooling unit is glued by thermal conductive paste on rear surface of module. And the performance of this modified module is compared with the normal module of same type, same rating and same make in similar operating conditions.

Both the modules, non-cooling and with cooling unit were mounted at an optimum angle of 30° tilt equal to the latitude of the location oriented due south for best year round performance.

Cooling / heat absorbing system consist of two rectangular hollow copper tanks of absorber and in thermal contact with standard PV module of 75 Wp. Absorber tank was fabricated with one inlet and one outlet arranged opposite to each other

and so water flows in reverse direction and cover 76 % back surface area of module. To avoid thermal losses from the absorber tank, tanks are thermal insulated. Inlet water from the overhead storage tank flow through cooling unit at pre- set flow rate, and absorb heat from the PV module surface and store in outlet tank. Water is flowing by gravity as head difference between inlet and outlet water tank and no pump is used.

Experiments were conducted to find Installed Normal Operating Cell Temperature at irradiance 800 W/m^2, ambient temperature 20^{o}C and wind speed 1m/s of both non - cooling and with cooling modules under similar mounting and operating conditions.

Water flow rate was pre-set for a single day and at 15 minutes interval following measurements were taken:-

- Solar irradiance at tilted surface
- Ambient temperature
- Wind speed
- Back surface temperature of non– cooling module
- Back surface temperature of module with cooling unit

To analyze collected data of each day for both non - cooling and with cooling modules:-

- Module temperature rise above ambient temperature as a function of solar irradiance (>400 W/m^2) is plotted.
- To fit data, linear regression is used and temperature above ambient at 800 W/m^2 was determine by regression equation
- Finally installed normal operating module temperature were determined at reporting conditions by adding 20^{o}C and corrected for average wind speed and ambient temperature from the following graph shown in fig. 2 [12].

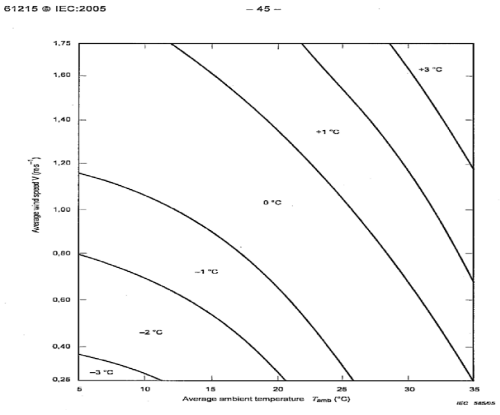

Figure 2. To correct NOCT for average wind speed and average ambient temperature [12]

IV. RESULT AND DISCUSSION

Eleven tests were conducted on different sunny days in the month of April 2014.Out of these four test are depicted in fig. 3-6 below and following equation is used to calculate INOCT on tested day:-

$INOCT_{day}$ = regression equation + 20^{o}C + correction factor

Where

- Correction factor is determined by using graph shown in fig. 2 above for average ambient temperature and average wind speed
- Regression equation of fitting collected data is obtained from the graphs plotted for each day.

Finally INOCT is obtained by correcting regression equation to 800 W/m^2 and adding 20^{o}C and correction factor.

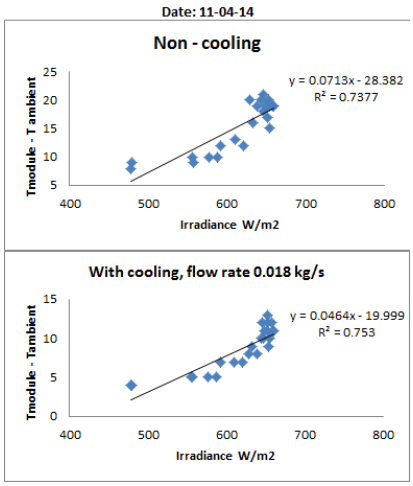

Figure 3. Test result of 11-04-14

Average wind speed = 1.02 m/s
Average ambient temperature = 31.63^{o}C
Correction factor = +1^{o}C
INOCT non-cooling,
T_{INOCT}= (0.0713*800-28.382) +20+1 = 49.66^{o}C
INOCT with cooling,
T_{INOCT} = 0.0464*800-19.999+20+1 = 38.12^{o}C

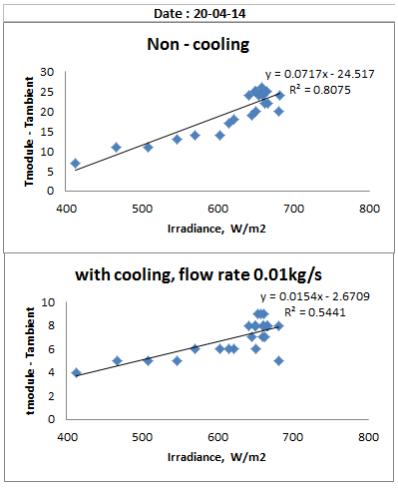

Figure 4. Test result of 20-04-14

Average wind speed = 1.15 m/s
Average ambient temperature = 29.2°C
Correction factor = +1°C
INOCT non-cooling,
T_{INOCT} = (0.0717*800-24.517) +20+1 = 53.84°C
INOCT with cooling,
T_{INOCT} = 0.0154*800-2.6709+20+1 = 30.64°C

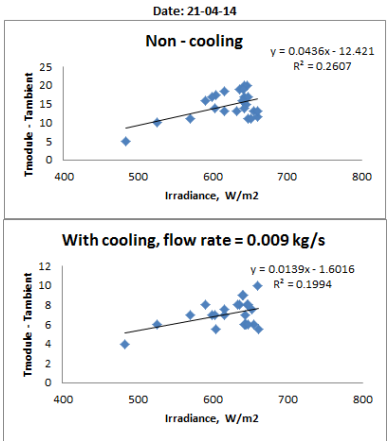

Figure 5. Test result of 21-04-14

Average wind speed = 0.858 m/s
Average ambient temperature = 33.77°C
Correction factor = +1°C
INOCT non-cooling,
T_{INOCT} = (0.0436*800-12.421) +20+1 = 43.5°C
INOCT with cooling,
T_{INOCT} = 0.0139*800-1.6016+20+1 = 30.5°C

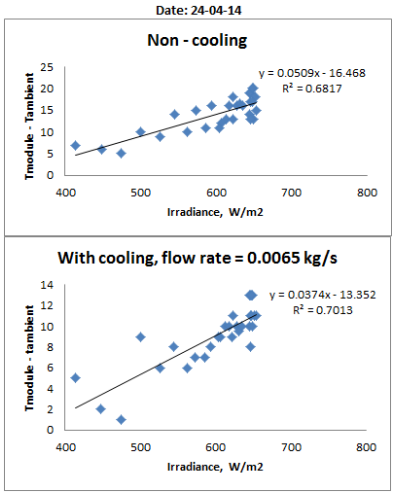

Figure 6. Test result of 24-04-14

Average wind speed = 1.09 m/s
Average ambient temperature = 31.61°C
Correction factor = +1°C
INOCT non-cooling,
T_{INOCT} = (0.0509*800-16.468) +20+1 = 45.3°C
INOCT with cooling,

T_{INOCT} = 0.0374*800-13.352+20+1 = 37.6°C
And result of all tests is summarized in table - I below

Table –I	Field Test Results		
	Flow	Operating Temp Non-cooled	Operating Temp with cooling
	(kg/s)	(°C)	(°C)
8/4/2014	0.032	51	43
11/4/2014	0.018	49.7	38.12
12/4/2014	0.016	56.56	37
14/4/2014	0.014	48.8	30.83
15/4/2014	0.013	52.5	30.66
20/4/2014	0.01	53.84	30.64
21/4/2014	0.009	43.5	30.5
22/4/2014	0.008	48.3	33.33
23/4/2014	0.0072	44.5	33.4
24/4/2014	0.0065	45.3	37.6
25/04/2014	0.0055	47.7	34

Based on experimental data, the effect of flow rate on operating temperature of modified module is presented in fig.6 below:

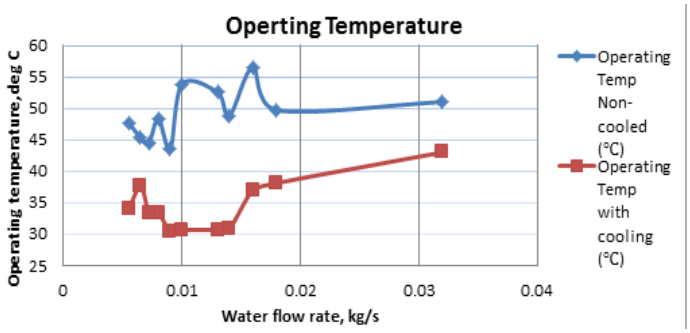

Figure 7. Test results at different flow rates

It is observed that non - cooling module is operating at much higher temperature than cooling one.Average operating temperature of non-cooled module is 49°C.It is also observed that in the water flow range of 0.009 kg/s to 0.014 kg/s operating temperature of module with cooling unit is almost constant.For poly crystalline module modify with cooling unit water flow rate is optimized at 0.01 kg/s for best operating temperature of about 30.6°C.

The calculated INOCT can consider as most representative of the module behavior. From available irradiance, ambient temperature and this INOCT value , module temperature can be calculated using equation below

$$Tm = Ta + (INOCT - 20)\ E / 800$$

Where Tm is module temperature and E is solar irradiance.

V. CONCLUSION

1) PV module efficiency is sensitive to module surface temperature and decrease with surface operating temperature increase.

2) Objective of the study is to prove the potential benefits of PV module with heat extraction unit (surface cooling units) system compared to typical PV module.

3) Polycrystalline silicon PV module combined with surface cooling system to extract heat was constructed and tested with respect to its operating temperature and compared with operating temperature of module of same rating without cooling system at the Geo graphic location of Dehradun installed similarly.

   Under same metrological and mounting conditions:

   - Installed normal operating temperature of non-cooling case is much higher than cooling one
   - There is wide variation in operating temperature of non - cooling unit tested and operating temperature variation is less with cooling unit in specified range of flow rate of water.
   - To maintain minimum operating temperature, optimum flow rate of water through cooling unit is 0.01 kg/sec for designed system.

4) Heat removed by the water flowing naturally by gravity through surface cooling unit at optimum flow rate is collected at the lower end of the panel and can be used as a utility for heating purposes.

5) Average installed nominal cell temperature of non-cooling module is found 49^{o}C and with cooling unit we are able to reduce it to 30.6^{o}C at optimum water flow rate. And accordingly efficiency will increase by 9.2 % if efficiency conversion coefficient is considered 0.45 %/^{o}C.

ACKNOWLEDGMENT

Special thanks to Dr. S.J. Chopra for support and suggestions. The work described in this paper was financially supported from University of Petroleum and Energy Studies, Dehradun.

REFERENCES

[1] John Hollick: Conserval Engineering Inc., Toronto Ontario, "PV thermal systems – Capturing the untapped Energy", Conference proceedings - "Solar Energy Society Conference in Cleveland". July 11, 2007,

[2] Kapil Kumar, S. D. Sharma, Lokesh Jain, "Standalone Photovoltaic (PV) module outdoor testing facility for UAE climate", CSEM-UAE Innovation Center LLC, Ras Al Khaimah, United Arab Emirates

[3] Sulaiman Shaari, Kamaruzzaman Sopian, Nowshad Amin and Mohd Nizan Kassim, "The Temperature Dependence Coefficients of Amorphous Silicon and Crystalline Photovoltaic Modules Using Malaysian Field Test Investigation", in American Journal of Applied Sciences 6 (4): 586-593, 2009, ISSN 1546-9239

[4] Pradhan Arjyadhara, Ali S.M and Jena Chitralekha, " Analysis of Solar PV cell Performance with changing Irradiance and Temperature", International Journal Of Engineering And Computer Science ISSN:2319-7242, Volume 2 Issue 1 Jan 2013 Page No. 214-220

[5] Gail-Angee Migan, "Study of the operating temperature of a PV module", Project Report, 2013 MVK160 Heat and Mass Transfer, May 16, 2013, Lund, Sweden

[6] Bert Herteleer, Jan Cappelle, Johan Driesen, "Quantifying low-light behavior of Photovoltaic modules by indentifying their irradiance – dependent efficiency from data sheets", 27th European Photovoltaic Solar Energy Conference proceeding 2012, pages 3714 – 3719, ISBN:3-936338-28-0

[7] A.Q. Malik and Mohamad Fauzi bin Haji Metali, "Performance of Single Crystal Silicon Photovoltaic Module in Bruneian Climate", International Journal of Applied Science and Engineering, 2010. 8, 2: 179-188

[8] V. Perraki and G. Tsolkas, "Temperature dependence on the photovoltaic properties of selected thin-film modules" , International Journal of Renewable and Sustainable Energy, 2013; 2(4): 140-146

[9] Joe-Air Jiang, Jen-Cheng Wang, Kun-Chang Kuo, Yu-Li Su, Jyh-Cherng Shieh and Jui-Jen Chou, "Analysis of the junction temperature and thermal characteristics of photovoltaic modules under various operation conditions", Energy 44 (2012), page 292-301

[10] M.C. Alonso Garcıa and J.L. Balenzategui, "Estimation of photovoltaic module yearly temperature and performance based on Nominal Operation Cell Temperature calculations", Renewable Energy 29 (2004), 1997–2010

[11] Fuentes MK, "A simplified thermal model for flat-plate photovoltaic arrays", SANDIA report no., SAND-85-0330; 1987

[12] Matthew Muller, "Measuring and Modeling Nominal Operating Cell Temperature (NOCT)", NREL, Test & Evaluation, Sept 22-23, 2010 PV Performance Modeling Workshop Albuquerque, NMNREL/PR-520-49505

Outlier Detection in Streaming Data A research Perspective

Neeraj Chugh
Deptt. of CSE
University of Petroleum
& Energy Studies,
Dehradun, India

Mitali Chugh
Deptt. of CSE
Tula's Institute of Engineering
& Management
Dehradun, India

Alok Agarwal
Deptt. of CSE
JP Institute of Engineering
& Technology
Meerut, India

Abstract—**Data mining is a system that brings up the light to hidden and valuable information from the data and the facts revealed by data mining which were previously not known, theoretically useful, and of high quality. Data mining offers a means by which we can explores the knowledge in database. *Data stream mining* and *finding outliers* are dynamic research areas of data mining. It is thought that 'data stream mining and outlier detection' research has drastically expanded the range of data analysis and will have profound impact on data mining methodologies and applications in the long run. However, there are still some difficult research problem that are to be answered before data stream mining and outlier detection can declare a keystone approach in data mining applications. The aim of this work is to simplify problems related to detecting outlier over dynamic data stream and exploring explicit techniques used for detecting outlier over streaming data in data mining presented by researchers in recent years and also to look at the future trends.**

IndexTerms—***Data mining, Outliers, data stream mining.***

I. INTRODUCTION

Data mining offers a way by which we can explore the knowledge in database. To discover knowledge, there are steps that are carried out before data mining such as selection of data, cleaning of data, pre-processing and data transformation. The rules are to be extracted from the bulk of available data. However, there is a concern about latest data, modification and deletion partly or fully of the currently available data set throughout the process of data mining. Earlier users had to reiterate the whole procedure which is time-consuming and also not much efficient. As a result the significance of dynamic data mining process comes into existence [1].

A data stream is a large series of data elements generated constantly with a fast rate. In streaming a large amount of data constantly inserted and queried so this requires huge database. A unique feature of data streams is that they are time-varying, i.e. only the current state is stored which is in contrast to traditional database systems [2]. As a result the traditional classification methods are not suitable. This alteration in the nature of the data results in the changes in the target classification model over time and is referred to as perception theme. For that reason the classification model should be such that it can adapt with the dynamics of the stream data [2]. Streaming data analysis has recently fascinated the attention over mining large data sets in data mining community.

Outlier, exceptional and not regular in the database detection is a dynamic research problem that aims to find objects that are significantly unlike. There are different definitions of outliers given by researchers which are:

Definition 1[Hawkins]: "An outlier is an observation that deviates so much from other observations as to arouse suspicious that it was generated by a different mechanism."[3]

Definition2 [Grubbs' outlier definition]: "An outlying observation, or outlier, is one that appears to deviate markedly from other members of the sample in which it occurs."[4]

Definition3 [Barnett and Lewis' outlier definition]: "An observation (or subset of observations) which appears to be inconsistent with the remainder of that set of data."[5]

These definitions give idea of outliers from a general point of view. For designing solutions related to mining outliers, operational notions are needed that facilitate us to design detection algorithms. However, as the nature of the detection problem is reliant on the application domain [6], across domains and even within each domain, the existing notions of outliers differ to a great extent. *Outlier detection* has significant role in data mining and deserves more consideration from data mining community. In recent years, conventional database querying methods are insufficient to remove useful information and hence researches nowadays focus on the development of new techniques to meet the increasing requirements.

II. RELATED WORK

Discovery, eliminating and identifying outliers has high worth in data mining. Error in large databases can be enormously collective, and so an essential property of a data mining algorithm is robustness in respect of outliers detection in the database. Some refined methods in data mining address this problem to some extent, but not fully, and can be enhanced by addressing the problem more directly. Outlier detection can lead to the finding of unsuspected knowledge in areas such as credit card fraud detection, calling card fraud detection, discovering criminal behaviors, discovering computer intrusion, etc.[7] . Work has been done in this area of

research. The early methods of outlier detection have mainly been related to the field of Statistics and are - Distribution based, and Depth based [8],[5]. This work is based on statistics [5],[9], and assume that a prior knowledge of distribution is mandatory. Most of the tests are depended on the distribution whether or not the distribution factors are known. Another area related to detecting outliers is clustering algorithms. These algorithms consider outliers as objects not found in clusters of a dataset and these algorithms produce outliers as by product.

Researchers have proposed distance-based, density-based and connectivity-based outlier detection methods and major advantage of these proposed methods is that they do not have any prior knowledge about the data distribution. However for stream data the performance results for these methods are not very efficient. The earlier work on outlier detection states online outlier and these are less correct and may lead to wrong decision. The interesting work on outlier detection in data stream declare a point due to limited memory resources as compared to huge data stream, as an outlier which can often lead to incorrect judgments because of vigorous nature of the received data[10]. Outlier detection over streaming data aim to identify objects which have dissimilar behavior, and they are exceptional in comparison to normal objects[11]. Depending upon different application domains these abnormal patterns are often referred to as outlier, exceptions, faults, defects, noise, errors, and contaminants. Identification of outlier in datasets results in discovery of valuable knowledge. This improves data analysis for further discovery within different application domains and helps to avoid a wrong conclusion. The outlier analysis in data streams leads in detection and prevention of fake activities, criminal activities, failures and improvement in security and safety in diverse applications, e.g. in credit card industry. Outlier detection is a challenging work because of the characteristics of data streams. Most of the outlier detection techniques work on static time sequences. They process outliers by working on the entire time sequences to detect global outliers. This would be computationally infeasible in case of data streams [2].

III. STREAMING TIME SERIES CLASSIFICATION

Classification is a method of data analysis that can be used to extract models which describe vital data classes or in prediction of future trends for data. Due to the characteristics of the stream data, the traditional classification methods are unsuitable for them. The most distinctive characteristic of data streams is that they are Abbreviations and Acronyms time-varying that is only the current state is stored, as opposed to traditional database systems. This change in the nature of the data takes the form of changes in the target classification model over time and is referred to as concept drift. Therefore the classification model should be such that it can adapt itself with the dynamics of the streaming data[2][12].

IV. OUTLIER DETECTION TECHNIQUES

For detecting outliers in static data statistics based approaches have primarily been developed. These approaches are based on assumptionthat dataset follows a statistical model, e.g. a normal or Poisson distribution[13]. In case of data streams unconventional knowledge about the data distribution may not be known. Cluster based approaches, such as DBSCAN, CLARANS [14], etc. have been used for outlier detection in different variety of datasets. During identification of clusters, outlier finding is treated as a byproduct. The problem with this approach is that it is mixing two problems instead of solving each problem individually. Density-Based Approaches adopt a Local Outlier Factor (LOF) for outlier detection[15]. Outlier detection (exception mining, deviation detection, novelty detection, etc.) is a critical issue that has attracted wide interest and different solutions by researchers. There are many outlier detection methods discussed in the literature and are in practical use. If data for analysis is given by domain expert and it is labelled then that data can be used to build outlier detection model. This method can be divided into: *Supervised, Semi-supervised, and Unsupervised methods,* whereas based on assumption, categorization of outlier detection methods are: *Statistical methods, Proximity-based methods, and clustering-based methods* [2].

a. Model-Based

Model based approach build a model based on domain values and the object that do not match with the model are marked [16].

Disadvantage: To build a model required the expertise of domain expert and an expensive task.

b. Connectedness

In this domain where objects are associated (social networks, biological networks), objects have few association, treated as prospective anomalies.[17].

Disadvantage: This approach works only for association information of datasets.

c. Density-Based

The objects that come into the low-density regions of space are flagged and treated as outliers [18].

Disadvantage: Density based models need the cautious settings of several factors. It requires quadratic time complexity. It may rule out anomalies close to some non-anomalies patterns that have low density.

d. Distance-Based

Objects that have distances to their nearest neighbors that exceed a specific threshold are considered probable anomalies. In compare to the above, distance-based methods are much more flexible and robust. They are defined for any data type for which we have a distance measure and do not require a detailed understanding of the application domain [19-23].

e. Cluster based approach

In this technique the data is partitioned into groups that have related objects. The expected performance of outliers is that they either do not belong to any cluster, or belong to very small clusters, or are enforced to fit in to a cluster where they are unlike from other members. This method specify that outliers do not fit in to any cluster since they are very few and different from the standard incidences [21][24][25].

f. K-Nearest Neighbor Based Approach

In this method each object is analyzed with respect to its local neighborhood. The basic view behind such schemes is that an outlier will have a neighborhood where it will position out while a normal object will have a neighborhood where all its neighbors will be exactly like it. It is to be highlighted that the strength of these techniques lies in the fact that they work in an unsupervised mode, i.e. they do not assume availability of class labels [22][26].

V. CHALLENGES IN DETECTION OF OUTLIER IN STREAMING OF DATA

In data analysis the most important task is Mining beneficial and interesting information from a large amount of data. Designing a suitable outlier detection technique is a challenging task in context of streaming data and type of data[27]. The following challenges are encountered in traditional outlier detection methods that are not able to detect outliers in data stream:

a. Distributed Streaming Data

Data coming from dissimilar datasets may change dynamically and in such situations distribution of data stream may not be known. As a result of dynamic nature of data direct computation of probability is a cumbersome task [28]. Traditional methods are not able to handle distributed data stream in the offline manner.

b. Massive Data Processing

Data stream have huge amount of data which changes dynamically, due to this it is difficult to scan the data in one go. In this scenario major challenge in traditional outlier detection methods is providing of a high detection rate in the dynamic data stream. Hence it is observed that traditional outlier detection techniques do not scale well to process bulk data of distributed data streams in an online manner.

c. Limited Computation Resources

In many application domain there is requirement of more calculating power and the other calculating factor such as intake of available memory at hand are not in accordance with huge amount of data in a data stream. Stream mining algorithms should learn fast and moreover it should consume less memory resources.

d. Uncertain and missing data

In most application domains we do not have enough data for operations. Such situations arise as a consequence of uncertain and missing data. If we do not have sufficient information about the data in data streaming it may lead us to wrong decisions. We require a technique to manage such indeterminate data and missing data in the data stream.

e. High Dimensional Data Stream

High dimensional data stream contain a tremendous amount of data. Such massive amount data contains a large data with high dimensions and complexity. For example in wireless sensor networks data, web logs, Google search, etc. traditional methods are not appropriate for high dimensional data as they require very high computation cost for processing data[29][30].

VI. CONCLUSION

In this paper a review of outlier detection over streaming data, issues and challenges in identifying outliers in data streams has been discussed. On the basis of review we can conclude that majority of outlier detection research is based on algorithms which are related to specific domain. We have also observed that assumption based methods are efficient if prior assumption made about data is accurate. Moreover, efficiency of detection methods is also dependent on nature of data and its distribution in a specific domain. The methods discussed in this paper for outlier detection have certain limitation as well. Methods work efficiently if a combination of methods is employed for identifying outliers in streaming data. It is also observed the obtained results are more accurate when compared to the result of individual method. Thus it is suggested that it is batter to use a combination of method for detection of outliers in streaming data.

REFERENCES

[1] H. H. Nasereddin, "Stream data mining," *International Jourmnal of Web Applicatios,* vol. 1, no. 4, pp. 183-190, december,2009.

[2] J. Han and M. Kamber, "Data Mining Concepts and Techniques," *Elsevier ,* 2008.

[3] D.Hawkins, " Identification of Outliers," Chapman and Hall, London, 1980.

[4] F. E. Grubbs, "Procedures for detecting outlying observations in samples no.," *Technometrics,* vol. 11, no. 1, pp. 1-21, 1969.

[5] V. Barnett and L. T, Outliers in Statistical Data, 3rd ed., John Wiley and Sons, 1994.

[6] H. V.J. and J. Austin, "A survey of outlier detection methodologies.," *Artificial Intelligence Review,* vol. 22, no. 2, pp. 85-126, 2004.

[7] M. O. Mansur and M. N. M. Sap, "Outlier Detection Technique in Data Mining: A Research Perspective," in *Proceedings of the Postgraduate Annual Research Seminar* , 2005 .

[8] M. O. Mansur and M. N. M. Sap, "Outlier Detection Technique in Data Mining: A Research Perspective," in *Proceedings of the Postgraduate Annual Research Seminar* , 2005.

[9] S. Ramaswamy, R. Rastogi and K.Shim, "Efficient algorithms for mining outliers from large data sets," in *Proceedings of the International Conference on Management of Conference Data*, Dallas,Texas, 2000.

[10] H. M. Koupaie, S. Ibrahim and J. Hooseinkhani, "Outlier Detection in Stream Data by Clustering Method," *International Journal of Advanced Computer Science and Information Technology(IJACSIT),* vol. 2, no. 3, pp. 25-34, 2013.

[11] J.Han and M.Kamber, "Data Mining: Concept and techniques,," in *Morgan Kaufmann*, San Francisco, 2006.

[12] D. Toshniwal and S. Yadav, "Adaptive Outlier Detection in

Streaming Time Series," in *IACSIT Press*, Singapoore , 2011.

[13] S.D.Pachgade and S. S.Dhande, "Outlier Detection over Data Set Using Cluster-Based and Distance-Based Approach," *International Journal of Advanced Research in Computer Science and Software Engineering*, vol. 2, no. 6, pp. 12-16, June 2012.

[14] K. Ishida and H. Kitagawa, "Detecting Current Outliers: Continuous Outlier Detection over Time-Series Data Streams," *Springer-Verlag Berlin Heidelberg*, vol. 5181, pp. 255-268, 2008.

[15] Breunig, M.M., K. H.P., N. R.T. and J. Sander, "LOF: Identifying Density- Based Local Outliers," *SIGMOD,*, p. 93–104, 2000.

[16] F. J. Anscombe and I. Guttman, "Rejection of Outliers," *Techno metrics*, vol. 2, pp. 123-147, May 1960.

[17] J. Tang, Z. Chen, A. W. Fu and D. W. Cheung, "Enhancing Effectiveness of Outlier Detections for Low Density Patterns," in *In Proceedings of PAKDD'02*, May 6-8 2002.

[18] M. Breunig, H. Kriege, T. N. Raymond and J. Sander, "LOF: Identifying Density Based Local Outliers," in *Proc. ACM SIGMOD 2000 Int. Conf. On Management of Data*, Dalles, TX,, 2000.

[19] F.Angiulli and F. Fassetti, "Detecting Distance-based Outliers in Streams of Data," in *In Proceedings of CIKM'07*, November 6-10 2007.

[20] E. M.Knorr, T.Ng.Raymond and V. Tucakov, "Distance-based outliers: algorithms and application," *VLDB*, vol. 8, pp. 237-253, 2000.

[21] E. M.Knorr and T. Raymond, "Alogorithms for Mining Distance-Base Outliers in Large Datasets," in *Proceedings of the 24th VLDB Conference*, New York, USA, 1998.

[22] M. Knorr and R. T. Ng., "Finding intentional knowledge of distance-based outliers," in *In VLDB '99: Proceedings of the 25thInternational Conference on Very Large Data Bases*, 1999.

[23] E. Knorr, R.T.Ng and R.H.Zamar, "Robust space transformations for distance-based operations," in *In Proc. ACM SIGKDD*, 2001.

[24] C. C. Aggarwal and P. S. Yu., "Outlier detection for high dimensional data," in *In Proc. of ACM-SIGMOD Int.Conf.Management of Data (SIGMOD'01)*, 2001.

[25] C. C. Aggarwal, J. Han, J. Wang and P. S. Yu, "A framework for clustering evolving data streams," in *In Proceedings of the 29th VLDB Conference*, 2003.

[26] D. Evans, A. J. Jones and W. M. Schmidt, "Asymptotic moments of near neighbor distance distributions," in *Proceedings of the Royal Society of London*, 2002.

[27] P. Chandore and P. Chatur, "Outlier Detection Techniques over Streaming Data in Data Mining: A Research Perspective," *International Journal of Recent Technology and Engineering (IJRTE)* , vol. 2, no. 1, pp. 157-162, March 2013.

[28] M. M. Gaber, "Data Stream Processing in Sensor N etworks," in *In J. Gama and M. M. Gaber ,Learning from Data Streams Processing,Springer*, Berlin,Heidelberg, 2007.

[29] C. C. Aggarwal, J. Han, J. Wang and P. S. Yu, "A Framework for Projected Clustering of High Dimensional Data Streams," in *Proceedings of the 30th VLDB Conference*, Toronto, Canada, 2004.

[30] I. Ntoutsi, A. Zimek, T. Palpanas, P. Kroger and H.-P. Kriegel, "Density-based Projected Clustering over High Dimensional Data Streams," in *SIAM International Conf. on Data Mining (SDM)*, Anaheim, CA, USA, 2012.

Short Term Load Forecasting for Uttarakhand using Neural Network and Time Series models

Prakash GL[1], K. Sambasivarao[2], Priyanka Kirsali [2] and Vibhuti Singh[2]

[1]*Research Scholar, Center for Information Technology,*
University of Petroleum and Energy Studies, Dehradun, India
glprakash78@gmail.com

[2]*M.Tech, (Artificial Intelligence and Artificial Neural Networks),*
Centre for Information Technology, University of Petroleum and Energy Studies,
Dehradun , India, k.sambasivarao222@gmail.com

***Abstract*— Accurate Load Forecasting is crucial in Power System operation and planning both for Regulated and De-regulated electricity markets. Short Term Load Fore-casting (STLF) is a tough job to handle because of the nonlinear behaviors of the electrical loads, climatic conditions. There is always a need for the sophisticated methods for STLF due to its complexity. This paper presented three models with neural network for both hour basis and day ahead prediction. The past load data as well as the weather data were collected and clustering technique is used for cleansing the data. The whole purified data is divided into three modules: Training data, Testing data and Validation data. The three NN models proposed were trained and tested by using the corresponding datasets. The presented models predicted the electric load, both daily and hourly, with high accuracy. The models proposed in this paper have been simulated using data obtained from State Load Dispatch Centre, Dehradun for the duration August 2011 to March 2013. The models are tested, results are compared with the actual load and Mean Absolute Percentage Error (MAPE) will be calculated.**

***Keywords*— Short Term Load Forecasting, Neural Network, NARX model, Curve fitting, MAPE.**

I. INTRODUCTION

One of the major drawbacks of electrical energy is that it cannot be stored. Electrical energy has to be generated whenever there is a demand. This causes a major challenge for generating units as start-up and shutdown of alternators takes some time. If we can estimate the required demand of consumers ahead with reasonable accuracy, we can schedule the generators accordingly. This process of estimating the future load demand is called as Load Forecasting. Load forecasting is an integral process with all phases of power system. Load forecasting is broadly classified into three categories: Long term, Medium term and Short term. Long term load forecasting deals with estimation of electric load for the next years. Medium term load forecasting estimates the electric loads ranging from few weeks to few months. Finally Short term load forecasting is used for predicting the future load ranging from few hours to few days. Long term load forecasting is useful for planning and setting up of new power plants to meet the long term demand. Medium load forecasting helps in power system maintenance planning and power purchase agreements and Tariff fixation. Short term load forecasting is very important as it is key for the whole power distribution system. Starting with the optimal load dispatch, STLF is useful in generator scheduling, unit commitment problems etc. So accurate prediction of load is very important for the proper operation of all phases of power systems. Wrong prediction of load leads to malfunction of power system as well as huge economic loss. Under estimation of STLF causes the increase in operating cost and load shedding causing problems to end users. Over estimation of STLF leads to unnecessary generation of excess amount of power which will go as loss in lines and increasing the operating cost.

The usage patterns of electricity by the consumers vary with so many factors such as climatic conditions, holiday effects, and their economic background and also include their random behavior. In order to forecast the load accurately, we have to consider all these factors. The integration of all these factors into the estimation process is a major challenge. In general, the relationship between load and these factors is very complex and nonlinear. It may vary according to the changes of the season, population and economic structure of the specified area and so on. Usually the future load prediction is carried out by making use of the past load data along with the influential factors. As the neural networks are the best tools for modelling nonlinear behavior, we proposed the NN models for accurate load prediction. There is a chance of presence of erroneous data in the past load data collected. This may be due to the measurement problems or some other problems. This erroneous data, if not treated properly, leads to wrong forecasting results. So we proposed a new methodology to eliminate the erroneous data from the collected load data.

In this paper, three models are proposed combining the Statistical Time Series Analysis Techniques with the Artificial Neural Networks to accurately forecast the load one day-ahead as well as one hour ahead. Both historical load data and historical temperature data is collected for Uttarakhand state. First the data is classified on seasonal basis and the erroneous data is purified by the method of outlier detection using clustering technique. A Multi-Layer Feed forward Neural

978-1-4799-6896-1/14/$31.00 ©2014 IEEE

network fore-casting model is constructed combining the reduced factors and typical training set. This proposed model is compared with the NAR and NARX models.

This paper is organized as follows: In Section II, the related work is discussed. The Neural network models and architectures are discussed in Section III. Section IV gives the problem definition and Section V discusses about the proposed methodology including data cleansing and training of models. The performance analysis is discussed in Section VI. Conclusion and the further possible research directions are discussed in section VII.

II. RELATED WORK

Various forecasting techniques have been applied to STLF to improve accuracy and efficiency. In general, The Short-term load forecasting is divided into two categories: Statistical approaches and Artificial Intelligence approaches [1]. In Statistical approaches, the relationship between the electric load and the influencing factors are modelled using mathematical equations and thus the future load will be predicted based on those modelled relationship. In artificial intelligence approaches, human beings way of thinking and reasoning are applied to the past load data to get the knowledge with which the future loads can be predicted. The statistical category includes multiple linear regression [2], stochastic time series [3], general exponential smoothing [4], state space [5], etc. Recently support vector regression (SVR) [6, 7], has shown good prediction results compared to the previous techniques. Statistical approaches are best for predicting the loads of normal days, but they are weak in predicting the loads of special days. The various regression models have been proposed for day ahead load prediction by Engle et al [8]. They incorporated the effects of holidays and weather into their models. The Auto regression and Integrated Moving Average models have been proposed for load prediction by Fan and McDonald [9] and Cho et al [10]. Artificial Intelligence category involves Expert system [11], artificial neural network (ANN) [12], fuzzy inference [13], and evolutionary algorithm. Expert systems are the earliest and simplest methods in artificial intelligence proposed for load forecasting. The knowledge of the experienced people in the problem domain is collected and programmed into expert systems as If-Then rules. An expert system for prediction of Taiwan power system load has been proposed by Ho et al [14]. They collected the past five years load data and incorporated into the system. [15] and [16] describe applications of fuzzy logic to load forecasting.

Artificial neural network is the best tool for modelling the nonlinear behavior. Many works have been proposed for load forecasting using neural networks. A three layer feed forward neural network has been proposed for energy control center of Greek Public Power Corporation [17]. A multilayer feed forward neural network for STLF has been proposed by Papalexopoulos et al [18]. Evolutionary algorithms have been proved to be very useful in multiobjective function optimization, this aspect is used to train the neural network to obtain better results. Generally computational intelligence methods are flexible in modelling the nonlinear relationship between load and its relative factors.

III. MODEL DESCRIPTION

A. Multi-Layer Perceptron Neural Network

Multi-Layer Perceptron is one of the most widely used Neural network model today due to its ability to construct a model for complex non-linear relationships between inputs and outputs. The network consists of number of layers each containing number of neuron units and weights associated with the connection between them where the information is passed as feed-forward manner.

In general, each node in the hidden and output layers is a simple computational unit. It sums all weighted signals from the lower layer and generates the output through a transfer function. In this work, the sigmoid function is used as the transfer function in our neural models, which is mathematically given by

$$Y_j = [1 + exp(\ {}_iW_{ij}X_i)]^{\ l} \quad (1)$$

Here Y_j is the output of node j, W_{ij} is the weight between node j and node i and X_i is the signal from node i.

B. *MLPNN Model For Hour Ahead And Day Ahead Load Forecasting*

The parameters of three layer perceptron artificial neural network for hour ahead as well as day ahead load forecasting are as given below:

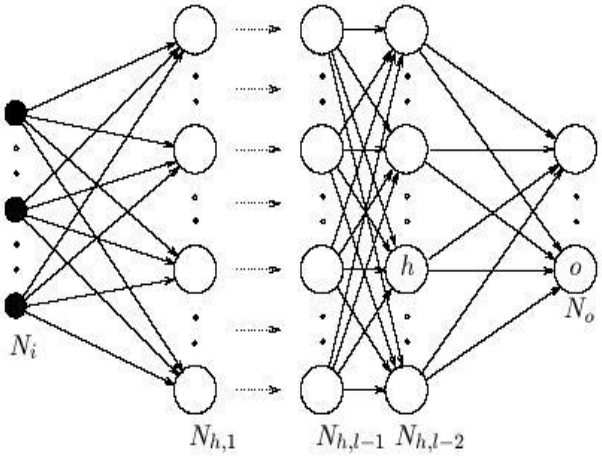

Fig. 1 Multi-Layer Perceptron Neural Network

TABLE I
MLPNN MODELS FOR HOUR AHEAD AND DAY AHEAD FORECASTING

S.No	Parameters	Hour ahead	Day ahead
1	No. of layers	3	3
2	No. of neurons in hidden layer	15 to 19	15 to 19
3	No. of neurons in output layer	1	1
4	Activation function of hidden Layer	Logsig	Logsig
5	Activation function of output Layer	Linear	Linear
6	Training Algorithm	Levenberg-Marquardt	Levenberg-Marquardt
7	Learning Rate	0.1	0.1
8	Momentum factor	0.98	0.98

Levenberg Marquardt algorithm is one of the best training algorithm for neural network. In LM algorithm, there is no need of calculating the Hessian matrix as in Gauss – Newton method. The Hessian matrix is approximated as the square of the Jacobian matrix, if the performance function can be viewed as the sum of squares.

$$H = J^T J \tag{2}$$

and the gradient of the error function can be given as

$$g = J^T e \tag{3}$$

Where J is the Jacobian matrix that contains first derivatives of the network errors with respect to the weights and biases, and e is a vector of network errors. Instead of computing the Hessian matrix, we can compute the Jacobian matrix using the standard backpropagation algorithm, which is much more simpler. This approximation of Hessian matrix is used for the updation as shown:

$$X_{k+1} = X_k \quad [J^T J + I]^{-1} J^T e \tag{4}$$

For large values, the Levenberg Marquardt algorithm can be approximated as gradient descent method with small step size. For small values, it can be approximated as Newtons method. As the Newton's method is faster and more accurate near an error minimum, our aim is to shift toward Newton's method as quickly as possible. In this way, after each iteration of the algorithm, there is a reduction in the error function.

IV. PROBLEM DEFINITION

Accurate prediction of the future load helps in planning and operation of power system. As Electrical energy should be supplied whenever there is demand, load forecasting is useful in generation scheduling. There are various factors which influences the load prediction such as seasonal variations, weather, time of day, day of week etc. So accurate prediction of load is necessary for proper operation of power system. The objectives of this work include:

i. Cleansing of past load data using data mining techniques
ii. Hour ahead load forecasting
iii. Day ahead load forecasting
iv. Analysis of dependency of load on temperature
v. comparison of various models

V. METHODOLOGY

Following steps have been proposed to formulate the above said problem:

1) First of all historical weather and load data are collected and scrutinized.
2) Data cleansing is performed by using data mining technique.
3) Then monthly deviations have been calculated excluding some special days e.g. holidays, Saturdays and Sundays.
4) Then data base has been created for developing load forecasting model(both training and testing).
5) After this classification, MLPNN can be used to train these input variables for getting the expected outcome for both hour ahead and day ahead load forecasting. System can be simulated with the help of MATLAB/ SIMULINK.
6) Building Nonlinear Auto regressive model (NAR) for one hour ahead forecasting without temperature effects.
7) Buidling Nonlinear Auto regressive model (NARX) with external temperature inputs
8) Then mean square percentage error (MSPE) will be calculated for the given forecasting models.
9) Comparison of results and visualizing the dependency of load on temperature.

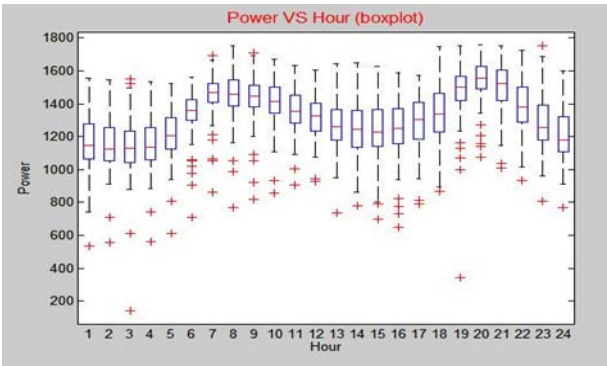

Fig. 2. Daily Load pattern for Dehradun city

A. Data Cleansing

The power consumption of the consumers at regular intervals of time recorded by the meters can be depicted graphically as Load curve. This load curve contains information regarding plant load factor, demand, peak demand, plant capacity factor etc. Analysis of load curves is very useful for finding the patterns in the power consumption. However there is chance of erroneous data in load which leads to false patterns in load curves. Our dataset consisted of intraday electricity demand from State Load Dispatch Centre, Dehradun from 1st August 2011 to 31st March 2013. We obtained hourly data for Dehradun. The load data till february 2013 were used to train the models to adapt the load behavior and the remaining 1 month data were used to evaluate the accuracy of forecasting for both day as well as hour ahead. The load pattern for Dehradun city is as shown in the Fig. 2.

The methodology of load data cleansing is:

1) Dividing the data into blocks based on seasons.

2) Calculating the Euclidean distance between entries of same block and removing the outliers.

3) Filling the gaps by the mean values of that respective block.

B. Neural Network Training

Training Algorithm plays a prominent role in the convergence of the problem. In this paper, we are using Levenberg Marquardt Algorithm for training our multilayer feed forward network. The Levenberg Marquardt algorithm was developed by Kenneth Levenberg and Donald Marquardt. This provides a numerical solution to the problem of minimizing a nonlinear function. It is fast and stable algorithm compared to other algorithms such as gradient descent and Gauss Newton etc. Small and medium sized problems can be solved by using this algorithm which needs fast and stable convergence.

The Levenberg Marquardt algorithm combines the steepest de-scent method and the Gauss Newton algorithm. The fast convergence of Gauss Newton algorithm is combined with the stability of gradient descent algorithm. This algorithm is superior to Gauss Newton, as it can solve the problems with error surface more than the quadratic approximation. Levenberg algorithm converges faster than the gradient descent algorithm but a bit slower than the gauss newton algorithm. Levenberg Marquardt algorithm is mostly preferred where the error surface is more complex than the quadratic approximation. The computational complexity of LM algorithm is very much simpler than the Gauss Newton algorithm as there is no need for the computation of hessian matrix. The block diagram for Levenberg Marquardt algorithm is as shown in figure 3.

The training process using Levenberg Marquardt algorithm is as follows:

1) Evaluate the Mean Square Error using the randomly generated initial weights.
2) Do an update to adjust weights by using Weight updation formula.
3) Evaluate the MSE again with the new updated weights.
4) If the MSE is increased because of updation of weights, reset the weight vector to the previous values and increase the coefficient by some factor, say 10. Do weight updation again as per step 2.
5) If the MSE is decreased because of updation of weights, accept the new weight vector and decrease the coefficient by the same factor as in step 4.
6) Until the current total error is smaller than the threshold limit value, repeat the same procedure starting from step 2 with new updated weights after every iteration.

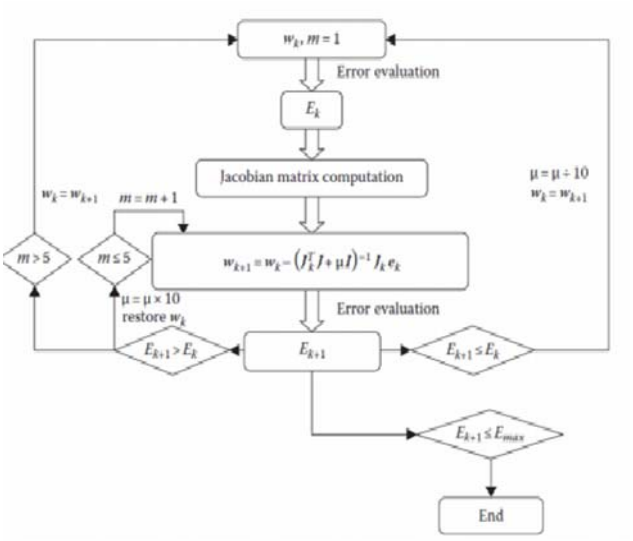

Fig.3.Leverberg Marquardt Algorithm

C. NAR and NARX models

Nonlinear Autoregressive Model can be built using an Multi-Layer Neural Network. NAR (nonlinear autoregressive) neural networks can be trained to predict a time series from that series past values. NAR takes the delayed values of output as

$$x_t = f(x_{t\ 1}; x_{t\ 2}; :::x_{t\ N}; W) + e_t \quad (5)$$

Similarly if we use the external information I available to make the prediction, the model becomes NARX. NARX model incorporating the external information is as shown:

$$x_t = f(x_{t\ 1}; x_{t\ 2}; :::x_{t\ N}; I_t; W) + e_t \quad (6)$$

For load forecasting problem, the number of input nodes is a key variable. Keeping the number of input nodes low may not

give enough information for the accurate prediction. Whereas if we select large number of input nodes, the model becomes more complex resulting in less effective training. We selected the lags L corresponding to the previous 24 hours L=[1,2,...24]. Actually there is a thumb rule for deciding about the number of hidden layers and the number of neurons in each hidden layer. The number of neurons in the output layer is also a considerable factor for the prediction. Based on the number of time intervals for which the model has to forecast in advance, we can select the number of output neurons. If we are doing one hour ahead prediction, we can set the number of output neurons as 1 and for one day ahead prediction, we took 24 neurons in the output layer. Both the NAR and NARX models are built in MATLAB using neural network toolbox.

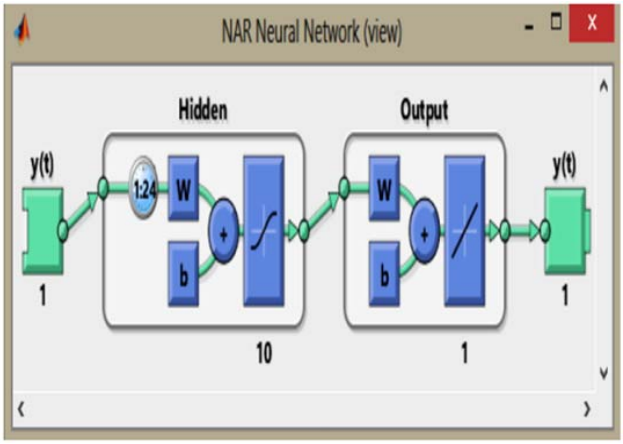

Fig 4. .Nonlinear Autoregressive Model

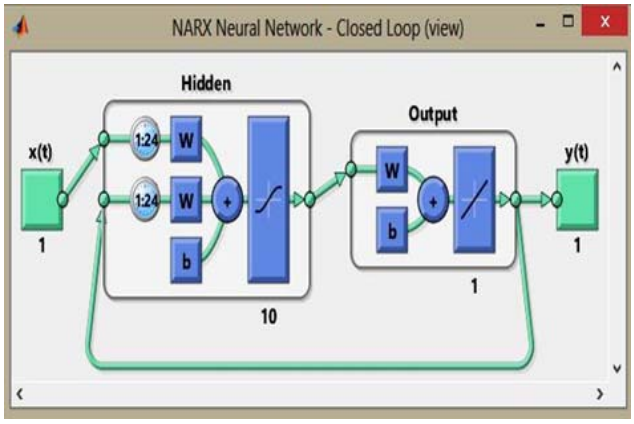

Fig. 5. Nonlinear Autoregressive Model with external inputs

The NAR model is as shown in Fig. 4. The temperature data is given as an external known information to NARX model which is shown in the Fig. 5. The results of both NAR and NARX are compared and the dependency of load on temperature is identified.

VI. PERFORMANCE ANALYSIS

The whole load data is divided into three blocks for training, testing and validation. The process of data cleansing is done by using R-an open source data mining software. The proposed models have been simulated using neural networks toolbox in MATLAB. Load forecasting is done for the month of April and the results are compared with the actual values. The forecasting performance can be evaluated by using Mean

Absolute Percentage Error (MAPE), which is defined as:

$$MAPE = \frac{1}{N}\Sigma\frac{|P_A - P_F|}{P_A} * 100 \qquad (7)$$

where PA, PF are the actual and forecast values of the load. N is the number of the hours of the day i.e. N = 1, 2,..,24. The forecasted result for day ahead forecasting as well as various performance plots are shown in Fig. 6-8

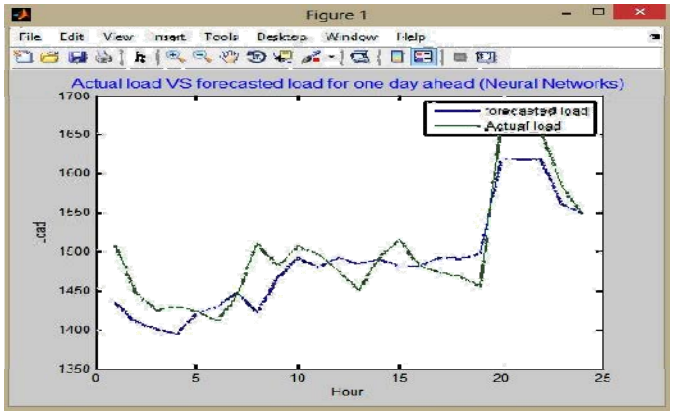

Fig. 6. Forecasted Load vs Actual Load

The Mean Absolute Percentage Error for the proposed models are shown in the Table 2.

TABLE II
MAPE FOR THE PROPOSED MODELS

S.No	Model	Hour ahead	Day ahead
1	Neural Network	1.764	1.827
2	NAR	1.92	2.01
3	NARX	1.83	1.924

As seen from the MAPE results, neural network performs better than the statistical methods in both hourly as well as daily ahead forecasting. As NAR model works without temperature data, the results are showing that with the nonlinear modeling capability of neural network, prediction models gives satisfiable results even without temperature data. But the weather data is necessary for getting accurate forecast results.

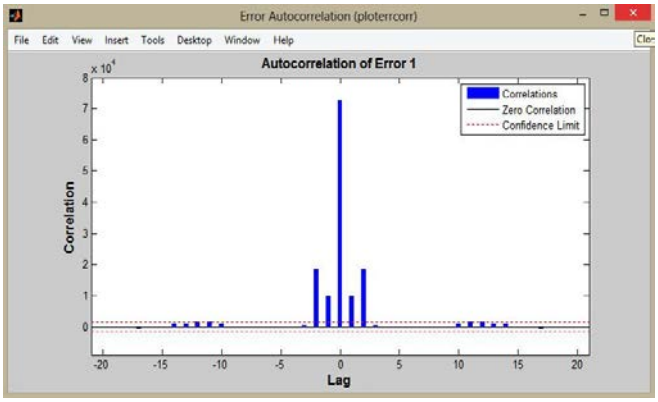

Fig. 7. Error Auto correlation plot

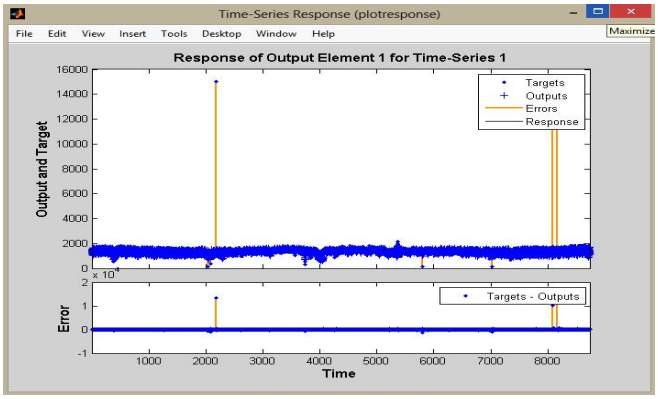

Fig. 8. Time Series Response plot

VII. CONCLUSION

In this paper, a Data Mining and Neural Network approach is presented for short term load forecasting. The main contribution of this paper is to propose a data cleansing method based on data mining approach and a comparative analysis of Multi-layer perceptron with statistical techniques. The proposed work also shows the dependency of load on temperature. The proposed models are built in MATLAB/Simulink environment and the performance of each model is calculated by using MAPE. We found that prediction results were better when temperature data is taken into consideration. Results have been shown the minimum percentage error of 1.76 with the neural network model considering temperature effects. This work can be further extended by using Adaptive Neuro Fuzzy Inference System (ANFIS) to obtain better results. The factors such as economic position, electricity prices can also be considered keeping in view the De Regulated electricity markets for obtaining good results.

VIII. ACKNOWLEDGEMENTS

The authors are grateful to State Load Dispatch Center, Dehradun for providing us the Load data for the previous 3 years for Uttarakhand. We express our sincere thanks to Indian Meteorological Department (IMD), for providing us the weather data for Dehradun.

REFERENCES

[1] I. Moghram and S. Rahman, ”Analysis and Evaluation of Five Short Term Load Forecasting Techniques,” IEEE Trans. Power Sys-tems, Vol. 4, No. 4, Oct. 1989, pp. 1484 1491.

[2] A. D. Papalexopoulos and T. C. Hesterberg, ”A Regression Based Approach to Short Term System Load Forecasting,” IEEE Trans. Power Systems, Vol. 5, No. 4, Nov. 1990, pp. 1535 1547.

[3] S. J. Huang and K. R. Shih, ”Short term load forecasting via ARMA model identification including non-Gaussian process considerations,” IEEE Trans. Power Syst., vol. 18, no. 2, pp. 673 679, 2003.

[4] J. W. Taylor, ”Short term load electricity demand forecasting using double seasonal exponential smoothing,” Journal of the Operational Research Society, vol. 54, pp. 799 805, 2003.

[5] P. E. McSharry, S. Bouwman, and G. Bloemhof, ”Probabilistic forecast of the magnitude and timing of peak electricity demand,” IEEE Trans. Power Syst., vol. 20, no. 2, pp. 1166 1172, 2005.

[6] J. Yang, H. Cheng, ”Application of SVM to power system short term load forecast,” Power System Automation Equipment China, 2004, 24(4), 30 32.

[7] B. J. Chen, M. W. Chang, and C.J. Lin, ”Load forecasting using support vector machines: a study on EUNITE competition 2001,” IEEE Trans. Power Syst., vol. 19, no. 4, p. 18211830, 2004.

[8] R.F. Engle, C. Mustafa, J. Rice, ”Modeling peak electricity demand,” Journal of Forecasting, 1992, 11, 241 251.

[9] J.Y. Fan, J.D. McDonald, ”A real-time implementation of short term load forecasting for distribution power systems,” IEEE Transactions on Power Systems, 1994, 9, 988 994.

[10] M.Y. Cho, J.C. Hwang, C.S. Chen, ”Customer short term load fore-casting by using ARIMA transfer function model,” Proceedings of the International Conference on Energy Management and Power Delivery, EMPD, 1995, 1, 317 322.

[11] K.J. Hwan, G.W. Kim, ”A short term load forecasting expert system,” Proceedings of The Fifth Russian-Korean International Symposium on Science and Technology, 2001, 112 116.

[12] Z. Yun, Z. Quan, S. Caixin, L. Shaolan, L. Yuming, and S. Yang, ”RBF neural network and ANFIS based short term load forecasting approach in real-time price environment,” IEEE Trans. Power Syst., vol. 23, no. 3, pp. 853 858, 2008.

[13] K.H. Kim, H.A.Youn, Y.C. Kang, ”Short term load forecasting for special days in anomalous load conditions using neural networks and fuzzy inference method,” IEEE Transactions on Power Systems, 2000, 15(2), 559 565.

[14] K.L. Ho et al, ”Short term load forecasting of Taiwan power system using a knowledge based expert system,” IEEE Transactions on Power Systems, 1990, 5, 1214 1221.

[15] V. H Hinojosa and A Hoese, ”Short-Term Load Forecasting Using Fuzzy Inductive Reasoning and Evolutionary Algorithms,” IEEE Trans-action on Power Systems, 25(1):565 574, 2010.

[16] S. C. Pandian, K. Duraiswamy, C. Christober, Asir Rajan, and N. Kanagaraj, ”Fuzzy approach for short term load forecasting,” Electric Power Systems Research, vol. 76, no. 6 7, pp. 541-548, Apr 2006.

[17] A.G.Bakirtzis, et al., ”A neural network short term load forecasting model for the Greek power system,” IEEE Transactions on Power Systems, 1996, 11, 858 863.

[18] A.D. Papalexopoulos, S. Hao, T.M. Peng, ”An implementation of a neural network based load forecasting model for the EMS,” IEEE Transactions on Power Systems, 1994, 9, 1956 1962.

Business Intelligence & Geo Tracking – A Novel Mining Technique to Identify Alerts and Pattern Analysis

M Vijaya Kamal
Dept of CIT,
University of Petroleum & Energy Studies,
Dehradun, Uttarakhand, India
kamalmv@gmail.com/mvkamal@ddn.upes.ac.in

D Vasumathi
Dept. of CSE,
Jawaharlal Nehru Technological University,
Hyderabad, India.
vasukumar_devara@yahoo.co.in

***Abstract* - Web mining plays vital role in day-to-day applications to improve intelligence of web in the context of business must be able to identify useful business intelligence. To achieve our model in web engineering, we are using mining techniques for next generation business intelligence development. In this research our approach identifies the weblogs error reports using comprehensive algorithms, applies the mining techniques to detect noisy and integrates the different models, finally our information patterns satisfies the need of client inputs. For web engineering retrieval system, list of web log bugs and web architecture, the system uses mining techniques to explore valuable web data patterns in order to meet better projects inputs and higher quality web systems that delivered on time. Our research uses association and machine learning applied to web architecture model pertaining to source code mining implementation tools improves software debugging business rules for novel projects and also presents strategies for efficient study text, graph mining. Presents the Geo Tracking system to identify messages from terrorist or threat persons and also from hackers detects the negative rates and improves the high positive which increases the quality of Government Private and Public sectors.**

Keywords *– Business Intelligence, Web mining, Geo-Tracking, Text Mining, Pattern Analysis*

I INTRODUCTION

Data mining is the nontrivial process of identifying valid novel, potentially useful, and ultimately understandable patterns in data Fayyad. Data mining research has drawn on a number of other fields such as inductive learning, machine learning and statistics etc. Machine learning is the automation of a learning process and learning is based on observations of environmental statistics and transitions. Machine learning examines previous examples and their outcomes and learns how to reproduce these make generalizations about new uses. Inductive learning means inference of information from data and Inductive learning is a model building process where the database is analyzed to find patterns. Main strategies are supervised learning and unsupervised learning. Statistics used to detect unusual patterns and explain patterns using statistical models such as linear models. Data mining models can be a discovery model – it is the system automatically discovering important information hidden in the data or verification model – takes an hypothesis from the user and tests the validity of it against the data.

The web contains collection of pages that includes countless hyperlinks and huge volumes of access and usage information. Because of the ever-increasing amount of information in cyberspace, knowledge discovery and web mining are becoming critical for successfully conducting business in the cyber world. Web mining is the discovery and analysis of useful information from the web. Web mining is the use of data mining techniques to automatically discover and extract information from web documents and services (content, structure, and usage). Two different approaches were taken in initially defining web mining: i. Process centric view web mining as a sequence of tasks ii. Data centric view web mining as a web data that was being used in the mining process. Text mining is concerned with the task of extracting relevant information from natural language text and to search for interesting relationships between the extracted entities.

SECTION - II

2. Related Work: Geo graphical systems captures manipulate analyze manage and present all types of geographical data used for geographical information science or geographical to extract large data. It digitally creates and manipulates spatial terms that may be jurisdictional. Generally geographical custom designed for an organization. One of the first applications of spatial analysis in epidemiology is the Rapport sur la marche et les effects du cholera dans paris modern geographical technology use digital information for which various digitized data creation methods are used where a hard copy map or survey plan is transferred into a digital capabilities. Data representation can be classified into discrete and continuous fields.

Web has tremendous success in building of users to identify such communities is useful for many purposes. Gibson identified web communities as core of central authorized pages linked together by hub pages. Web crawling applies the maximum flow minimum cut model to

978-1-4799-7552-5/14 $31.00 © 2014 IEEE
DOI 10.1109/ISCBI.2014.19

the web graph for identifying web communities flow approaches and strengths bipartite graph method followed to find a related concept of friends and neighbors was introduced who are in the cyber world would form a community. Analyzing web log data with visualization tools has evoked a lot of interest developed a web ecology visualization is to understand the relationship between web content, structure, usage over a period of time. Interactive web log site at a global level display each browsing path on the pattern displayed in an incremental manner. Google is popular search engine provides access to information from over billion web pages that it has indexed on its server.

Mining techniques like Association Rule Mining predict the association and correlation among set of items "where the presence of one set of items in a transaction implies with a certain degree of confidence. 1) Discovers the correlations between pages that are most often referenced together in a single server session/user session. 2) Provide the information: i. what are the set of pages frequently accessed together by web users? ii. What page will be fetched next? iii. What are paths frequently accessed by web users. 3) Associations and correlations: i. Page association from usage data – user sessions, user transactions ii. Page associations from content data – similarity based on content analysis iii. Page associations based on structure – link connectivity between pages. Advantages: a) Guide for web site restructuring – by adding links that interconnect pages often viewed together. B) Improve the system performance by prefetching web data. Sequential pattern discovery is applied to web access server transaction logs to discover sequential patterns that indicate user visit patterns over a certain period. That is, the order in which URLs tend to be accessed benefits are a) useful user trends can be discovered b) predictions concerning visit pattern can be made c) to improve website navigation d) personalize advertisements e) dynamically reorganize link structure and adopt web site contents to individual client requirements or to provide clients with automatic recommendations that best suit customer profiles. Clustering is a group together items that have similar characteristics. a) Page clusters groups of pages that seem to be conceptually related according to users' perception. b) User Cluster groups or users that seem to be behave similarly when navigating through a web site.

Classification maps a data item into one of several predetermined classes for example describing each users category using profiles. Classification algorithms are decision tree, naïve Bayesian classifier, neural networks. Path Analysis is a technique that involves the generation of some form of graph that "represents relations defined on web pages. This can be the physical layout of a web site in which the web pages are nodes and links between these pages are directed edges. Most graphs are involved in determining frequent traversal patterns/ more frequently visited paths in a web site for example what paths do users traversal before they go to a particular URL.

SECTION - III

3. Web Mining Techniques: Web mining can be categorized into three areas of interest based on which part of the web to mine

3.1. Web content mining: Useful information from the web contents/documents is the application of data mining techniques to content published on the Internet. The web contains types of data. Basically, the web content consists of several types of data such as plain text (unstructured), image, audio, video, meta data as well as HTML (semi Structured), or XML (structured documents), dynamic documents, multimedia documents. The research around applying data mining techniques to unstructured text is termed knowledge discovery in texts/ text data mining/ text mining. Hence consider text mining as an instance as an instance of web content mining.

Issues in Web content Mining:

Finding keywords and key phases

- Discovering grammatical rules collections
- Hypertext classification/categorization
- Extracting key phrases from text documents
- Learning extraction rules
- Hierarchical clustering
- Predicting relationships

Web content mining involves in artificial intelligence systems that can "act autonomously or semi autonomously on behalf of a particular user, to discover and organize web based information". Agent Based approaches focus on intelligent and autonomous web mining tools based on agent technology. i. Some intelligent web agents can use a user profile to search for relevant information, then organize and interpret the discovered information. Example Harvest. ii) Some use various information retrieval techniques and the characteristics of open hypertext documents to organize and filter retrieved information. iii) Learn user preferences and use those preferences to discover information sources for those particular users. Example: Xpert Rule Rminer.

Data base approach: focuses on "integrating and organizing the heterogeneous and semi-structured data on the web into more structured and high level collections of resources". These organized resources can then be accessed and analyzed. These "metadata or generalization

are then organized into structured collections and can be analyzed.

3.2. Web Structure Mining: Operates on the web hyperlink structure can provide information about page ranking or authoritativeness and enhance search results through filtering i.e., tries to discover the model underlying the link structures of the web. This model is used to analyze the similarity and relationship between different web sites. This type of mining can be based on the kind of structural data used. a) A hyperlink is a structural unit that connects a web page to different location, either within the same web page (intra_document hyperlink) or to a different web page (inter_document) hyperlink. b) Document structure, the content within a web page can also be organized in a tree structured format, based on various HTML and XML tags within the page. Mining efforts here have focused on automatically extracting document object model (DOM) structures out of documents.

Web structure analysis used for:

- Ordering documents matching a user query
- Deciding what pages to add to a collection
- Page categorization
- Finding related pages
- Finding duplicated web sites
- Find out similarity between them.

3.3. Web Usage Mining: To discover interesting usage patterns from web data, in order to understand and better serve the needs of web-based applications. It tries to make sense of the data generated by the web surfer's sessions/behaviors. While the web content and structure mining utilize the primary data on the web, web usage mining mines the secondary data derived from the interactions of the users while interacting with the web. The web usage data includes the data from web server logs, proxy server logs, browser logs, and user profiles. (The usage data can also be classified into three different kinds on the basis of the source of its collection, on the server side (there is an aggregate picture of the usage of a service by all users), the client side (while on the client side there is complete picture of usage of all services by a particular client), and the proxy side (with the proxy side being somewhere in the middle). Web usage mining analyzes results of user interactions with a web server, including web logs, click streams, and database transactions at a web site of a group of related sites.

Web usage mining process can be regarded as a three-phase process consisting:

a. Preprocessing/ data preparation - web log data are preprocessed in order to clean the data – removes log entries that are not needed for the mining process, data integration, identify users, sessions, and so on

b. Pattern discovery - statistical methods as well as data mining methods (path analysis, Association rule, Sequential patterns, and cluster and classification rules) are applied in order to detect interesting patterns.

c. Pattern analysis phase - discovered patterns are analyzed here using OLAP tools, knowledge query management mechanism and Intelligent agent to filter out the uninteresting rules/patterns.

After discovering patterns from usage data, analysis has to be conducted. The most common ways of analyzing such patterns are either by using query or by loading the results into a data cube and then performing OLAP operations. Then, visualization techniques are used for a results interpretation. The discovered rules and patterns can then be used for improving the system performance / for making modifications to the web site. The purpose of web usage mining is to apply statistical and data mining techniques to the preprocessed web log data, in order to discover useful patterns. Usage mining tools discover and predict user behavior in order to help the designer to improve the web site, to attract visitors, or to give regular users a personalized and adaptive service.

SECTION - IV

4. Business Intelligence: Business intelligence is software represents the tools and systems that play a role in the strategic planning processes of the corporation. System allows an organization to gather store access and analyze corporate data in decision making. Generally systems illustrate business intelligence in the areas of customer profiling, support, market research, segmentation, product profitability, statistical analysis inventory. Most of the companies collect large data from their business operations. A business would need to use a wide range of software programs, such as Excel, Access, databases applications. Business intelligence software for web mining help to gather information in a timelier, this will search for the trade magazines and newspapers relevant to business to provide the growth information. Entering a new revenue market is always frightening but diversification is key factor to surviving difficult timelines. Business intelligence software for mining provides predictive analysis of various growth potentials according to the search criteria determine. With assistance of a business intelligence service can we face the most difficult of financial times with more confidence and need to diversify because will have intelligence smart choice.

Web mining can help in improving the business decision is challenging task to engineer,

implement the search engine. This specifies that indexing of web pages involves a huge task as per tens of millions of queries are given to search engine. The problems of scaling traditional search techniques to magnitude new technical challenges are involved in using the additional information present in hypertext to produce better search results. Hypertext information can be answered by using web mining techniques and improving the capabilities of the search engines by giving better results to clients. Web mining applications have been used by these web sites such as web search for example Google Yahoo web vertical search Amazon, applications of web mining such as ERP CRM , E-Business

Business Intelligence Architecture: web content is responsible for fetching content from diverse sources into the web business intelligence system.

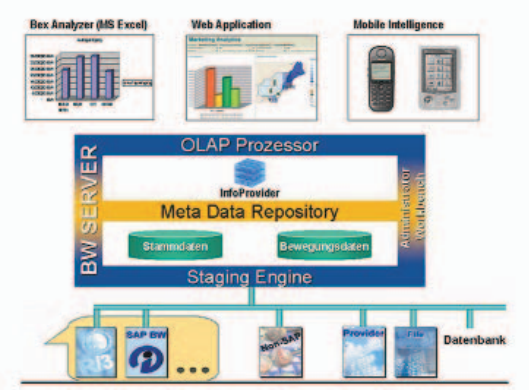

Figure 1: Business Intelligence Architecture.

As a component of the SAP Netweaver platform business intelligence brings together a powerful business intelligence infrastructure and numerous tools and functions for planning for data warehousing. We can integrate internal and external data and convert it into valuable information.

Online analytical processing data mining alerts data to be accessed and represented to be searched for patterns. Queries reports and analysis as well as the development of web applications will allow creating analysis reports to support decision making all levels of business solutions available on the internet. Business content and metadata as well as collaborative business intelligence can track progress report templates ensure data consistency and promote cooperation between decision make. Functionally business intelligence improves the efficiency of queries simplify administrative tasks and speed up background processes.

SECTION - V

5. Problem Definition: In previous research we found some text mining, sequence mining. Research in web mining is ultimate goal of developing computational approaches for monitoring public opinion in regions of conflict, indicators, and social media correlating these risk signals with commonly accepted quantitative assessments. Geo-tracking web system includes blogs, social media forum data from several countries. Our system supports automated social media collection updates from multiple search, visualization and machine translation through web interface application only.

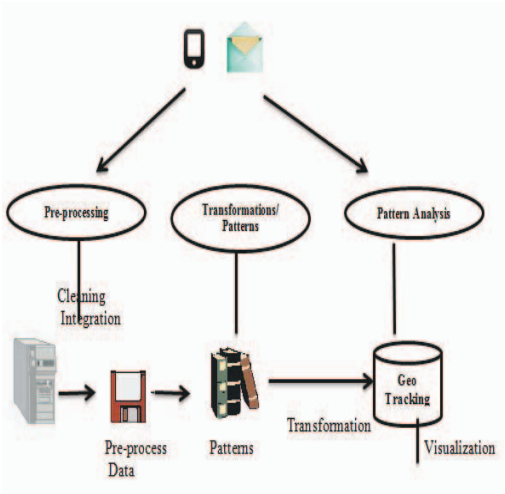

Figure 2: Geo Tracking system Mining

SECTION - VI

6. Early research on web mining

Web mining research on Google apps, text mining, semantic webs, information retrieval, graph mining, and museum mining, we briefly describe on web mining applications.

6.1. Text Mining: Text mining is to process of extracting relevant patterns (text, numeric indices) from unstructured information. It filter out automatically most undesirable junk emails based on certain terms or words that are not likely to appear in legitimate message but instead identify undesirable electronic mail. Automatically process the contents of web pages in a particular domain for example open a webpage and begin crawling the links to find there process all web pages that are referenced. The automatic search of large numbers of documents based on key words is the domain for example the popular internet search engines that have been developed over the last decade to provide efficient access to web pages with certain content.

6.2. Sequence Analysis: A set of sequence is to find the complete set of frequent subsequences. An element may contain a set of items within an

element are unordered and we list them alphabetically. Huge number of possible sequential patterns are hidden in databases mining algorithm should find the complete set of patterns when possible satisfying the minimum support frequency threshold. Highly efficient scalable involving only a small number of databases scans and incorporates various kinds of user-specific constraints. A sequence of two events is generated from frequent sequences consisting of one event and so on after generating a new sequence is checked in a database of customer histories.

6.3. Graph Mining: Graph mining has become an important research because of numerous applications to a wide variety of data mining problems in computational biology chemical data analysis, drug discovery and communication networking. Traditional data mining algorithms such as clustering classification frequent pattern and indexing have now been extended to the graph scenario. A graph is a set of nodes pairs of which might be connected by edges in a wide array of disciplines data can be intuitively cast into this format. Computer networks consists of routers computers and links between them. Social networks consists of individuals and interconnections, aims to design a graph mining tool that provides facilities for input data preprocessing for upload of source data into graph representations, frequent substructure discovery dense substructures especially the interactions within themselves.

6.4. Museums Mining: Museums development is a text mining to improve image access the goal is to collect digital image art historians and personalize retrieval. Text combines social tagging and trust inferencing to enrich metadata retrieval. By processing related text through the CLiMB toolkit evidence for evaluating the role of trust and for assessing the relationship between tags and text terms.

SECTION-VII

7. Evaluation: In our work web mining is a most innovative role to identify messages from hackers and terrorist which focus to capture mobile information data. To report all the information it uses business intelligence technique at the same time it also identify the hackers, anyone going to attack our Geo Tracking.

Step 1: Capture mobile information from all the networks

Step2: Preprocessing the data (relevant information to be mined from large database)

Step 3: Transforms in Pattern analysis.

Step 4: Apply the Mining Technique.

Step 5: Track the message into Geo Tracking System.

Evaluates the Geo Tracking system using information object that are available in particular dataset results will be shown either in percentage or notification alerts.

CONCLUSION-VII

Aassociation and machine learning applied to web architecture model pertaining to source code mining implementation tools improves software debugging business rules for novel projects and also presents strategies for efficient study text, graph mining. Capture the information available in mobile calls internet and call conversations from all the networks availability apply the data mining technique to track the alerts or attacks. We implements the system ”Geo Tracking” to identify messages from terrorist or threat persons which only finds the alert messages or misuse conversations at time Geo Tracking not expose to capture the confidential information is advantage and also from hackers detects the negative rates and improves the high positive which increases the quality of Government Private and Public sectors.

Reference:

[1] K. Bollacker, S. Lawrence, and C.L. Giles. CiteSeer: An autonomous web
agent for automatic retrieval and identification of interesting publications. In
Katia P. Sycara and Michael Wooldridge, editors, Proceedings of the Second International Conference on Autonomous Agents, pages 116–123, New York, 1998.
ACM Press.

[2] J. Borges and M. Levene. Mining Association Rules in Hypertext Databases. In
Knowledge Discovery and Data Mining, pages 149–153, 1998.

[3] S. Brin and L. Page. The anatomy of a large-scale hypertextual Web search engine. Computer Networks and ISDN Systems, 30(1-7):107–117, 1998.

[4] Ananiadou, S. and McNaught, J. (Editors) (2006). *Text Mining for Biology and Biomedicine*. Artech House Books. ISBN 978-1-58053-984-5

[5] Bilisoly, R. (2008). *Practical Text Mining with Perl*. New York: John Wiley & Sons.

[6] Feldman, R., and Sanger, J. (2006). *The Text Mining Handbook*. New York: Cambridge University Press. ISBN 9780521836579